ISSN 0021-9673

VOL. 663 NO. 1 MARCH 4, 1994

JOURNAL OF CHROMATOGRAPHY A

INCLUDING ELECTROPHORESIS AND OTHER SEPARATION METHODS

ELSEVIER

JOURNAL OF CHROMATOGRAPHY A

INCLUDING ELECTROPHORESIS AND OTHER SEPARATION METHODS

Scope. The *Journal of Chromatography A* publishes papers on all aspects of **chromatography, electrophoresis** and related methods. Contributions consist mainly of research papers dealing with chromatographic theory, instrumental developments and their applications. In the *Symposium volumes*, which are under separate editorship, proceedings of symposia on chromatography, electrophoresis and related methods are published. *Journal of Chromatography B: Biomedical Applications* —This journal, which is under separate editorship, deals with the following aspects: developments in and applications of chromatographic and electrophoretic techniques related to clinical diagnosis or alterations during medical treatment; screening and profiling of body fluids or tissues related to the analysis of active substances and to metabolic disorders; drug level monitoring and pharmacokinetic studies; clinical toxicology; forensic medicine; veterinary medicine; occupational medicine; results from basic medical research with direct consequences in clinical practice.

Submission of Papers. The preferred medium of submission is on disk with accompanying manuscript (see *Electronic manuscripts* in the Instructions to Authors, which can be obtained from the publisher, Elsevier Science B.V., P.O. Box 330, 1000 AH Amsterdam, Netherlands). Manuscripts (in English; *four* copies are required) should be submitted to: Editorial Office of *Journal of Chromatography A*, P.O. Box 681, 1000 AR Amsterdam, Netherlands, Telefax (+31-20) 5862 304, or to: The Editor of *Journal of Chromatography B: Biomedical Applications*, P.O. Box 681, 1000 AR Amsterdam, Netherlands. Review articles are invited or proposed in writing to the Editors who welcome suggestions for subjects. An outline of the proposed review should first be forwarded to the Editors for preliminary discussion prior to preparation. Submission of an article is understood to imply that the article is original and unpublished and is not being considered for publication elsewhere. For copyright regulations, see below.

Publication information. *Journal of Chromatography A* (ISSN 0021-9673): for 1994 Vols. 652–682 are scheduled for publication. *Journal of Chromatography B: Biomedical Applications* (ISSN 0378-4347): for 1994 Vols. 652–662 are scheduled for publication. Subscription prices for *Journal of Chromatography A*, *Journal of Chromatography B: Biomedical Applications* or a combined subscription are available upon request from the publisher. Subscriptions are accepted on a prepaid basis only and are entered on a calendar year basis. Issues are sent by surface mail except to the following countries where air delivery via SAL is ensured: Argentina, Australia, Brazil, Canada, China, Hong Kong, India, Israel, Japan, Malaysia, Mexico, New Zealand, Pakistan, Singapore, South Africa, South Korea, Taiwan, Thailand, USA. For all other countries airmail rates are available upon request. Claims for missing issues must be made within six months of our publication (mailing) date. Please address all your requests regarding orders and subscription queries to: Elsevier Science B.V., Journal Department, P.O. Box 211, 1000 AE Amsterdam, Netherlands. Tel.: (+31-20) 5803 642; Fax: (+31-20) 5803 598. Customers in the USA and Canada wishing information on this and other Elsevier journals, please contact Journal Information Center, Elsevier Science Inc., 655 Avenue of the Americas, New York, NY 10010, USA, Tel. (+1-212) 633 3750, Telefax (+1-212) 633 3764.

Abstracts/Contents Lists published in Analytical Abstracts, Biochemical Abstracts, Biological Abstracts, Chemical Abstracts, Chemical Titles, Chromatography Abstracts, Current Awareness in Biological Sciences (CABS), Current Contents/Life Sciences, Current Contents/Physical, Chemical & Earth Sciences, Deep-Sea Research/Part B: Oceanographic Literature Review, Excerpta Medica, Index Medicus, Mass Spectrometry Bulletin, PASCAL-CNRS, Referativnyi Zhurnal, Research Alert and Science Citation Index.

US Mailing Notice. *Journal of Chromatography A* (ISSN 0021-9673) is published weekly (total 52 issues) by Elsevier Science B.V., (Sara Burgerhartstraat 25, P.O. Box 211, 1000 AE Amsterdam, Netherlands). Annual subscription price in the USA US$ 4994.00 (US$ price valid in North, Central and South America only) including air speed delivery. Second class postage paid at Jamaica, NY 11431. **USA POSTMASTERS**: Send address changes to *Journal of Chromatography A*, Publications Expediting, Inc., 200 Meacham Avenue, Elmont, NY 11003. Airfreight and mailing in the USA by Publications Expediting.

See inside back cover for Publication Schedule, Information for Authors and information on Advertisements.

0021-9673/94/$07.00

Printed in the Netherlands

VOL. 663, NO. 1 JOURNAL OF CHROMATOGRAPHY A MARCH 4, 1994

CONTENTS

(Abstracts/Contents Lists published in Analytical Abstracts, Biochemical Abstracts, Biological Abstracts, Chemical Abstracts, Chemical Titles, Chromatography Abstracts, Current Awareness in Biological Sciences (CABS), Current Contents/Life Sciences, Current Contents/Physical, Chemical & Earth Sciences, Deep-Sea Research/Part B: Oceanographic Literature Review, Excerpta Medica, Index Medicus, Mass Spectrometry Bulletin, PASCAL-CNRS, Referativnyi Zhurnal, Research Alert and Science Citation Index)

REGULAR PAPERS

Column Liquid Chromatography

Gas Chromatography

Electrophoresis

(Continued overleaf)

Contents (continued)

SHORT COMMUNICATIONS

BOOK REVIEW

JOURNAL OF CHROMATOGRAPHY A

VOL. 663 (1994)

JOURNAL OF CHROMATOGRAPHY A

INCLUDING ELECTROPHORESIS AND OTHER SEPARATION METHODS

ELSEVIER

AMSTERDAM — LONDON — NEW YORK — TOKYO

0021-9673/94/$07.00

Printed in the Netherlands

Journal of Chromatography A, 663 (1994) 1–10
Elsevier Science B.V., Amsterdam

CHROM. 25 708

Adsorption and ion-exchange isotherms in preparative chromatography

Ajoy Velayudhan[☆] and Csaba Horváth*

Department of Chemical Engineering, Yale University, New Haven, CT 06520-8286 (USA)

(First received July 5th, 1993; revised manuscript received November 1st, 1993)

ABSTRACT

A systematic characterization of ion-exchange and adsorption isotherms is presented. This treatment serves to emphasize the singular nature of monovalent ion-exchange and classical Langmuir isotherms, and describes the more general homovalent and heterovalent isotherms that are applicable to both ion-exchange and adsorption. Such formalisms are applied to adsorptive systems for the first time, and could prove to be useful additions to the canon of available isotherms. The shielding effect of macromolecular adsorbates on the binding of other macromolecules is discussed, and its parallel to the characteristic charge of a macromolecule is brought out. The application of the general adsorptive formalism to reversed-phase chromatography yields a relationship between the retention factor and the modifier concentration that, in two limiting cases, reduces to two well-known results. The first, which is characteristic of small molecules, gives a linear relationship between the logarithmic retention factor and a linear or quadratic term in the modifier. The second, which is characteristic of large molecules, gives a linear relationship between the logarithmic retention factor and the logarithm of the modifier concentration. The use of appropriate concentration units is shown to resolve certain apparently non-standard (non-Tiselian) displacement patterns. The measurement of characteristic charges by displacement described above could be an interesting complement to the more common elution method, and could provide further insight into the underlying physico-chemical phenomena.

INTRODUCTION

Preparative chromatography is of ever-increasing importance in the downstream processing of biotechnological products. Non-linear chromatography, in which the feed components are at high enough mobile phase concentrations to lie within the non-linear regions of their respective adsorption isotherms and thus interfere both with themselves and with each other, is an attractive approach to preparative and process-scale separation, in that the stationary phase is more efficiently utilized and the throughput is higher than in linear elution chromatography [1]. One of the key pieces of information needed in the design of preparative chromatographic separations is multicomponent adsorption isotherms. This paper attempts to characterize the isotherm formalisms used in adsorption and ion exchange, and to resolve certain anomalies found in the literature related to isotherm formalisms.

ION-EXCHANGE ISOTHERM FORMALISMS

The most common isotherm used in ion-exchange chromatography is based on the monovalent form of the mass-action formalism [2,3]. This can be represented for two feed components A and B by

$$A + S^* \rightleftharpoons A^* + S \quad (1)$$

and similarly for B. Here, asterisks denote the corresponding adsorbed species, and S is the salt

* Corresponding author.
☆ Present address: Laboratory of Renewable Resources Engineering, 1295 Potter Center, Purdue University, West Lafayette, IN 47907-1295, USA.

0021-9673/94/$07.00
SSDI 0021-9673(93)E1167-X

buffer counterion that maintains stationary phase electroneutrality and serves as the mobile phase modulator. For a species i, c_i is its mobile phase and q_i its stationary phase concentration. Electroneutrality then gives

$$q_S + q_A + q_B = \Lambda \tag{2}$$

where Λ is the total concentration of binding sites (fixed charges) on the ion exchanger. It can be seen that several assumptions have been made to arrive at this formalism. Activities have been replaced by concentrations; the binding process is assumed to be a stoichiometric exchange of counterions, *i.e.*, processes that involve the coions non-trivially, such as Donnan exclusion, are negligible. Further, the equilibrium constants, K_i, which are given by

$$K_i = \frac{q_i c_S}{c_i q_S}, \quad i = A, B \tag{3}$$

are assumed to be constant. Eq. 3 gives the familiar constancy of separation factors, S_{ij}:

$$S_{AB} = \frac{q_A c_B}{c_A q_B} = \frac{K_A}{K_B} \tag{4}$$

Eqns. 2 and 3 can be used to arrive at explicit expressions for the stationary phase concentrations:

$$q_i = \frac{\Lambda K_i c_i}{c_S + K_A c_A + K_B c_B}, \quad i = A, B \tag{5}$$

These results can be easily generalized to n feed components [4], for which

$$q_i = \frac{\Lambda K_i c_i}{c_S + \sum_j K_j c_j} \tag{6}$$

where the summation variable j runs over all the adsorbable components other than the buffer counterion (in this case, all the n feed components). The constancy of separation factors has the important consequence that the order of affinity of the components for the stationary phase, *i.e.*, the order of their selectivities, remains unchanged throughout the separation. Then column dynamics follow well-established trends [4,5]. As will be seen later, more complex isotherm formalisms can lead to non-constant selectivities, and thus the possibility of selectivity reversal in the composition range under consideration. This in turn leads to much more complex column dynamics, which have not yet been fully characterized.

A more general description, which will be called the "homovalent" formalism, applies when all the feed counterions involved have the same valence α, while the buffer is still monovalent. If the buffer is of the same valence as the feed components, the problem reduces to that of monovalent exchange, treated above. All other assumptions being the same as for the monovalent case, the binding process for homovalent exchange with a monovalent counterion, which could therefore be called ideal homovalent exchange, is represented by

$$A + \alpha S^* \rightleftharpoons A^* + \alpha S \tag{7}$$

and similarly for B. The appropriate electroneutrality condition is

$$q_S + \alpha q_A + \alpha q_B = \Lambda \tag{8}$$

and the equilibrium constants are given by

$$K_i = \frac{q_i (c_S)^\alpha}{c_i (\Lambda - \alpha q_A - \alpha q_B)^\alpha}, \quad i = A, B \tag{9}$$

It can be seen from eqn. 9 that the separation factor is still constant and equal to the ratio of the equilibrium constants. However, general explicit expressions are no longer available for the stationary phase concentrations, which have to be found numerically from eqns. 8 and 9. The constancy of separation factor implies that selectivity reversal will not occur, and that the standard theories of column dynamics will still apply (*e.g.*, ref. 5).

However, the most common situation in practice involves several adsorbable components with different valences. When large molecules such as proteins and other biopolymers are involved, the number of charges on their surfaces that interacts with the stationary phase is smaller than their net charges, because their surface charges are in general too widely distributed for all of the charges to interact with the stationary phase [6]. In these cases, the valence is replaced by the characteristic charge [7,8], which must in general

be determined by experiment at the conditions under which the separation is run.

The ion-exchange process involving species of difference valences (or characteristic charges) is described by a heterovalent mass-action formalism. With all other assumptions as before, a system of two feed components, A with a characteristic charge of α and B with a characteristic charge of β, is considered. The binding processes are given by

$$A + \alpha S^* \rightleftharpoons A^* + \alpha S \quad (10)$$

$$B + \beta S^* \rightleftharpoons B^* + \beta S \quad (11)$$

The electroneutrality condition becomes

$$q_S + \alpha q_A + \beta q_B = \Lambda \quad (12)$$

The equilibrium constant for A is

$$K_A = \frac{q_A (c_S)^\alpha}{c_A (\Lambda - \alpha q_A - \beta q_B)^\alpha} \quad (13)$$

and that for B is

$$K_B = \frac{q_B (c_S)^\beta}{c_B (\Lambda - \alpha q_A - \beta q_B)^\beta} \quad (14)$$

From eqns. 13 and 14, it can be seen that the separation factor is no longer constant: it varies with the concentrations of all the adsorbing components. This allows for the possibility of concentration-dependent selectivity reversal, where the affinity order of the components for the stationary phase changes as the mobile-phase concentrations are varied. When selectivity reversal occurs during a chromatographic separation, unusual concentration profiles can result [9–12]. For example, it becomes possible in isocratic elution for one component to completely envelop another. Standard theories no longer account for column dynamics, and numerical simulations of the chromatographic process are needed to predict column effluent profiles.

ADSORPTION ISOTHERM FORMALISMS

In the same way as was done above for ion exchange, isotherms for adsorption can be classified. The most common isotherm used in adsorption chromatography is the Langmuir isotherm, whose well-known multicomponent form is:

$$q_A = \frac{\Lambda_A K_A c_A}{(1 + K_A c_A + K_B c_B)} \quad (15)$$

The result above, for a binary feed mixture, is shown for comparison with the earlier ion-exchange results. This form assumes that each adsorbate molecule interacts with a single binding site on the stationary phase, and is thus in a sense equivalent to the monovalent ion-exchange process. In fact, Helfferich and Klein [4] have shown that the multicomponent Langmuir isotherms are in a sense equivalent to, and can be converted into, monovalent ion-exchange isotherms by the addition of a "dummy" component. As would be expected, the separation factor is constant, precluding selectivity reversal, and consequently detailed theories of column dynamics are available [4,5]. It is also well known that the multicomponent Langmuir form is thermodynamically consistent only when the saturation concentrations of all the adsorbates is equal [13,14]. The Langmuir description is in fact better suited to, and was originally derived [15] for, the description of gas adsorption, where fixed adsorption sites and a non-adsorbing carrier gas are more realistic. Nevertheless, multicomponent Langmuir adsorption is still the most widely used isotherm for non-linear liquid chromatography studies.

It is intriguing to view the binding sites in ion exchange as analogous to hydrophobic patches on the stationary phase available for binding in liquid adsorption; then the analogue to the characteristic charge in ion exchange is a "binding area" for each adsorbate in adsorption.

In the light of the above parallel between the monovalent ion-exchange isotherms and the Langmuir isotherms, we wish to examine whether analogues of the homovalent and heterovalent ion-exchange forms exist for adsorptive systems. Such generalizations can easily be formulated, as shown below.

The "adsorptive-homovalent," or "homosorptive," formalism would involve each feed component occupying α sites on binding; the adsorption equilibria would then take the form

$$A + \alpha I \rightleftharpoons A^* \quad (16)$$

and similarly for B, where I is a single binding site on the stationary phase. The equilibrium constants are given by

$$K_i = \frac{q_i}{c_i(\Lambda - \alpha q_A - \alpha q_B)^\alpha}, \quad i = A, B \quad (17)$$

where Λ is the total concentration of binding sites available. The similarity between eqns. 9 and 17 is striking, the only difference being the term involving the buffer counterion in the numerator of eqn. 9. Again, it can be seen that the separation factor is constant, as for the ion-exchange equations, and selectivity reversal will not occur. Similarly, no explicit expression is in general available for the stationary phase concentrations in the adsorptive-homovalent formalism.

The more general case is that of adsorbates with different binding areas or, in terms of the Langmuir adsorption formalism, that occupy different numbers of binding sites. This is analogous to the heterovalent version of the ion-exchange process. The formal representation of the "adsorptive-heterovalent," or "heterosorptive," binding equilibria are therefore

$$A + \alpha I \rightleftharpoons A^* \quad (18)$$

$$B + \beta I \rightleftharpoons B^* \quad (19)$$

The distribution coefficients are given by

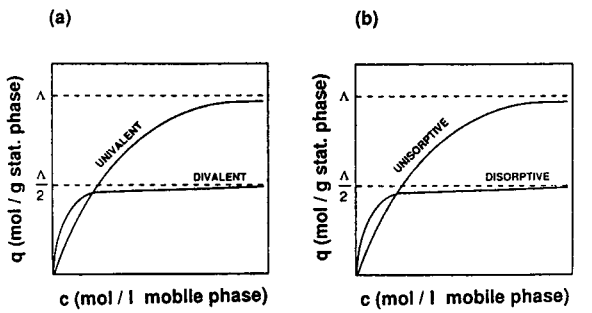

Fig. 1. The similarity between ion-exchange and adsorption isotherm formalisms. (a) Single-component isotherms for an univalent and a divalent adsorbate; (b) analogous case for heterosorptive single component isotherms, for species with binding areas of 1 and 2.

$$K_A = \frac{q_A}{c_A(\Lambda - \alpha q_A - \beta q_B)^\alpha} \quad (20)$$

and similarly for B; note the analogy to eqns. 13 and 14. Again, eqns. 13 and 20 are identical except for the modulator concentration term in the numerator of eqn. 13. The separation factors are not constant, and selectivity reversal becomes possible. As before, no explicit form for the stationary phase concentrations is available, and the single-component isotherms cross, as seen in Fig. 1.

GENERAL FEATURES OF THE ISOTHERMS

The extension of the homovalent and heterovalent binding models from ion-exchange to adsorption processes can be viewed as a generalization of the classical Langmuir formalism. In this context, it could be interesting to examine the special case of a single component A. For both the homo- and heterosorptive cases, the equilibrium distribution can be expressed as:

$$K_A = \frac{q_A}{c_A(\Lambda - \alpha q_A)^\alpha} \quad (21)$$

This expression can be recast as

$$q_A = K_A c_A(\Lambda - \alpha q_A)^\alpha = K_A c_A \Lambda^\alpha \left(1 - \frac{\alpha q_A}{\Lambda}\right)^\alpha \quad (22)$$

For relatively small q_A, the last term in brackets in eqn. 22 can be expanded as a binomial series, since this term is always non-negative. Keeping only the linear term gives a Langmuirian form:

$$q_A = \frac{K_A \Lambda^\alpha c_A}{1 + K_A \Lambda^{\alpha-1} c_A} \quad (23)$$

Including the second-order term gives a quadratic algebraic equation for q_A. The result is

$$\frac{\alpha q_A}{\Lambda} = \frac{(\alpha\psi - 1) + \sqrt{(1 - \alpha\psi)^2 - 2\alpha(\alpha - 1)\psi^2}}{\alpha(\alpha - 1)\psi} \quad (24)$$

where

$$\psi = \alpha K \Lambda^{\alpha-1} c_A \quad (25)$$

A similar quadratic form can be obtained for the mass-action heterovalent ion-exchange formalism. In all cases, these approximate explicit forms will be monotonic and concave-down, like their parent isotherms.

The perturbative approximation above was only carried out for a single component, in order to avoid algebraic complexity. The generalization could be carried out to multicomponent systems with the aid of a symbolic calculation (or computer algebra) program such as Maple or Mathematica. The potential use for such approximations to the original isotherm is in computer simulations, which are widely used to model preparative chromatographic separations (*e.g.*, ref. 16). While it is easy enough to solve the original equations (a system of equations like eqn. 20) numerically on a computer, this step, of finding the stationary phase composition in equilibrium with a particular mobile phase composition, could occur several times in the calculation of the actual compositions at a given point in the column at a given time. When the number of discrete points in both space and time used in an accurate numerical program is considered, it is clear that the equilibrium calculation could prove to consume an appreciable fraction of the overall computing time. Thus explicit isotherm forms, such as those in eqns. 23 and 24, could prove valuable, in spite of their approximate nature.

However, one caveat must be emphasized: the approximate forms may not exhibit selectivity reversal in the same composition range as their original exact forms do. For instance, the approximation given by eqn. 22 is Langmuirian, even though the original isotherm was heterovalent. If the first-order approximations to the corresponding multicomponent isotherms were also Langmuirian, they could only be used in a composition range where the original exact isotherm did not exhibit selectivity reversal. Thus only those approximate explicit isotherms that exhibit similar selectivity-reversal behavior to the original exact isotherm in the composition range of interest can safely be used.

The characteristics of the various isotherms described above are summarized in Table I. The close analogy between the ion-exchange and adsorptive forms of the mono-, homo- and heterovalent formalisms is evident. All these isotherms are concave-down and monotonic, and their slopes obey the relations

$$\frac{\partial q_i}{\partial c_i} > 0\,; \quad \frac{\partial q_i}{\partial c_j} < 0\,, \quad i \neq j \tag{26}$$

These are the standard conditions for competitive binding [5], and imply that, if selectivity reversal does not occur in the range of compositions encountered during a separation, column effluent profiles that are qualitatively similar to those calculated for the monovalent ion-exchange and classical Langmuir formalisms [5,9] will result.

TABLE I

CHARACTERISTIC FEATURES OF VARIOUS ISOTHERM FORMALISMS IN ION EXCHANGE (IEX) AND ADSORPTION (ADS)

AV = Always valid; NV = never valid; E = explicit; I = implicit, NP = not possible; P = possible.

Features	Monovalent		Homovalent		Heterovalent	
	IEX	ADS	IEX	ADS	IEX	ADS
Constancy of separation factors	AV	AV	AV	AV	NV	NV
Expression for stationary phase concentration	E	E	I	I	I	I
Selectivity reversal	NP	NP	NP	NP	P	P

In both the monovalent and the homovalent cases, the single-component isotherms will not cross, regardless of the units in which the concentrations are expressed (molarity, molality, equivalents, etc.) However, the heterovalent isotherms will, in general, cross, as has been shown [8]. We briefly repeat the argument here for completeness. Consider a monovalent adsorbate A and a divalent adsorbate B. If an adsorbent with Λ binding sites (in molar units, *e.g.*, moles of binding sites per unit area of stationary phase) is being used, the saturation concentration of A would be Λ M if it were the only adsorbable counterion. Under the same conditions, the saturation concentration of B would be $\Lambda/2$ M. Thus B would have a lower saturation concentration than A, but it would have the higher initial isotherm slope, reflecting its higher affinity for the adsorbent. The single-component isotherms of A and B would therefore cross, as seen in Fig. 1.

As mentioned earlier, Helfferich and Klein [4] have pointed out how the Langmuirian formalism (which we have called above monosorptive) can be converted into a monovalent ion exchange formalism by the inclusion of a dummy component, whose stationary phase concentration varied so as to keep the sum of all stationary phase concentrations constant, in analogy to an electroneutrality condition. The present work has described the forms of the homosorptive and heterosorptive generalizations of the Langmuir (monosorptive) isotherm. It remains an intriguing possibility to attempt to convert these formalisms into equivalent homo- and heterovalent ion-exchange (mass-action) formalisms by an analogous application of the method of Helfferich and Klein.

IMPLICATIONS FOR REVERSED-PHASE CHROMATOGRAPHY

Another interesting parallel between the ion exchange and adsorptive formalisms arises in the context of reversed-phase chromatography. It is well-known that, in ion exchange, the logarithmic retention factor varies linearly with the logarithm of the salt concentration in the mobile phase [2,7,8] when the adsorbate concentration is low enough to ensure that its adsorption is linear. Here we derive analogous expressions for the adsorption isotherm formalisms.

Consider an organic modifier S with unit adsorptive binding area, and an adsorbate A with binding area α. The equilibrium relations are

$$K_A = \frac{q_A}{c_A(\Lambda - \alpha q_A - q_S)^\alpha} \tag{27}$$

$$K_S = \frac{q_S}{c_S(\Lambda - \alpha q_A - q_S)} \tag{28}$$

from which follows

$$\left(\frac{q_A}{K_A c_A}\right)^{1/\alpha} = \left(\frac{q_S}{K_S c_S}\right) \tag{29}$$

Substituting eqn. 29 into eqn. 27 and neglecting αq_A with respect to Λ under the restriction of linear adsorption on A, we get

$$\left[\Lambda - K_S c_S \left(\frac{q_A}{K_A c_A}\right)^{1/\alpha}\right]^\alpha = \frac{q_A}{K_A c_A} \tag{30}$$

Let the distribution coefficient D_A represent q_A/c_A. Then

$$\Lambda - K_S c_S \left(\frac{D_A}{K_A}\right)^{1/\alpha} = \left(\frac{D_A}{K_A}\right)^{1/\alpha} \tag{31}$$

$$\frac{1}{\alpha} \ln D_A - \frac{1}{\alpha} \ln K_A = \ln \Lambda - \ln(1 + K_S c_S) \tag{32}$$

$$\ln D_A = \ln(K_A \Lambda^\alpha) - \alpha \ln(1 + K_S c_S) \tag{33}$$

When the product $K_S c_S$ is small with respect to unity, the last term in eqn. 33 can be simplified by using the usual approximation for the logarithm:

$$\ln(1 + x) \approx x - \frac{x^2}{2} \tag{34}$$

which gives

$$\ln D_A = \ln(K_A \Lambda^\alpha) - \alpha K_S c_S + \alpha \cdot \frac{K_S^2}{2} \cdot c_S^2$$

$$= K_1 - K_2 c_S + K_3 c_S^2 \tag{35}$$

where K_1, K_2, K_3 are constants. This is the usual expression for the dependence of adsorbate retention factor on organic modifier concentration in reversed-phase chromatography. It is

interesting that a formalism that is based solely on adsorbate interactions with the stationary phase can generate this result, since most reversed-phase retention theories are based on the interaction of adsorbates with the mobile phase [17–21]. However, it must be emphasized that the deviation above is limited to organic modifiers of unit binding area. (The binding area of the modulator can be regarded as the basic unit of interaction with the stationary phase, since it is unlikely that any feed component will be smaller than the modulator.) The calculation does not carry through in the general case, where the binding area of the modulator is arbitrary.

On the other hand, when the product $K_S c_S$ is large with respect to unity, the last term on the right-hand side of eqn. 33 can be simply replaced by the logarithm of $K_S c_S$; this leads to a linear relationship between the logarithmic retention factor and the logarithm of the modulator concentration:

$$\ln D_A = \ln(K_A \Lambda^\alpha K_S^\alpha) - \alpha \ln c_S \quad (36)$$

An analogous result has been reported by Geng and Regnier [22,23] based on a "displacement" model, in which the stationary phase is effectively considered to be saturated at all times, and adsorption of one species is necessarily accompanied by the desorption of another. Thus, Geng and Regnier's model is essentially the mass-action or ion-exchange formalism discussed earlier. Here we have shown that an adsorptive model, in which saturation of the stationary phase is not required, can also yield the usual log–log relationship as one limiting case, as seen in eqn. 36. Further, the other limiting case gives the "semilog" relation commonly used for small adsorbates (eqn. 35), and further provides a basis for the quadratic term in c_S that is frequently found necessary to describe experiments [19,24].

The two limiting cases described above can be physically motivated as follows. Prior to the introduction of feed components, the stationary phase can be regarded as saturated by the mobile phase components, *e.g.*, water and the modulator (here, an organic modifier). However, it cannot be concluded that the stationary phase is essentially covered by the modifier alone. In many cases of practical interest [25–27] the excess isotherm exhibits an adsorption azeotrope. If it is then assumed that the modifier alone adsorbs, the resultant individual isotherm for the modifier has a local maximum, which is physically unreasonable. It is therefore necessary to assume that the water also adsorbs. In fact, acetonitrile and water have been found to adsorb to comparable amounts over a wide range of mobile phase composition on octadecyl silica [25,26].

Given that both the modifier and the water adsorb, eqn. 35 can be regarded as corresponding to the region where the adsorption of a feed component is not necessarily accompanied by the desorption of the modifier. Instead, the feed can easily displace adsorbed water molecules. The other limiting condition corresponds to the region in which the only mobile phase component that is adsorbed to any appreciable extent is the modifier, and the adsorption of a feed component now results in the desorption of the modifier. The displacement model, eqn. 36, then results.

SHIELDING OF BINDING SITES BY MACROMOLECULAR ADSORBATES

All the isotherm formalisms described above are based on the assumption that all the adsorbates are able to access all the available binding sites on the stationary phase, *e.g.*, that a protein of characteristic charge α will adsorb on to an ion exchanger of binding site concentration Λ, and in the absence of other counterions, have a stationary phase (saturation) concentration of Λ/α. However, this excludes the possibility of shielding and exclusion, whereby the size of the protein makes a certain number of fixed charges on the stationary phase unavailable for binding by a molecule of comparable size. Thus, let the number of such excluded (occluded) binding sites associated with the protein A be ε_A; then the number of sites unavailable for binding after a single molecule of A has adsorbed is $(\alpha + \varepsilon_A)$, and the saturation concentration is decreased to $\Lambda/(\alpha + \varepsilon_A)$. Of course, electroneutrality requires that all the sites on the stationary phase be

bound, and thus ε_A molecules of salt (buffer or modulator) must adsorb to the ε_A binding sites occluded by molecule of A. The adsorption of large molecules on, say, reversed-phase sorbents, can be similarly generalized from the adsorptive formalisms presented earlier. Again, an excluded binding area, which we will also represent by ε_A, is associated with the binding of a protein A with binding area α. Such a shielding or screening effect was proposed by Velayudhan [28], and has been expanded upon by Cramer and co-workers [29,30].

One important consequence of this generalized formalism is that it is no longer necessary for single-component isotherms to cross. Consider a protein A with characteristic charge 6 and occluded charge 3, which is found to be more retentive in analytical runs than another protein B with characteristic charge 5 and occluded charge 5. The effective saturation concentration of A is $\Lambda/9$, while that of B is $\Lambda/10$. In this example, the single-component isotherms need not cross.

Implications for displacement chromatography

As we have pointed out in the previous section, all the isotherms discussed above should give "normal" separation profiles as long as selectivity reversal (for the heterovalent formalisms only) does not occur during the separation. Thus, in displacement, a final pattern of contiguous rectangular bands of pure feed components should result on using a sufficiently long column. This is the classical Tiselian description of displacement [31], and is based upon monotonic, concave-down, non-crossing single-component isotherms for all the feed components as well as the displacer. Since these isotherms do not cross, there is a natural retention order of the feed components; by excluding selectivity reversal, this order is maintained throughout the separation. The displacer's single-component isotherm must overlie all of the others, so that it is the most-strongly retained component, and its front can displace the bands of all the other components, eventually forming a displacement train (final pattern). The concentrations of the bands in the final pattern increase monotonically in increasing order of retention, with the displacer's concentration being the highest.

However, it has sometimes been found that displacement trains are formed even though the single-component isotherms cross, and that the concentrations in the final pattern do not form a monotonic sequence. We seek to clarify these results based on the previous discussion on isotherms. This is clearly a heterovalent case, since the single-component isotherms cross. However, if the concentrations were replaced by equivalents —this would involve scaling by the valence or characteristic charge in ion exchange, and by the binding area in adsorption— the single-component isotherms would no longer cross, since they would all have the same saturation concentrations. In effect, we have converted heterovalent isotherms into monovalent isotherms by using equivalents. The same conversion is obviously also applicable to homovalent systems.

In the example given above, the saturation levels of both A and B would be Λ equivalents, and the single-component isotherms no longer cross. Further, consider a displacement of A and B in which a final pattern of fully resolved bands of A and B are formed, but the concentration of A —which emerges first— is higher than that of the later-eluting band of B. If the concentrations in the displacement train were replaced by equivalents, the equivalents of B would be twice its concentration, while the numerical value of A in equivalents would be identical to that in concentration units. Thus the non-monotonicity of concentrations in the final pattern could well be removed. Fig. 2 shows a schematic of such a displacement, using a trivalent displacer. This situation, in which heterovalent ion exchange in the absence of selectivity reversal gives rise to apparently non-Tiselian behavior, is apparently quite widespread. The remedy of using equivalents, while standard in classical ion-exchange batch studies [3], does not seem to have been widely used, to the best of our knowledge, for heterovalent systems in column chromatography.

It must be emphasized that the suggestion offered here is purely formal: it does not in any way affect the dynamics of separation. For instance, if selectivity reversal is observed ex-

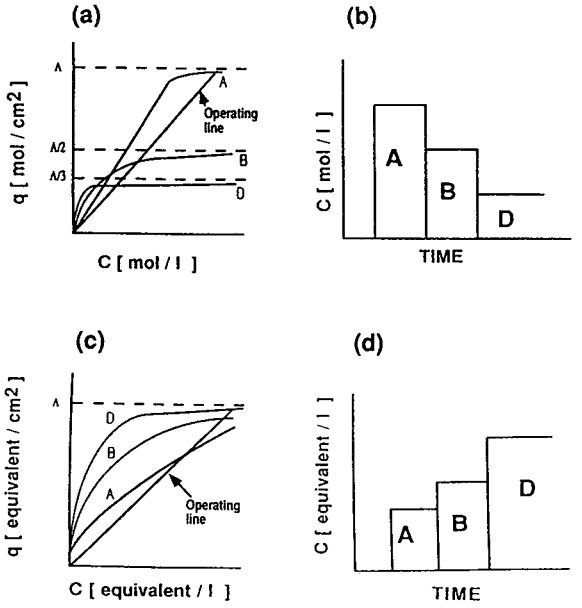

Fig. 2. Representation of single-component isotherms and consequences for final patterns in displacement. (a) Crossing single-component isotherms for two feed components and the displacer; here shielding effects are not considered; (b) the resulting displacement chromatogram; (c) the isotherms in (a) redrawn in terms of equivalents; now the single-component isotherms no longer cross, since they all have the same saturation level in equivalents; (d) the final pattern in (b) redrawn in terms of equivalents. The normal Tiselian final pattern is shown. C = mobile phase concentration; q = stationary phase concentration.

perimentally, changing concentrations into equivalents will not alter the non-Tiselian behavior found in practice. The present suggestion is merely intended to add a modicum of conceptual clarity to the understanding of systems that might be regarded theoretically as non-Tiselian, but do in fact give fully resolved displacement trains (as opposed to systems where selectivity reversal is encountered during the separation, and fully resolved component bands are not in general formed). The result might be summarized thus: in the absence of selectivity reversal, ion-exchange and adsorptive systems exhibiting crossing single-component isotherms can give fully resolved displacement trains. In these situations, using equivalents rather than concentrations will clarify why such results are obtained, and reduce them to classical Tiselian patterns.

CONCLUSIONS

The preceding discussion assumes that the heterovalent ion-exchange (ideal mass-action) formalism is applicable, *i.e.*, that stationary and mobile phase activities can be replaced by their respective concentrations, and that mechanisms other than pure mass-action, such as Donnan equilibrium, can be neglected. While certainly being far from the truth [32], the ideal mass-action formalism is still widely used to approximate chromatographic behavior in the ion-exchange mode for a large class of realistic operating conditions.

The use of valences is essential to converting concentrations to equivalents. However, the equivalent for proteins and other macromolecules, the "characteristic charge," [7,32] is by no means as well-defined a concept. In fact, the characteristic charge is unlikely to be solely a function of the adsorbate, even when the environmental conditions such as temperature and pH are fixed: it could well vary with the adsorbent. For example, the characteristic charge of a protein is likely to be low on an adsorbent with a very low density of fixed charges, since there are not too many fixed charges available within a protein diameter. If another adsorbent with a higher density of fixed charges were used, all other conditions remaining the same, it is likely that the measured characteristic charge of the protein would increase. The characteristic charge could also vary with loading. In addition, the charge carried by the ionogenic groups of the protein can depend on the dielectric of the local microenvironment as well as on the electrostatic field generated by the fixed charges. These points merely emphasize the need for more fundamental studies on protein adsorption. Nevertheless, the use of characteristic charges measured at the conditions under which the displacement separation is to be run should prove adequate to remove the kind of anomaly described above.

In turn, fully resolved displacement trains could be used to measure characteristic charges in the absence of selectivity reversal, as long as the characteristic charge or valence for one component is known. It would be interesting to

see how the characteristic charges measured from displacement runs compare with those measured in the standard fashion from analytical elution experiments (as the slope of a log–log plot of retention factor *versus* the salt concentration in the mobile phase [7], or from a plot of the logarithmic retention factor against the reciprocal square root of the ionic strength [32]).

ACKNOWLEDGEMENTS

This work was supported by grants No. GM20993 from the National Institutes of Health, US Public Health Service, and No. BCS-9014119 from the National Science Foundation.

REFERENCES

1 A.L. Lee, A. Velayudhan and Cs. Horváth, in G. Durant, L. Bobichon and J. Florent (Editors), *Proceedings of the 8th International Biotechnology Symposium*, Vol. 1, Société Francaise de Microbiologie, Paris, 1988, pp. 593–611.
2 N.K. Boardman and S.M. Partridge, *Biochem. J.*, 59 (1955) 543.
3 F. Helfferich, *Ion Exchange*, McGraw-Hill, New York, 1962.
4 F. Helfferich and G. Klein, *Multicomponent Chromatography*, Marcel Dekker, New York, 1970.
5 H.-K. Rhee, R. Aris and N.R. Amundson, *Phil. Trans. Roy. Soc. (London)*, 267 (1970) 419.
6 H.P. Jennissen, *Biochemistry*, 15 (1976) 5683.
7 W. Kopaciewicz, M.A. Rounds, J. Fausnaugh and F.E. Regnier, *J. Chromatogr.*, 266 (1983) 3.
8 A. Velayudhan and Cs. Horváth, *J. Chromatogr.*, 443 (1988) 13.
9 E. Glückauf, *Disc. Faraday Soc.*, 7 (1949) 12.
10 A.L. Lee, *Ph.D. Dissertation*, Yale University, New Haven, CT, 1990.
11 A. Velayudhan, A.L. Lee and Cs. Horváth, in preparation.
12 F. Antia and Cs. Horváth, *J. Chromatogr.*, 550 (1991) 411.
13 J.B. Butler and C. Ockrent, *J. Phys. Chem.*, 34 (1930) 2841.
14 D.B. Broughton, *Ind. Eng. Chem.*, 40 (1948) 1506.
15 I. Langmuir, *J. Chem. Soc.*, 40 (1918) 1361.
16 M.Z. El Fallah and G. Guiochon, *Biotechnol. Bioeng.*, 39 (1992) 877.
17 Cs. Horváth, W. Melander and I. Molnár, *J. Chromatogr.*, 125 (1976) 129.
18 A. Nahum and Cs. Horváth, *J. Chromatogr.*, 203 (1981) 53.
19 P. Jandera and J. Churáček, *Gradient Elution in Column Liquid Chromatography—Theory and Practice*, Elsevier, Amsterdam, 1985.
20 N. Chen, Y. Zhang and P. Lu, *J. Chromatogr.*, 633 (1993) 31.
21 N. Chen, Y. Zhang and P. Lu, *J. Chromatogr.*, 603 (1992) 35.
22 X. Geng and F.E. Regnier, *J. Chromatogr.*, 296 (1984) 15.
23 X. Geng and F.E. Regnier, *J. Chromatogr.*, 332 (1985) 147.
24 L.R. Snyder and M.A. Stadalius, in Cs. Horváth (Editor), *High-Performance Liquid Chromatography—Advances and Perspectives*, Academic Press, New York, Vol. 4, 1986, p. 195.
25 E.H. Slaats, W. Markovski, J. Fekete and H. Poppe, *J. Chromatogr.*, 207 (1981) 299.
26 K. Tani and Y. Suzuki, *J. Chromatogr. Sci.*, 27 (1989) 698.
27 C.S. Koch, F. Köster and G.H. Findenegg, *J. Chromatogr.*, 406 (1987) 257.
28 A. Velayudhan, *Ph.D. Dissertation*, Yale University, New Haven, CT, 1990.
29 C.A. Brooks and S.M. Cramer, *AIChE J.*, 38 (1992) 1969.
30 J.A. Gerstner and S.M. Cramer, *Biotechnol. Prog.*, 8 (1992) 540.
31 A. Tiselius, *Ark. Kemi Mineral. Geol.*, 16A (18) (1943) 1.
32 J. Ståhlberg, B. Jönsson and Cs. Horváth, *Anal. Chem.*, 63 (1991) 1867.

ELSEVIER

Journal of Chromatography A, 663 (1994) 11–26

JOURNAL OF CHROMATOGRAPHY A

Group-type separation of middle petroleum distillates by adsorption and charge-transfer liquid chromatography with dielectric constant detection

Lante Carbognani

INTEVEP, S.A., P.O. Box 76343, Caracas 1070A, Venezuela

(First received June 7th, 1993; revised manuscript received November 3rd, 1993)

Abstract

A fast (<15 min) LC method was developed for the group-type separation of low olefinic (<5%, v/v) petroleum middle distillates. Dinitroanilinopropyl- and underivatized silica columns were used with Freon 123 as mobile phase and dielectric constant detection. Aliphatic hydrocarbons and mono-, di- and triaromatics were the determined group types. A response factor of 1.12 to correct the total aromatic content by volume was found. Some applications are described, including fingerprinting of refinery cuts and monitoring of upgrading processes.

1. Introduction

The predicted worldwide increase in the use of Diesel fuel during the last decade [1] has forced refiners to introduce higher levels of cracked components into these energy sources [2]. High aromatic contents in such blends were of concern from the pollution [2,3], performance [2] and health [4] standpoints.

The aromatic content of middle distillates was traditionally measured by using techniques such as fluorescent indicator adsorption [5], aniline point [6], mass spectrometry (MS) [7,8] and high-performance liquid chromatography (HPLC) [9–12]. However, the poor accuracy of the first two techniques suggested the adoption of better methodologies. This was especially noticeable with coloured samples when analysed by fluorescent indicator adsorption and naphthenic samples evaluated with the aniline point method. Further, the high analytical skills required in MS methodologies, their inherent inapplicability to olefinic cuts and the wide range of response factors of HPLC with refractive index (RI) detection make the routine use of these methods difficult.

In addition to the above methods, many approaches have been described for group-type analysis of light and middle distillates. UV spectrophotometry has been used for the determination of naphthalenes [13]. Fourier transform infrared (FT-IR) spectrometry gave correlations between Diesel composition and particulate emissions [14]. Gas chromatography (GC) with polar stationary phases has been proposed for the determination of aromatics in non-olefinic kerosenes [15]. Nuclear magnetic resonance (NMR) spectrometry has been proposed for the determination of aromatics content [3,16–18]. The advantage of using a universal detection

0021-9673/94/$07.00
SSDI 0021-9673(93)E1174-X

system such as flame ionization detection (FID) has been exploited by coupling LC and GC instruments. This has proved effective for virgin and low-olefin content kerosenes [19,20]. Likewise, FID has commonly been used in supercritical fluid chromatography (SFC)-based methodologies [21–23]. ASTM has approved a method for aromatics determination based on these techniques [24]. Chemical methods have been similarly explored, some of them directed at olefin compounds, such as hydroboration [25] and complex formation with the stationary phase [26].

Complexation with the stationary phase has received particular attention for more than a decade in the case of derivatized packing materials. Many phases for LC have been synthesized that are specially suited for aromatic complexation, according to the number of π-electrons and/or number of conjugate aromatic rings present in the molecules. Some reviews [27,28] and a recent monograph [29] have been published on this topic. Owing to the strong absorbing nature of chromophores with aromatic structures, most of the work described has relied on UV detection. This posed a quantification problem as absorptivities vary greatly between aromatics. To solve this problem, some workers have used UV spectrophotometry for qualitative purposes and the quantification was then performed gravimetrically [30,31]. Information-rich detection systems have been used simultaneously for identification in some instances, such as an on-line UV diode-array detector and of-line MS [31]. Also, LC–FID with detectors developed for LC has been described [32]. However, all of these approaches are well suited only for heavier distillates, as removal of solvents generally causes sample losses with lighter materials, such as petroleum middle distillates.

A dielectric constant detector for LC was introduced commercially over a decade ago [33]. This detector operates like a universal detection system for hydrocarbons if the dielectric constant of the mobile phase used is greater than 5, as was shown by Hayes and Anderson [34]. Many applications were described by these workers. With a combination of a tetranitrofluoreneimino-derivatized silica (TENF) column (charge-transfer) and aminocyanosilicas (adsorption), it was possible to determine aliphatic and alkylbenzene polycyclic aromatics [34]. *n*-Butyl chloride was chosen as the mobile phase, requiring small response factors for quantitative analysis. By adoption of Freon 123 as the mobile phase, quantification was simplified, as a response of unity was appropriate for different hydrocarbon groups. With this solvent and several cationic columns loaded with silver, it was possible to determine saturated compounds, aromatics and olefins [35], or *n* + isoparaffins and cycloparaffins and aromatics + olefins [36]. Naphthenic selective columns [37] were added in the last example to separate the cycloparaffins. PONA (paraffins, olefins, naphthenes and aromatics)-type analysis was also achieved with a multidimensional system employing five columns and two selection valves [38]. Preparative separations have also been described [39,40] and many of the possibilities have been discussed in a review [41].

This paper describes a fast and simple LC method used for routine monitoring of hydrocarbon groups during the upgrading of middle petroleum distillates. Charge-transfer (dinitroanilinopropylsilica) together with adsorption columns (underivatized silica) were used with Freon 123 as the mobile phase and dielectric constant detection. The groups determined were aliphatic hydrocarbons and mono-, di- and triaromatics. Small response factors were required for quantitative volumetric analysis. Comparison with MS permitted the applicability of the methodology exclusively for atmospheric cuts to be assessed. No interferences were detected from bicycloparaffins, compounds typically present in hydrotreated products. Olefin-rich samples, such as thermal cracked gasoils, cannot be analysed owing to interference from such hydrocarbon types.

2. Experimental

2.1. Reagents and solvents

Standard compounds were obtained from Aldrich (Milwaukee, WI, USA) or Chem-Service

(West Chester, PA, USA). Solvents were purchased from Burdick and Jackson (Muskegon, MI, USA) or Fisher (Pittsburgh, PA, USA). Reagents and solvents were used as received.

Envron 123 (1,1,1 - trifluoro - 2,2 - dichloroethane) from Halocarbon Products (North Augusta, SC, USA) was used as the HPLC mobile phase. The solvent was commonly reused and was purified monthly by percolation through a bed of basic alumina. Halogen acids and heavy aromatics and polar compounds were removed in this way. Additionally, every 6 months, hydrocarbon stripping was achieved by distillation under a dry atmosphere.

2.2. HPLC system

The HPLC system is shown in Fig. 1. The main components were a glass pressurized solvent reservoir from Altex (Berkeley, CA, USA) (2), a model LC-3A HPLC pump from Shimadzu (Columbia, MD, USA) (6), a six-port injection valve from Valco (Houston, TX, USA), furnished with a 5-μl sampling loop (7), an HPLC column bank (8), a Model 410 dielectric constant detector from Laitec (Bartlesville, OK, USA) (10), a chart recorder (from Linear or Kipp & Zonen) (15) and an A/D interface for data acquisition, analysis and storage in an HP-3350S laboratory automation system.

2.3. Chromatographic conditions

HPLC was performed at room temperature (*ca.* 24°C). The mobile phase was pumped at 1.5 ml/min and 90–100 bar when using four columns (total length 85 cm). Slight pressure variations were observed, depending on the setting of the sample cell restrictor. The detector was usually operated at a sensitivity of 2. To avoid bubbling in the pump head and also to maintain a flow-rate of *ca.* 0.3 ml/min in the reference cell, the solvent was pressurized with nitrogen at 40 p.s.i. (1 p.s.i. = 6894.76 Pa).

2.4. Columns

The column bank was assembled with one 25 cm × 4 mm I.D. 2,4-dinitroanilinopropylsilica (DNAP) column and two or three 60 cm × 4 mm I.D. silica columns. Preliminary experiments were carried out with two 30-cm silica columns. Most of the experiments described were performed with two 25-cm plus one 10-cm column. The DNAP stationary phase was supplied by Dr. J.B. Green [National Institute for Petroleum and Energy Research (Niper), Bartlesville, OK, USA] and has been described previously [42,43]. Underivatized silica gel was obtained from Alltech Associates (Deerfield, IL, USA) and consisted of 10-μm irregular Adsorbosil-LC. The

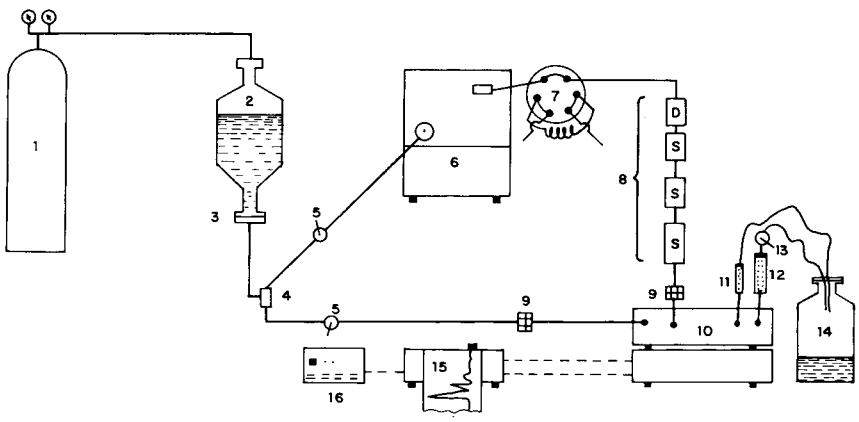

Fig. 1. Schematic diagram of HPLC system. 1 = Nitrogen cylinder; 2 = solvent reservoir; 3 = line filters (20 μm); 4 = tee; 5 = PTFE on–off valves; 6 = HPLC pump; 7 = injection valve; 8 = column bank; 9 = line filters (2 μm); 10 = detector; 11 = reference cell restrictor; 12 = sample cell restrictor; 13 = metering valve; 14 = effluent receiver; 15 = chart recorder; 16 = A/D interface; D = dinitroanilinopropylsilica column; S = underivatized silica columns.

columns were packed in-house with a Haskel (Burbank, CA, USA) pneumatic high-pressure pump. Carbontetrachloride was used for slurry preparation and pentane was employed as a driving solvent (10 000 p.s.i.).

2.5. Standard mixtures prepared from real samples

Aliphatic and aromatic fractions were preparatively separated in a silica column (60 cm × 1.5 cm I.D.) packed with 32–63-μm Woelm Pharma SiO_2 (ICN, Cleveland, OH, USA). Pentane was used as the mobile phase. Simultaneous UV (254 nm) and refractive index (RI) detection were used. A 0.5-g amount was loaded in each injection and the fractions from six successive separations were pooled.

Saturated compounds and olefins were also preparatively separated from the aliphatic fraction of thermal cracked medium distillates. A 21 cm × 1.5 cm I.D. column packed with SiO_2–$AgNO_3$ (80:20, w/w) was used. Saturated compounds were eluted with pentane and detected by differential RI detection. Olefins were then back-flushed with *n*-pentane–dichloromethane (30:70, v/v) and the column was regenerated with pentane. The sample load was 180 μl in each separation. Argentation chromatography of olefins has been described previously [26].

The preparative fractions were finally obtained by solvent stripping using Kuderna–Danish-type evaporators. The recoveries were 100 ± 3%. Solvent absence was confirmed by GC. Standard mixtures were obtained by mixing precisely measured amounts of preparative fractions. Straight-run, catalytically and thermal cracked and also hydrotreated and solvent-extracted middle distillates from Petróleos de Venezuela (PDVSA) refineries were employed for standards formulation. The samples originated from PDVSA refineries at Cardón, Amuay and El Palito.

2.6. Mass spectrometry

Mass spectrometric analyses were performed at the Analysis and Evaluation Department in INTEVEP. Group-type results were obtained according to the Robinson methodology [8] and/or the ASTM standard [44] if very volatile materials were present in the samples.

3. Results and discussion

Pollution and health hazards have forced the adoption of specifications regarding the aromatic content of middle distillates. Until now, in our laboratories the common way to measure this parameter was based on MS [7,8,44] and HPLC techniques [11]. Probably, in the near future, SFC techniques [24] will also be adopted.

MS has proved to be a reliable technique for non-olefinic distillates. However, it is a highly demanding technique for routine process monitoring. On the other hand, HPLC with RI detection and response factors [11] is a fast and simple procedure used in our laboratories for group-type quantitative analyses of virgin distillates. Nevertheless, process monitoring has been hampered by the fact that unpredictable refractive indices are obtained under widely diverse test conditions. In such circumstances, quantification is not accurate (Table 1).

Table 1
Determination of aromatics in processed matrices

Sample	Aromatics (%, w/w)	
	Known[a]	HPLC–RI[b]
Thermal cracked gasoil	40.0	51.5
Catalytically cracked gasoil	50.0	60.9
Hydrotreated products		
I (650 p.s.i. H_2)	25.0	35.4
II (650 p.s.i. H_2)	40.9	39.8
III (1500 p.s.i. H_2)	50.0	55.6
Virgin + cracked + hydrotreated synthetic blends		
I	16.7	26.5
II	34.0	42.8
III	54.6	57.5
IV	72.8	73.1
V	86.4	84.2

[a] Blending of preparatively separated fractions.
[b] Response factor [11]: saturates, 1.00; aromatics, 0.70.

Table 2
Reference compounds employed for the evaluation of the chromatographic system

Group-types	Standard compounds[a]					
Saturated compounds	(6.26) n-C_{28}	(6.54) n-C_{16}	(6.62) n-C_{13}	(6.71) n-C_{10}	(6.86) n-C_5	(6.94) 
	1	2	3	4	5	6
	(6.97) 					
	7					
Olefins	(6.52) 1-Docosene	(6.58) 1-Eicosene	(6.70) 1-Hexadecene	(6.82) 1-Dodecene	(6.97) 1-Nonene	
	8	9	10	11	12	
	(6.95) 1-Octene	(7.04) 3-Me-3-heptene		(7.14) 4 Me-2-pentene		
	13	14		15		
Monoaromatics	(7.17) 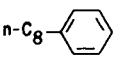	(7.39) 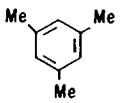	(7.42) 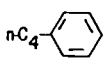	(7.59) 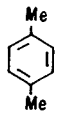	(7.69) 	
	16	17	18	19	20	
	(7.69) 	(7.80) 	(7.89) 			
	21	22	23			
Diaromatics	(8.06) 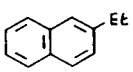	(8.32) 	(8.45) 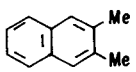	(8.46) 		
	24	25	26	27		
	(8.56) 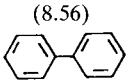		(9.34) 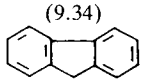			
	28		29			
Triaromatics	(10.08) 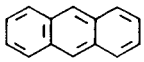	(10.14) 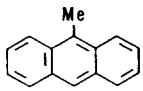	(10.30) 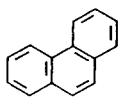			
	30	31	32			
Tetraromatics	(12.59) 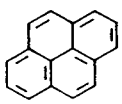	(15.5) 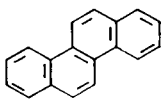	(16.32) 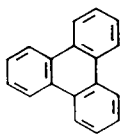	(19.1) 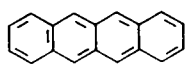		
	33	34	35	36		

[a] Values in parentheses are retention times (min). Numbers 1–36 denote the standards in Fig. 2.

In order to devise an easier and faster method for process monitoring, research was initiated 4 years ago to explore the feasibility of HPLC with dielectric constant detection. Initial experiments were carried only with a DNAP charge-transfer column, as we had previous experiences with this phase [45]. Under such conditions, saturated compounds and monoaromatics co-eluted, so silica columns were sequentially combined until saturated compounds and mono-, di- and triaromatics could be separated. Freon 123 was employed as the mobile phase because reportedly its use facilitates the determination of hydrocarbons [35,36,38–40]. The final column bank required a DNAP column to achieve the separation of di- and triaromatics. The eluent was too strong a solvent for silica columns alone to be employed. The elution range of each hydrocarbon group was initially ascertained with the aid of reference compounds (see Table 2 and Fig. 2).

In addition to charge-transfer and adsorption mechanisms obtained with the combination of DNAP and silica columns, it was possible to observe a simultaneous exclusion mechanism. Among the families of saturated compounds and olefins, larger members elute first (Table 2). In a similar fashion, the length of the alkyl substituent in monoaromatics governs the retention properties. However, isomerism effects can be observed and are not easily explained. This effect has also been noted by other workers in similar studies [35]. Attempts to control this sizing effect with wide-pore silica columns (300 Å) proved unsuccessful. Similarly, improvements in resolution were pursued by adding more

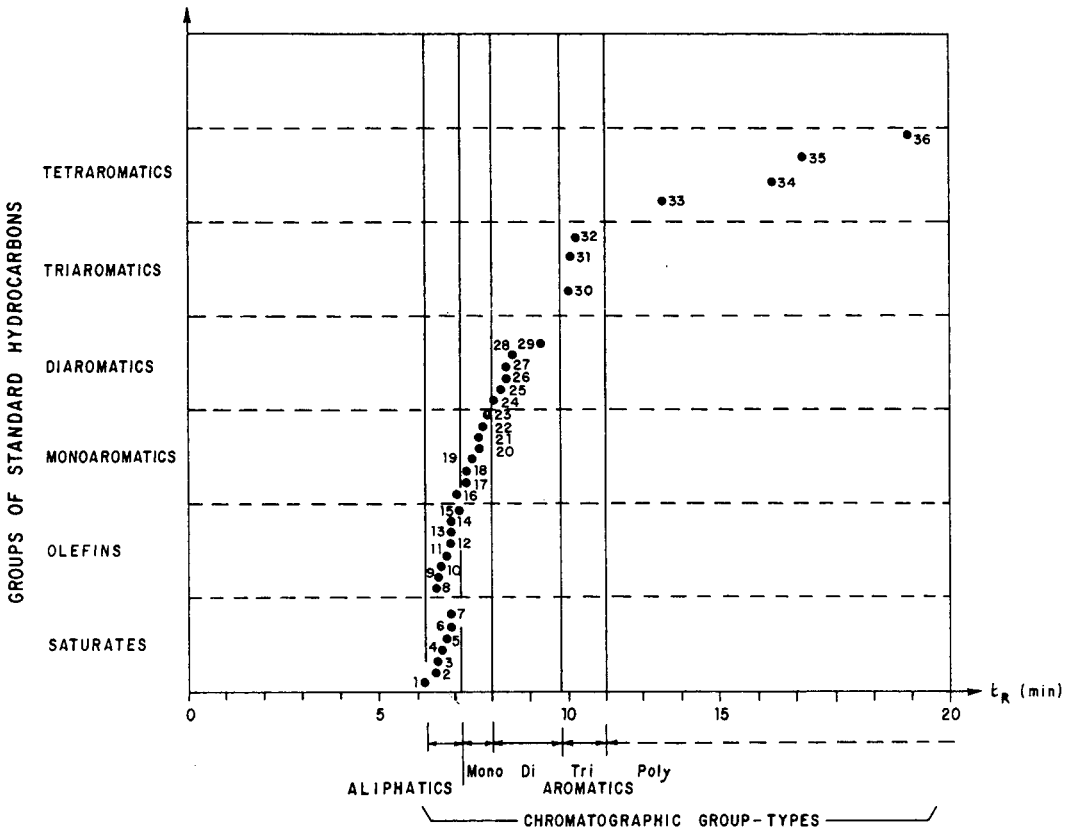

Fig. 2. Chromatographic group-types determined. Numbers 1–36 denote reference compounds, detailed in Table 2.

Table 3
Detector response for pure preparative hydrocarbon groups, determined after HPLC separation

Sample	Integrator counts[a] × 10^{-4}		Response factor for total aromatics
	Aliphatics	Total aromatics	
Hydrotreated middle distillate	4433	4017	1.10
Virgin gasoil	4556	3809	1.20
Catalytically cracked gasoil	4445	4095	1.09
Hydrotreated LCO	4420	4052	1.09
Kerosene	4613	3946	1.17
LCO	4404	4062	1.09
Thermal cracked light gasoil	4271	3781	1.13
Mean ± S.D.			1.12 ± 0.04

[a] 5 μl of neat sample and detector at sensitivity 2. Means of three determinations.

columns, employing spherical Nucleosil particles instead of the irregular Adsorbosil-LC, or replacing these by Partisil 5-PAC columns (Whatman). None of these approaches was successful.

Before trying to perform quantitative analysis, response factors for saturates and total aromatics were checked. Several preparatively separated fractions were analysed. It was found that with the chromatographic system employed, a factor of 1.12 for total aromatics corrected the volumetric content of such hydrocarbon types (see

Table 4
Detector response for pure hydrocarbons

Hydrocarbon group	Compound	Detector response[a] (counts × 10^{-3})	Average response for hydrocarbon group (counts × 10^{-3})
Saturated compounds	*n*-C_5	2323	
	Cyclopentane	2127	
	n-C_{11}	2013	2077
	n-C_{13}	1977	
	n-C_{15}	1942	
Olefins	2,4,4-Trimethyl-1-pentene	1136	
	1-Nonene	1350	
	1-Dodecene	1613	1484
	1-Tridecene	1515	
	1-Hexadecene	1807	
Monoaromatics	Toluene	2152	
	o-Xylene	1948	
	n-Butylbenzene	1814	1826
	n-Decylbenzene	1774	
	Tetralin	1527	
	n-Hexadecylbenzene	1742	
Diaromatics	1-Methylnaphthalene	1641	1695
	2-Ethylnaphthalene	1750	

[a] 1.0 μl of neat sample and detector at sensitivity 10. Means of three determinations.

Table 3). The non-unity correction factor may arise from several causes. Band broadening due to the very long column bank used might contribute. In our system, this effect could definitely be present. However, it was not evaluated. Another possibility is a structural effect. This was verified with pure hydrocarbon groups, as shown in Table 4. By plotting the dielectric constants of pure compounds [46] (see Fig. 3), it was possible to rationalized the decrease in response along the sequence saturates–monoaromatics–diaromatics. The differences in signal between solvent and sample follow the same sequence, which explains the results found. Nevertheless, we do not have an explanation for the very low response of olefins (see Table 4). Experiments were not performed to test for the irreversible loss of such compounds over metallic surfaces of the injector, the connecting tubing and the detector itself.

The selection of chromatographic conditions for quantitative analysis was based on compromises. A sample load of 5 μl (neat) with the detector operated at a sensitivity of 2 were in our opinion the optimum conditions from a pragmatic point of view. In such way, it was possible to avoid the cumbersome handling of very volatile solutions, as the eluent boils under ambient conditions. Detector sensitivities were evaluated in the range 1–5 and sample loads of a light cycle oil (LCO) between 1 and 10 μl. The response of triaromatics was lower than expected, with a 1-μl injection, and, on the other hand, the resolution decreased with a 10-μl injection. Baseline drift was noticeable at a detector setting of 1, and also the noise was very high owing to the pulsating pumping system. At a detector sensitivity of 2 and a 5-μl sample load, the resolution was comparative to that obtained with a 1-μl injection. The signal-to-noise ratio was

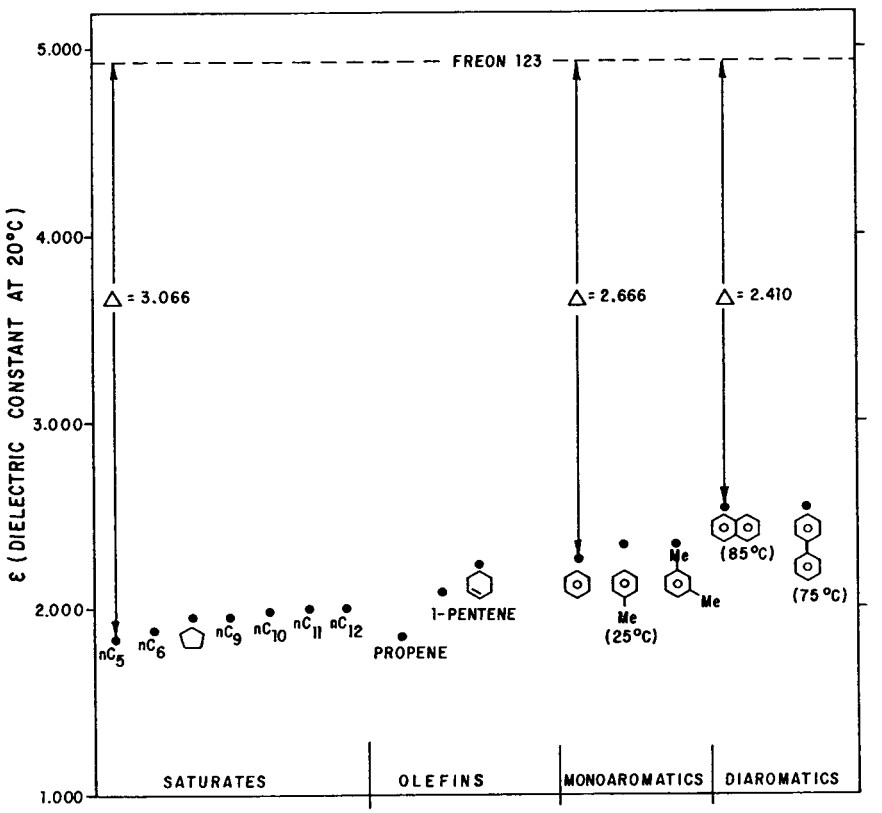

Fig. 3. Dielectric constants of some reference compounds.

improved from 3 to 15 for the worst signal (triaromatics) when the sample load was changed from 1 to 5 μl. The optimum sample load (5 μl) was close to the upper limit of the linearity range reported by Hayes and Anderson [34]. With the present chromatographic system, this load decreased the effect of instrumental noise, caused by the pulsating pump employed, making it unnecessary to use the generally recommended pulseless syringe-type pumps. In addition, the larger adsorbent capacity of the stationary phase allowed the handling of such sample loads without noticeable overload problems.

Fig. 4 shows some chromatograms obtained with the system described. The catalytic LCO separation resembled that obtained by Pedley *et al.* [47] employing a very apolar eluent (pentane) with amino- and underivatized silica columns. Baseline resolution was usually not achieved. For this reason, peak-area integration was performed by drawing lines parallel to the ordinate axis, passing through the frontier points. These frontiers were defined by valleys and/or inflection points, maintaining the general time domains previously stated (see Fig. 2). To verify the accuracy of the determination of the aromatics content, 28 standard blends were prepared. Saturated compounds and aromatics separated preparatively from catalytic LCO (5 standard blends), thermal cracked light gasoil (2), virgin light gasoil (6), kerosene (1) and hydrotreated middle distillates (9) were quantitatively mixed. Five additional blends were prepared by mixing diverse proportions of all the cited fractions. The aromatics contents of prepared standards spanned the range 5–84% (v/v). A linear correlation was found between known and measured aromatic contents, the slope being 0.9956 and the intercept 0.6648. The correlation coefficients obtained were $r = 0.9973$ and $r^2 = 0.9946$, and the standard deviations of the slope and intercept were 0.01 and 0.78, respectively. The standard error of residuals was 2.02.

Regarding precision, short-term repeatability was evaluated by analysis performed over a 2-day period. Table 5 shows an example of short-term repeatability. Appropriate standard deviations were obtained for all hydrocarbon groups except for triaromatics. Long-term repeatability was checked with different type of samples, measured 1 and 5 months after the first determination. Table 6 presents the results obtained, showing greater standard deviations than for the short-term repeatability. The precision was still reasonable for total aromatics and monoaromatics, but was poorer for more conju-

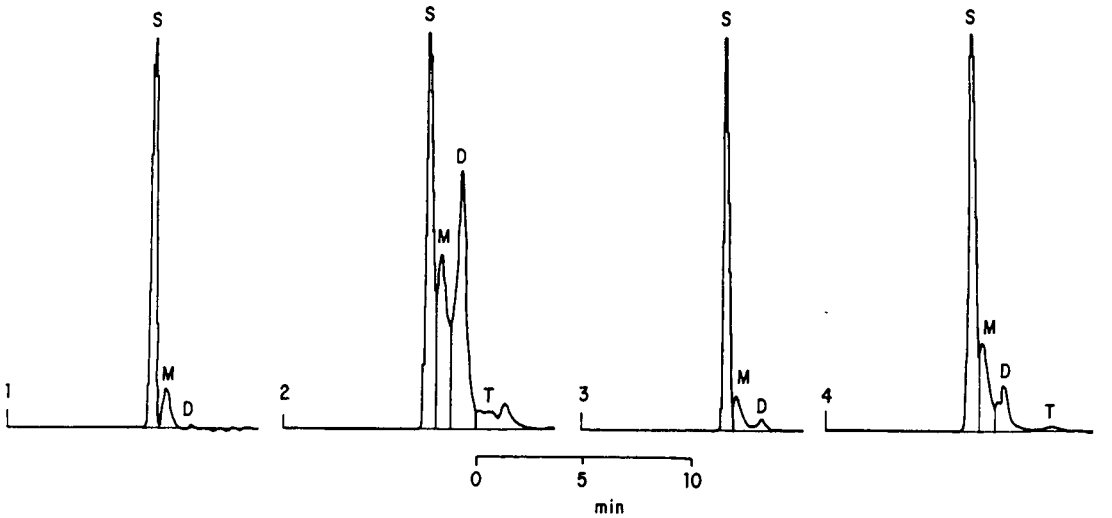

Fig. 4. Selected chromatograms obtained with the described HPLC system. 1 = Kerosene; 2 = LCO; 3 = desulphurized middle distillate; 4 = partially hydrotreated LCO; S = aliphatics; M = monoaromatics; D = diaromatics; T = triaromatics.

Table 5
Repeatability of analysis during a 2-day interval [% (v/v) of hydrocarbon groups from an LCO]

Aliphatics	Total aromatics	Monoaromatics	Diaromatics	Triaromatics
17.0	83.0	18.5	55.1	9.4
17.6	82.4	19.0	56.0	7.4
17.8	82.4	19.5	56.3	6.4
17.6	82.4	19.2	56.3	6.9
17.5	82.5	19.1	55.6	7.8
Mean ± S.D.				
17.5 ± 0.3	82.5 ± 0.3	19.1 ± 0.4	55.9 ± 0.5	7.6 ± 1.2

Table 6
Repeatability of analysis during a 5-month interval

Sample	Hydrocarbon group (%, v/v)[a]				
	Aliphatics	Aromatics			
		Total	Mono-	Di-	Tri-
Hydrotreated middle distillate (350 p.s.i.)	64.7	35.3	20.3	13.8	1.2
	61.2	38.3	23.6	12.0	3.1
	61.5	38.5	21.3	15.0	2.3
	62.5 ± 1.9	37.4 ± 1.8	21.7 ± 1.7	13.6 ± 1.5	2.2 ± 1.0
Hydrotreated middle distillate (1500 p.s.i.)	71.9	28.1	26.1	1.4	0.6
	72.9	27.1	27.6	1.8	0.1
	69.7	30.3	26.6	2.7	1.0
	71.5 ± 1.6	28.5 ± 1.6	26.8 ± 0.8	2.0 ± 0.7	0.6 ± 0.5
LCO	35.2	64.9	21.9	37.7	5.2
	33.6	66.4	22.8	37.2	6.3
	34.7	65.4	21.7	38.2	5.5
	34.5 ± 0.8	65.6 ± 0.8	22.1 ± 0.6	37.7 ± 0.5	5.7 ± 0.6
Kerosene	81.6	18.4	14.6	3.8	ND[b]
	82.9	17.1	15.2	1.9	ND
	82.2	17.8	15.1	2.7	ND
	82.2 ± 0.7	17.8 ± 0.7	15.0 ± 0.3	2.8 ± 1.0	
Desulphurized middle distillate	65.8	34.2	27.4	5.5	1.3
	61.6	38.4	26.7	9.4	2.3
	61.6	38.4	26.8	9.0	2.6
	63.0 ± 2.4	37.0 ± 2.4	27.0 ± 0.4	8.0 ± 2.1	2.1 ± 0.7
Kerosene	83.3	16.7	16.0	0.8	ND
	81.2	18.8	17.7	1.1	ND
	80.5	19.5	17.2	2.2	ND
	81.7 ± 1.5	18.3 ± 1.5	17.0 ± 0.9	1.4 ± 0.7	

[a] Means ± S.D. are additionally reported.
[b] ND = Not detected.

gated aromatics. This was especially noticeable for samples with low levels of di- and triaromatics. The poor precision for triaromatics was caused by the low sensitivity, due to band broadening (last-eluted signals in a long chromatographic system) and a lower response (lower dieletric constant difference, according to the findings in Fig. 3).

Other evidence of repeatibility arises from the fact that the columns were successfully used for 3 years without noticeable changes in the quantitative analysis of the samples used as references. Very small resolution losses were observed during this period. Silica columns were finally replaced for a different reason, *i.e.*, increases in pressure drop were observed as consequence of corrosion of fritted discs. The DNAP column is still in use after 4 years of operation.

The methodology described has found practical applications for the routine monitoring of processes and to obtain rapidly fingerprints of samples from different refineries or from changes in feeds within the same refinery. Examples of the latter are shown in Fig. 5 for LCO samples.

Processes usually monitored with this methodology involved distillation, solvent extraction of aromatics and hydrotreating. Fig. 6 shows sequential chromatograms from distillation and hydrotreating experiments. Hydrocarbon distribution and balances can easily be obtained (see Table 7). This represents the main advantage of the HPLC–dielectric constant detection methodology described here over the commonly used HPLC–RI detection methods [11]. In the same way, trends in total aromatic contents (see Fig. 7) or specific aromatic group distributions can easily be followed during processing, owing to the short time and simple protocol involved in the measurement.

In order to validate this methodology it was compared with MS. This comparison is also useful to assess the applicability of the LC method to distillates with different boiling ranges. Table 8 shows that the results agreed reasonably well for light distillates, such as typical atmospheric cuts. On the other hand, the aromatic contents determined by LC were always lower for heavy distillates. This confirms

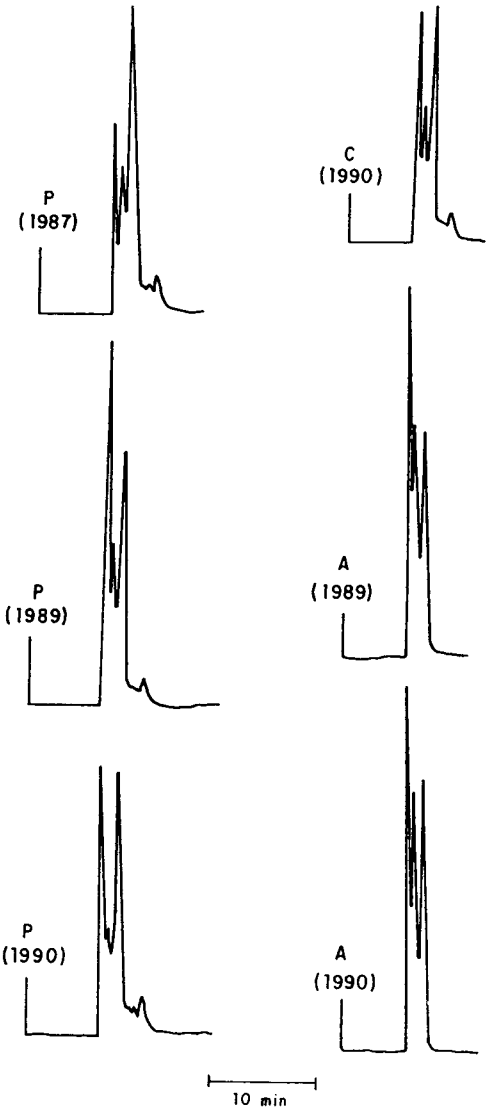

Fig. 5. HPLC fingerprinting of light cycle oils from different Venezuelan refineries (A, C, P). Samples were taken in different years (given in parentheses).

the applicability of the developed methodology exclusively to atmospheric cuts. For heavier materials such as vacuum gasoil, the signal of tetraaromatics, although detectable, is not measured correctly. This is a consequence of the peak broadening and its poor sensitivity owing to the low dielectric constant difference compared with the solvent.

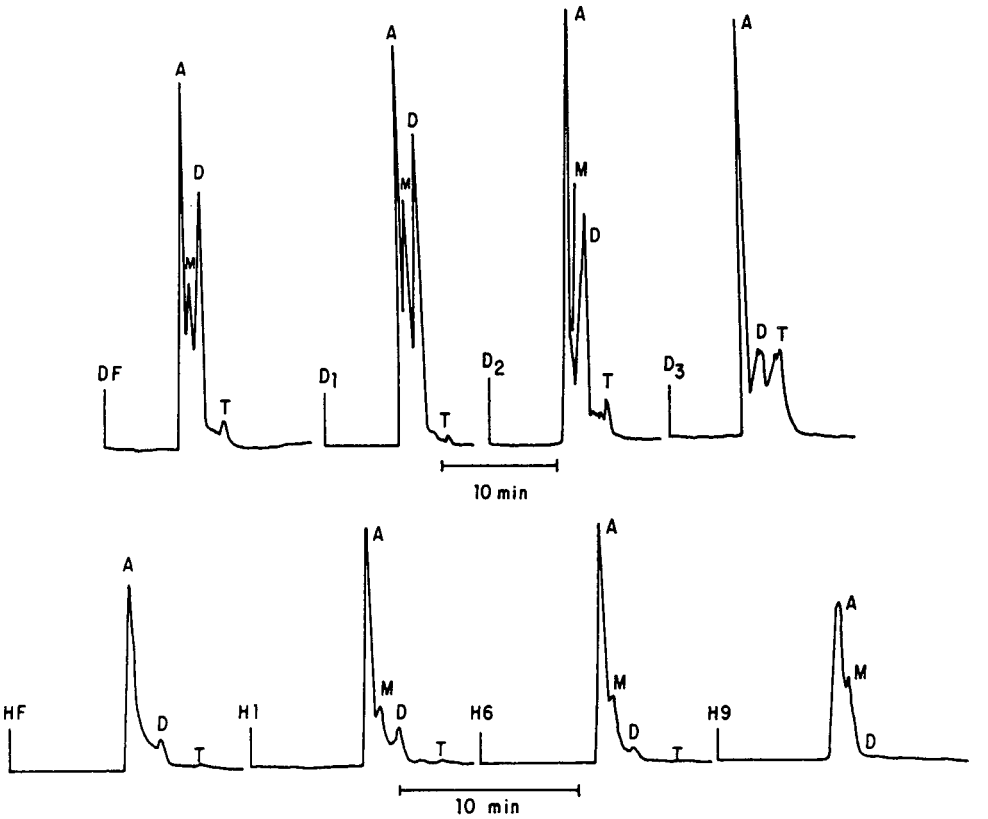

Fig. 6. HPLC monitoring of distillation and hydrotreating processes. DF = Distillation feed; D_1 = 200–300°C cut; D_2 = 300–343°C cut; D_3 = 343°C+ cut; HF = hydrotreating olefinic feed; H_1 = hydrotreated at 350 p.s.i. H_2; H_6 = hydrotreated at 650 p.s.i. H_2; H_9 = hydrotreated at 1500 p.s.i. H_2; A = aliphatics; M = monoaromatics; D = diaromatics; T = triaromatics.

Table 7
Group-type distributions in distillation cuts obtained from an LCO

Sample	Boiling range (°C)	Yield (% P)	Hydrocarbon group by HPLC (%, v/v)			
			Aliphatics	Aromatics		
				Mono-	Di-	Tri-
LCO	NM[a]	100.0	29.6	21.9	38.3	10.3
Cut 1	222–300	67.2	26.6	29.6	39.7	4.1
Cut 2	300–343	26.0	34.2	6.8	43.9	15.2
Cut 3	343+	6.8	40.1	NS[a]	24.5	35.4
Balance of fractions	–	–	29.5	21.7	39.8	9.1

HPLC chromatograms traces are shown in Fig. 6.
[a] NM = Not measured; NS = no signal separated.

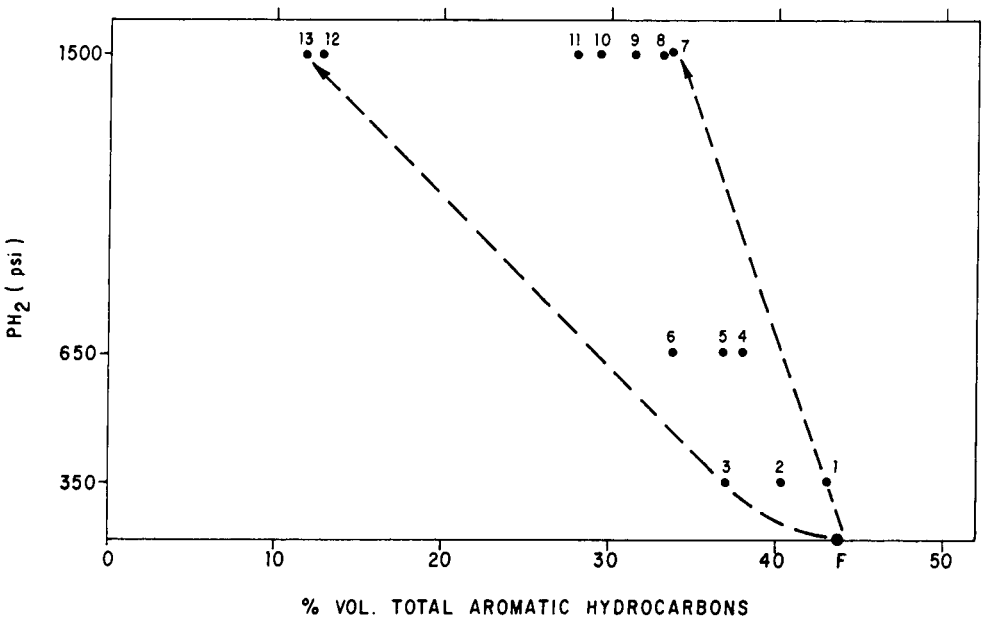

Fig. 7. HPLC mapping of hydrotreating conditions. Selected chromatograms of products 1, 6 and 9 are shown in Fig. 6. F = Feed.

Table 8
Comparison of HPLC and MS for total aromatic content determination of petroleum products

Sample	Average molecular mass[a]	Distillation[b]					Total aromatics (%, v/v)	
		IBP	10%	50%	95%	FBP	HPLC	MS
Hydrotreated middle distillate	182						31.5	35.8[c]
Kerosene	186	154	166	186	238	250	20.2	18.3
LCO	189	210	210	273		332	67.3	65.9
Hydrotreated middle distillate	190						57.0	60.3[c]
Light virgin gasoil	208	180	212	250	308	320	14.6	17.0
Light virgin gasoil	210	180	212	250	308	320	22.5	18.1
Medium gasoil	230	190	245	304	360	390	16.9	30.6
Hydrotreated vacuum gasoil	230						29.4	40.9
Heavy gasoil	254	270	303	334	380	386	12.6	29.9
Heavy gasoil	266						NS[d]	21.5
Vacuum gasoil	309						NS	42.9

[a] Cryoscopy in dioxane for light products; vapour-pressure osmometry in chloroform for heavier materials.
[b] IBP and FBP = Initial and final boiling points.
[c] MS determined by Robinson method [8], with the exceptions noted [44].
[d] NS = No aromatic signal separated.

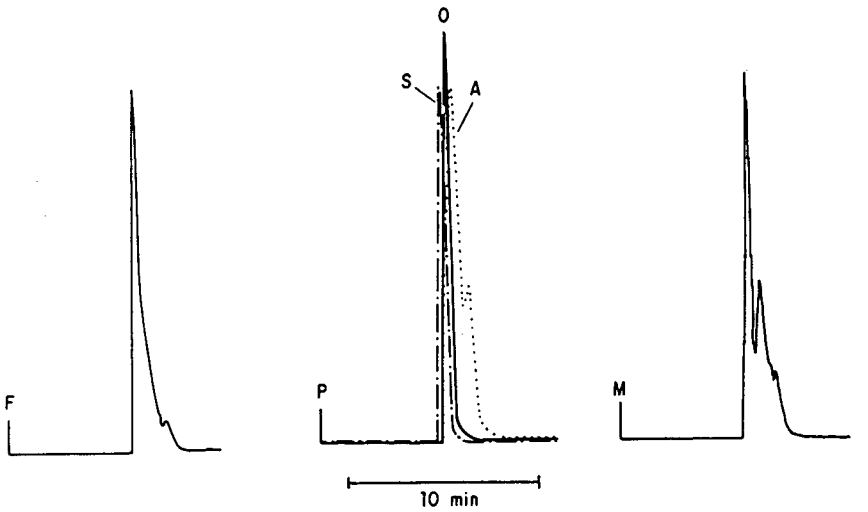

Fig. 8. HPLC of thermal cracked light gasoil and its preparative fractions. F = Thermal cracked light gasoil; P = preparatively separated fractions; M = saturates plus aromatics mixture; S = saturates; O = olefins; A = aromatics.

When analysing pure thermal cracked components by the present LC method, in most instances only one broad signal was obtained. To clarify this finding, saturated compounds, olefins and aromatics from a light thermal cracked gasoil were preparatively separated. Olefins produced in the process eluted exactly between saturated compounds and monoaromatics (see Fig. 8). When mixed in the concentration usually found (*ca.* 40%, v/v), only one signal was detected. Apparently, low levels of olefins do not interfere to a great extent as LCOs were correctly analysed for saturates and aromatics content. The typical olefin content of LCO ranges between 3 and 5% (v/v). Nevertheless, a possibility not addressed until now is based on probable differences between thermal and catalytically cracked olefins.

Interferences from cycloparaffins and naphthenes were finally investigated. In addition to the appearance of a double aliphatic signal (see shoulder increasing as function of hydrotreating severity in Fig. 9), no bias was found during the quantitative analysis of real samples. This was confirmed by MS. Qualitative analysis showed that most of the cycloparaffins present in these samples were decalins. Pure tetralin, a naphthenoaromatic spiked in some samples, was found to elute in the monoaromatic region.

4. Conclusions

A fast LC method was developed for group-type separations of middle petroleum distillates, in terms of aliphatic hydrocarbons and mono-, di- and triaromatics. Freon 123 was employed as the eluent in combination with DNAP and silica columns. Dielectric constant detection was used. A response factor of 1.12 corrected the total aromatic content by volume. The method was found useful for process monitoring and fingerprinting of refinery streams. Its applicability is restricted to low-olefinic (<5%, v/v) atmospheric cuts.

5. Acknowledgements

Thanks are due to INTEVEP and Drs. Galiasso and J. Medina for sponsoring this work. Discussions held with R. Flores, A. Izquierdo and D. Páez of INTEVEP are greatly appreciated. Mass spectra were measured by H.

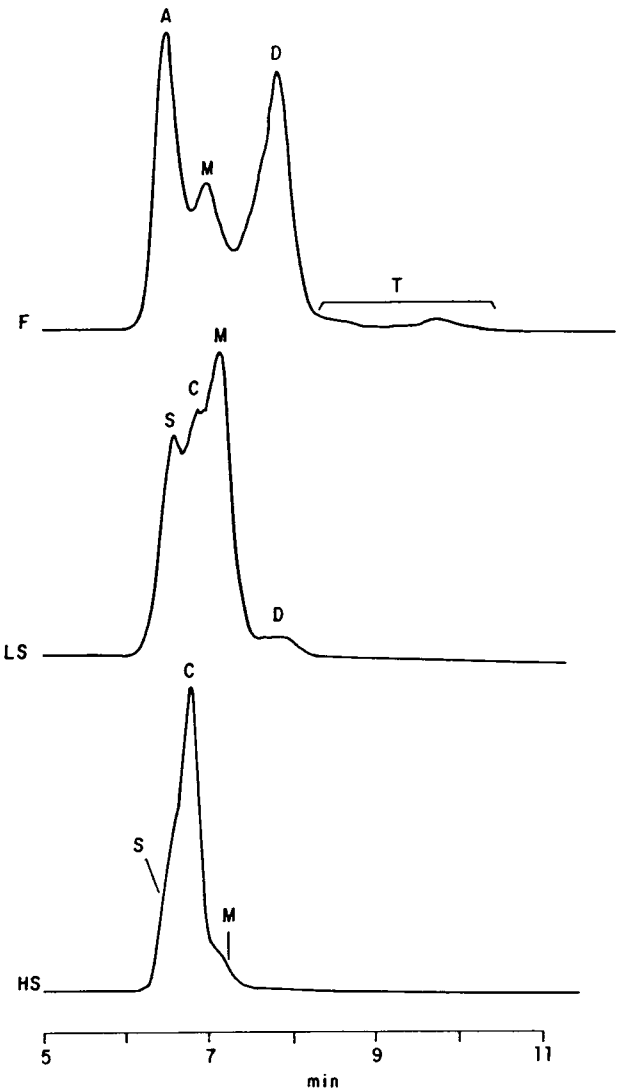

Fig. 9. HPLC monitoring of an LCO hydrotreatment. F = Feed; LS = low-severity product; HS = high-severity product; A = aliphatics; M = monoaromatics; D = diaromatics; T = triaromatics; S = non-cyclic saturates; C = cycloalkanes.

Enríquez of INTEVEP. Dr. J.B. Green (Niper, Bartlesville, OK, USA) is thanked for providing the DNAP stationary phase. Thanks are due to Dr. S.D. Anderson (Air Force Wright Aeronutical Labs./POSF, Wright-Paterson Air Force Base, OH, USA) for suggestions regarding the use of the Model 410 detector. Thanks are expresed to S. Colaiocco for statistical analysis support and to Dr. A. Parisi for reviewing the manuscript.

6. References

[1] J.M. Collins and G.H. Unzellman, *Diesel Trends Emphasize Cetane Economics, Quality and Prediction; API Paper Order 820-0002*, American Petroleum Institute, Washington, DC, 1982.
[2] D.L. Lenane, M.E. Gluckstein and J.R.R.C. Reid, *Impact of Diesel Fuel Quality Trends and Effect of Diesel Performance Improver Additives, Japan Petroleum Institute Conference, Products Section, Tokyo, October 18–19, 1984*, Ethyl Corporation, Baton Rouge, LA.
[3] S.W. Lee, *Prepr. Am. Chem. Soc. Div. Fuel Chem.*, 32 (1988) 883.
[4] R.D. Harvey, *Polycyclic Aromatic Hydrocarbons and Carcinogenesis (ACS Symposium Series*, No. 283), American Chemical Society, Washington, DC, 1985.
[5] *Annual Book of ASTM Standards*, Vol. 05-01, ASTM, Philadelphia, 1989, p. 516, Standard D-1319.
[6] *Annual Book of ASTM Standards*, Vol. 05-01, ASTM, Philadelphia, 1989, p. 226, Standard D-611.
[7] *Annual Book of ASTM Standards*, Vol. 05-01, ASTM, Philadelphia, 1989, p. 174, Standard D-2425.
[8] C.J. Robinson, *Anal. Chem.*, 43 (1971) 1425.
[9] J.C. Suatoni and R.E. Swab, *J. Chromatogr. Sci.*, 13 (1975) 361.
[10] T.N. Tate, in G.B. Crump (Editor), *Petroanalysis 1981. Advances in Analytical Chemistry in the Petroleum Industry*, Butterworths, Boston, and Wiley, London, 1982, p. 268.
[11] J.M. Collins and G. Vion, *J. Chromatogr.*, 280 (1983) 152.
[12] L.J. Cookson, C.J. Rix, L.M. Shaw and B.E. Smith, *J. Chromatogr.*, 312 (1984) 237.
[13] *Annual Book of ASTM Standards*, Vol. 05-01, ASTM, Philadelphia, PA, 1989, p. 739, Standard D-1840.
[14] D.G. Hamblen, P.R. Solomon, K.S. Tarantul and P.M. Carangelo, *Prepr. Am. Chem. Soc. Div. Pet. Chem.*, 32 (1987) 530.
[15] A.H.H. Tameesh, M.H. Hanna and R. Komers, *J. Chromatogr.*, 328 (1985) 207.
[16] W.J. Danaher and P.A. Johnston, *Fuel Sci. Technol. Int.*, 5 (1982) 1870.
[17] J. Muhl, V. Srica, B. Mimica and M. Tomaskovic, *Anal. Chem.*, 54 (1982) 1871.
[18] B. Glavincevski, O.L. Gulder and L. Gardner, *Prepr. Am. Chem. Soc. Div. Pet. Chem.*, 34 (1989) 897.
[19] I.L. Davies, K.D. Bartle, G.E. Andrews and P.T. Williams, *Anal. Chem.*, 60 (1988) 204.
[20] I.L. Davies, K.D. Bartle, G.E. Andrews and P.T. Williams, *J. Chromatogr. Sci.*, 28 (1988) 125.
[21] T.A. Norris and M.G. Rawdon, *Anal. Chem.*, 56 (1984) 1767.

[22] B.J. Fuhr, L.R. Holloway, S.W. Lee and A.C.S. Hayden, *Prepr. Am. Chem. Soc. Div. Fuel Chem.*, 32 (1987) 30.
[23] F.P. DiSanzo and R.E. Yoder, *J. Chromatogr. Sci.*, 29 (1991) 4.
[24] *Annual Book of ASTM Standards*, Vol. 05-03, ASTM, Philadelphia, 1989, p. 855, Standard D-5186.
[25] M.A. Poirier and A.E. George, *Fuel*, 60 (1981) 194.
[26] F.P. DiSanzo, *Prepr. Am. Chem. Soc. Div. Pet. Chem.*, 26 (1981) 13.
[27] L. Nondek, *J. Chromatogr.*, 373 (1986) 61.
[28] P. Jadaud, M. Caude and R. Rosset, *Analusis*, 14 (1986) 491.
[29] D. Cagniant (Editor), *Complexation Chromatography (Chromatography Science Series*, Vol. 57), Marcel Dekker, New York, Basle, 1991.
[30] P.L. Grizzle and D.M. Sablotny, *Anal. Chem.*, 58 (1986) 2389.
[31] M.M. Boduszynski, *Energy Fuels*, 2 (1988) 597.
[32] C.D. Pearson and S.G. Garfeh, *Anal. Chem.*, 58 (1986) 307.
[33] L.V. Benningfield and R.A. Mowery, Jr., *J. Chromatogr. Sci.*, 19 (1981) 115.
[34] P.C. Hayes, Jr., and S.D. Anderson, *Anal. Chem.*, 57 (1985) 2094.
[35] P.C. Hayes, Jr., and S.D. Anderson, *Anal. Chem.*, 58 (1986) 2384.
[36] P.C. Hayes, Jr., and S.D. Anderson, *J. Chromatogr.*, 387 (1987) 333.
[37] T.V. Alfredson, *J. Chromatogr.*, 218 (1981) 715.
[38] P.C. Hayes, Jr., and S.D. Anderson, *J. Chromatogr.*, 437 (1988) 365.
[39] P.C. Hayes, Jr., and S.D. Anderson, *J. Chromatogr. Sci.*, 26 (1988) 250.
[40] P.C. Hayes, Jr., and S.D. Anderson, *Prepr. Am. Chem. Soc. Div. Pet. Chem.*, 32 (1987) 550.
[41] S.D. Anderson and P.C. Hayes, Jr., *J. Chromatogr. Sci.*, 26 (1988) 210.
[42] P.L. Grizzle and J.S. Thomson, *Anal. Chem.*, 54 (1982) 1071.
[43] J.S. Thomson and J.W. Reynolds, *Anal. Chem.*, 56 (1984) 2434.
[44] *Annual Book of ASTM Standards*, Vol. 05-02, ASTM, Philadelphia, 1988, p. 451, Standard D-2789.
[45] J.A. Green, J.B. Green, R.D. Grigsby, C.D. Pearson, J.W. Reynolds, J.Y. Shay, G.P. Sturm, Jr., J.S. Thomson, J.W. Vogh, R.P. Vrana, S.K.-T. Yu, B.H. Diehl, P.L. Grizzle, D.E. Mirsch, K.W. Hornung, S.Y. Tang, L. Carbognani, M. Hazos and V. Sanchez, *Analysis of Heavy Oils: Method Development and Application to Cerro Negro Heavy Petroleum, Niper 452*, Vols. 1 and 2, Niper, Bartlesville, OK, 1989.
[46] R.C. Weast (Editor), *Handbook of Chemistry and Physics*, CRC Press, Cleveland, OH, 57th ed., 1976–77, p. E.-55–E-58.
[47] J.F. Pedley, R.W. Hiley and R.A. Hancock, *Fuel*, 67 (1988) 1124.

ELSEVIER

Journal of Chromatography A, 663 (1994) 27–33

JOURNAL OF CHROMATOGRAPHY A

Indirect photodetection of pregnanolone on a Cyclobond column by high-performance liquid chromatography

Benoit Agnus[a], Noëlle-Martine Gosselet*[,b], Bernard Sebille[b]

[a]*Laboratoires Besins Iscovesco, 10 Rue Morel, 92120 Montrouge, France*

[b]*Laboratoire de Physico-Chimie des Biopolymères, CNRS–Université Paris XII, UM 27, 2 Rue Henri Dunant, 94320 Thiais, France*

(First received July 7th, 1993; revised manuscript received October 18th, 1993)

Abstract

The chromatographic properties of eight steroids were studied on a Cyclobond column in order to select those which can be used as markers for the indirect photodetection of pregnanolone. Testosterone was shown to be the best compound, enhancing the pregnanolone detection by a factor of 6.5 with respect to the direct detection of pregnanolone at 280 nm under the optimum conditions: 0.0085 m*M* testosterone with methanol–water (65:35) as mobile phase. The influence of the percentage of methanol and the marker concentration in the mobile phase was studied. The models developed previously on a reversed-phase column were successfully applied and the apparent inclusion constants for progesterone and testosterone in the β-cyclodextrin cavity were determined. They were 103 and 2200 l mol^{-1} for progesterone and testosterone, respectively, with methanol–water (65:35) and 50 and 780 l mol^{-1} with methanol–water (75:35) as mobile phase.

1. Introduction

Cyclodextrins are natural macrocyclic polymers of glucose in toroidal shape. They have the ability to trap molecules in their hydrophobic internal cavity, thus forming inclusion complexes.

Immobilized cyclodextrin stationary phases developed by Armstrong and Demond [1,2] were essentially used for the separation of enantiomers [2–6], diastereoisomers [6], and structural isomers [7–9]. However, a cyclodextrin bonded phase column behaves also as a conventional phase when it is used with water–organic mixtures as mobile phase for the separation of barbiturates [2] and vitamins [8].

Compounds with a poor detector response can be detected and determined using indirect ultraviolet or fluorescence detection. In this technique an ultraviolet- or fluorescence-absorbing species is added to the mobile phase. The detection results from perturbation of the distribution equilibria of the probe on injection of the sample. Reversed-phase chromatography is the main field of application of the indirect detection of both charged and uncharged species. In this work, we examined the possibility that pregnanolone may be detected by indirect photodetection on a β-cyclodextrin bonded phase (Cyclobond I) for comparison with results obtained previously on a C_4 reversed-phase column

* Corresponding author.

0021-9673/94/$07.00
SSDI 0021-9673(93)E1192-3

in the presence of β-cyclodextrin in the mobile phase [10]. Pregnanolone has a low molar absorption coefficient, $\varepsilon = 500$ l mol^{-1} cm^{-1}, at 280 nm and its more sensitive detection is of interest.

2. Experimental

2.1. Apparatus

The chromatographic equipment included a pump (Varian Model 5500), a variable-wavelength detector (Varian Model UV 200) with a 9-mm flow cell length, a 20-μl loop injector (Rheodyne Model 7125), an integrator for data acquisition (Spectra-Physics Model 4400) and a diode-array detector (Varian UV 9065). The columns (250 × 4.6 mm I.D.) were made of stainless steel equipped with Swagelock connectors.

2.2. Chemicals and reagents

Methanol of HPLC grade was purchased from SDS (France). Progesterone, testosterone, estradiol and pregnanolone were purchased from Diosynth (Netherlands) and the other steroids from Sigma (France).

2.3. Chromatography

Separations were carried out with a Cyclobond I column (250 × 4.6 mm I.D.) purchased from Astec (USA) and used at room temperature (20 ± 1°C). The flow rate was 0.6 ml min^{-1}. The samples were injected as solutions in the mobile phase. Peak areas were determined with the integrator and were expressed in arbitrary peak-area units. The void volume was obtained from the methanol front peak of the chromatogram.

3. Results and discussion

3.1. Choice of the probe

In order to select the best probe for the indirect photodetection of pregnanolone, which has a low absorption at 280 nm, we studied the chromatographic properties of eight steroids (see Table 1). The capacity factors (k') reflect the different stabilities of the inclusion complexes, the highest corresponding to testosterone. As expected, all the k' values decrease with increasing amount of methanol in the mobile phase.

The selectivity factor, α_s, of each steroid calculated with respect to the steroid to be detected, pregnanolone, is also reported in Table 1. Depending on the stability of the inclusion complexes and the steric hindrance of the steroid, the variation of α_s with methanol concentration in the mobile phase is large or small. The α_s value calculated for testosterone with respect to pregnanolone does not vary with increasing concentration methanol. The α_s value calculated for progesterone decreases with increasing concentration methanol, in contrast to the α_s values for the other steroids, which increase with increasing methanol content.

Owing to their different selectivities, which are greater or smaller than 1, and their high molar absorption coefficients, progesterone and testosterone were selected to serve as markers for the indirect detection of pregnanolone. The molar absorption coefficients are $\varepsilon = 13\,700$ and 12 000 l mol^{-1} cm^{-1}, respectively.

Table 1
Capacity factors and selectivity factors for the studied steroids on a Cyclobond I column

Compound	Methanol–water					
	85:15		75:25		65:35	
	k'	α_s	k'	α_s	k'	α_s
Pregnanolone	0.52	–	1.08	–	2.60	–
Progesterone	0.38	1.37	0.64	1.69	1.46	1.78
Testosterone (T)	1.22	0.43	2.34	0.46	5.90	0.32
T. propionate	0.60	0.87	1.34	0.81	3.96	0.66
T. benzoate	1.02	0.51	2.52	0.43	8.22	0.32
Estradiol (E)	0.28	1.86	0.70	1.54	2.44	1.27
E. propionate	0.50	1.04	1.32	0.82	4.30	0.61
E. benzoate	0.38	1.37	1.10	0.98	3.70	0.70

3.2. Qualitative results

The chromatograms in Figs. 1 and 2 show the possibility of indirect photodetection of pregnanolone with progesterone (Fig. 1a) and testosterone (Fig. 2a) as markers with methanol–water (85:15, v/v) as mobile phase. For each case, we compared the response of indirect photodetection with that of direct photodetection of pregnanolone at 280 nm. For 0.048 m*M* progesterone as marker in the mobile phase, there was a 1.4-fold enhancement of the pregnanolone signal. For 0.017 m*M* testosterone as enhancement by a factor 1.1 was observed.

The direction of the marker and sample peaks differs according to the marker selected. We observed, as previously reported by Schill and Crommen [11] for uncharged species, a positive sample peak when k'_{sample} is lower than k'_{marker} (Fig. 2a) and a negative sample peak when k'_{sample} is greater than k'_{marker} (Fig. 1a). The peak corresponding to the marker, negative or positive, is marked out by the system peak (SP).

In order to identify the species corresponding to the different peaks, we used a diode-array detector. With progesterone as marker (Fig. 1b) the first chromatographic peak corresponds to progesterone and the second is the sum of a known amount of pregnanolone (32 nmol) with a deficiency in progesterone. When the testosterone marker is used (Fig. 2b) the first chromatographic peak, which appears at the retention time of pregnanolone, corresponds to the simultaneous presence of pregnanolone and testosterone, and the second peak, which appears at the retention time of testosterone, corresponds to a deficiency in testosterone.

3.3. Quantitative results

For the determination of the optimum conditions for the indirect detection of pregnanolone, we varied the concentrations of the marker and methanol in the mobile phase.

Figs. 3 and 4 show a linear correlation between the response and the amount of pregnanolone injected (8–64 nmol), the concentrations varying from 0.0032 to 0.048 m*M* for

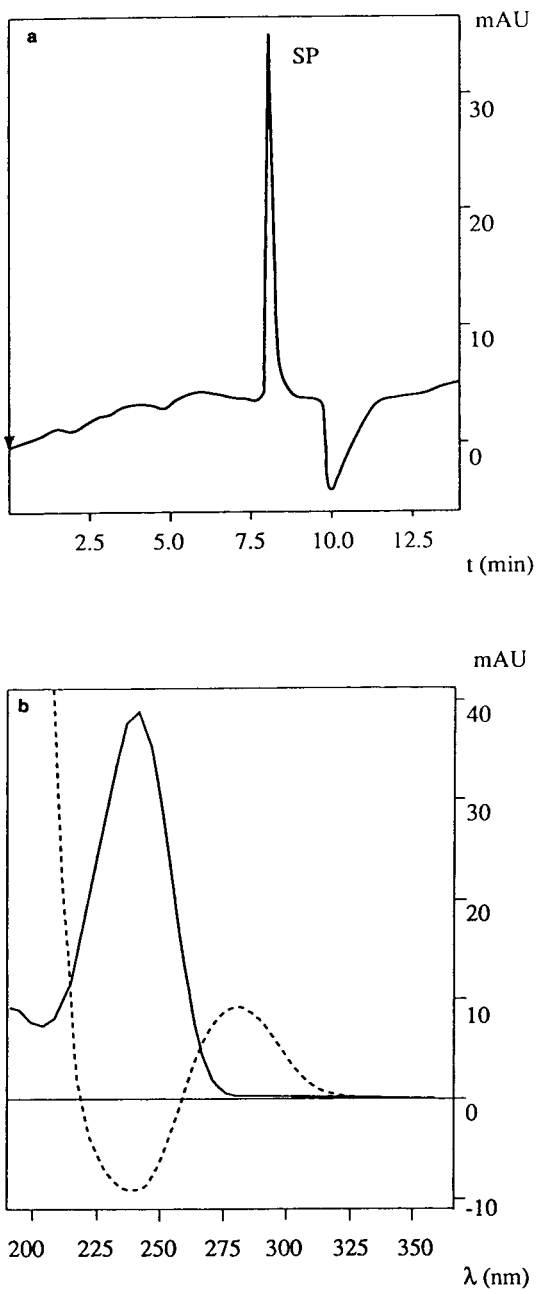

Fig. 1. (a) Indirect chromatographic detection of pregnanolone with progesterone as probe. Chromatographic conditions: mobile phase, methanol–water (85:15, v/v); λ = 241 nm; flow-rate, 0.6 ml min^{-1}; amount of pregnanolone injected, 32 nmol. SP refers to system peak, *i.e.*, progesterone. (b) Diode-array detector spectra corresponding to (solid line) first peak and (dashed line) second peak.

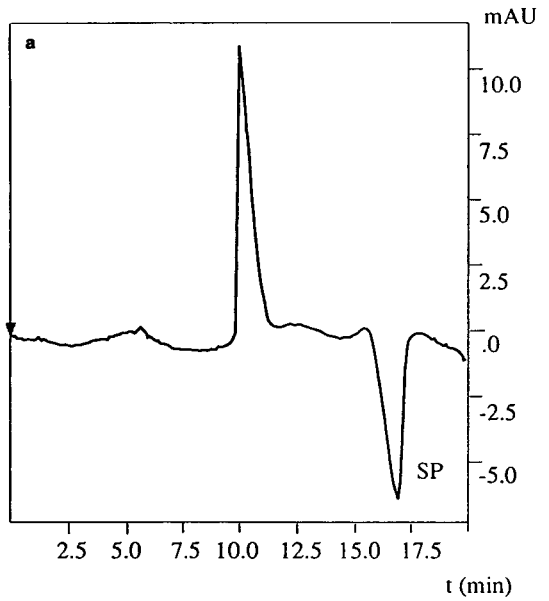

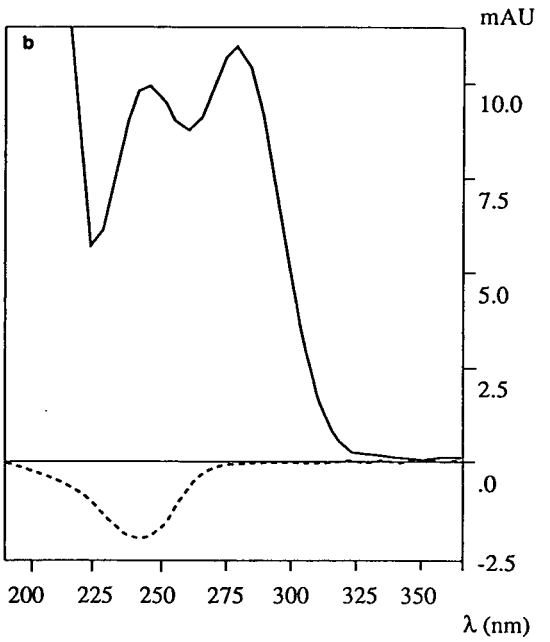

Fig. 2. (a) Indirect chromatographic detection of pregnanolone with testosterone as probe. Chromatographic conditions as in Fig. 1. SP is the system peak, *i.e.*, testosterone. (b) Diode-array detector spectra corresponding to (solid line) first peak and (dashed line) second peak.

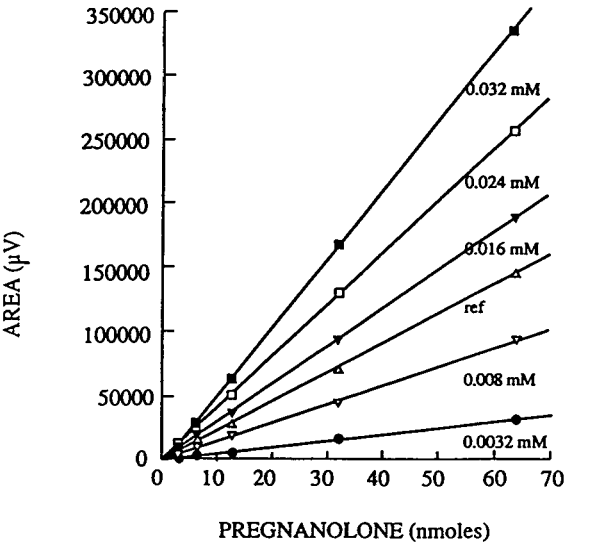

Fig. 3. Quantitative indirect detection of pregnanolone with various concentrations of progesterone with methanol–water (65:35) as mobile phase. Other chromatographic conditions: flow-rate, 0.6 ml min^{-1}; $\lambda = 241$ nm;. The reference curve (△) corresponds to direct detection of pregnanolone at 280 nm.

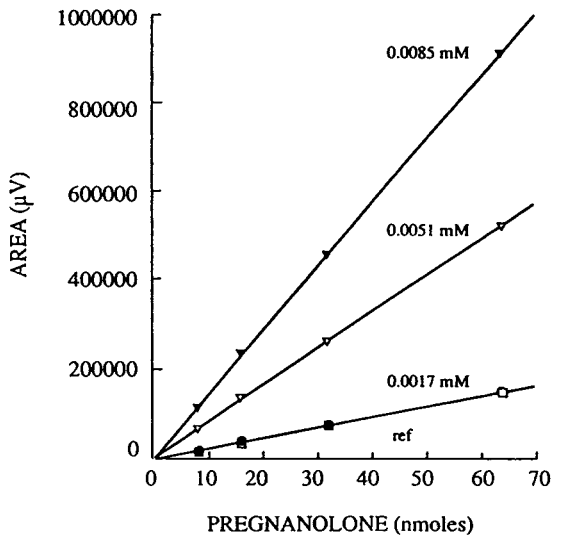

Fig. 4. Quantitative indirect detection of pregnanolone with various concentrations of testosterone with methanol–water (65:35) as mobile phase. Other chromatographic conditions: flow-rate, 0.6 ml min^{-1}; $\lambda = 241$ nm. The reference curve (●) corresponds to direct detection of pregnanolone.

progesterone or from 0.0017 to 0.0085 m*M* for testosterone when methanol–water (65:35) is used as the mobile phase. The highest response is obtained for the highest concentration in progesterone or testosterone in the mobile phase. With 0.032 m*M* progesterone and methanol–water (65:35) an enhancement of the pregnanolone signal by a factor of 2.4 is observed compared with the direct detection of pregnanolone at 280 nm. With 0.0085 m*M* testosterone and methanol–water (65:35) the signal is enhanced by a factor of 6.5.

For higher methanol concentrations in the mobile phase, we also observed linear correlations between the response and the amount of pregnanolone injected.

Figs. 5 and 6 show the influence of methanol on the response. An increasing methanol content in the eluent decreases the response. The variation of the response is not proportional to the amount of methanol.

Crommen and co-workers [11–13] developed three models to explain the sense and the intensity of the peaks observed with indirect photodetection. These models were developed

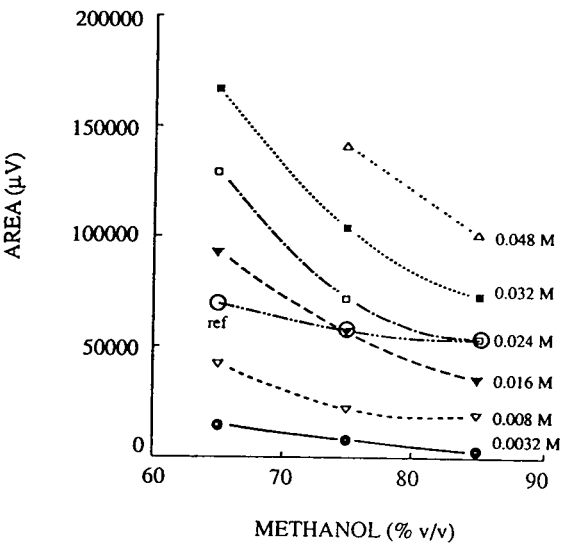

Fig. 5. Influence of methanol on the indirect response for the progesterone probe. Flow rate, 0.6 ml min^{-1}; $\lambda = 241$ nm; amount of pregnanolone injected, 32 nmol. The reference curve (○) corresponds to direct detection of pregnanolone at 280 nm.

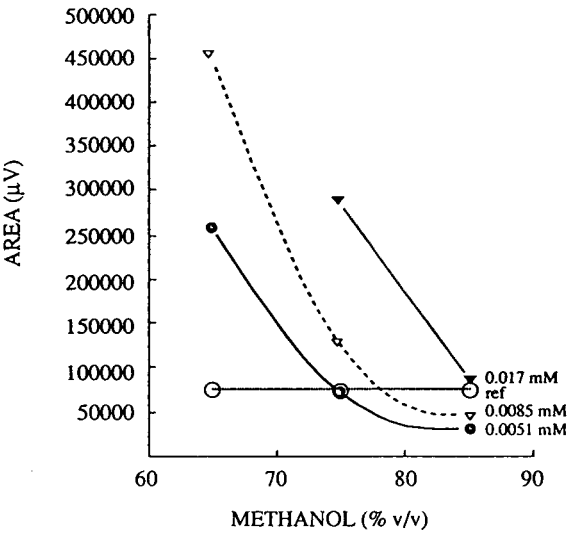

Fig. 6. Influence of methanol on the indirect response for the testosterone probe. Flow rate, 0.6 ml min^{-1}; $\lambda = 241$ nm; amount of pregnanolone injected, 32 nmol. The reference curve (○) corresponds to direct detection of pregnanolone at 280 nm.

on the assumption of a pure Langmuir adsorption isotherm on a C_{18} stationary phase, which was also assumed for the Cyclobond column. Therefore, we applied the Crommen models [12] after calculating the $(\varepsilon^*/\varepsilon)$ ratio according to Hackzell and Shill [14]:

$$\varepsilon^* = \frac{ysu}{mdb} \tag{1}$$

where y is the sample peak area, s the detector range, u the flow-rate, m the amount of compound injected, d the chart speed and b the path length of the detector cell. We determined for each marker the ε value under the same conditions as ε^*.

For a system with only two components competing for the adsorption, Crommen *et al.* [12,13] gave the following equations:

$$\frac{\Delta C_k}{\Delta C_j} = \frac{\varepsilon^*}{\varepsilon} = \theta_k \cdot \frac{\alpha_s}{1-\alpha_s} \tag{2}$$

$$\frac{\varepsilon^*}{\varepsilon} \cdot \frac{1-\alpha_s}{\alpha_s} = \frac{K_k C_{k,M}}{1 + K_k C_{k,M}} \tag{3}$$

where K_k is the absorption constant of marker k

and $C_{k,M}$ its concentration in the mobile phase, ΔC_k and ΔC_j are the concentration variations of marker k and sample j, respectively, in the elution sample zone, θ_k is the partial coverage of the stationary phase by the marker and α_s is equal to the ratio of the capacity factors of sample j and marker k:

$$\alpha_s = \frac{k'_j}{k'_k} \tag{4}$$

This first model was applied successfully to the testosterone marker (Fig. 7). This model is compatible with a positive sample peak and an increasing sensitivity when the marker concentration is higher. We were then able to determine the testosterone adsorption constant, K_k, at various methanol concentrations. These K_k values are apparent inclusion constants and correspond to the slope of the straight lines representing the variation of $(\varepsilon^*/\varepsilon)[(1-\alpha_s)/\alpha_s]$ with $C_{k,M}$. The product $K_k C_{k,M}$ can be neglected with respect to unity. We found for K_k values of 2200 and 780 l mol^{-1} for 65:35 and 75:25 methanol–water mobile phases, respectively. The slopes

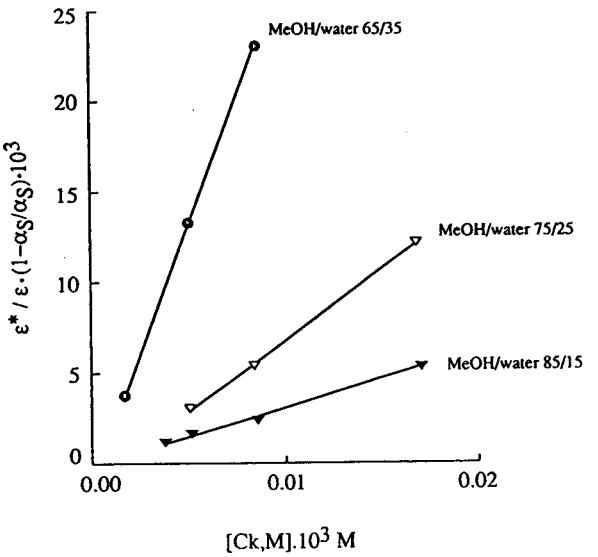

Fig. 7. Estimation of the apparent inclusion constant of testosterone from pregnanolone response. Concentration: $1.7 \cdot 10^{-3}$–$1.7 \cdot 10^{-2}$ mM in methanol–water mobile phases of the proportions indicated. Flow-rate, 0.6 ml min^{-1}; $\lambda = 241$ nm.

are positive because the peak signal is positive. These apparent constant K_k values are of the same order of magnitude as that determined by Liu *et al.* [15] for a 1:1 complex ($K_k = 5058$ l mol^{-1}) in water using phase solubility and spectroscopic techniques.

Despite the fact that the selectivity factor of progesterone is closest to unity, the highest sensitivity was obtained when testosterone was used as a marker in the mobile phase.

For a system corresponding to the simultaneous adsorption of free (j) and associated sample with the marker (jk), competing with the marker adsorption, Crommen developed a second model [12,13] taking into account the formation of the associated form (jk), according to

$$\frac{\varepsilon^*}{\varepsilon} \cdot \frac{1-\alpha_s}{\alpha_s} = \theta_k\left(1 - \frac{K_{jk}}{K_k K_{j0}}\right) = K_k\left(1 - \frac{K_{jk}}{K_k K_{j0}}\right) C_{k,M} \tag{5}$$

where $K_{j,k}$ is the adsorption constant of the associated sample jk, K_k that of marker k and K_{j0} that of free sample j. This equation is based on the hypothesis that the product $K_{j,k}C_{k,M}$ is much lower than K_{j0}, *i.e.*, a low fraction of sample j is associated with the marker k.

This model was used to explain the indirect detection results obtained with progesterone as marker. Fig. 8 shows a good proportionality between $(\varepsilon^*/\varepsilon)[(1-\alpha_s)/\alpha_s]$ and $C_{k,M}$. We therefore conclude that a fraction of sample j (pregnanolone) is associated with the marker k (progesterone) on the stationary phase. This association of pregnanolone and progesterone can explain the lower sensitivity of the response for the highest concentration of progesterone as compared with that obtained with testosterone, which only exists as a free species. Indeed, $(\varepsilon^*/\varepsilon)[(1-\alpha_s)/\alpha_s]$ is not equal to θ_k but to $\theta_k[1-(K_{jk}/K_k K_{j0})]$, which explains why the sensitivity does not increase as much as with testosterone. The slopes are negative, as is the direction of the signal peak. The slopes only permit an approximate K_k calculation because K_k is decreased by $1-(K_{jk}/K_{j0})$.

We found for K_k values of 103 and 50 l mol^{-1}

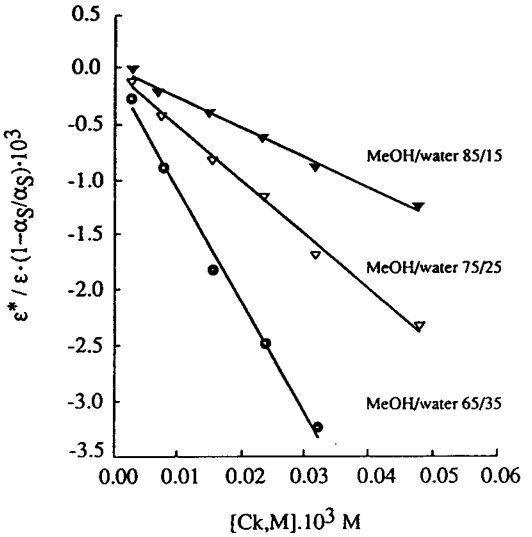

Fig. 8. Estimation of the apparent inclusion constant of progesterone from pregnanolone response. Concentration: $32 \cdot 10^{-4}$–$4.8 \cdot 10^{-2}$ mM in methanol–water mobile phases of the proportions indicated. Flow-rate, 0.6 ml min^{-1}; $\lambda = 241$ nm.

for 65:35 and 75:25 methanol–water mobile phases, respectively. These values are of the same magnitude as those determined previously by another method [10].

In conclusion, we have shown that indirect detection of pregnanolone was possible on a β-cyclodextrin stationary phase and that the models developed by Crommen [12,13] could be applied successfully to this particular stationary phase. Testosterone, which is the best marker, allowed us to detect 2 nmol of pregnanolone with methanol–water (65:35, v/v). These results can be compared with those obtained previously [10] on a C_4 column. We observed a sixfold enhancement of the signal obtained with indirect detection of the pregnanolone in the presence of 4.9 mM of β-cyclodextrin and 0.032 mM progesterone in comparison with the signal obtained at 280 nm by direct detection with methanol–water (47:53) as the mobile phase. The 2.4-fold enhancement observed in this work with the progesterone marker at 0.032 mM with methanol–water (65:35) as mobile phase, which is lower than that observed on the C_4 column, can be explained by two facts: a lower progesterone coverage on the β-cyclodextrin column than on the C_4 column, and a higher percentage of methanol in the mobile phase, which is unfavourable.

Testosterone at 0.0085 mM with methanol–water (65:35) as the mobile phase offers a sensitivity comparable to that obtained on a C_4 column with 0.032 mM progesterone with methanol–water (47:53) mobile phase. This method can be an alternative for the detection of poor UV-absorbing species, but both the sample and the marker must interact with β-cyclodextrin.

4. References

[1] D.W. Armstrong, *US Pat.*, 4 539 399 (1985).
[2] D.W. Armstrong and W. Demond, *J. Chromatogr. Sci.*, 22 (1984) 411.
[3] D.W. Armstrong, W. Demond and B.P. Czech, *Anal. Chem.*, 57 (1985) 481.
[4] C.A. Chang, H. Abdel-Aziz, N. Melchor, Q. Wu, K.H. Pannel and D.W. Armstrong, *J. Chromatogr.*, 347 (1985) 51.
[5] W.L. Hinze, T.E. Riehl, D.W. Armstrong, W. de Mond, A. Alak and T. Ward, *Anal. Chem.*, 57 (1985) 237.
[6] D.W. Armstrong, T.J. Ward, R.D. Armstrong and T.E. Beesley, *Science*, 232 (1986) 1132.
[7] D.W. Armstrong, A. Alak, K. Bui, W. Demond, T. Ward, T.E. Riehl and W.L. Hinze, *J. Inclus. Phenom.*, 3 (1985) 533.
[8] D.W. Armstrong, W. Demond, A. Alak, W.L. Hinze, T.E. Riehl and K. Bui, *Anal. Chem.*, 57 (1985) 234.
[9] C.A. Chang, Q. Wu and L. Tan, *J. Chromatogr.*, 361 (1986) 199.
[10] B. Agnus, B. Sebille and M. Gosselet, *J. Chromatogr.*, 552 (1991) 583.
[11] G. Schill and J. Crommen, *Trends Anal. Chem.*, 6 (1987) 111.
[12] J. Crommen, G. Schill and P. Herne, *Chromatographia*, 25 (1988) 397.
[13] J. Crommen, *Thesis*, University of Liège, Liège, 1989.
[14] L. Hackzell and G. Schill, *Chromatographia*, 15 (1982) 437.
[15] F.Y. Liu, D.O. Kildsig and A.K. Mitra, *Pharm. Res.*, 7 (1990) 869.

ELSEVIER

Journal of Chromatography A, 663 (1994) 35–41

JOURNAL OF CHROMATOGRAPHY A

Application of radioluminography to off-line counting of radioactivity in high-performance liquid chromatographic eluates

Shigeo Baba*[,a], Yoshikatsu Terazawa[a], Hideki Kimata[b], Yoshihiko Shinohara[a], Kazuki Akira[a], Hiroshi Hasegawa[a],

[a]*Tokyo College of Pharmacy, 1432-1 Horinouchi, Hachioji, Tokyo 192-03, Japan*

[b]*Tokyo Research Laboratories, Kowa Co., Ltd., Noguchi-cho, Higashimurayama, Tokyo 189, Japan*

(First received August 6th, 1993; revised manuscript received October 19th, 1993)

Abstract

An off-line counting method for the determination of carbon-14 in HPLC eluates was developed using radioluminography (RLG). A succession of aliquots of the eluate were collected in the flat-bottomed wells of a polystyrene microplate, evaporated to dryness and contacted with an imaging plate, and radioactivity was determined with a Bio-image analyser. The limit of detection was 0.35 Bq per injection. The inter-assay relative standard deviation was less than 3% over the range 2–20 Bq. The RLG off-line counting method was utilized to determine [^{14}C]eicosapentaenoic acid metabolites formed by rat hepatic microsomes. The results were compared with those obtained with an off-line liquid scintillation counting method and an on-line counting method.

1. Introduction

A radioisotope tracer technique using soft β-ray emitters such as carbon-14 is widely used in biological and pharmaceutical studies. In this tracer technique, HPLC has been used for the separation of compounds [1–3]. The measurement of radioactivity has been performed by fractionating the eluate in vials, mixing with a liquid scintillation cocktail and counting with a liquid scintillation counter (LSC), *i.e.*, namely the LSC off-line counting method. In order to maintain the chromatographic resolution, a large number of fractions must be collected, which requires a large volume of liquid scintillation fluid and a considerable time for counting. This method was not easily adaptable to the large number of samples that can be generated by HPLC. Karmen and co-workers [4,5] reported the collection of eluates in wells formed in a non-wetting fluorocarbon film and off-line counting by autoradiography. However, it is difficult to obtain quantitative information directly from the autoradiograms using conventional X-ray film. Radioactivity in HPLC eluates can also be monitored in real-time with a flow-through on-line detector. The method is classified into two types, homogeneous and heterogeneous. In the homogeneous counting method, the eluate is mixed with a liquid scintillation cocktail and the mixture is passed continuously through the counting cell placed between a pair of photo-

* Corresponding author.

0021-9673/94/$07.00
SSDI 0021-9673(93)E1095-H

multiplier tubes. In the heterogeneous counting method, the eluate is passed through a cell packed with a solid scintillator. However, these types of detectors do not permit a simultaneous improvement in both the detection sensitivity and the chromatographic resolution.

Recently, radioluminography (RLG) [6,7] using an imaging plate (IP) had made possible the measurement of β-ray emitters on TLC plates and in tissue slices [8,9]. The IP is composed of polyester film coated with microcrystals of a photostimulable phosphor ($BaFBr:Eu^{2+}$) which memorizes the energy of radioactivity in the form of quasi-stable colour centres and emits photostimulated luminescence (PSL) by laser beam stimulation with its intensity proportional to the absorbed radiation energy. By digitizing the intensity of the emission, a digital image showing the radioactivity distribution is obtained. Data analysis including scanning can be completed in *ca.* 3 min for an IP. The image stored on the IP can be easily erased by irradiation with visible light, allowing repeated use. The sensitivity of IP was shown to be over 100 times higher than that of X-ray film, and further IP has a considerably wider dynamic range than X-ray film [8].

VanRollins *et al.* [10] reported the HPLC determination of [^{14}C]eicosapentaenoic acid (EPA) metabolites formed by rat hepatic microsomes using the LSC off-line counting method. As a single injection generated about 550 fractions, it required 4 days for counting and produced about 3000 ml of scintillation waste per chromatographic analysis. In the previous paper [11], we proposed a method alternative to LSC for detecting carbon-14 using RLG. The method involves placing an aqueous radioisotope sample in flat-bottomed wells of a polystyrene microplate, evaporating the solvent and determining the radioactivity in each well using RLG. This method permitted the detection of the radioactivity of several hundred samples simultaneously and required no scintillation fluids. These advantages are useful for the off-line counting of radioactivity in HPLC eluates. This paper describes the determination of [^{14}C]EPA metabolites with rat hepatic microsomes by HPLC to assess the feasibility of the RLG off-line counting method.

2. Experimental

2.1. Materials

Eicosapentaenoic acid (EPA) was purchased from GL Sciences (Tokyo, Japan). [1-^{14}C]EPA (specific radioactivity 2.05 GBq/mmol) was purchased from American Radiolabeled Chemicals (St. Louis, MO, USA). This compound was diluted with non-labelled EPA to give an ethanol solution of 27.6 MBq/mmol (100 Bq per 0.1 ml). Working standard solutions were prepared by diluting the solution with ethanol to give radioactivity concentrations of 5, 0.5, 0.35, 0.05 and 0.005 Bq/μl. Polystyrene flat-bottomed microplates (85 × 127 mm) with 48 wells (11.3 mm in diameter) were purchased from Costar (Cambridge, MA, USA) and the depth of the wells was adjusted to 5.0 mm by cutting the plates horizontally.

2.2. HPLC system and conditions

A block diagram of the HPLC system is shown in Fig. 1. The HPLC system consisted of two Shimadzu (Kyoto, Japan) LC-6A pumps, a Shimadzu SLC-6B system controller, a Rheodyne Model 7125 injector and a Shimadzu SPD-6A UV spectrophotometric detector. The column was LiChrosorb RP-18 (7 μm; 250 × 4 mm I.D.) (Merck, Darmstadt, Germany). The

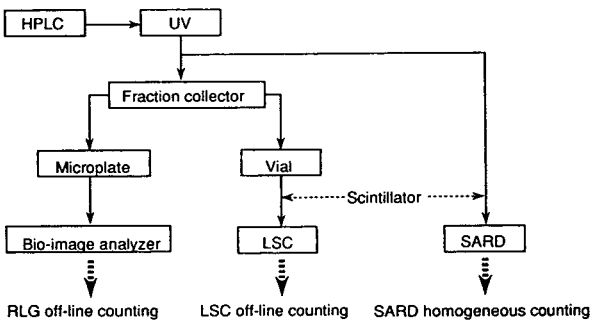

Fig. 1. Block diagram of HPLC system.

mobile phases were (A) 0.1% trifluoroacetic acid (TFA) in water and (B) 0.1% TFA in acetonitrile. Elution was performed isocratically with a solution of 15% of solvent A in solvent B, except for the determination of [^{14}C]EPA metabolites, which was carried out by gradient elution as indicated in Fig. 4. The flow-rate was 1 ml/min in each instance.

2.3. RLG off-line counting

The HPLC eluate was fractionated into the wells of microplates at 10-s intervals (20-s intervals for the determination of [^{14}C]EPA metabolites) using a Gilson (Middleton, WI, USA) Model 222 fraction collector. The microplates were allowed to stand for 5–12 h at room temperature for evaporation of the solvent. The samples were overlaid with Diafoil plastic film (0.52 mg/cm^2) (Mitsubishi, Tokyo, Japan) and contacted with an IP (20 × 40 cm) in the brass chamber (30 × 50 × 3 cm; thickness 1 cm) for 24 h. The absorbed dose recorded on the IP was quantified using a BAS-2000 Bio-image analyser (Fuji Film, Tokyo, Japan).

2.4. LSC off-line counting

The HPLC eluate was collected in Minivials at 10-s intervals using a Gilson fraction collector. A 3-ml volume of a hydrophilic liquid scintillation cocktail (dioxane–toluene–ethyl Cellosolve (75:15:10, v/v/v) containing 100 g of naphthalene, 4 g of 2,5-diphenyloxazole and 0.4 g of 1,4-bis[2-(5-phenyloxazoyl)]benzene per litre) was added to each Minivial. The radioactivity was counted for 3 min per sample in an Aloka (Tokyo, Japan) LSC-1000 liquid scintillation counter.

2.5. Homogeneous counting

The HPLC eluate was mixed with a fivefold volume of the hydrophilic liquid scintillation cocktail and the mixture (6 ml/min) was passed through an Aloka synchronized accumulating radioisotope detector (SARD) [12,13]. The SARD was composed from five counting cells with a 1-ml cell volume and five pairs of photomultiplier tubes.

2.6. Cross-talk ratio between wells

A 100-Bq amount of [^{14}C]EPA in 0.1 ml of ethanol was applied to a well of the microplate and was allowed to stand for 5 h at room temperature for evaporation of the solvent. The sample was overlaid with a Diafoil and contacted with the IP in the brass chamber for 24 h. The absorbed dose recorded on the IP was measured with the BAS-2000.

2.7. Preparation of rat hepatic microsomes

Rat hepatic microsomes were prepared by the method of VanRollins and co-workers [10,14]. In brief, a Wistar male rat (*ca.* 200 g) was given daily intraperitoneal injections for 3 days of 10% phenobarbital in saline (0.1 ml per 100 g body mass). After the third injection, the rat was deprived of food overnight. The rat was decapitated 24 h after the last injection and the liver was removed. All subsequent steps were performed at 0–4°C. The liver was homogenized (0.25 g/ml) in a buffered salt solution consisting of 150 m*M* KCl and 50 m*M* Tris–HCl (pH 7.5). The homogenate was centrifuged at 10000 *g* for 10 min. The supernatant was then centrifuged at 105 000 *g* for 60 min. The microsomal pellets were washed once, resuspended in buffer (6–8 μg protein/ml) and stored at −80°C.

2.8. Incubation of [^{14}C]EPA with rat hepatic microsomes

A 1-ml volume of 1 m*M* NADPH was added to 0.5 ml of the microsomes and the solution was incubated at 37°C for 3 min. To the solution were added 8.33 kBq of [^{14}C]EPA in 50 μl of 0.01 *M* $NaHCO_3$ and the mixture was incubated at 37°C for 20 min. Reaction was stopped by the addition of 2 ml of ice-cold ethanol. The mixture was centrifuged at 1000 *g* for 20 min at 4°C and the pellets were suspended in ethanol and recentrifuged. The washing step was repeated twice and the combined supernatants were con-

centrated and acidified with formic acid to pH 3. Separation of EPA metabolites from the samples was performed as described previously [15]. In brief, the solution was applied to a Sep-Pak C_{18} cartridge (Waters, Milford, MA, USA) which was washed with 5 ml each of methanol and water immediately before use. The cartridge column was washed with 10 ml each of water, 5% ethanol in water and light petroleum and then eluted with 6 ml of methyl formate. The eluate was evaporated to dryness under a stream of nitrogen. The residue was dissolved in 50 μl of ethanol and aliquots of the solution were injected into the HPLC column.

3. Results and discussion

The feasibility on the present RLG off-line counting method was determined by injecting [^{14}C]EPA into the HPLC column. Elution was performed with acetonitrile–water–TFA (85:15:0.1, v/v/v) at 1.0 ml/min and the eluate was collected in the wells of microplates at 10-s intervals. The solvents (167 μl per well) could be evaporated by standing overnight at room temperature. Fig. 2A shows a representative radioluminogram. The intensity of PSL in the images is proportional to the number of β-particles registered from the samples in the wells. As each image was placed in order of separation, a chromatogram (Fig. 2B) was obtained by processing the radioluminogram.

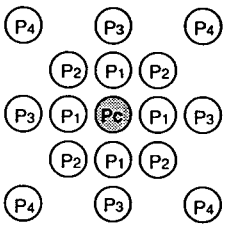

Fig. 3. Scanned area for cross-talk examination.

If high radioactivity exists in a well, an unexpected high intensity of PSL may be obtained over the adjacent wells, that is "cross-talk" between wells occurs. In order to access the cross-talk, 100 Bq of [^{14}C]EPA were applied homogeneously to a well of a microplate and the intensity of PSL in the surrounding wells (Fig. 3) was measured. The cross-talk ratios (Table 1) were negligibly small and were calculated using the following equation:

$$\text{cross-talk } (\%) = \frac{PSL_n - PSL_{B.G.}}{PSL_{centre} - PSL_{B.G.}} \cdot 100$$

The accuracy of the RLG off-line counting method was determined over the range 0.35–20

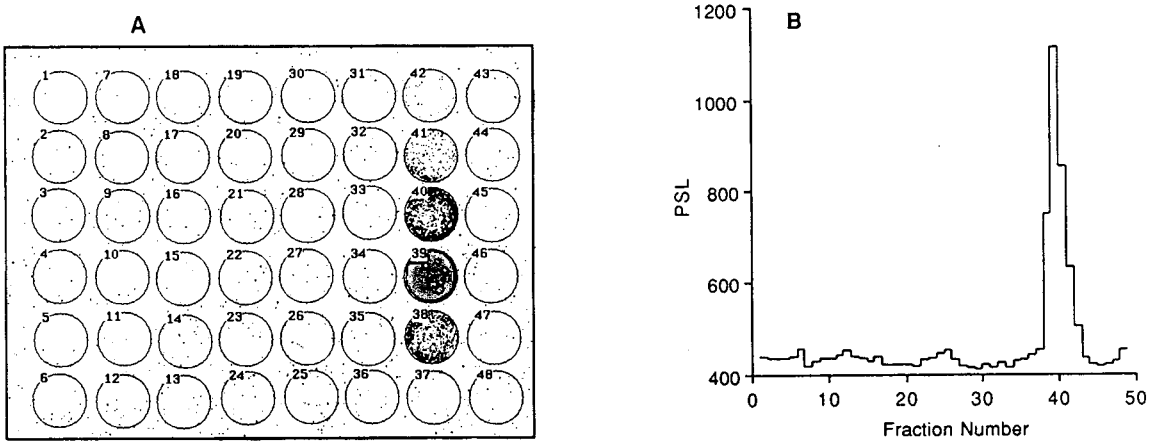

Fig. 2. (A) Radioluminogram and (B) chromatogram following the injection of 15 Bq of [^{14}C]EPA into the HPLC system. HPLC was performed on a LiChrosorb RP-18 (7 μm; 250 × 4 mm I.D.) column with acetonitrile–water–TFA (85:15:0.1, v/v/v) at a flow rate of 1 ml/min. The eluate was collected in the wells of a microplate at 10-s intervals. The plate was exposed with an IP for 24 h.

Table 1
Cross-talk ratio between wells

Position No.[a]	PLS		Cross-talk (%)
	Mean ± S.D.	R.S.D. (%)	
P_{centre}	13702.1[b]		
P_1	289.5 ± 10.8	3.7	0.098
P_2	282.4 ± 2.4	0.8	0.045
P_3	279.7 ± 4.0	1.4	0.024
P_4	276.8 ± 3.6	1.3	0.003
$P_{B.G.}$	276.4 ± 4.2[c]	1.5[c]	

[a] The numbers of the wells are shown in Fig. 3.
[b] The PSL value corresponded to 100 Bq of [^{14}C]EPA placed in the P_{centre} well.
[c] The value was obtained with the wells of the same microplate except P_{centre} and P_n ($n = 1$–4).

Bq of [^{14}C]EPA. There was strict linearity between the values of PSL and the radioactivity injected into the HPLC column. The results were compared with those from other methods (LSC off-line counting method and a homogeneous counting method by SARD), as shown in Table 2. The inter-assay relative standard deviations (R.S.D.s) in the RLG method were constant and less than 3% regardless of the radioactivity over the range 2–20 Bq of [^{14}C]EPA injected. On the other hand, the R.S.D.s in the LSC off-line counting method and the homogeneous counting method became progressively greater as the amounts of radioactivity decreased. The reason may be that the number of radioactive decays for a constant period of 24 h in the RLG method is so high as to make statistical variations irrelevant. In the RLG method, the detection limit was reported to be *ca.* 0.2 Bq for ^{14}C [11]. Further studies demonstrated that the background was reduced by exposure in a brass chamber and the detection limit could be decreased to 0.05 Bq. The limit of detection for [^{14}C]EPA in the present HPLC method was *ca.* 0.35 Bq injected. This is smaller than those of the LSC off-line counting method (0.7 Bq) and the homogeneous counting method (2 Bq).

Table 2
Comparison of accuracy ($n = 3$) among the RLG off-line counting method, the LSC off-line counting method and the SARD homogeneous counting method

Injected amount (Bq)	RLG		LSC[a]		SARD	
	PSL	R.S.D. (%)	dpm	R.S.D. (%)	cpm	R.S.D. (%)
0.35	39.6	4.6	n.d.[b]		n.d.[b]	
0.7	66.0	3.1	57.3	6.4	n.d.[b]	
2.0	189.2	3.0	132.4	12.9	122.0	9.7
5.0	561.1	2.8	304.6	5.0	264.3	7.3
10.0	1138.2	1.7	550.6	8.0	531.0	2.6
15.0	1720.2[c]	2.0[c]	807.6[c]	3.7[c]	732.4[c]	2.1[c]
20.0	2292.5	2.6	1068.2[d]	1.4[d]	885.7	2.0

[a] Counting time 3 min.
[b] Not detected.
[c] $n = 5$.
[d] $n = 4$.

To assess the feasibility of using the RLG off-line counting method, the determination of [^{14}C]EPA metabolites formed by rat hepatic microsomes was performed. [^{14}C]EPA metabolites were prepared by the method of VanRollins *et al.* [10]. Sep-Pak C_{18} cartridges were used to separate EPA metabolities from biological samples as described previously [15]. About 833 Bq of the sample were injected into the HPLC column. As the eluate was collected in the wells of microplates at 20-s intervals from 15 min to 225 min after injection, twelve sheets of the microplates (576 wells) were used per injection. After the solvents (333 μl per well) had evaporated, the samples were exposed with two sheets of IP because an IP can be contacted with six sheets of the microplates. On the other hand, equal amounts of [^{14}C]EPA metabolite sample were analysed by SARD, in which an improvement by a factor of $\sqrt{5}$ in detection accuracy was achieved without sacrificing the chromatographic resolution as compared with conventional detector [12,13]. Fig. 4 shows the chromatograms obtained by the RLG off-line counting method and the homogeneous counting method. Although there was no appreciable difference between the two chromatograms for the separation of the metabolites, the signal-to-noise ratio in the RLG off-line counting method was better. The homogeneous counting method has the advantage that it can yield immediate access to data. However, it produced about 1200 ml of liquid scintillation waste per injection. In the RLG off-line counting method, no scintillation fluid was required and the used plates were disposed of easily because they were flammable and inexpensive. Although about 2 days were required to obtain the data (5–12 h for evaporation, 24 h for contact and 3 min for data analysis including scanning with the BAS-2000, many chromatograms could be obtained in this period because the time for evaporation and contact could be kept almost constant regardless of the number of samples. This suggested that the RLG off-line counting method is a useful method for the routine analysis of radioactive samples requiring long analysis times.

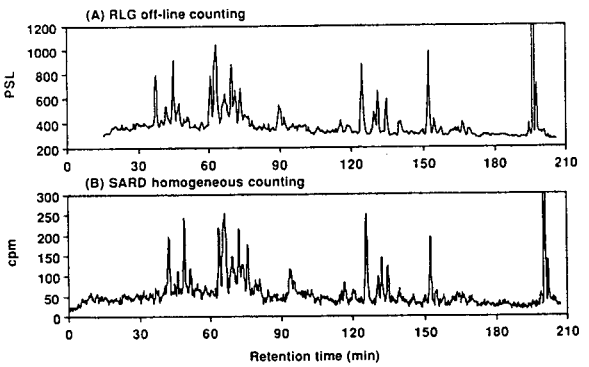

Fig. 4. Chromatograms obtained by (A) RLG off-line counting method and (B) SARD homogeneous counting method after injecting 833 Bq of [^{14}C]EPA metabolities formed by rat hepatic microsomes. Chromatographic conditions: column, LiChrosorb RP-18 (7 μm; 250T × 4 mm I.D.); mobile phase, (A) 0.1% TFA in water and (B) 0.1% TFA in acetonitrile; flow-rate, 1 ml/min. Elution was carried out with a stepwise linear gradient from 30 to 50% solvent B over 180 min, from 50 to 100% solvent B over 10 min and isocratic at 100% solvent B for 30 min. In (A) the fraction interval was 20 s.

The proposed method provided high sensitivity and a reliable procedure for determining the radioactivity of several hundred fractions simultaneously. As no scintillation cocktail is required in this method, the volume of radioactive waste produced per analysis is much smaller than that in the LSC off-line method. In addition, the radioactive compounds can be recovered from the wells and re-analysed by other methods.

4. References

[1] T.R. Roberts, *Radiochromatography —the Chromatography and Electrophoresis of Radiolabelled Compounds* (*Journal of Chromatography Library*, Vol. 14), Elsevier, Amsterdam, 1978.

[2] A.R. Reich, S. Lucas-Reich and H. Parvez, in H. Parvez, A.R. Reich, S. Lucas-Reich and S. Parvez (Editors), *Flow Through Radioactivity Detection in HPLC* (*Progress in HPLC*, Vol. 3), VSP, Utrecht, 1988, p. 1.

[3] A.C. Veltkamp, in K. Zech and R.W. Frei (Editors), *Selective Sample Handling and Detection in High-Performance Liquid Chromatography*, Part B (*Journal of Chromatography Library*, Vol. 39B), Elsevier, Amsterdam, 1989, p. 133.

[4] A. Karmen, G. Malikin and S. Lam, *J. Chromatogr.*, 302 (1984) 31.

[5] A. Karmen, G. Malikin, L. Freundlich and S. Lam, *J. Chromatogr.*, 349 (1985) 267.
[6] Y. Amemiya, K. Wakabayashi, H. Tanaka, Y. Ueno and J. Miyahara, *Science*, 237 (1987) 164.
[7] Y. Amemiya and J. Miyahara, *Nature*, 336 (1988) 89.
[8] K. Kawai, E. Nakajima and T. Komai, *Sankyo Kenkyusho Nempo*, 40 (1988) 101.
[9] Y. Ito, Y. Sugawara, O. Takaiti and S. Nakamura, *J. Pharmacobio-Dyn.*, 14 (1991) 547.
[10] M. VanRollins, P.D. Frade and O.A. Carretero, *Biochim. Biophys. Acta*, 966 (1988) 133.
[11] S. Baba, H. Kimata, S. Haruki and Y. Shinohara, *Appl. Radiat. Isot.*, 44 (1993) 1011.
[12] S. Baba, M. Horie and K. Watanabe, *J. Chromatogr.*, 244 (1982) 57.
[13] S. Baba, Y. Suzuki, Y. Sasaki and M. Horie, *J. Chromatogr.*, 392 (1987) 157.
[14] M. VanRollins, R.C. Baker, H.W. Sprecher and R.C. Murphy, *J. Biol. Chem.*, 259 (1984) 5776.
[15] K. Akira, T. Nakamura, Y. Shinohara and S. Baba, *Lipids*, 28 (1993) 361.

Journal of Chromatography A, 663 (1994) 43–51
Elsevier Science B.V., Amsterdam

CHROM. 25 625

Reversed-phase high-performance liquid chromatography assay for recombinant acidic fibroblast growth factor in *E. coli* cell suspensions and lysate samples

P. DePhillips* B. Buckland, K. Gbewonyo, S. Yamazaki and R. Sitrin

Merck Research Labs, P.O. Box 4, West Point, PA 19406 (USA)

(First received July 16th, 1993; revised manuscript received October 5th, 1993)

ABSTRACT

A reversed-phase HPLC assay for acidic Fibroblast Growth Factor (aFGF) expressed in *E. coli* is described. The assay was developed on a Polymer Labs. PLRP-S macroporous poly(styrene-benzene) column. A sample preparation procedure was developed to permit quantitation of aFGF in crude samples, such as cell suspensions and cell lysates. The assay was linear over the range of 25–140 μg/ml with an accuracy of 5%. By using a POROS column containing a stationary phase with "through-pores" and a superficial mobile phase velocity of 1440 cm/h, the analysis could be performed in 3 min. The polymeric supports used for this assay were durable; periodic washing with sodium hydroxide maintained column performance for extended periods.

INTRODUCTION

In order to develop and subsequently validate a large-scale recombinant protein purification process, a careful and detailed evaluation of the process performance is required. Typically, during the development phase of a multi-step purification process, dozens of in-process samples may be generated for analysis of purity and recovery. Early on, when many possible steps are being simultaneously evaluated for possible inclusion, the length of time required for this analysis can be considerable, and can dictate to a significant extent the overall development time. Developing fast assays, or assays that require minimal sample preparation but are nonetheless applicable throughout the process, is therefore an important aspect of any process development effort.

In the case of *E. coli* derived proteins, determining host cell expression levels, monitoring fermentations, and optimizing a capture step requires that the concentration of a target protein be accurately determined in cell suspensions or cell lysates. Analysis of samples such as these, in complex matrices with high levels of endogenous protein, lipids, DNA and other cellular contaminants, can be problematic. Enzyme or biological assays may require substantial sample purification prior to assay and can give misleading information when truncated or chemically modified products are present. Immunoassays, such as ELISA [1], and particle concentration fluorescence assays [2] have been used to quantitate protein concentrations in crude samples. In most cases however these may require specialized reagents and equipment, such as antibodies, and are difficult to automate. SDS-PAGE is slow, difficult to quantitate and offers limited sample throughput.

Reversed-phase HPLC offers very high res-

* Corresponding author.

0021-9673/94/$07.00
SSDI 0021-9673(93)E1065-8

olution, sensitivity and precision and has often been applied to difficult protein separation problems. It is a valuable method for in-process monitoring, and for determination of chemical modification [3], protein conformation, or enzymatic degradation. In addition, HPLC systems are widely available and completely automated. For the crude samples described above however, silica-based reversed-phase columns may lose efficiency and resolution very rapidly due to non-specific adsorption of contaminants. They are also difficult to clean once degraded. Recently, polymer-based reversed-phase columns have been developed and utilized [4] for protein separations. Polymeric columns have exhibited higher recoveries [5], and increased column stability at both low and high pHs [6,7]. As we will demonstrate, polymeric columns appear much less prone to degradation with crude samples, and can be regenerated easily and repeatedly. By using these supports, the benefits of RP-HPLC, namely high speed, high resolution, and high recovery, along with complete automation, can be applied to samples generated through a protein purification process, including very crude early stage samples (cell suspensions and lysates).

We describe herein the assay of acidic fibroblast growth factor, (aFGF) [8,9] in both cell suspensions and cell lysates, as well as a rapid sample preparation procedure applicable for both cell lysate samples and cell suspensions. The method was evaluated for linearity, accuracy, precision and specificity. With some modification, the method was adapted for high-speed analysis.

EXPERIMENTAL

HPLC grade acetonitrile was obtained from J.T. Baker (Phillipsburg, NJ, USA). Trifluoroacetic acid was obtained from Pierce (Rockford, IL, USA). Water was obtained from a Millipore Milli-Q system (Bedford, MA, USA). Ultrapure grade guanidine hydrochloride was obtained from Bethesda Research Laboratories (Gaithersburg, MD, USA).

A polymeric PLRP-S column 50 mm × 4.6 mm I.D. with a particle diameter of 8 μm and nominal pore size of 300 Å was obtained from Polymer Laboratories (Amherst, MA, USA). A POROS RP/H column 50 mm × 4.6 mm I.D. was obtained from PerSeptive Biosystems (Cambridge, MA, USA).

The gradient HPLC system consisted of two Rainin Rabbit pumps, a Macintosh SE computer with Rainin Dynamax HPLC Method Manager software (version 1.1), a Gilson Model 811 gradient mixer, and a Gilson Model 231 autosampler. The autosampler rack was chilled by a Lauda circulating chiller to a temperature of 6°C. Columns were heated to 60°C by an Eldex lCH-150 column heater unless indicated otherwise. A Gilson Model 116 UV detector set at 280 nm was used for detection.

Cell disruptions were carried out with a Manton Gaulin Laboratory Homogenizer (Model 15M-8TA).

Preparation of aFGF stock solutions in PBS

Purified aFGF in phosphate buffered saline (PBS) from a trial purification process was concentrated using an Amicon Centriprep 10 (Amicon, Beverly, MA, USA) membrane to a final concentration of 14.0 mg/ml. The concentrated stock solution was diluted in PBS to obtain stock solutions of 2.5, 5.0, 7.0 and 10.0 mg/ml.

Preparation of aFGF standards and control samples

Preparation of blank cell lysate. E. coli cells of the same host strain used for aFGF expression but without the aFGF plasmid were suspended in PBS (1:4, v/v). The suspended cells were lysed by two passes through a Manton Gaulin Homogenizer operated at a pressure of 9000 p.s.i. (1 p.s.i. = 6894.76 Pa). The resultant cell lysate was aliquoted and stored at − 70°C until use.

Preparation of aFGF standards in blank cell lysate. The aFGF stock solutions described above were diluted 1 in 100 with blank cell lysate to obtain standards with final aFGF concentra-

tions of 25, 50, 70, 100, and 140 μg/ml cell lysate.

Preparation of aFGF control samples in blank cell lysate. Stock solutions of 2.5, 7.0, and 14.0 mg/ml were diluted 1 in 100 with blank cell lysate to obtain 3 control standards with aFGF concentrations of 25 (Low control), 70 (Mid control), and 140 (High control) μg aFGF/ml blank cell lysate. Five samples were prepared for each control concentration.

Sample preparation procedures

Cell lysate samples. In-process aFGF lysate samples were prepared by passing cell suspensions two times through a Manton Gaulin Laboratory Homogenizer at a pressure of 9000 p.s.i. To prepare cell lysate samples for HPLC assay, an aliquot of lysate (100 μl) is placed in a 1.5-ml microcentrifuge tube. 7 *M* guanidine hydrochloride (200 μl) with 5 m*M* DTT (dithiothreitol) is added and vortexed. After mixing, 500 μl of acetonitrile–7 *M* guanidine–TFA (20:80:0.2, v/v/v) is added to the same tube and vortexed, then centrifuged for 5 minutes (10 000 *g*). The supernatant is removed and placed in an autosampler vial.

Chemical cell disruption. Frozen cell paste samples were thawed and suspended in 4 volumes of PBS buffer then vortexed for 30 s. A 500-μl aliquot of each of the samples of suspended cells was added to 4.0 ml of 7 *M* guanidine hydrochloride containing 5 m*M* DTT and rotated for 10 min. After rotation, an aliquot (300 μl) was placed in a 1.5-ml microcentrifuge tube. The sample is then vortexed with 500 μl of acetonitrile–7 *M* guanidine–TFA (20:80:0.2) and centrifuged for 5 min (10 000 *g*). The supernatant is removed and placed in an autosampler vial.

Whole fermentation broth samples were centrifuged for 5 min (10 000 *g*). The resulting cell pellets were resuspended in 2 to 4 volumes of PBS and vortexed for 30 s. The resulting cell suspension was prepared as noted above for resuspended frozen cell paste samples.

HPLC methods

For the Polymer Labs PLRP-S column the HPLC assay was performed using a two-stage linear gradient. Following injection the gradient increased linearly from 8% acetonitrile–0.1% TFA to 28% acetonitrile–0.1% TFA over 1 min then linearly to 42% acetonitrile–0.1% TFA over 14 min at a flow rate of 2 ml/min throughout. The injection volume was 100 μl. Column temperature was maintained at 60°C.

For the POROS RP/H column the gradient increases linearly from 8% acetonitrile–0.1%TFA to 28% acetonitrile–0.1% TFA over 20 s, then linearly to 41% acetonitrile–0.1% TFA over 2 min 25 s, at a flow rate of 4 ml/min throughout. The injection volume was 20 μl. Column temperature was maintained at 60°C.

Assessment of linearity, precision, specificity, viability and column durability

The aFGF standards prepared in blank cell lysate were assayed to determine linearity. The five replicates of the control samples were assayed to assess variability in the method. Specificity was determined by comparison of a blank cell lysate sample to the spiked standards. Column durability was determined by making 40 injections of a cell lysate sample and comparing retention times and peak areas for these injections.

RESULTS AND DISCUSSION

Sample preparation procedure

To develop and optimize a capture step for aFGF, it was necessary to quantitate the amount of aFGF present in lysate samples obtained from pilot scale cell breakages. To determine the mass of aFGF present in these samples with a high degree of accuracy (± 5%) presented problems because no enzymatic assay existed and the mitogenic bioassay [8] could not be used because of interference of *E. coli* lipopolysaccharide in the sample. It was therefore desirable to develop a sample preparation procedure that would allow for quantitation by HPLC.

aFGF has limited solubility at the low pH typically used for reversed-phase chromatography and, at concentrations encountered in cell

lysates, can precipitate when the pH is rapidly lowered. The addition of 200 μl 7 *M* guanidine to 100 μl of cell lysate produces a final guanidine concentration of about 4.6 *M*. At this guanidine concentration, aFGF unfolds rapidly; this unfolded aFGF is soluble at low pH and does not precipitate upon subsequent acidification. This high guanidine concentration should also assist in disassociation of any aFGF in electrostatic aggregation with cell constituents as well as solubilization of inclusion bodies if present. This unfolding/disaggregation step proved critical to the entire sample preparation scheme; if omitted, the recovery of aFGF was drastically lowered for these samples. When 6 *M* urea was substituted for guanidine, the yield of aFGF in lysate samples was higher than obtained with omission of the unfolding/disaggregation step, but not as high as obtained with guanidine. High concentration of urea was less effective in dissociating electrostatic interactions between aFGF and cell constituents, resulting in loss of aggregated aFGF. After unfolding, the solution is acidified by addition of acetonitrile–7 *M* guanidine–TFA (20:80:0.2), and centrifuged at high speed to remove insoluble material.

A chromatogram of a typical cell lysate sample is shown in Fig. 1A. The aFGF peak is well resolved from all the *E. coli* contaminants, which are confined to the early portion of the gradient and the portion of the gradient used to clean off the column between injections, thereby producing a clean chromatographic profile amenable to accurate quantitation.

The method is specific for aFGF. When a blank *E. coli* cell paste that does not express aFGF is prepared, no interfering peaks are detected in the region of aFGF elution, as shown in Fig. 1B.

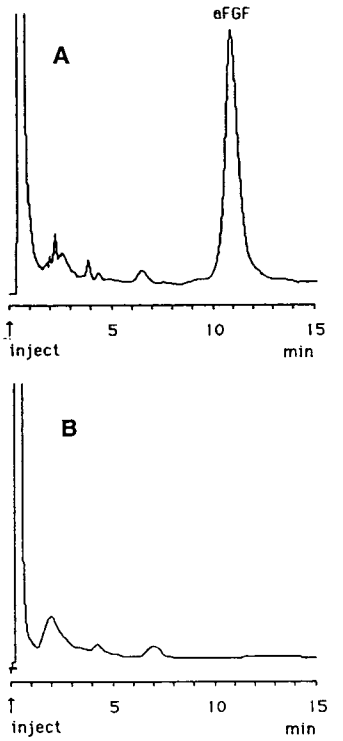

Fig. 1. Chromatographic profiles of an aFGF cell lysate sample (A) and a blank cell lysate sample (B) containing no aFGF. No interference peaks were detected in the aFGF region of the blank cell lysate. Preparation of samples is described under Sample preparation procedures. Chromatographic conditions: Polymer Labs PLRP-S column (50 mm × 4.6 mm I.D.); eluent A, 0.1% TFA in water, eluent B 0.1% TFA in 80:20 acetonitrile–water; two-stage linear gradient program, 1 min linear gradient from 10 to 35% B; followed by a 14-min linear gradient from 35 to 52% B at a flow rate of 2 ml/min throughout. Injection volume 100 μl for each, detection wavelength 280 nm.

Linearity, accuracy, precision and specificity

A standard curve prepared from the spiked cell lysate standards described in Experimental is shown in Fig. 2. The regression coefficient of 0.999 for the least-squares fit to the data is quite good considering the crude state of the samples and demonstrates linearity for the concentration range of 25–140 μg aFGF/ml.

Data from the spiked control samples are shown in Table I. Five replicate samples were prepared for each concentration level. The low control standard, with a nominal concentration of 25.0 μg/ml shows a mean measured concentration of 26.2 μg/ml, with an R.S.D. of 5.4%. The mid control standard with a nominal concentration of 70.0 μg/ml shows a mean measured concentration of 70.2 with an R.S.D. of 2.0%. The high control standard, with a nominal concentration of 140.0 μg/ml shows a mean measured concentration of 136.0 μg/ml, with an R.S.D. of 3.0%. The percentage difference be-

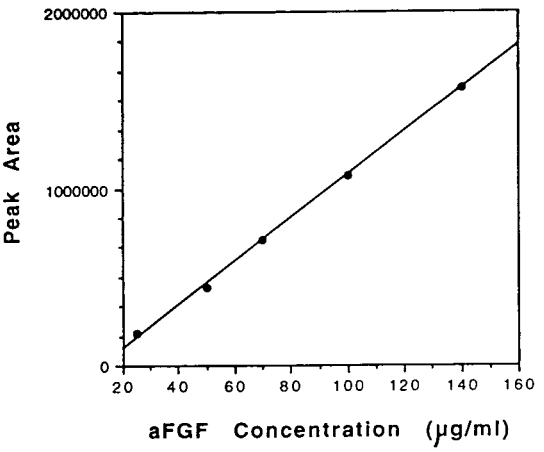

Fig. 2. A five-level calibration curve prepared from aFGF standards. Preparation of aFGF standards is described under Preparation of aFGF standards and control samples. Chromatographic conditions as in Fig. 1.

tween the nominal and measured concentration was under 5.5% for all concentration levels, which was within the desired accuracy range.

Repeatability and column degradation

The ability to process multiple samples from crude matrices can be difficult due to column degradation. Initial attempts to develop this assay on silica based reversed-phase columns were unsuccessful: these columns were significantly and irreversibly degraded after fewer than 10 injections of lysate samples prepared as described above (data not shown).

Polymeric supports have been shown to give higher protein recoveries and significantly longer lifetimes [5–7]. In addition, these supports can be regenerated with sodium hydroxide to restore performance. The durability of the PLRP-S column was tested by making 40 consecutive injections of a prepared lysate sample. Both the retention times and peak areas obtained for these injections were very stable. The average peak area was 2 169 209 uV ± 27 076 uV, the R.S.D. value is therefore less 1.3%, indicating that prepared lysate samples do not appreciably degrade the column over at least 40 consecutive injection cycles. Fig. 3 shows an overlay of the chromatograms of the first and fortieth injection of prepared lysate; peak shape is virtually identical, and more importantly, the peak area of the first and fortieth injection were within 1.5%. Following these injection sequences, blank gradients showed no evidence of "ghosting". For this assay application the polymeric column proved to be more resistant to degradation than silica-based columns, in practice this allowed for heavy use. Periodic (bimonthly) washing with 60

TABLE I

DATA FROM SPIKED CONTROL SAMPLES

Five samples were prepared for each control concentration.

Sample	Measured concentrations (μg/ml)		
	Low control (25 μg/ml)	Mid control (70 μg/ml)	High control (140 μg/ml)
1	26.3	69.9	138.4
2	25.9	69.3	131.6
3	28.7	70.8	129.6
4	24.4	68.7	137.0
5	25.7	72.3	138.3
Mean	26.18	70.20	135.99
S.D. (μg)	1.4	1.4	4.1
R.S.D. (%)	5.3	2.0	3.0
Diff. (%)	4.7	0.2	2.9

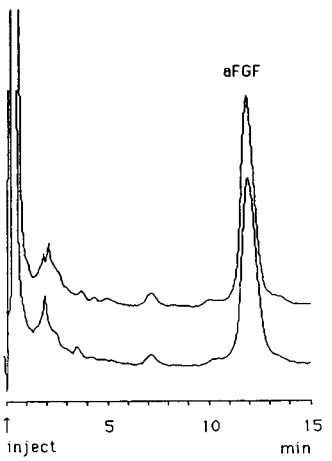

Fig. 3. Comparison of the 1st (lower trace) and 40th (upper trace) chromatograms obtained from consecutive injections of a cell lysate sample. Peak areas and retention times for aFGF remained stable through the injection series. Chromatographic conditions as in Fig. 1.

ml of methanol–0.2 *M* NaOH (1:1, v/v) prevented deterioration in peak height and separation quality.

Comparison of mechanical and chemical disruption of cells

In order to rapidly prepare cell paste and cell suspensions for HPLC assay, a guanidine disruption procedure was developed as described in Experimental. Chaotropic agents such as guanidine are commonly and effectively used to solubilize protein samples prior to assay [7]. Recently, guanidine has also been shown to be capable of releasing protein from intact *E. coli* by solubilizing the inner membrane and altering the outer wall to allow protein release without causing cell fragmentation [10]. Since preserving native conformation through the sample pretreatment is neither required nor desirable for this aFGF assay, very high guanidine concentrations were examined for aFGF release. The release and solubilization of aFGF from chemically disrupted cells was compared to that obtained by mechanical disruption. Frozen cells were resuspended in PBS buffer (1:4, v:v). A sample of this suspension was retained and the remainder lysed by two passes through a Manton Gaulin at 9000 p.s.i. The retained cells were chemically disrupted by adding 500 μl of cell suspension to 4 ml of 7 *M* guanidine and rotating at room temperature for 20 min. Samples were prepared in triplicate for both the chemically and mechanically disrupted cell suspensions. The assay results were normalized to account for the difference in total dilution between the two disruption methods. The mean concentration for chemically disrupted cells was 97% of the value obtained for mechanically disrupted cells (S.D. = 3.4%), indicating that the chemical disruption is as effective as homogenization in causing release of aFGF from the cells.

Fig. 4 shows a typical chromatogram of a chemically disrupted cell suspension. The chromatographic profile of this sample is virtually identical to the profile obtained by mechanical disruption (Fig. 1A), with no contaminants eluting in the region of aFGF. The addition of 500 μl of cell suspension to 4 ml of 7 *M* guanidine results in a final guanidine concentration of about 6 *M*. As with the sample preparation of cell lysates described earlier, it is envisioned that disruption of cells in the presence of a high concentration of a charged chaotrope will enhance both the solubilization of inclusion bodies and the disaggregation of aFGF from cellular constituents. Since the chemical disruption procedure is so simple, multiple samples can be rapidly processed.

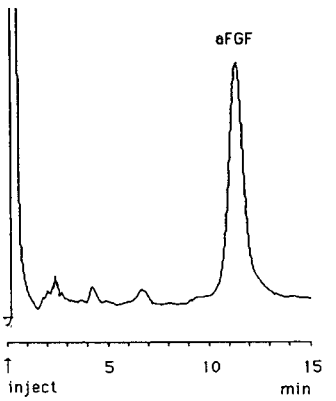

Fig. 4. The chromatogram of a cell suspension sample. The sample was chemically disrupted by guanidine HCi as described under Chemical cell disruption. Chromatographic conditions as in Fig. 1.

Monitoring fermentations and determining aFGF expression levels

In the development of a bacterial fermentation process both the yield and quality of a target protein need to be determined for different expression systems and under differing fermentation conditions to optimize product expression. A rapid, accurate assay for the target protein that can differentiate small changes in product concentration can greatly enhance this development process. The chemical disruption of cell suspensions followed by the sample pretreatment method described above have been applied to this fermentation effort for aFGF.

By removing small samples from active fermentations at different time points, the aFGF production in fermentors can be followed. In a typical analysis, whole broth samples are centrifuged to obtain a cell pellet. Equivalent cell mass samples are generated for each time point.

A comparison of aFGF concentration per cell mass can then be made. The production of aFGF in a fermentor monitored at 12, 14, and 16 h after induction is shown in Fig. 5. The aFGF titers could be accurately quantitated through the entire fermentation; because the chemical lysis and sample preparation procedures are simple and can be performed quickly, this information can be obtained concurrently with the fermentation. The ability to accurately determine aFGF levels in cell suspensions allowed for fermentation conditions to be more readily optimized. As media or fermentation conditions are varied, relatively small differences in the resulting aFGF expression levels can be determined. This is exemplified by the chromatograms shown in Fig. 6. In this comparison, the maximum aFGF titers from two different trial fermentations differed by less than 15%. Yet this difference could be easily discerned; the ability to accurately discriminate these smaller percentage improvements is significant since optimization usually consists of making several such stepwise improvements.

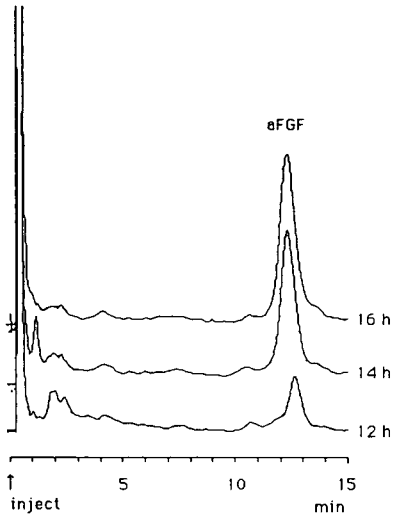

Fig. 5. The production of aFGF in a fermentation monitored at 12, 14, and 16 h after induction. Whole broth samples were removed at each time point and centrifuged to produce a cell pellet. The cell pellet is suspended in buffer and chemically disrupted by guanidine HCl as described under Chemical cell disruption. Chromatographic conditions as in Fig. 1.

High-speed analysis

For fermentation and process development projects, where large numbers of samples must be analyzed, obtaining a high sample throughput is important. The recent development of "perfusion chromatography" has resulted in significant reduction in analysis times. Chromatography on POROS supports permits very high superficial velocities to be achieved (>1000 cm/h) while maintaining efficiency and resolution [11–13]. To reduce analysis time, the aFGF assay was adapted to a POROS R/H column. By increasing the flow rate to 4 ml/min (superficial velocity = 1445 cm/h) and modifying gradient conditions a decrease in run time from 15 min to 3 min was achieved while maintaining the quality of the separation. A chromatogram of an aFGF cell lysate sample assayed on the POROS R/H column is shown in Fig. 7. The aFGF is well resolved from the sample constituents at the higher superficial mobile phase velocity used for POROS supports. Duplicate sample sets analyzed on both columns and similar validation experiments showed equivalent accuracy and reproducibility for the POROS column; R.S.D. values of 5% or less for 3 control samples

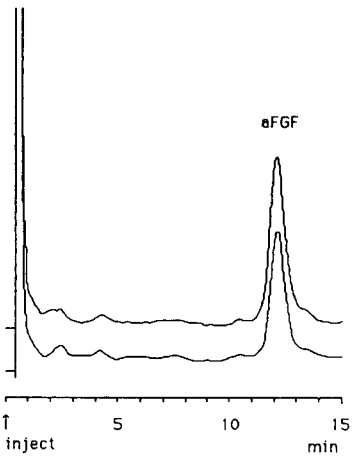

Fig. 6. A comparison of aFGF titers from two different trial fermentations. Lower trace, fermentation 1 (145 units/ml); upper trace, fermentation 2 (178 units/ml). Sample preparation and chromatographic conditions as in Fig. 5.

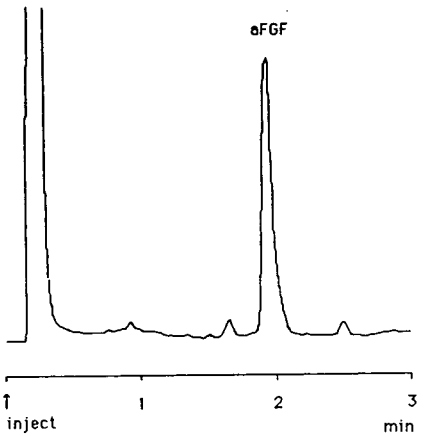

Fig. 7. High-speed analysis of an aFGF cell lysate sample. Chromatographic conditions: PerSeptive Biosystems POROS R/H column (50 mm × 4.6 mm I.D.); eluent A, 0.1% TFA in water, eluent B 0.1% TFA in 80:20 acetonitrile–water; two-stage linear gradient program, 20 s linear gradient from 10 to 35% B; followed by a 2:25-min linear gradient from 35 to 51% B at a flow rate of 4 ml/min throughout. Injection volume 20 μl, detection wavelength 280 nm.

analyzed in quadruplicate over the range of 50–250 μg/ml.

The quantitation of aFGF recovery through the entire process scheme, starting with the whole cell paste can be done very rapidly using one HPLC method for all sample streams. A purification procedure for aFGF consisted of cell lysis, centrifugation to remove cell debris, capture chromatography on an ion-exchange column to concentrate and purify the aFGF, followed by an affinity chromatography polishing step. The HPLC analysis of the suspended cells prior to lysis, the lysed cells and the chromatography column eluates are shown in Fig. 8. The cell suspension and lysate samples require the sample preparation methods previously described, samples from the capture column and other chromatographic products are sufficiently clean that simple dilution in 0.1% TFA is all that is required prior to analysis. Because the aFGF concentration could be determined for any sample type in 3 min, a complete process recovery analysis, (including side-fractions, column flow through and waste streams) comprising 60–80 samples, can be completed in about four h.

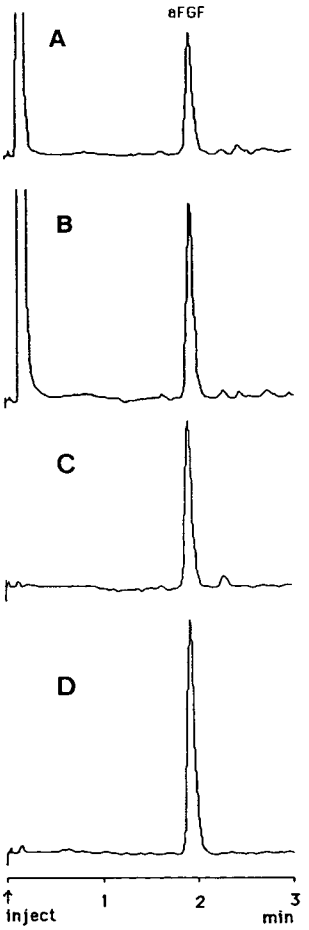

Fig. 8. Chromatograms from a pilot scale purification of aFGF. The cell suspension sample (A) was chemically disrupted by guanidine HCl as described under Chemical cell disruption, then prepared as described under Sample preparation procedures. The cell lysate sample (B) was prepared as described under Sample preparation procedures. The capture column product (C) and the affinity column product (D) were diluted with PBS prior to chromatography. Chromatographic conditions as in Fig. 7.

CONCLUSIONS

The use of polymeric reversed-phase supports in tandem with a simple sample preparation procedure has enabled the development of an assay for aFGF in cell suspensions and cell lysates with mean precision and accuracy values of 5%. The polymeric columns described here have been in use for over six months, periodic (biweekly) washing with 60 ml of 50%

methanol–0.2 *M* NaOH have prevented any noticeable deterioration in separation quality. Samples generated from either fermentation or any processing step can be assayed with the same HPLC method, eliminating the need for immunoassays to quantitate aFGF in very crude matrices. Enhanced throughput can be obtained using Perfusion Chromatography columns operated at high superficial velocity. The resulting chromatography is fast enough to obtain results concurrent with either fermentation or processing operations, with the potential for real time on-line analysis.

REFERENCES

1 K. Hayashibe, D. Sassano and M. Reza Ziai, *J. Immunoassay*, 11 (1990) 89.
2 B.J. Del Tito, Jr., D.W. Zabriskie and E.J. Arcuri, *J. Immunol. Methods*, 107 (1988) 67.
3 R.M. Riggin, G.K. Dorulla and D.J. Miner, *Anal. Biochem.*, 167 (1987) 199.
4 K.A. Tweeten and T.N. Tweeten, *J. Chromatogr.*, 359 (1986) 111.
5 W.G. Burton, K.D. Nugent, T.K. Slattery, B.R. Summers and L.R. Snyder, *J. Chromatogr.*, 443 (1988) 381.
6 W. Dong, J. Gant and B. Larsen, *BioChromatography*, 4 (1989) 19.
7 K.D. Nugent, W.G. Burton, T.K. Slattery, B.F. Johnson and L.R. Snyder, *J. Chromatogr.*, 443 (1988) 363.
8 K.A. Thomas, *Methods Enzym.*, 147 (1987) 120.
9 K.A. Thomas and G. Gimenez-Gallago, *Trends Biochem. Sci.*, 11 (1986) 81.
10 D. Hettwer and H. Wang, *Biotechnol. Bioeng.*, 33 (1989) 886.
11 N.B. Afeyan, N.F. Gordon, I. Mazsaroff, L. Varady, S.P. Fulton, Y.B. Yang and F.E. Regnier, *J. Chromatogr.*, 519 (1990) 1.
12 N.B. Afeyan, S.P. Fulton and F.E. Regnier, *J. Chromatogr.*, 544 (1991) 267.
13 S.P. Fulton, N.B. Afeyan, N.F. Gordon and F.E. Regnier, *J. Chromatogr.*, 547 (1991) 452.

ELSEVIER

Journal of Chromatography A, 663 (1994) 53–63

JOURNAL OF CHROMATOGRAPHY A

Examination of glutathione S-transferase isoenzyme profiles in human liver using high-performance affinity chromatography

Jeffrey B. Wheatley[a], M. Kathleen Kelley[b], Julie A. Montali[a], Christopher O.A. Berry[c], Donald E. Schmidt, Jr.*[,a]

[a]*Terrapin Technologies, Inc., 750-H Gateway Boulevard, South San Francisco, CA 94080, USA*
[b]*Brain Tumor Research Center, UC San Francisco, San Francisco, CA 94103, USA*
[c]*Friedrich Miescher Institut, Basel, Switzerland*

(First received September 22nd, 1993; revised manuscript received December 1st, 1993)

Abstract

A method for the examination of the glutathione S-transferase isoenzyme profiles in human liver using a new HPLC affinity support is described. Liver cytosol was injected directly onto an HPLC column (5 × 0.46 cm) containing a support with a covalently bound affinity ligand (S-octylglutathione) specific for the isoenzymes. Contaminating cytosolic proteins were removed in a washing step. The isoenzymes were eluted with a linear gradient of a different affinity ligand in the mobile phase. Coinciding with the affinity ligand gradient, a salt gradient (0–200 m*M* sodium chloride) was applied. In this manner the isoenzymes were fractionated into the enzymatically active homodimers and heterodimers. The classes of the affinity fractionated isoenzymes were determined by SDS-PAGE and ELISA while the subunit content was determined by reversed-phase chromatography. For one liver three Alpha class isoenzyme subunits, forming three heterodimers and two homodimers, were detected. Five livers were examined, and the homodimer A1–1 was found to be the predominant glutathione S-transferase isoenzyme. Minor amounts of Pi and Mu class isoenzymes were also detected. This non-denaturing high-performance affinity chromatography method reduced analysis time by a factor of ten when compared to other affinity analysis methods for the glutathione S-transferases.

1. Introduction

Glutathione S-transferases (GSTs, E.C. 2.5.1.18) are a group of cytosolic enzymes which catalyze the conjugation of electrophilic xenobiotics with glutathione via the free sulfhydryl group present in this abundant intracellular tripeptide [1]. This process generally leads to the detoxification of the xenobiotics since the resulting adducts are normally metabolized to mercapturates and excreted. These human cytosolic enzymes belong to a supergene family comprised of at least four multigene classes: Alpha, Mu, Pi, and Theta. The enzymes exist as dimers with subunit molecular masses between 23 000 and 27 000 and have a range of isoelectric points from 4.8 to 8.9. Both heterodimers and homodimers exist, but heterodimers only form from subunits within the same class [2]. A dimeric enzyme is named by class followed by an Arabic numeral designation of the subunit composition. For example A1–2 designates a heterodimer of the Alpha class consisting of the monomeric subunits A1 and A2 [3].

* Corresponding author.

0021-9673/94/$07.00
SSDI 0021-9673(93)E1286-9

Individual isoenzymes show significant preference for particular compounds, including some in use as cancer chemotherapeutics [4–9]. Current chemotherapy often fails due to the appearance of tumor cells resistant to the chemotherapeutic agents [1,10]. Elevated levels of the GSTs have been associated with this resistant state [11–13] and as a predictor of early cancer recurrence [14]. This accumulated body of evidence suggests that GSTs are important in several aspects of cancer therapy. To substantiate this idea, improved methods are needed for determining the types and levels of the native isoenzymes.

Previously described sodium dodecyl sulphate polyacrylamide gel electrophoresis (SDS-PAGE) separations of human GSTs allow the determination of class but not of subunit composition. Similarly, prior work has shown that the sensitive, high-resolution reversed-phase HPLC analysis of GSTs identifies many of the known subunits but gives no information as to the dimeric composition [15–17]. Both separation techniques are conducted under denaturing conditions which is of concern with regard to the discovery of any new GST isoenzymes in the genetically diverse human population. A number of ion-exchange [18–20] and chromatofocusing [21,22] methods have been described for the analysis of GSTs, and in some cases intact, enzymatically active dimers have been isolated. Before the application of any of these analytical techniques, a batch purification of the GSTs from cytosol is required. This partial purification is traditionally performed by affinity chromatography [23–25].

A method for the separation of a range of GSTs in dimeric, active form is affinity chromatography using isocratic and/or gradient elution with a counter ligand. This method combines the purification of the GSTs from the cytosol by affinity chromatography and the separation of the individual GSTs. Resolution of GST homodimers and heterodimers has previously been accomplished using this technique with either S-hexylglutathione or glutathione as the affinity ligand bound to agarose [26–28]. Due to the large particle diameter and slow flow-rates inherent with agarose gels, the fractionation time for these studies was approximately 25 h [29] which explains why this technique is not used for the routine analysis of the GSTs. Appreciable savings in time and increases in sensitivity would be anticipated if this affinity technique were performed on a small particle stationary phase [30]. An HPLC column containing immobilized glutathione as the affinity ligand has been described for the preparative purification of GSTs [31], but no attempt was made to separate the individual enzymes.

This report describes the affinity separation of GSTs from human liver as active dimers using a novel HPLC method. A stationary phase with a GST affinity ligand (S-octylglutathione) covalently linked to an HPLC particle was developed and used to determine liver profiles of this important family of detoxifying isoenzymes.

2. Materials and methods

2.1. Reagents

Iodobutane, iodooctane, sodium borohydride, 1,4-butanediol diglycidyl ether and EDTA were purchased from Aldrich (Milwaukee, WI, USA). Glutathione, dithiothreitol, 1-chloro-2,4-dinitrobenzene (CDNB), Tris, Tween-20, *p*-nitrophenyl phosphate and phenylmethylsulfonyl fluoride were obtained from Sigma (St. Louis, MO, USA). Alkaline phosphatase labeled goat anti-rabbit IgG was purchased from Kirkegaard and Perry (Gaithersburg, MD, USA). Recombinant GST enzymes rA1–1, rP1–1, rM1a–1a and rM1b–1b were obtained from B. Mannervik (University of Uppsala, Uppsala, Sweden), and rA2–2 was obtained from A. Townsend (Bowman Gray School of Medicine, Winston-Salem, NC, USA). Rabbit antisera against rA1–1, rP1–1 and rM1a–1a were obtained from rabbits, immunized with the appropriate recombinant GST, from BAbCo (Richmond, CA, USA). HEMA BIO 1000 (10 μm) was purchased from Melcor Technologies (Sunnyvale, CA, USA).

2.2. Synthesis of peptides

S-butylglutathione and S-octylglutathione were synthesized by the method of Vince *et al.* [32]. The tripeptide γ-glutamyl-(*S*-benzyl) cysteinyl-β-alanine (TER106) was synthesized as previously reported [33]. All peptides had greater than 90% purity when analyzed by reversed-phase HPLC and had acceptable elemental analyses.

2.3. Chromatography

The HPLC system consisted of two HPLX pumps equipped with 10 ml/min titanium pump heads, a Rheodyne 7125-081 titanium injector and a Dynamax UV-C detector (Rainin Instrument, Woburn, MA, USA). For both reversed-phase (214 nm) and affinity chromatography (280 nm), 1000 mV were equivalent to 1 absorbance unit.

For reversed-phase analyses a 1.2-ml titanium, dynamic mixer (Rainin Instrument) was used to form the gradient. A 25 × 0.46 cm Vydac (Hesperia, CA, USA) reversed-phase column 218ATP54 with a mobile phase of water and acetonitrile containing 0.1% trifluoroacetic acid (Pierce Chemical, Rockford, IL, USA) was used to separate the GST subunits. The elution times of P1, M1a, M1b, A1 and A2 were determined by injection of the appropriate recombinant GST.

For affinity chromatography the gradient was formed with a static mixing tee (Upchurch Scientific, Oak Harbor, WA, USA). A biocompatible 100 p.s.i. (1 p.s.i. = $6.9 \cdot 10^3$ Pa) back-pressure regulator (Upchurch Scientific) was placed between the injector and the mixing tee. The back-pressure regulator was placed in-line to insure the proper function of the HPLC pump check valves at the low pressure generated during affinity chromatography. All pathways in contact with the mobile phase were of either titanium or biocompatible polymer construction. Fractions (0.8 min/fraction) were collected with a Gilson FC203 fraction collector (Rainin Instrument) into a polystyrene, 96-well plate (Costar, Cambridge, MA, USA, Catalog No. 9017). To reduce protein adsorption, the 96-well plate was pretreated with a solution of 0.1% Tween-20 for 16 h, washed with deionized water and air dried.

2.4. Tissue treatment

Human liver samples were obtained from the Cooperative Human Tissue Network (Columbus, OH and Birmingham, AL, USA) and stored at − 80°C. Liver tissues were designated with the prefix L affixed to a three digit number followed by the suffix CA (cancer) or N (normal). Samples were slightly thawed, minced with scissors and homogenized at 25% (w/v) in buffer containing 10 m*M* Tris–HCl (pH 7.8), 1 m*M* EDTA, 1 m*M* dithiothreitol and 0.10 m*M* phenylmethylsulfonyl fluoride using an OMNI stator generator homogenizer (Marietta, GA, USA). Cytosol was prepared by ultracentrifugation at 135 000 *g* for 35 min at 4°C in a Beckman Optima TL-100 tabletop ultracentrifuge (Fullerton, CA, USA). Protein concentrations were determined using a 96-well plate Coomassie dye binding assay (Bio-Rad, Richmond, CA, USA) read on a Tmax Plate Reader (Molecular Devices, Menlo Park, CA, USA) with bovine serum albumin as a standard [25].

2.5. Pooled GST fractions

To obtain the total pooled population of GSTs from cytosol, a batch purification was performed using a Sepharose-6B affinity matrix with S-hexylglutathione ligand in a 96-well microplate equipped with a membrane on the bottom surface [25]. GSTs were eluted with S-hexylglutathione.

2.6. Gel electrophoresis

SDS-PAGE was performed according to standard methods [34] at a 12.5% (w/v) acrylamide concentration. Proteins were visualized after electrophoresis by silver staining [35].

2.7. CDNB conjugating activity

GST enzymatic activity was determined by measuring the conjugation of CDNB with glutathione at 340 nm with a Tmax Plate Reader. Aliquots (10 μl) of fractions from affinity chromatography or from fractions collected to determine activity recoveries were placed in the wells of a 96-well plate and mixed with 190 μl of a standard reaction solution. Standard reaction conditions were 200 m*M* sodium phosphate (pH 6.8) with 1 m*M* glutathione and 1 m*M* CDNB at 30°C [36].

2.8. Recovery of CDNB conjugating activity

Cytosol was diluted (1 to 50) into 200 m*M* sodium phosphate (pH 6.8) and 10 μl of this solution was used to determine the true activity. Unretained activity was determined from the column effluent collected during the loading step. The eluate containing the GSTs was collected as one fraction and the activity determined. A correction factor [25] to compensate for the inhibition of GST activity by the S-butylglutathione eluent was determined by comparing the true cytosolic activity with the activity of cytosol diluted (1 to 50) in a solution containing a concentration of S-butylglutathione equivalent to that in the GST eluate. This equivalent concentration of S-butylglutathione was obtained by collecting a fraction containing S-butylglutathione from a blank gradient. The time interval of collection of the fraction from the blank gradient was identical to the time interval for collection of the GST fraction from affinity chromatography. The ratio of true cytosolic activity to inhibited cytosolic activity was used to correct the activity of the eluted GST fraction. For the recovery studies the GSTs were collected over an interval of 10 min.

2.9. Enzyme-linked immunosorbent assay (ELISA)

Aliquots of 50 μl of PBS (140 m*M* sodium chloride, 37 m*M* potassium dihydrogen phosphate, 11.2 m*M* disodium hydrogen phosphate, pH 7.2) were pipetted into each well of a Nunc MaxiSorp 96-well plate (VWR Scientific, Brisbane, CA, USA). To each well was added an aliquot (usually 10 μl) from the corresponding well of the collection plate from the affinity separation. The ELISA plate was then covered and left overnight at room temperature. The next day, contents of the plate were shaken out and the plate was blocked with 5% non-fat dry milk in PBS, 200 μl/well, for 1 h at 37°C or 2 h at room temperature. The plate contents were shaken out and the plate was washed once with a PBS solution with 0.05% Tween 20. To each well, 50 μl of the appropriate rabbit antisera diluted in the PBS–Tween solution was added and incubated for 1 h at 37°C. Plates were then washed three times with PBS–Tween, and alkaline phosphatase labeled goat anti-rabbit IgG, diluted 1:2500 in PBS–Tween, was added, 50 μl to each well. This was also incubated for 1 h at 37°C, and the plate was then washed three times with deionized water. Finally, color was developed by the addition of 100 μl/well of *p*-nitrophenyl phosphate, 1 mg/ml in 10 m*M* diethanolamine and 0.5 m*M* magnesium chloride. After color development (typically 30 min), the absorbance was read at 405 nm.

2.10. Affinity matrix

The synthesis of the affinity matrix follows the general procedure of Sundberg and Porath [37]. HEMA BIO 1000, 1,4-butanediol diglycidyl ether and 0.6 *M* sodium hydroxide containing 2 mg/ml of sodium borohydride (0.03:1:1, w/v/v) were mixed overnight. The particles were filtered and washed with water, ethyl alcohol and acetone.

To 700 mg of the dried particles was added S-octylglutathione (75 mg) dissolved in 3.5 ml of 0.5 *M* sodium carbonate. The suspension was mixed for approximately 90 h. After filtration the particles were washed with (i) 1 *M* sodium chloride, 0.1 *M* sodium phosphate (pH 9), (ii) 1 *M* sodium chloride, 0.1 *M* sodium acetate (pH 4.5), (iii) water, (iv) ethyl alcohol and (v) acetone.

2.11. Packing of HPLC columns

The affinity material (650 mg) was slurried in 20 ml of water and was packed at high pressure into stainless-steel columns 5 × 0.46 cm (Supelco, Bellefonte, PA, USA). The column frits were 2-μm (average pore diameter) titanium encased in a CTFE ring (Upchurch Scientific, Oak Harbor, WA, USA). A Haskell (Burbank, CA, USA) DSTV-122 liquid pump was used to provide the drive solvent (water) during the packing process. The columns were packed at 2000 p.s.i. with 50 ml of water and then 4000 p.s.i. with 50 ml of water.

3. Results

The chromatogram and activity profile for a typical affinity separation of GSTs from a human liver cytosol (L006N) is shown in Fig. 1. During loading (0–10 min) and washing (10–35 min) steps, GSTs were bound to the column and contaminating proteins were removed. Sodium chloride was required during the washing step to facilitate the elution of the contaminating proteins presumably adsorbed to the stationary phase by ionic interactions. GSTs were then eluted (50–120 min) with a gradient of the glutathione analog TER106. In subsequent affinity chromatograms only the portion of the separation corresponding to the activity profile for the retained GSTs is shown.

The average recovery of CDNB conjugating

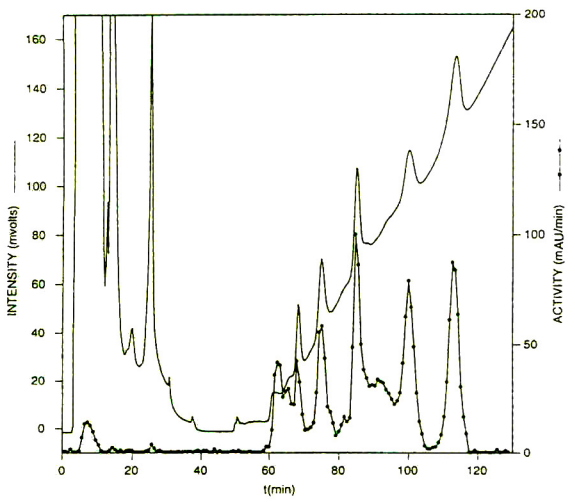

Fig. 1. Profiles of CDNB conjugating activity (●) and intensity at 280 nm (—) for the affinity separation of liver L006N using TER106 as the eluting ligand. Mobile phase: (A) 10 m*M* sodium phosphate (pH 6), (B) 200 m*M* sodium chloride in A, (C) 40 m*M* TER106 in B. Gradient: 0–10 min, 100% A, 0.1 ml/min; 10–30 min, 100% B, 0.4 ml/min; 30–35 min, 100% B, 1 ml/min; 35–50 min, 100% A, 1 ml/min; 50–108 min, 100% A to 48% C, 0.1 ml/min; 108–150 min, 48% to 100% C, 0.1 ml/min.

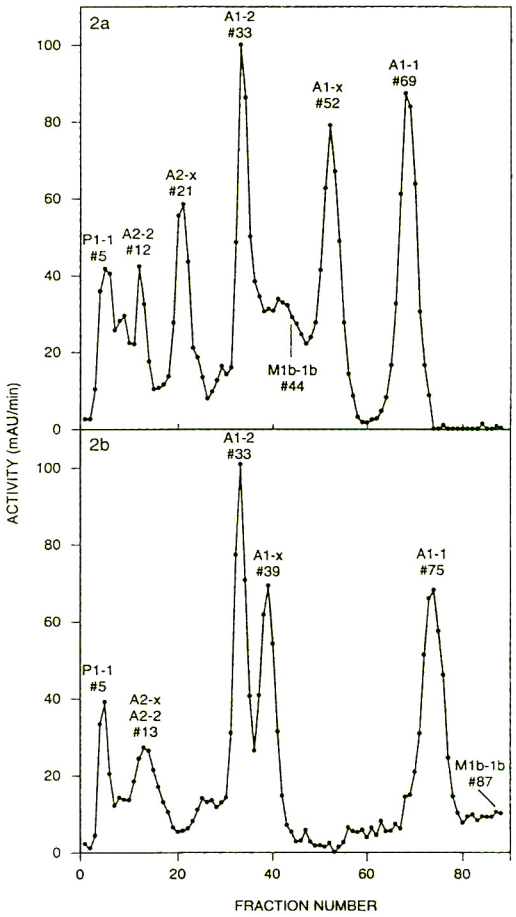

Fig. 2. Profiles of the CDNB conjugating activity for the affinity separations of liver L006N using different eluting ligands. (a) Eluting ligand TER106 (40 m*M* in buffer C); (b) eluting ligand S-butylglutathione (20 m*M* in buffer C). See Fig. 1 for the gradient profile. Fraction No. 1 in Fig. 2 corresponds to 59.2 min in Fig. 1.

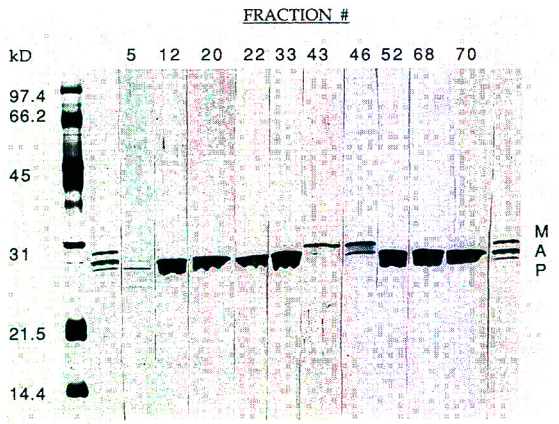

Fig. 3. SDS-PAGE of selected fractions from the affinity separation of L006N using TER106 as the eluting ligand. Lanes 4–13 contain aliquots from the corresponding fractions of Fig. 2a. Lanes 3 and 14 contain a mixture of the recombinant M1a–1a (M), A1–1 (A) and P1–1 (P).

activity during an affinity separation was 76%. The activity recoveries for three liver samples were 66% (L002N), 60% (L002CA) and 103% (L004CA). The proportion of unretained activity for the three livers varied from 3 to 13%. The reproducibility of the GST affinity extraction was determined by comparing the amounts of unretained activity from a series of repetitive injections of the same cytosol (L005N). On the first day, two affinity separations were performed and the amount of unretained activity was 2.5 and 2.3%. In a separate series of experiments made two days later the amount of unretained activity was 2.6, 2.6 and 3.5%.

Fig. 2 shows the GST isoenzyme content of the major peaks eluted with TER106 (Fig. 2a) or with S-butylglutathione (Fig. 2b). Note that fraction No. 1 in Fig. 2a corresponds to 59.2 min of Fig. 1. The GST isoenzyme content of the peaks in Fig. 2a was identified from the analysis of the collected fractions by SDS-PAGE, ELISA and reversed-phase chromatography while in the case of Fig. 2b the fractions were analyzed by SDS-PAGE and reversed-phase chromatography. The class of the GST in the fractions was determined by SDS-PAGE and ELISA with representative data shown in Figs. 3 and 4, respectively. There appeared to be some cross-

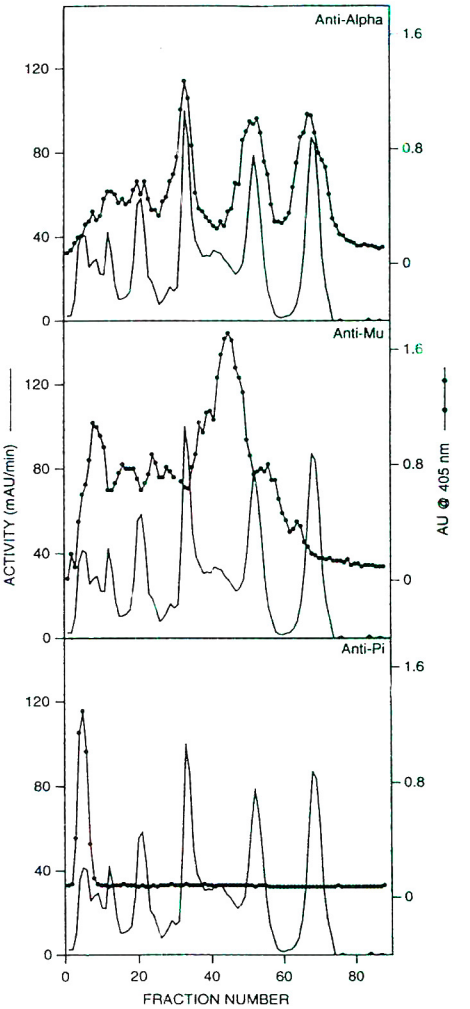

Fig. 4. ELISA analysis (●) and CDNB conjugating activity (—) of fractions from the affinity separation of L006N using TER106 as the eluting ligand. On separate plates the aliquots from the corresponding fractions of Fig. 2a were analyzed with anti-Alpha, anti-Mu or anti-Pi IgG. See Materials and Methods for experimental details.

reactivity of the anti-Mu IgG with Alpha isoenzymes in fraction Nos. 9 and 52. This cross-reactivity was not investigated further. The major Mu peak as detected by ELISA was centered at fraction No. 44 in agreement with the SDS-PAGE and reversed-phase chromatography results.

To assess the subunit composition of the isoenzymes, the fractions corresponding to the

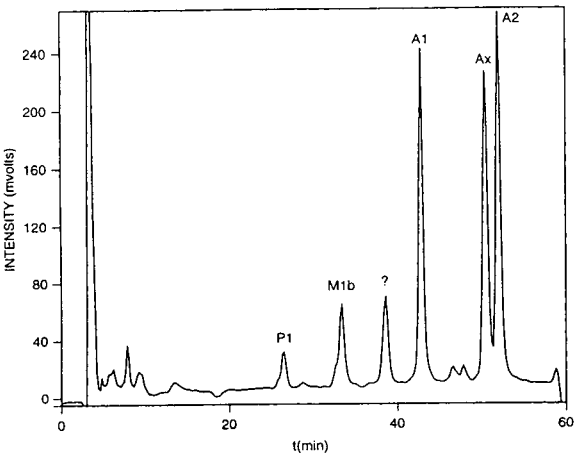

Fig. 5. Reversed-phase chromatogram of the pooled GSTs of liver L006N. Mobile phase: (A) acetonitrile with 0.1% trifluoroacetic acid, (B) water with 0.1% trifluoroacetic acid. Gradient: 41% A to 55% A in 55 min at 1 ml/min.

major peaks found in Fig. 2 were individually analyzed by reversed-phase chromatography. Subunits were identified by comparison of their retention times with the retention times of recombinant GSTs. Liver L006N contained a protein component which eluted between A1 and A2 during reversed-phase chromatography (Fig. 5) and which had an elution time not corresponding to any of the recombinant enzyme standards. This protein component was tentatively assigned as Ax (see Discussion). Representative chromatograms are shown in Fig. 6 for fractions Nos. 21 and 33 of the TER106 elution. Affinity peaks assigned as containing heterodimers showed two peaks of equal area corresponding to the two subunits in the isoenzyme (Fig. 6). For affinity peaks containing homodimers, only one major peak was detected by reversed-phase chromatographic analysis.

The isoenzyme content of five liver cytosols, shown in Table 1, was determined from affinity chromatographic analysis using S-butylglutathione as the eluting ligand. Peak assignments for the affinity separations were based on retention of the isoenzymes identified for L006N, as described above (Fig. 2b). Isoenzyme identities were further substantiated (see Discussion) from the subunit content determined by the

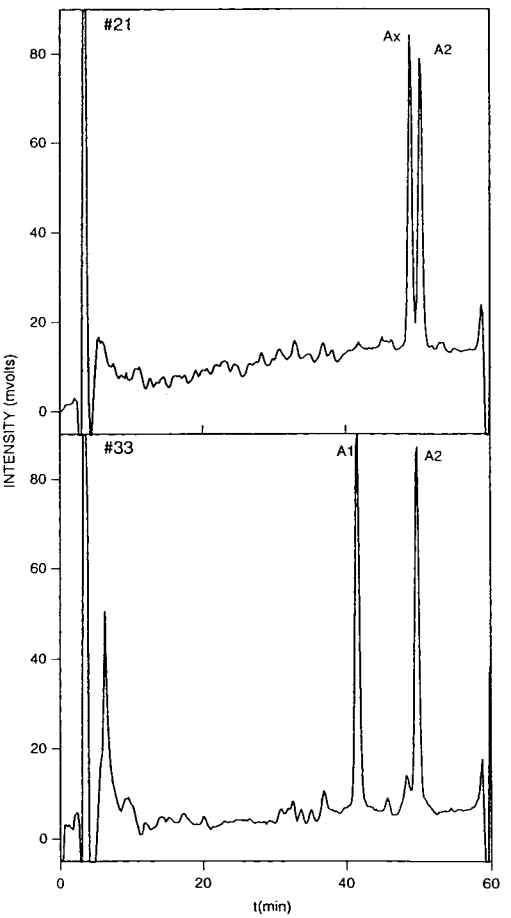

Fig. 6. Reversed-phase chromatograms of fractions Nos. 21 and 33 from the affinity separation of liver L006N using TER106 as the eluting ligand. Fraction numbers correspond to the fractions of Fig. 2a. See Fig. 5 for chromatographic conditions.

reversed-phase analysis of pooled GSTs derived from S-hexylglutathione–Sepharose 6B extractions of the cytosols [25]. The reversed-phase chromatogram from the pooled GST extract of L006N, corresponding to the affinity separation shown in Fig. 2b, can be seen in Fig. 5. Peak assignments were based on the retention of rGSTs. The peak between M1b and A1 and centered at 39 min, which was observed for all five livers, has not been identified and was not investigated further. A peak at a similar retention time, also unidentified, has been reported by Van Ommen *et al.* [16]. Minor

Table 1
GST profiles of human liver

Liver	Isoenzyme content[a]						Subunit content[b]				
	P1–1	A2–x A2–2	A1–2	A1–x	A1–1	M1b–1b	P1	M1b	A1	Ax	A2
L006	+[c]	++	++	++	++	+	+	+	++	++	++
L007	+	++	++	–	++	–	+	–	++	–	++
L004	+	++	–	++	++	+	+	+	++	++	+
L005	+	–	–	+	++	++	+	+	++	+	+
L002	–	+	+	–	++	+	+	+	++	–	+

[a] The GST isoenzyme content of a liver as determined by affinity analysis. Buffers: (A) 10 m*M* sodium phosphate (pH 6.0); (B) 200 m*M* sodium chloride in A; (C) 20 m*M* S-butylglutathione in B. Conditions: 0–5 min, A, 0.1 ml/min; 5–21 min, B, 1.5 ml/min; 21–34 min, A, 1 ml/min; 34–35 min, A, 0.1 ml/min; 35–155, 0–42% C, 0.1 ml/min.
[b] The GST subunit content of the liver as determined by reversed-phase analysis.
[c] + + = Greater than 10% of total peak area; + = less than 10% of total peak area; – = not detected.

amounts of M1a were also observed at 28 min for two of the livers, L005N and L002N (data not shown). The GST subunit composition, along with the isoenzyme content, is shown in Table 1 for the five liver cytosols.

4. Discussion

A significant saving in GST analysis time was achieved by performing the separation on the novel HPLC packing described here. Liver samples were analyzed in 2 h, more than ten times faster than similar separations using Sepharose-6B based affinity supports [29]. Washing and eluting steps were significantly shorter in duration with the HPLC method. Although the washing step in the separation shown in Fig. 1 was conducted at 0.4 and 1.0 ml/min, the HPLC packing is capable of withstanding higher pressures. In the analysis of the five human livers (Table 1) advantage was taken of this pressure stability by conducting the washing step at 1.5 ml/min thereby reducing the washing time by 9 min. In preliminary experiments we have found that flow-rates of 2 ml/min during the washing step can be tolerated in this system with no loss of affinity bound GST isoenzymes.

The affinity separation of the GST isoenzymes described here depended upon the simultaneous application of two concentration gradients. One gradient consisted of a linearly increasing concentration of either TER106 (Fig. 2a) or S-butylglutathione (Fig. 2b), both known competitive inhibitors of the GSTs [36]. The general mechanism for this type of chromatographic separation has been reviewed [38]. In the loading step, a GST complexes with an affinity ligand covalently linked to the stationary phase. As the concentration of the competitive inhibitor (TER106 or S-butylglutathione) increases during the elution step, the GST increasingly partitions into the mobile phase and finally elutes. The order of elution of a mixture of GSTs is a complex function of their affinities for both the immobilized affinity ligand and the competitive inhibitor in the mobile phase. For instance a change in elution order was observed when comparing the difference in GST elution profiles using two different eluting ligands. Elution with S-butylglutathione as compared with elution with TER106 shifted the Mu class isoenzyme to a longer retained peak relative to the Alpha class peaks. In addition, the S-butylglutathione elution resulted in the co-elution of A2–x and A2–2 which were resolved with TER106 elution. Note that twice the concentration of TER106 to S-butylglutathione was needed to produce similar chromatograms, reflecting their differing affinities for the isoenzymes [36].

Second, a salt gradient was also applied, coinciding with the ligand gradient. Without this

gradient the first three components (P1–1, A2–x and A2–2 in Fig. 2b) co-eluted. The salt gradient may be acting to overcome ionic interactions between the proteins and the stationary phase bound affinity ligand, S-octylglutathione, which was expected to have a net negative charge at pH 6.0. Another interpretation of the salt effects is possible. The chloride ion may act as a competitive inhibitor of the GSTs and thus affect their retention on the affinity stationary phase. Small anions have been shown to act as competitive inhibitors in another enzyme system [39].

The recovery of CDNB conjugating activity eluted with an affinity ligand from the affinity column averaged 76% for three livers while the average yield of total activity (affinity ligand eluted activity plus unretained activity) was 83%. The yield of CDNB conjugating activity from the affinity column described here was comparable to that described in previous reports. Reported yields of the recovery of CDNB conjugating activity from affinity chromatography of tissues from various sources have varied from 30–95% [31]. For human liver cytosol eluted from agarose columns using S-hexylglutathione as the affinity ligand, yields varied from 84 [40], 80–100 [41], to 51% [42] while in a study of two livers using the affinity ligand S-octylglutathione on agarose yields were 47 and 67% [22].

There are several possible reasons for the variation in the fraction of unretained activity. Competitive inhibitors of GSTs may exist in liver and these competitive inhibitors may cause a decrease in the binding of isoenzymes to the column. The concentrations and types of these competitive inhibitors may vary from liver to liver, giving rise to the observed inconsistency of unretained activities for different livers. In addition Hayes [29] has noted that different affinity matrices have different selectivities. The affinity matrix described in this report may not bind certain GST isoenzymes. The levels and amounts of these non-binding GST isoenzymes can be expected to vary depending on the liver source, and this variation could give rise to the observed inconsistencies in yield. Variation in the unretained activity from different rat livers processed by affinity chromatography has been noted [28].

The class of GST isoenzymes in the major peaks were identified by both SDS-PAGE (Fig. 3) and ELISA (Fig. 4). The subunit composition of the isoenzymes was determined by reversed-phase HPLC (Fig. 6). Liver L006N appears to contain three forms of Alpha subunits. The reversed-phase chromatogram of the GSTs isolated from liver L006N shows a peak which elutes between A1 and A2 (Fig. 5). We have tentatively designated this later eluting protein as subunit Ax. This designation was based on the following evidence. The SDS-PAGE analysis (Fig. 3) of the TER106 affinity fraction No. 21 containing A2–x and fraction No. 52 containing A1–x (Fig. 2a) showed subunits with molecular masses characteristic of Alpha class subunits. The reversed-phase HPLC analysis indicated equal amounts of subunits A1 and A2 in fraction No. 33 which indicates that this analysis method is valid for identifying heterodimers (Fig. 6). Equal amounts of subunits A2 and Ax in fraction No. 21 (Fig. 6), is consistent with heterodimer formation. In addition a dimer of A1 and Ax is detected by reversed-phase chromatography in fraction No. 52 (data not shown). We surmise that Ax is capable of forming a heterodimer with Alpha class subunits. To date heterodimers have only been found to form among members of the same class [2]. The association of Ax with A1 and A2 suggests that this subunit belongs to the Alpha class of GSTs. Moreover, the ELISA analysis of the affinity HPLC fractions (Fig. 4) shows that the fractions containing Ax are only reactive with the anti-Alpha IgG.

Human liver cytosol has previously been analyzed for both GST subunit [16,41,43] and dimeric content [21,22,40,42,44]. Using an isoelectric focusing technique [41], six different Alpha subunits were identified. From reversed-phase HPLC analysis of GST subunits, two Alpha subunits were identified in human liver [16,43]. In one report of dimer isolation by chromatofocusing [40], 13 forms of GST were found, but no attempt was made to differentiate them into classes. Other investigators [22,42,44] of GST dimers in human liver have found two types of Alpha subunits which form two homodimers and one heterodimer. For L006N we have identified

three subunits which form two homodimers (A1–1 and A2–2) and three heterodimers (A2–x, A1–x, and A1–2). Interestingly the potential homodimer Ax–x was not identified in this liver.

For the examination of five livers, S-butylglutathione was chosen as the eluting ligand because it separated Mu class GSTs from the Alpha class. The five human livers were examined for dimeric content by affinity chromatography and for subunit content by reversed-phase chromatography (Table 1). The amount of cytosol injected onto the affinity column was equivalent to approximately 20 mg of liver. In previous reports [16,21,22,41–44] the predominant forms of GST in human liver were A1 subunits and A1–1 dimers. This was the case for the five livers examined in this report. When appreciable amounts of Ax or A2 subunits were detected, heterodimers with A1 were also found. For L007N, which had appreciable amounts of subunit A2, both the homodimer A2–2 and the heterodimer A1–2 as well as A1–1 were detected. Human liver L005N which had A1 and Ax but only a minor amount of A2 exhibited A1–x and A1–1, but no Ax–x was detected. Minor amounts of P1 were detected by reversed-phase analysis in all five samples and were also detected by affinity analysis in four of the five livers. Previous investigations also showed Pi to be a minor component in human liver [41,42]. Small amounts of the Mu class GSTs were detected by the reversed-phase method. Due to poor peak shape in affinity chromatography, the detection of the Mu class is difficult when it constitutes only a minor portion of the total GST content.

This new affinity chromatography system using HPLC technology has significant advantages over conventional soft gel affinity systems for the analysis of the GST dimeric content of tissues. The time of analysis is reduced by a factor of ten. In addition the sensitivity for this affinity system is greater because the peak volumes for HPLC affinity are only about 0.5 ml compared to 50–100 ml when using conventional soft gels [29]. This technique also has the advantage of combining both sample cleanup and analysis into a single step. Other techniques such as reversed-phase HPLC, chromatofocusing or electrophoresis require a separate affinity step to batch purify the GSTs before the final analysis.

Affinity chromatography using gradients of a counter ligand in the eluent is a powerful separation technique. Variation of the biospecific ligand in the eluent results in chromatographic separations exhibiting different selectivities. The different selectivities observed are due to the unique set of binding constants that exist among ligands in their associations with various isoenzymes. This was the case for the GSTs when comparing elution profiles using TER106 or S-butylglutathione as the counter ligand. Many more ligands interact with GSTs [36], and any of these could give a unique separation allowing a custom separation to be developed. In particular, the analytical methods reported here can be readily scaled-up for preparative isolation of particular GSTs of interest.

5. Acknowledgements

The authors thank Larry M. Kauvar for comments on this manuscript. This work was supported in part by a Small Business Innovative Research grant to L.M.K. from the US National Science Foundation (No. ISI-9022271).

6. References

[1] D.J. Waxman, *Cancer Res.*, 50 (1990) 6449.
[2] H. Sies and B. Ketterer (Editors), *Glutathione Conjugation, Mechanisms and Biological Significance*, Academic Press, London, 1988, p. 74.
[3] B. Mannervik, Y.C. Awasthi, P.G. Board, J.D. Hayes, C. Di Ilio, B. Ketterer, I. Listowsky, R. Morgenstern, M. Muramatsu, W.R. Pearson, C.B. Pickett, K. Sato, M. Widersten and C.R. Wolf, *Biochem. J.*, 282 (1992) 305.
[4] B. Mannervik and U.H. Danielson, *CRC Crit. Rev. Biochem.*, 23 (1988) 283.
[5] P.J. Ciaccio, K.D. Tew and F.P. LaCreta, *Cancer Commun.*, 2 (1990) 279.
[6] P.J. Ciaccio, K.D. Tew and F.P. LaCreta, *Biochem. Pharmacol.*, 42 (1991) 1504.
[7] M.T. Smith, C.G. Evans, P. Doane-Setzer, V.M. Castro, M.K. Tahir and B. Mannervik, *Cancer Res.*, 49 (1989) 2621.

[8] D.M. Dulik, C. Fenselau and J. Hilton, *Biochem. Pharmacol.*, 35 (1986) 3409.
[9] D. Ross, *Pharmacol. Ther.*, 37 (1988) 231.
[10] R.A. Kramer, J. Zakher and G. Kim, *Science*, 241 (1988) 694.
[11] R.B. Puchalski and W.E. Fahl, *Proc. Natl. Acad. Sci. USA*, 87 (1990) 2443.
[12] S.M. Black, J.D. Beggs, J.D. Hayes, A. Bartoszek, M. Muramatsu, M. Sakai and C.R. Wolf, *Biochem. J.*, 268 (1990) 309.
[13] K.D. Tew, C.B. Pickett, T.J. Mantle, B. Mannervik and J.D. Hayes (Editors), *Structure and Function of Glutathione S-Transferases*, CRC Press, Boca Raton, FL, 1993, p. 251.
[14] L. Gilbert, L.J. Elwood, M. Merino, S. Masood, R. Barnes, S.M. Steinberg, D.F. Lazarous, L. Pierce, T. d'Angelo, J.A. Moscow, A.J. Townsend and K.H. Cowan, *J. Clin. Oncol.*, 11 (1993) 49.
[15] D.J. Meyer, E. Lalor, B. Coles, A. Kispert, P. Alin, B. Mannervik and B. Ketterer, *Biochem. J.*, 260 (1989) 785.
[16] B. van Ommen, J.J.P. Bogaards, W.H.M. Peters, B. Blaauboer and P.J. van Bladeren, *Biochem. J.*, 269 (1990) 609.
[17] J.A. Johnson, T.L. Neal, J.H. Collins and F.L. Siegel, *Biochem. J.*, 270 (1990) 483.
[18] L.L. Radulovic and A.P. Kulkarni, *Biochem. J.*, 239 (1986) 53.
[19] H.V. Singh, G.A.S. Ansari and Y.C. Awasthi, *J. Chromatogr.*, 361 (1986) 337.
[20] E. Martínez-Lara, P. Pascual, F. Toribio, J. López-Barea and J.A. Bárcena, *J. Chromatogr.*, 609 (1992) 141.
[21] P. Ålin, H. Jensson, C. Guthenberg, U.H. Danielson, M.K. Tahir and B. Mannervik, *Anal. Biochem.*, 146 (1985) 313.
[22] M. Sugimoto, H. Takikawa, A. Stolz and N. Kaplowitz, *Pharmacology*, 35 (1987) 65.
[23] W.B. Jakoby (Editor), *Methods in Enzymology*, Academic Press, New York, Vol. 77, 1981, p. 231.
[24] W.B. Jakoby (Editor), *Methods in Enzymology*, Academic Press, New York, Vol. 77, 1981, p. 398.
[25] V.M. Castro, M.K. Kelley, Å. Engqvist-Goldstein and L.M. Kauvar, *Biochem. J.*, 292 (1993) 371.
[26] J.D. Hayes, *Biochem. J.*, 255 (1988) 913.
[27] J.D. Hayes, L.A. Kerr and A.D. Cronshaw, *Biochem. J.*, 264 (1989) 437.
[28] P.J. Dierickx, *J. Chromatogr.*, 530 (1990) 263.
[29] J.D. Hayes, in C.B. Pickett and T.J. Mantle (Editors), *Glutathione S-Transferases and Drug Resistance*, Taylor and Francis, London, 1989, p. 17.
[30] L.R. Snyder and J.J. Kirkland, *Introduction to Modern Liquid Chromatography*, Wiley, New York, 1976, p. 3.
[31] F.P. LaCreta, J.J. Olszewski and K.D. Tew, *J. Chromatogr.*, 434 (1988) 83.
[32] R. Vince, S. Daluge and W.B. Wadd, *J. Med. Chem.*, 14 (1971) 402.
[33] M.H. Lyttle, D.T. Aaron, M.D. Hocker and B.R. Hughes, *Peptide Res.*, 5 (1992) 336.
[34] U.K. Laemmli, *Nature*, 227 (1970) 680.
[35] H. Blum, H. Beier and H.J. Gross, *J. Electrophor.*, 8 (1987) 93.
[36] J.E. Flatgaard, K.E. Bauer and L.M. Kauvar, *Cancer Chemother. Pharmacol.*, 33 (1993) 63.
[37] L. Sundberg and J. Porath, *J. Chromatogr.*, 90 (1974) 87.
[38] R.R. Walters, in I.M. Chaiken (Editor), *Analytical Affinity Chromatography*, CRC Press, Boca Raton, FL, 1987, p. 117.
[39] C.V. Braun and D.E. Schmidt, *Biochemistry*, 12 (1973) 4878.
[40] D.L. Vander Jagt, L.A. Hunsaker, K.B. Garcia and R.E. Royer, *J. Biol. Chem.*, 260 (1985) 11603.
[41] K.A. Killick, *Anal. Biochem.*, 195 (1991) 255.
[42] Y. Soma, K. Satoh and K. Sato, *Biochim. Biophys. Acta*, 869 (1986) 247.
[43] F. Morel, O. Fardel, D.J. Meyer, S. Langouet, K.S. Gilmore, B. Meunier, C.D. Tu, T.W. Kensler, B. Ketterer and A. Guillouzo, *Cancer Res.*, 53 (1993) 231.
[44] P.K. Stockman, G.J. Beckett and J.D. Hayes, *Biochem. J.*, 227 (1985) 457.

ELSEVIER

Journal of Chromatography A, 663 (1994) 65–69

JOURNAL OF CHROMATOGRAPHY A

Automated high-performance liquid chromatographic method for the determination of acyclovir in plasma☆

K.J. Swart*, H.K.L. Hundt, A.M. Groenewald

Department of Pharmacology (G6) and Farmovs Institute for Clinical Pharmacology and Drug Development, UOFS, Bloemfontein, South Africa

(First received May 9th, 1993; revised manuscript received November 13th, 1993)

Abstract

Owing to the low plasma concentrations of acyclovir obtained during pharmacokinetic studies after low-dosage oral administration, a sensitive, automated HPLC method had to be developed for determining acyclovir in a large number of plasma samples. Extraction and injection of the samples were done automatically by a Gilson ASPEC system using tC_{18}, 100-mg Sep-Pak Vac extraction columns. The extracts were chromatographed on a Nova-Pak C_{18} column with sodium octanesulphonate and methanol in the mobile phase. The analyte was detected at 250 nm. The calibration graphs were linear up to at least 1200 ng/ml and the limit of quantification was 10 ng/ml.

1. Introduction

Acyclovir {9-[(2-hydroxyethoxy)methyl]guanine}, an acyclic analogue of the natural nucleoside 2′-deoxyguanosine, selectively inhibits replication of members of herpes groups of DNA viruses, with low host cell toxicity [1]. Acyclovir is slowly and poorly absorbed from the gastrointestinal tract (20%) [2] and reaches its peak concentration in plasma *ca.* 1.5–2 h after an oral dose.

A number of radioimmunoassay [3–5] and HPLC [6–11] methods have been published for the determination of acyclovir in plasma. These methods did not meet our requirement, as we needed a sensitive and automated method to determine acyclovir in a large number of plasma samples for up to five half-lives of the drug after a single 400-mg oral administration to human volunteers. A sensitive assay procedure was required in order to obtain the necessary data for pharmacokinetic calculations. Published radioimmunoassay methods are sensitive enough but they require the proper antibody, which was not available to us. Of the published HPLC methods, only that of Mascher *et al.* [10] was sensitive enough, but it required step-gradient elution to wash the column after every injection and it was not automated.

This paper describes the first fully automated procedure for the determination of acyclovir in plasma using solid-phase extraction and UV detection.

* Corresponding author.

☆ Presented at the *17th International Symposium on Column Liquid Chromatography, Hamburg, May 9–14, 1993.* The majority of the papers presented at this symposium were published in *J. Chromatogr. A*, Vols. 660 + 661 (1994).

0021-9673/94/$07.00
SSDI 0021-9673(93)E1226-P

2. Experimental

2.1. Chemicals and reagents

All the reagents were of guaranteed analytical grade and were used as received. Sodium octanesulphonate (SOS) was obtained from Tokyo Kasei Kogyo (Tokyo, Japan). Acyclovir was 99.7% pure. Water was purified by passing it through a Millipore Milli-Q filtration system (18 MΩ cm resistivity) (Waters, Milford, MA, USA).

2.2. Analytical systems

A modular HPLC system was used which consisted of a pump (LC-6A; Shimadzu, Kyoto, Japan), a Waters Nova Pak C_{18}, 4-μm particle size, 150 mm × 3.9 mm I.D., stainless-steel cartridge (batch T12632) protected by an Upchurch (20 mm × 2 mm I.D.) precolumn, dry-packed with Perisorb RP-18 (30–40 μm) packing. A Shimadzu SPD-6A UV detector was used to measure the absorbance of the eluate at 250 nm. The chromatograms were recorded on an SP4290 integrator (Spectra-Physics, San Jose, CA, USA) and the data were sent via a LABNET network to a workstation with Winner for Windows software for automated data manipulation.

Sample processing and injections were done by an ASPEC system (automated sample preparation with extraction columns) from Gilson (Villiers le Bel, France) utilizing Waters Sep-Pak Vac trifunctional C_{18} (tC_{18}) (100 mg; 1 ml) extraction columns.

2.3. Chromatography

The mobile phase consisted of methanol–Na_2HPO_4 (0.01 *M*) containing 0.01 *M* sodium octanesulphonate (7:93, v/v), with the final apparent pH of the mobile phase adjusted to pH 2.80 with concentrated orthophosphoric acid, pumped at a flow-rate of 1 ml/min, and the column temperature was maintained at 40°C. The retention time of acyclovir was *ca.* 3.6 min.

2.4. Sample preparation

Plasma standards and quality controls. An accurately weighed amount of acyclovir was dissolved in water and an aliquot was added to drug-free plasma to obtain a stock standard solution containing *ca.* 1.2 μg of acyclovir per millilitre of plasma. Subsequent dilutions with plasma were made to obtain eight adequate working standard solutions covering the expected range. For quality controls a stock standard solution in water was prepared and different amounts were individually added to three different volumes of drug-free plasma to obtain quality controls with concentrations $C_{max} = 601$ ng/ml, $C_{av} = 301$ ng/ml and $C_{min} = 88$ ng/ml. These standards and quality controls were divided into aliquots and stored at −20°C under the same conditions as the actual trial samples. With each batch of samples analysed each day a set of standards and quality controls were processed and were scattered among the 68 samples of each batch.

Plasma samples (0.5 ml) were transferred to 5-ml glass tubes and mixed with 0.5 ml of 5 m*M* sodium octanesulphonate (adjusted to pH 2.85 with concentrated orthophosphoric acid). The samples were briefly vortex mixed to achieve thorough mixing and placed in the ASPEC system.

The apparatus was programmed to condition each Sep-Pak Vac extraction column with 1 ml of methanol, followed by 1 ml of 5 m*M* sodium octanesulphonate (pH 2.85), just before use. The plasma mixture was loaded on to the column and washed with 0.5 ml of 5 m*M* sodium octanesulphonate (pH 2.85). The analytes were eluted with 300 μl of 5 m*M* sodium octanesulphonate (adjusted to pH 8.50 with 4 *M* NaOH)–methanol (4:1) into a clean tube and mixed by bubbling air and a 130-μl aliquot was automatically injected on to the HPLC column.

Validation. During the validation of the analytical method, standards and quality controls were prepared in plasma over the range of concentrations estimated to be $2 \cdot C_{max}$ expected (1244 ng/ml) down to $1/8 \cdot C_{min}$ expected (2.71

ng/ml). The controls were analysed five times to determine the accuracy and precision of the procedure. As the lower concentration controls often fall in a range close to the limit of detection, these serve as a measure of the limit of quantification (LQ). The limit of quantification was chosen as that concentration at which the analyte could still be determined with acceptable precision and accuracy (maximum R.S.D. = 15%). The LQ was set at 10 ng/ml with an R.S.D. of 5% and an accuracy of 97% with a signal-to-noise ratio of 7. The specificity of the assay with respect to related endogenous compounds was tested by analysing samples from six different volunteers during the method development and from 24 different volunteers during the study. No interfering peaks from endogenous plasma compounds were found during chromatography of these samples. As this was a pharmacokinetic study performed with volunteers, the assay procedure was not tested against possible interferences by concomitantly ingested drugs.

The absolute recovery was tested at concentrations of 601, 301 and 88 ng/ml by comparison with directly injected aqueous standard solutions. The recoveries were 87%, 82% and 88%, respectively.

3. Results and discussion

3.1. Selection of extraction method

From a number of experiments involving plasma precipitation with perchloric acid, trifluoracetic acid, acetonitrile and heavy metals, it was apparent that we would not obtain the necessary sensitivity required to measure acyclovir in plasma for five half-lives of the drug after a single 400-mg oral dose unless the samples could be prepurified and concentrated. Acyclovir is very hydrophilic and therefore it is very difficult to extract it from plasma using organic solvents. We tried to extract it from plasma at various pH levels (1–12) using from very non-polar solvents such as hexane to more polar solvents such as methylene chloride, without success. Ion-pairing extractions using di(2-ethylhexyl)phosphoric acid in chloroform as an ion-pairing reagent also proved unsuccessful. Solid-phase extraction columns tested unsuccessfully included silica, aminopropyl and non-polar phases such as C_2, C_8 and C_{18}, using buffers at various pH values. The retention of acyclovir on the benzenesulphonylpropyl ion-exchange cartridge was acceptable when the acyclovir was dissolved in water but not in plasma, even after plasma precipitation before loading of the sample on to the SPE column.

Good retention of acyclovir on a Novapak C_{18} analytical column was obtained when the mobile phase contained 5 m*M* sodium octanesulphonate at pH 2.8. This prompted us to investigate whether we could achieve a similar retention of acyclovir on a C_{18} SPE column using the same SOS solution. The optimum conditions for retention of acyclovir on a Bond-Elut C_{18} column (1 ml, 100 mg; Varian) were obtained when the plasma was mixed with an equal volume of 5 m*M* sodium octanesulphonate at pH 2.8 and the extraction column prepared with the SOS solution. At any pH value of the SOS solution below or above 2.8, a marked decrease in the retention of acyclovir on the SPE column was found. The recovery of acyclovir from C_{18} extraction columns from different manufacturers and from the same manufacturer with different batch numbers varied considerably (Table 1). With the Waters tC_{18} columns we obtained the best recoveries and batch-to-batch variation.

Elution of acyclovir from the extraction column can easily be achieved with organic solvents such as methanol, but direct injection of the eluate on to the analytical column results in peak broadening due to the low concentration of organic modifiers in the mobile phase. A solution containing 20% methanol in 5 m*M* sodium octanesulphonate (pH 8.5) gave 100% elution of acyclovir from the extraction column and did not compromise the peak shape after direct injection on to the analytical column. Higher concentrations of methanol caused severe peak-shape deterioration.

TABLE I

Differences in recovery of acyclovir from different C_{18} solid-phase extraction (SPE) columns.

SPE column	Lot No.	Recovery (%)
Supelclean LC_{18} (Supelco)	SP0386	45
Extra Sep C_{18} (Lida)	1253	51
Clean-UP C_{18} (World Wide Monitoring)	Test sample	59
Sep-Pak Vac tC_{18} (Waters)	P0334A1	85
	P0342A2	79
Bond Elut C_{18} (Varian)	071365	45
	070695	24
	070975	57

Fig. 1 shows representative chromatograms obtained from plasma analyses and demonstrates the lack of interfering endogenous compounds in the blank plasmas. Quantification was achieved using the peak-height values of acyclovir. The calibration graphs constructed with eight standard concentrations were linear over a wide range (5–1200 ng/ml) and almost passed through the origin [$y = -69.348 + 29.793x$ correlation coefficient $r^2 = 0.999$; y = peak height (arbitrary units) and x = concentration (ng/ml)]. The within- and between-day precision of the method is indicated in Table 2.

Although previous workers claimed better sensitivity for the detection of acyclovir using fluorescence detection, we decided to use UV detection as it avoided the need to work at very low pH values or low temperatures, as is required with fluorescence detection to obtain adequate sensitivity. Using an automated preconcentration step and UV detection, our method was sensitive enough for use in pharmacokinetic studies. The extraction and chromatographic procedures are fully automated and take only 10 min from injection of a sample to extraction and injection of a second sample. Minimum sample handling is required and analyses can be done 24 h per day.

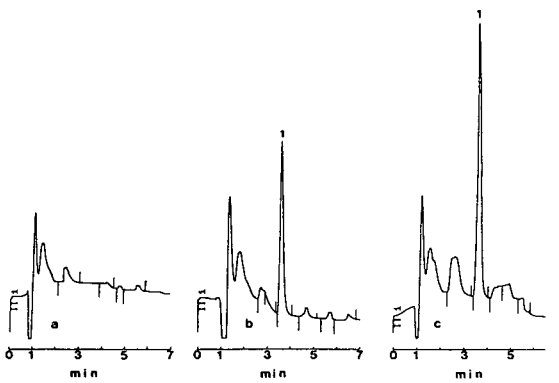

Fig. 1. Representative chromatograms obtained showing extractions from (a) blank plasma, (b) a trial sample equivalent to 567 ng/ml and (c) a plasma standard equivalent to 863 ng/ml. For HPLC conditions, see text.

3.2. *Factors affecting chromatographic resolution*

Smith and Walker [9] described the relationship between pH, an ion-pair reagent, sodium heptanesulphonate and the k' values for acyclovir. From that it was clear that appreciable retention of acyclovir occurred once the eluent pH decreased below 3.2. An acidic mobile phase containing sodium octanesulphonate was chosen as it permitted better retention of the compound on the reversed-phase column. Slight changes in pH significantly affected the retention of acyclovir. It was found that the pH of the mobile phase had to be lowered slightly after 200–300 injections in order to obtain reasonable retention times and optimum resolution from co-extracted endogenous components. Smith and Walker [9] used a polystyrened–divinylbenzene stationary phase to obtain better column stability, but large relative standard deviations were found below 1.2 μg/ml owing to the low column efficiencies for acyclovir.

Although the pH of the mobile phase eventually approached the commonly suggested limit (pH 2) for use with silica-based analytical columns, reasonable column lifetimes were observed. The columns were replaced after about 1000–1500 injections as lowering of the pH no longer resulted in separation of the analyte from the endogenous compounds. These columns were later tested and found to be still useful in the chromatography of other compounds. The analytical column appears to be modified by the

TABLE II

Within- and between-day precision of the method

Within-day ($n = 5$)			Between-day ($n = 20–24$)		
Nominal plasma concentration (ng/ml)	Nominal/found (mean) (%)	R.S.D. (%)	Nominal plasma concentration (ng/ml)	Nominal/found (mean) (%)	R.S.D. (%)
1244	93	7.2	1006	96	7.2
623	95	7.8	457	99	9.3
312	92	3.7	31.8	105	8.4
155	98	4.6			
77.3	98	7.2			
38.2	101	2.2			
20.4	109	2.3			
10.1	103	5.1			
5.44	106	10			

injection of the plasma extracts, which later renders them useless for further determinations of acyclovir but not for other compounds; the guard-column packing was changed every day to protect the analytical column from extracted plasma residues.

4. Conclusions

The method is sensitive enough to determine concentrations of acyclovir in low plasma volumes for 24 hs after a single 400-mg oral dose. Analyses can be done 24 h per day as the extraction, injection, chromatographic and data manipulation steps are completely automated.

5. References

[1] J.J. O'Brien and D.M. Campoli-Richards, *Drugs*, 37 (1989) 233.

[2] W.M. Sullender, A.M. Arvin, P.S. Diaz, J.D. Connor, R. Straube, W. Dankner, M.J. Levin, S. Weller, M.R. Blum and S. Chapman, *Antimicrob. Agents Chemother.*, 31 (1987) 1722.

[3] M. Hintz, R.P. Quinn, S.A. Spector, R.E. Keeney and J.D. Connor, in J.D. Nelson and C. Grassi (Editors), *Current Chemotherapy and Infectious Disease, Proceedings of the 11th International Congress of Chemotherapy and the 19th Interscience Conference on Antimicrobial Agents and Chemotherapy*, Vol. 2, American Society for Microbiology, Washington, DC, 1980, p. 1385.

[4] C.G. Prober, L.E. Kirk and R.E. Kenney, *J. Pediatr.*, 101 (1982) 622.

[5] P.P. Quinn, P. de Miranda, L. Gerald and S.S. Good, *Anal. Biochem.*, 98 (1979) 319.

[6] G. Land and A. Bye, *J. Chromatogr.*, 224 (1981) 51.

[7] J. Cronqvist and I. Nilsson-Ehle, *J. Liq. Chromatogr.*, 11 (1988) 2593.

[8] A.M. Molokhia, E.M. Niazy, S.A. El-Hoofy and M.E. El-Dardari, *J. Liq. Chromatogr.*, 13 (1990) 981.

[9] R.L. Smith and D.D. Walker, *J. Chromatogr.*, 343 (1985) 203.

[10] H. Mascher, C. Kikuta, R. Metz and H. Vergin, *J. Chromatogr.*, 583 (1992) 122.

[11] J. Salamoun, V. Sprta, T. Sladek and M. Smrz, *J. Chromatogr.*, 420 (1987) 197.

ELSEVIER

Journal of Chromatography A, 663 (1994) 71–78

JOURNAL OF CHROMATOGRAPHY A

Analysis of amino acids by gas chromatography–flame ionization detection and gas chromatography–mass spectrometry: Simultaneous derivatization of functional groups by an aqueous-phase chloroformate-mediated reaction

Jian Wang [a], Zhi-Heng Huang [b], Douglas A. Gage [b], J. Throck Watson *,[ab]

[a] *Department of Chemistry, Michigan State University, East Lansing, MI 48824, USA*

[b] *Department of Biochemistry, Michigan State University, East Lansing, MI 48824, USA*

(First received August 24th, 1993; revised manuscript received November 18th, 1993)

Abstract

The one-step ethyl chloroformate derivatization of amino acids in an aqueous medium is extended with the use of a variety of alkyl chloroformate reagents. This provides a new and convenient procedure for preparing esters with different alkoxy groups. A new mechanism for esterification during chloroformate derivatization is proposed based on the formation of an intermediate mixed carboxylic–carbonic acid anhydride followed by the exchange with an alcohol. Among the different reagents investigated, isobutyl chloroformate derivatized amino acids were found to provide more sensitivity for analyses by GC–flame ionization detection and GC–MS relative to derivatives prepared by other alkyl chloroformates.

1. Introduction

Analysis of protein hydrolysates for usual amino acids by gas chromatography is now routine. The foundation for the most commonly used method was laid by Gehrke and co-workers [1] who developed a procedure for quantitative derivatization to provide N(O,S)-trifluoroacetyl (TFA) amino acid *n*-butyl esters (TAB amino acids). Other perfluoroacyl alkyl esters [2,3] have also been useful in the vapor phase analysis of amino acids. Procedures for preparation of TAB and related derivatives require two reactions.

An alternative approach for the analysis of amino acids by GC was introduced by Hušek [4–6] and fatty acids [7]. Briefly, the Hušek procedure uses an aqueous medium in which ethyl chloroformate (EtCF) reacts instantaneously with the amino, carboxyl, and the side-chain functional groups (excluding the guanidino- and aliphatic hydroxyl groups). Results of a comprehensive study on the mass spectrometric fragmentation of this family of derivatives have been reported by this laboratory [8].

Here we report an extended and improved chloroformate derivatization method by applying

* Corresponding author. Address for correspondence: Department of Biochemistry, Room 116A, Biochemistry Building, Michigan State University, East Lansing, MI 48824-1319, USA

0021-9673/94/$07.00
SSDI 0021-9673(93)E1268-5

alternate alkylchloroformate reagents, as well as different combinations of reagents to derivatize amino acids prior to analysis by GC and GC–MS. Specifically, the incorporation of different alcohols in the reaction mixture provides a convenient means to prepare a variety of different esters. Some of these newly described derivatives provide higher sensitivities than the ethyl chloroformate amino acid derivatives. A reaction mechanism for carboxyl group derivatization is proposed which differs from that suggested by Hušek [4–7].

2. Experimental

The amino acids were purchased from Sigma (St. Louis, MO, USA), alkyl chloroformates and alcohols were purchased from Aldrich (Milwaukee, WI, USA). A solution of 20 amino acids in 0.1 *M* HCl at a concentration of 0.5 μg/μl each was prepared.

The N(O,S)ethoxycarbonyl ethyl ester of amino acids (ECEE) were prepared by adding 10 μl of the amino acid mixture to a H_2O–ethanol (EtOH)–pyridine (Py) (60 μl–30 μl–10 μl) solution. 5–10 μl of ethylchloroformate (EtCF) were then added and the reaction mixture was vortexed for 5–10 s and extracted with 100–200 μl $CHCl_3$. A 1-μl aliquot of the $CHCl_3$ layer was injected for analysis. Other chloroformate derivatives were prepared by adding the amino acids to a solution of H_2O–alcohol–Py (80 μl–30 μl–10 μl) and 10 μl of the chloroformate reagent following the same procedure.

Analyses by GC–MS were carried out on a JEOL AX-505H double focusing mass spectrometer coupled to a Hewlett-Packard 5890J gas chromatograph. GC separation was achieved on a DB-1701 (15 m × 0.25 mm I.D.) fused-silica capillary column with a 0.25 μm film coating from J&W Scientific (Rancho Cordova, CA, USA). Direct (splitless) injection was used. Helium gas flow was approximately 1 ml/min. MS conditions were as follows: interface temperature 275°C, ion source temperature *ca.* 150–200°C, electron energy 70 eV, scan rate of the mass spectrometer 1 s/scan over the range of *m/z* 50–750. GC–FID (flame ionization detection) was carried out on the same gas chromatographic column with injector and detector temperatures 260°C and 280°C, respectivelt; N_2 was the carrier gas.

3. Results and discussion

Initial experiments using different combinations of alkyl chloroformate reagents and various alcohols in the reaction medium indicated that the type of ester formed during the derivatization process with chloroformate reagents is directly dependent upon the type of alcohol present in the reaction medium. When using an alcohol with an alkyl group different from that in the alkyl chloroformate, the alkoxy group found in the ester derivative corresponds to the alcohol in the reaction medium, and not to the alkyl group of the chloroformate reagent. For example, when phenylalanine reacts with isobutyl chloroformate (iBuCF) in an aqueous medium also containing trimethylsilylmethanol [$(CH_3)_3SiCH_2OH \equiv TMSCH_2OH$], the derivative produced is that in which the carboxylic group is esterified with the trimethylsilylmethyl group, not the isobutyl group. The mass spectrum of this derivative and its structure are shown in Fig. 1. Similarly, when Phe is derivatized by reaction with isobutyl chloroformate in the presence of *n*-heptafluorobutanol in an aqueous reaction medium, the ester derivative formed includes a heptafluorobutoxyl group. The mass spectrum of this derivative and its structure are shown in Fig. 2.

The results presented in Figs. 1 and 2 are in conflict with those expected for carboxyl group derivatization based on the mechanism proposed by Hušek *et al.* [4–7]. According to the Hušek mechanism, the mixed anhydride formed by reaction between the alkyl chloroformate and carboxyl group should decarboxylate ($-CO_2$) to yield the ester containing the alkyl group derived from the alkyl chloroformate. Rather, the results reported here are consistent with a mixed anhydride–alcohol exchange mechanism for derivatization of the carboxyl group as illustrated in

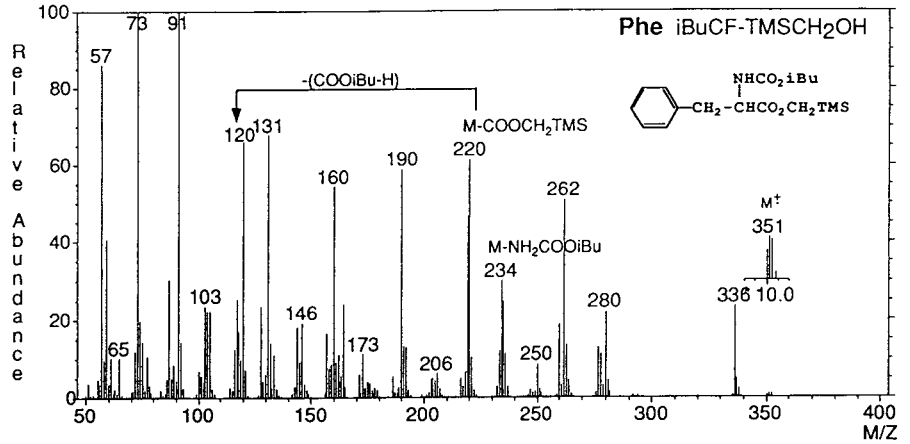

Fig. 1. EI mass spectrum of Phe derivatized by reaction with iBuCF–TMSCH$_2$OH.

Fig. 3. The carboxylic–carbonic acid mixed anhydride proposed as an intermediate in Fig. 3 has precedence in classical organic synthesis utilizing chloroformate reagents. The mixed anhydride reacts with the alcohol in the reaction medium to undergo an exchange reaction as illustrated via pathway A leading to the principal product. A small amount of derivative is also found in which the alkyl group in the ester moiety is the same as that in the alkyl chloroformate reagent. It is likely that this minor product derives from one or both of the possible routes indicated as B and C in Fig. 3. Via route B, it is possible that there is some decarboxylation of the mixed anhydride that takes place to produce the minor product. It is also possible, however, that the mixed anhydride reacts with a small amount of alcohol (having the same alkyl moiety as the chloroformate reagent) produced *in situ* from hydrolysis of the chloroformate reagent in the reaction medium.

Additional evidence for the direct involvement of alcohol constituents in the aqueous reaction medium containing the chloroformate reagent is given in Fig. 4. These data were obtained during analysis of Phe after treatment with isobutyl chloroformate in an aqueous solution containing equimolar amounts of seven alcohols: pentaflu-

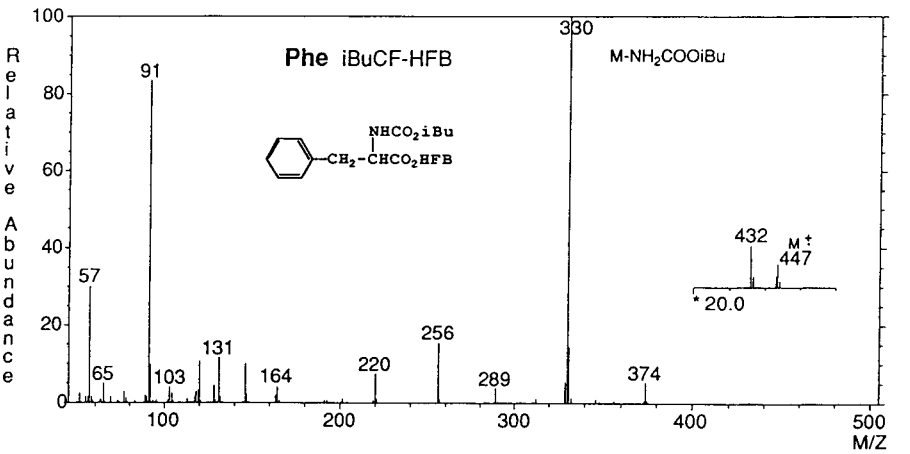

Fig. 2. EI mass spectrum of Phe derivatized by reaction with iBuCF–HFB.

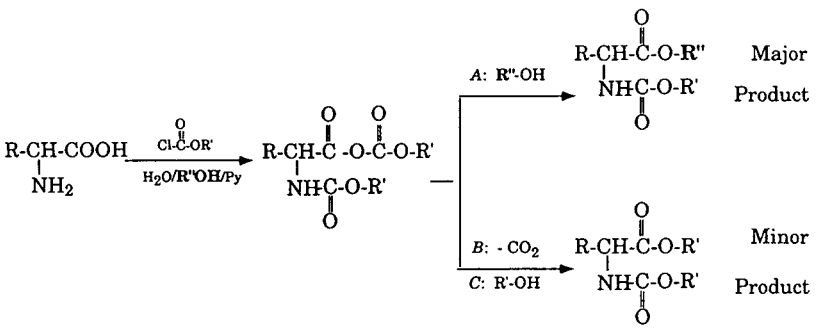

Fig. 3. Mixed anhydride–alcohol exchange mechanism for carboxyl group derivatization of amino acids reacting with ClCOOR' in a medium of H_2O–R"OH–pyridine.

oropropanol (PFP), heptafluorobutanol (HFB), trifluoroethanol (TFE), methanol, ethanol, propanol, and trimethylsilylmethanol. Fig. 4 is a reconstructed total ion current chromatogram resulting from analysis of the reaction mixture by GC–MS. Seven major peaks are obtained, corresponding to the esters formed by reactions with the alcohols in the reaction medium. The different intensities of the peaks result from the differential reactivity of these alcohols with the mixed anhydride and/or responses of the corresponding derivatives under EI–MS conditions.

Various combinations of chloroformate reagents and alcohols were used to generate a wide variety of N(O,S)-alkoxycarbonyl amino acid alkyl esters for analyses by GC or GC–MS with the objectives of optimizing the chromatographic separation of the amino acid derivatives, and evaluating the influence of the alkyl group of the chloroformate (alkyl carbamate in the derivative) and also the structure of the alcohol (alkoxyl group in the ester of the derivative) in the reaction medium on the response of the derivatives detected by FID or by EI-MS. These different combinations of the chloroformate reagents and alcohol systems are tabulated in Table 1 in groups I–III for ease of discussion. Within group I, the derivatives formed by the

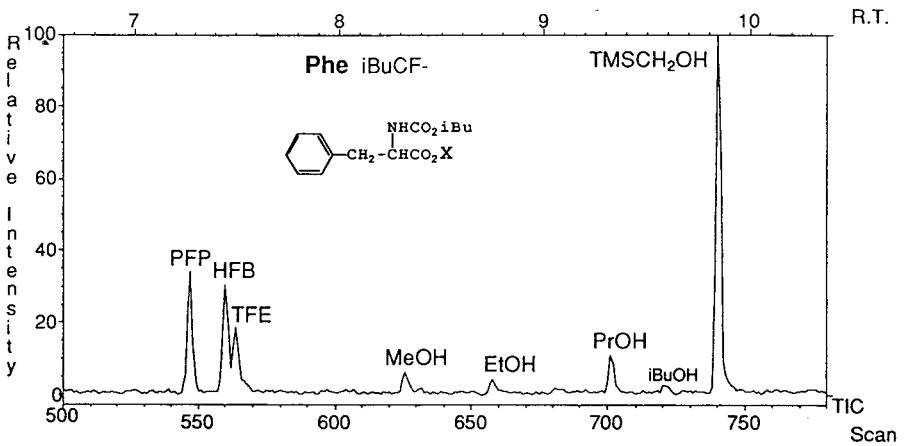

Fig. 4. Reconstructed TIC from analysis by GC–MS of the reaction mixture of Phe and iBuCF in an aqueous solution of an equimolar mixture of seven alcohols. The peaks correspond (as proved from corresponding mass spectra, not shown) to esters formed by exchange reaction with pentafluoropropanol (PFP), heptafluorobutanol (HFB), trifluoroethanol (TFE), methanol, ethanol, propanol, and trimethylsilylmethanol ($TMSCH_2OH$). The peak labeled iBuOH represents a trace of the ester product formed with the alkoxyl group corresponding to the alkyl group of the chloroformate reagent (see text)

Table 1
Composition of chloroformate reagent–alcohol systems studied

Reagent	Derivative
Group I	
EtCF–EtOH [a]	N(O,S)-ethoxycarbonyl ethyl ester
PrCF–PrOH [b]	N(O,S)-propoxycarbonyl propyl ester
iBuCF–iBuOH [c]	N(O,S)-isobutoxycarbonyl isobutyl ester
Group II	
EtCF–TFE	N(O,S)-ethoxycarbonyl trifluoroethyl ester
–PFP	N(O,S)-ethoxycarbonyl pentafluoropropyl ester
–HFB	N(O,S)-ethoxycarbonyl heptafluorobutyl ester
PrCF –TFE	N(O,S)-propoxycarbonyl trifluoroethyl ester
–PFP	N(O,S)-propoxycarbonyl pentafluoropropyl ester
–HFB	N(O,S)-propoxycarbonyl heptafluorobutyl ester
iBuCF–TFE	N(O,S)-isobutoxycarbonyl trifluoroethyl ester
–PFP	N(O,S)-isobutoxycarbonyl pentafluoropropyl ester
–HFB [d]	N(O,S)-isobutoxycarbonyl heptafluorobutyl ester
Group III	
iBuCF–$TMSCH_2OH$ [e]	N(O,S)-isobutoxycarbonyl trimethylsilymethyl ester
–$TMS(CH_2)_2OH$	N(O,S)-isobutoxycarbonyl trimethylsilyethyl ester
–$TMS(CH_2)_3OH$	N(O,S)-isobutoxycarbonyl trimethylsilypropyl ester

The order of response by GC–FID and by GC–MS: $e \sim d \sim c > b > a$.

reagents generates a response in MS analysis and by FID that increases with the size of the alkyl groups for the groups studied: (isobutyl > propyl > ethyl) in the chloroformate reagent as well as in the derivatizing alcohol. Thus, the responses of the iBuCF–iBuOH amino acid derivatives are higher than those of EtCF–EtOH derivatives. In group II, for any particular chloroformate reagent (EtCF, PrCF, or iBuCF), the detectability increases with the size of the perfluoroalcohol (HFB > PFP > TFE). Also in group II, for any particular alcohol (TFE, PFP, or HFB), the detectability increases with the size of the chloroformate (iBuCF > PrCF > EtCF). In group III, when using iBuCF and various TMS alcohols similar results as those in group II were found, but an increase in the size of the alcohol ($TMS(CH_2)_3OH > TMS(CH_2)_2OH > TMSCH_2OH$) causes greater production of the derivatives esterified with the alkyl group of the chloroformate reagent. The reason for increased competition from this side reaction is unclear, although it may result from slower alcohol–mixed anhydride exchange reactions for bulkier alcohols. In general, the formation of minor products from hydrolysis/exchange (pathway B + C, Fig. 3) were typically much less than 10% as indicated by the total ion current chromatogram of the derivatives; however, the yields of side products were not systematically investigated.

The highest detectability and the best chromatographic separations are produced by iBuCF–iBuOH, iBuCF–HFB, and iBuCF–$TMSCH_2OH$ derivatization reagents. Fig. 5 shows that the GC–FID responses of the 20 amino acids derivatized with iBuCF–iBuOH, iBuCF–HFB, and iBuCF–$TMSCH_2OH$ are higher than those prepared with EtCF–EtOH. Tyr and Hyp also can be derivatized and separated from the other 20 amino acids (even though these two were not included in the mixture represented in Fig. 5). The guanidino group on the side chain of Arg is not derivatized by the reaction mixture described here as verified by detection with FAB; Arg in this form cannot be eluted from the GC column. A quantitative comparison of the detector response to

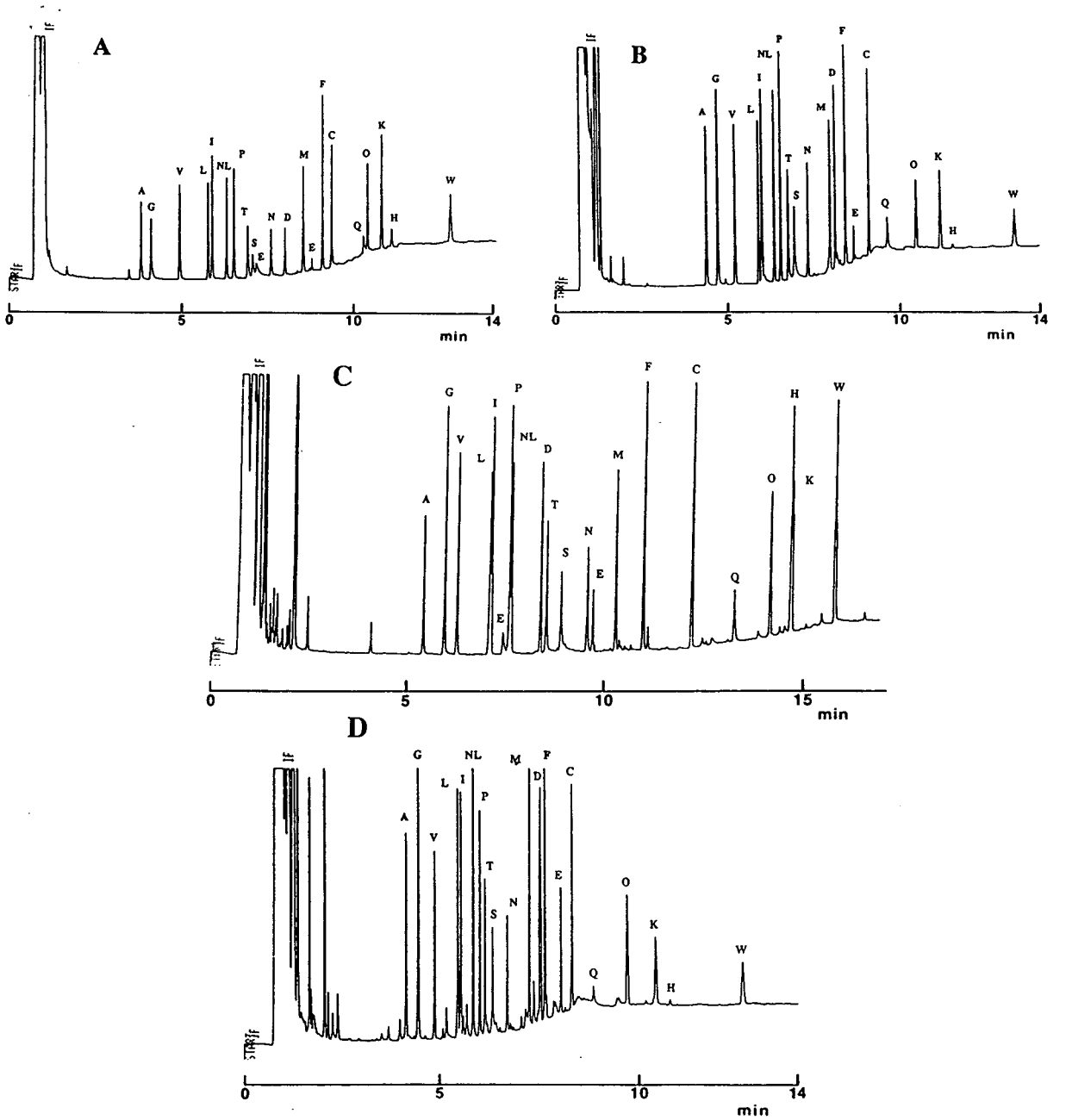

Fig. 5. Comparison of GC–FID chromatograms of derivatives of 20 amino acids prepared from four different chloroformate derivatization mixtures: (A) EtCF–EtOH; (B) iBuCF–iBuOH; (C) iBuCF–HFB; (D) iBuCF–TMSCH$_2$OH. The chromatograms result from injection of an aliquot of the reaction mixture containing 50 ng of each amino acid on to a 15m × 0.25 mm I.D. column containing a 0.25-μm film of DB-1701. Temperature programs: (A) from 110°C to 180°C at 10°C/min, then 30°C/min to 280°C; (B) from 140°C to 200°C at 10°C/min, then 30°C/min to 280°C; (C) from 100°C to 200°C at 10°C/min, then 15°C/min to 280°C; (D) from 150°C to 200°C at 10°C/min, then 40°C/min to 280°C. Norleucine (NL) is also included in the mixture. Tyrosine (Tyr) and hydroxyproline (Hyp)can also be derivatized, although the hydroxyl group of the latter is not modified. Arg is derivatized at the N- and C-terminus, but not on the side chain, and, as such, cannot be eluted from the GC column.)

Table 2
Ratio of peak area on GC–FID of indicated derivatives relative to those prepared with EtCF–EtOH

	PrCF–PrOH /EtCF–EtOH	iBuCF–iBuOH /EtCF–EtOH	iBuCF–HFB /EtCF–EtOH
Ala	1.5	2.0	1.4
Gly	1.8	2.6	2.4
Val	1.2	1.6	1.5
Leu	1.3	1.7	1.4
Ile	1.1	1.6	1.4
n-Leu	1.5	1.7	1.9
Pro	1.2	1.7	1.2
Thr	1.3	1.7	1.5
Ser	1.8	1.3	2.0
Asn	1.5	1.9	1.6
Asp	0.5	3.1	2.9
Met	1.7	1.5	1.4
Glu	1.3	2.2	4.3
Phe	1.2	1.5	1.4
Cys	1.3	1.4	2.0
Gln	4.1	3.2	4.5
Orn	1.1	1.2	1.4
Lys	1.0	1.1	1.2
His	0.7	0.4	5.7
Trp	0.9	1.2	2.7

Responses for EtCF–EtOH derivatives are the averages of results from triplicate analyses; responses for the indicated derivatives are the averages of results from duplicate analyses.

various derivatives is given in Table 2, which lists the ratio of GC–FID peak area produced by the derivatives made from PrCF–PrOH, iBuCF–iBuOH or iBuCF–HFB to those made from EtCF–EtOH. For derivatives prepared with PrCF and iBuCF, pyro-Glu is not resolved from isoleucine. Table 3 compares the reconstructed TIC responses of different groups of derivatives relative to those prepared from EtCF–EtOH. In nearly all cases, derivatives prepared from EtCF–EtOH gave a lower response. The mass spectra of the amino acid derivatives reported herein are produced through fragmentation pathways similar to those described earlier for mass spectra of EtCF–EtOH derivatives of amino acids [8]. The amino acid derivatives described in this paper are expected to have recoveries similar to those of amino acids derivatized with EtCF–EtOH [4–6]. Although quantitative experiments were not conducted, the inclusion of a suitable internal standard, such as norleucine (see Fig. 5) or stable isotope labelled amino acids, would make the approach described here suitable for quantitative analyses. Derivatization by iBuCF–iBuOH has been applied to the determination of isotopic amino acid incorporation into photosynthetic proteins of Synechocystis PCC 6803 [9].

4. Conclusions

The one-step chloroformate derivatization of amino acids in an aqueous medium has been extended with the use of a variety of alkyl chloroformate and alcohol reagents. It was discovered that the ester moiety of the amino acid derivatives is directly dependent upon the type of alcohol used in the aqueous reaction medium. Based on these findings, a new mechanism for ester formation is proposed to involve an alcohol exchange reaction with an intermediate mixed anhydride of the carboxyl group. These results have provided new insight into the one-step

Table 3
Ratio of both peak area and peak height of reconstructed TIC corresponding to the indicated derivatives relative to those made with EtCF–EtOH from analyses by GC–MS (EI)

	PrCF–PrOH /EtCF–EtOH		iBuCF–iBuOH /EtCF–EtOH		iBuCF–HFB /EtCF–EtOH	
	Area	Height	Area	Height	Area	Height
Ala	0.99	0.95	1.79	2.09	2.05	1.93
Gly	1.13	1.13	1.98	2.24	3.33	3.02
Val	0.90	0.81	1.09	1.21	1.70	1.57
Leu	0.97	1.01	1.49	1.58	2.24	2.96
Ile	0.78	0.81	0.87	0.91	1.37	1.75
Leu	0.98	0.92	1.42	1.45	2.01	1.83
Pro	1.06	1.16	1.60	1.92	1.88	1.88
Thr	1.14	1.39	1.58	1.70	1.87	2.02
Ser	0.85	0.67	1.10	1.08	1.05	1.43
Asn	1.23	1.18	1.69	1.72	2.49	2.42
Asp	0.37	0.37	1.88	2.66	3.51	2.81
Met	1.81	1.55	1.52	1.53	1.84	1.52
Glu	1.20	1.30	0.94	0.83	2.33	2.16
Phe	1.22	1.79	1.41	1.90	1.83	1.82
Cys	1.48	1.85	0.62	0.83	2.02	2.25
Gln	2.03	1.96	1.70	1.68	1.40	1.22
Orn	1.22	1.87	1.01	1.58	1.02	1.27
Lys	1.07	1.42	0.95	1.14	0.71	0.67
His	1.68	1.65	1.17	0.83	2.93	3.17
Trp	1.10	0.84	1.20	0.86	1.52	1.05

derivatization reaction and have provided the basis for preparing a variety of derivatives that can be assessed for optimizing the analysis of amino acids by GLC with FID or by GC–MS. Discovering the influence of the alcohol on the chloroformate reaction in an aqueous medium opens the possibility for preparing a wide variety of ester derivatives that can be tailored to the analytical needs of a specific problem. A variation of the chemical procedure reported here to prepare perfluorinated derivatives with chloroformate–alcohol reagents is being undertaken to facilitate analyses by electron capture negative ionization mass spectrometry.

5. Acknowledgements

Mass spectral data were acquired at the MSU Mass Spectrometry Facility which is supported, in part, by a grant (RR00480) to JTW. from the National Institutes of Health, National Center for Research Resources and by several units at Michigan State University.

6. References

[1] C.W. Gehrke, R.W. Zumwalt and L.L. Wall, *J. Chromatogr.*, 37 (1967) 398.
[2] S.L. Mackenzie in R.E. Clement (Editor), *Gas Chromatography: Biochemical, Biomedical and Clinical Application*, Vol. III, John Wiley and Sons, Inc., New York, 1990, Ch. 10, p. 267.
[3] W. Vetter, in G.R. Waller and O.C. Dermer (Editors), *Biochemical Applications of Mass Spectrometry*, Suppl. Vol., Wiley-Interscience, New York, 1980, p. 439.
[4] P. Hušek, *FEBS Lett.*, 280 (1991) 354.
[5] P. Hušek and C.C. Sweeley, *J. High Resolut. Chromatogr.*, 14 (1991) 751.
[6] P. Hušek, *J. Chromatogr.*, 552 (1991) 289.
[7] P. Hušek, J.A. Rijks, P.A. Leclercq and C.A. Cramers, *J. High Resolut. Chromatogr.*, 13 (1990) 633.
[8] Z.-H. Huang, J. Wang, P. Hušek, D.A. Gage, J.T. Watson and C.C. Sweeley, *J. Chromatogr.*, 635 (1993) 271.
[9] N.R. Bowlby, M. Espe, R. Bhatnagar, J. Wang, C. Hoganson, L. McIntosh and G.T. Babcock, *Photosynthesis Research*, in press.

ELSEVIER

Journal of Chromatography A, 663 (1994) 79–85

JOURNAL OF CHROMATOGRAPHY A

Gas chromatographic separation of the enantiomers of volatile fluoroether anesthetics by derivatized cyclodextrins II. Preparative-scale separations for isoflurane

Daniel U. Staerk, Aroonsiri Shitangkoon, Gyula Vigh *

Department of Chemistry, Texas A & M University, College Station, TX 77843-3255, USA

(First received October 19th, 1993; revised manuscript received November 30th, 1993)

Abstract

Preparative-scale gas chromatographic separation of the enantiomers of isoflurane, a volatile anesthetic, has been achieved with 2 m × 10 mm I.D. columns, packed with 80–100 mesh Chromosorb W AW, coated with up to 23% (w/w) trifluoroacetyl γ-cyclodextrin as stationary phase. The type and particle size of the support, the concentration of the stationary phase and the separation conditions were varied to improve product purity and the production rate under overloaded elution mode conditions. Using a sampling interface located between the exit of the preparative column and the fraction collector, effluent samples were directed onto a short, high-efficiency analytical capillary column every 30 s to achieve on-line enantiomeric analysis of the eluting bands, which allowed the calculation of purity, recovery and production rate for the separations.

1. Introduction

In the early 1970s, there were some exciting developments in preparative-scale gas chromatography (GC) which culminated in 1–4 in. (1 in. = 2.54 cm) I.D. packed columns with plate heights on the order of 1 mm, cycle times less than 1 h and production rates of 50 mg/day to 100 g/day [1–3]. Though preparative GC never replaced distillation as an industrial production method, due to advances in modelling and engineering in the 1980s, Bonmati *et al.* [4] were able to design and realize systems with production rates as high as 100 g/day to 100 kg/day.

Though there is a strong, documented need for pure enantiomers in the life sciences [5], very little has been published about the efforts aimed at their production by preparative GC. Schurig and Leyrer [6,7] were able to isolate, in 2- to 20-h long runs, up to 10-mg quantities of the pure enantiomers of pheromones using 3.5 m × 4 mm I.D. columns packed with 60–80 mesh (approximately 175–250 μm) Chromosorb W, coated with 0.7% (w/w) of nickel(II) bis[(6-heptafluorobutanoyl)-(5 *S*)-carvonate] in squalane as stationary phase. The limited success is due, primarily, to the small chiral selectivity factors ($\alpha \leq 1.5$), and the accompanying large k' values that are commonly observed with the current, mostly cyclodextrin-based, chiral GC stationary phases [8–11].

Following the first report [12] on the successful capillary GC analysis of fluoroethers, in Part I of this series [13] we studied the factors that led to maximized separation selectivities for the enantiomers of one of the volatile fluoroether

* Corresponding author.

0021-9673/94/$07.00
SSDI 0021-9673(93)E1280-D

anesthetics, isoflurane [2-chloro-2-(difluoromethoxy)-1,1,1-trifluoroethane]. Of the commercially available cyclodextrin-based chiral stationary phases, trifluoroacetyl γ-cyclodextrin, operated at 40°C, showed both sufficiently high α and acceptably low k' values, suggesting that preparative-scale enantiomer separations using a packed GC column could be attempted. Trifluoroacetyl γ-cyclodextrin is, as most derivatized cyclodextrins used as neat stationary phases, a mixture of isomers and homologues [8], a viscous, honey-like liquid that can be coated onto the walls of capillary columns, or onto the surface of diatomite-based GC supports. In this paper, we will describe some of the early results of these preparative-scale separation efforts including column preparation, the development of an on-line fraction analysis scheme for the determination of the enantiomeric purity of the eluting bands, as well as load, recovery and production rate studies.

2. Experimental

Preparative-scale GC separations were completed on a PSGC 10-40 preparative gas chromatograph (Varex, Burtonsville, MD, USA), equipped with a septumless injector, a large-capacity oven and a thermal conductivity detection (TCD) system. A Chrom-1 AT data acquisition board (Keithley-Metrabyte, Tauton, MA, USA) installed in a 386SX-20 NEC personal computer, and our ChromPlot1 software [14] was used for data acquisition and analysis. An HP 5890 Series II gas chromatograph (Hewlett-Packard, Avondale, PA, USA), equipped with a cryostate, a septumless split/splitless injector, a flame ionization detector, and a ChemStation data collection/analysis system was used for the semi-preparative and analytical-scale separations.

An effluent sampling interface, based on a Series 7000 switching valve (Rheodyne, Cotati, CA, USA), which was connected between the TCD outlet of the PSGC 10-40, the cooled fraction collector unit and the inlet of an analytical capillary column, allowed for the on-line enantiomeric purity analysis of the effluent of the preparative column. A 15 m × 0.25 mm I.D. fused-silica capillary, coated with a 0.25-μm thick film of trifluoroacetyl 2,6-O-dipentyl γ-cyclodextrin (ASTEC, Whippany, NJ, USA) was used as the analytical column for the on-line analysis. A 0.5–3-s wide effluent sample could be injected into the capillary column (and the enantiomeric analysis could be completed) every 30 s. Semi-preparative and preparative columns of 2.1 mm I.D., 5.3 mm I.D. (Supelco, Bellefonte, PA, USA) and 10.0 mm I.D. (Varex) were constructed from copper and stainless-steel tubing. Chromosorb W AW and W HP, 80–100, 100–120 and 120–140 mesh (Supelco) were used as support materials (approximately 150–175 μm, 125–150 μm and 105–125 μm fractions, respectively).

Hydrogen and helium were used as carrier gases at various average linear velocities with methane as the unretained compound. All separations were performed isothermally in the −10 to 70°C range. Isoflurane was obtained from Anaquest (Murray Hill, NJ, USA), a division of BOC Health Care.

Semi-preparative (2.1 mm I.D.) and preparative (> 2.5 mm I.D.) columns were fabricated in essentially the same fashion. The calculated amount of trifluoroacetyl γ-cyclodextrin was dissolved in enough dichloromethane to yield a thin slurry when mixed with the desired amount of dry diatomite support. Dichloromethane was then removed in a Rotavap (Fisher Scientific, Pittsburgh, PA, USA), under slight vacuum, and the packing was transferred into a fluidization apparatus where it was conditioned with dry nitrogen at 105°C for 1–1.5 h. Columns were packed with a combination of tapping and turning, while drawing dry nitrogen through the column. Plate heights were determined by injecting dichloromethane, which is as retained on trifluoroacetyl γ-cyclodextrin as isoflurane.

3. Results and discussion

3.1. Column packing studies

Chromosorb W AW and W HP supports (80–100, 100–120 and 120–140 mesh) were coated

with 4.7% (w/w) trifluoroacetyl γ-cyclodextrin and packed into straight, 1 m × 1/4 in. O.D. columns using different packing methods. Invariably, the denser 80–100 mesh Chromosorb W AW material yielded more efficient columns (Fig. 1), with varying degrees of lumping for both the W HP material and the smaller particle size fractions. Next, the concentration of the trifluoroacetyl γ-cyclodextrin stationary phase was increased through 7.5, 10, 15 and 20% (w/w) to 23.4% (w/w). Up to this point, the plate heights did not increase with increasing loading of the stationary phase (Fig. 1). Finally, when the 23.4% (w/w) trifluoroacetyl γ-cyclodextrin coated 80–100 mesh Chromosorb W AW material was packed into 10 mm I.D. columns (the largest used in this study), the column efficiency increased slightly indicating that the efficiencies were limited by the homogeneity of the bed structure, rather than by liquid phase mass transfer problems. [Incidentally, about twice as many plates were obtained when 25% (w/w) PS255-coated 80–100 mesh Chromosorb W AW was packed into the same 10 mm I.D. columns.]

Therefore, in the rest of the studies, 2-m long sections of 10 mm I.D. columns packed with 23.4% (w/w) trifluoroacetyl γ-cyclodextrin on 80–100 mesh Chromosorb W AW were used.

3.2. Loading studies

The loading characteristics of the 2 m × 10 mm I.D. columns were tested next. The injected sample size was increased from 6 mg to 1200 mg and the elution profiles were determined as shown in Fig. 2. The separation cycle can be completed in about 30 min.

In order to determine the enantiomeric purity *vs.* sample load characteristics, as well as the positions of the cut-points for fraction collection, the enantiomeric composition in the effluent of the preparative column has to be known. Since no chiroptical GC detector was available for this study, a capillary column, coated with the same trifluoroacetyl γ-cyclodextrin as the preparative column, but capable of completing the enantiomer analysis in less than 30 s was made using the static coating procedure [15]. The width of the effluent plug injected into the capillary column could be varied from 0.5 s upwards; 3-s aliquots

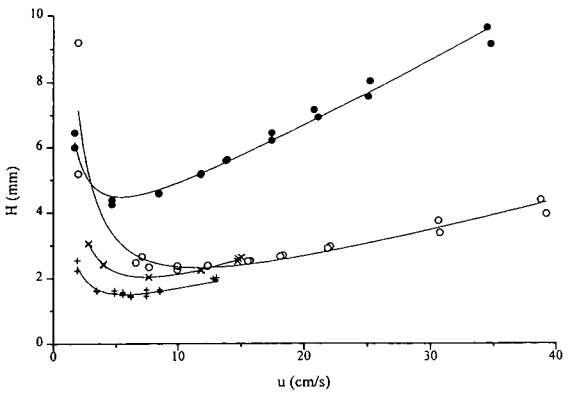

Fig. 1. Van Deemter plots (H = plate height, u = linear velocity) for the packed trifluoroacetyl γ-cyclodextrin columns. Column length: 1 m; temperature: 40°C, isothermal; carrier gas: hydrogen. Packing: 4.7% (w/w) trifluoroacetyl γ-cyclodextrin on Chromosorb W HP 80–100 mesh (●), 4.7% (w/w) trifluoroacetyl γ-cyclodextrin on Chromosorb W AW 80–100 mesh (○) in 2.1 mm I.D. semi-preparative columns; 23.4% (w/w) trifluoroacetyl γ-cyclodextrin on Chromosorb W AW 80–100 mesh in 5.3 mm I.D. column (x); 23.4% (w/w) trifluoroacetyl γ-cyclodextrin on Chromosorb W AW 80–100 mesh in 10 mm I.D. column (+).

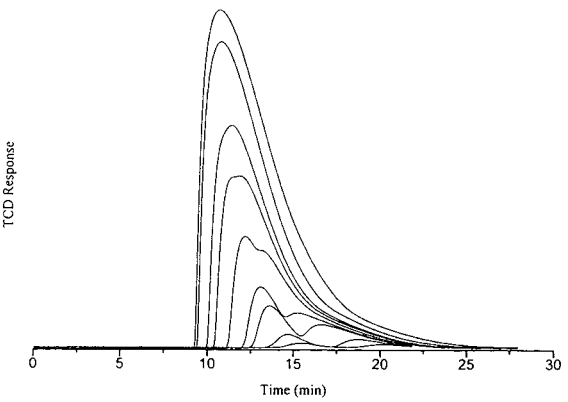

Fig. 2. Sample load study on the 2 m × 10 mm I.D. preparative column packed with 23.4% (w/w) trifluoroacetyl γ-cyclodextrin on 60–80 mesh Chromosorb W AW. Column temperature: 40°C, isothermal; carrier gas: helium at 2.2 cm/s. Racemic isoflurane sample loads: 12, 36, 120, 195, 335, 525, 675, 900 and 1200 mg, increasing as peak height.

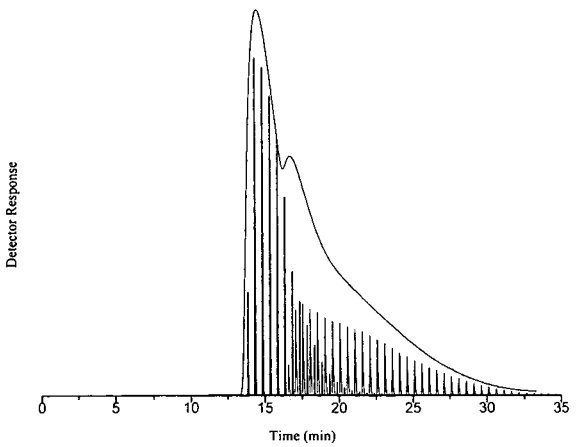

Fig. 3. Example of an on-line enantiomeric fraction analysis. Sample: 195 mg racemic isoflurane. 2 m × 10 mm I.D. preparative column packed with 23.4% (w/w) trifluoroacetyl γ-cyclodextrin on 80–100 mesh Chromosorb W AW, operated at 40°C with 2.2 cm/s helium as carrier gas. Analytical column: 15 m × 0.25 mm I.D. fused-silica capillary coated with a 0.25-μm thick film of trifluoroacetyl γ-cyclodextrin. Analysis temperature: 40°C, isothermal; carrier gas hydrogen at 50 cm/s. Sampling time: 3 s, sampling interval: 30 s. Dark peaks: (+)-isoflurane; light peaks: (−)-isoflurane.

allowed for the analysis of less than 0.01% of the minor enantiomer, so that value, coupled with a 30-s analysis cycle time, was used in the rest of the studies.

The TCD trace of the effluent of the preparative column, together with the corresponding on-line enantiomer analysis chromatograms, is shown in Fig. 3 for a 195-mg injection of racemic isoflurane sample. The peaks in the fraction analysis corresponding to the less retained enantiomer are in black, and those for the more retained enantiomer in white. The peak areas and the respective calibration curves allow for the determination of the quantities of the individual enantiomers in each fraction, and the calculation of production, production rate and enantiomeric purity of the pooled fractions.

The enantiomeric purity *vs.* production (lower horizontal axis) curves and recovery (upper horizontal axis) curves are shown in Figs. 4–7, with the actual reconstructed chromatogram appearing as an inset, for sample loads of 75, 195, 375 and 675 mg, respectively. The normalized

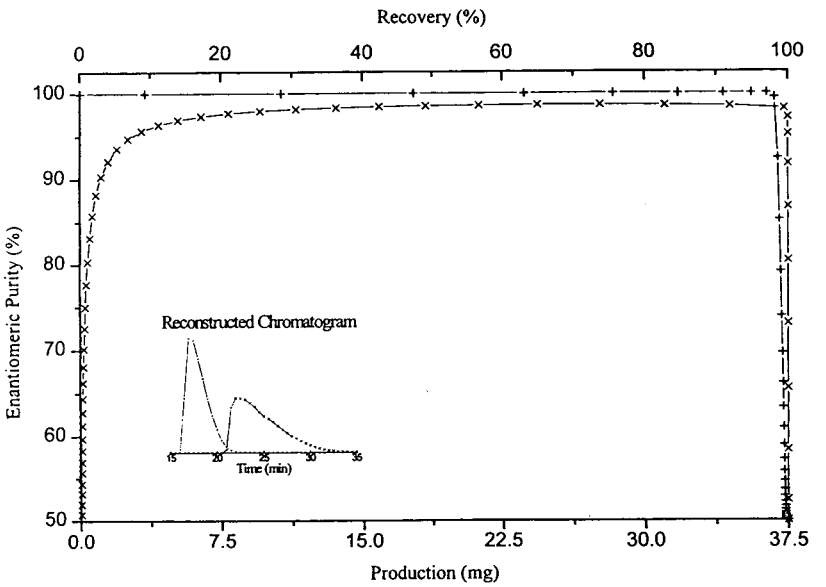

Fig. 4. Cumulative enantiomeric purity of the effluent as a function of enantiomer production (mg) on the lower horizontal axis, recovery (%) on the upper horizontal axis, with the reconstructed chromatogram shown in the inset. Sample load: 75 mg racemic mixture. Symbols: + = (+)-isoflurane; x = (−)-isoflurane.

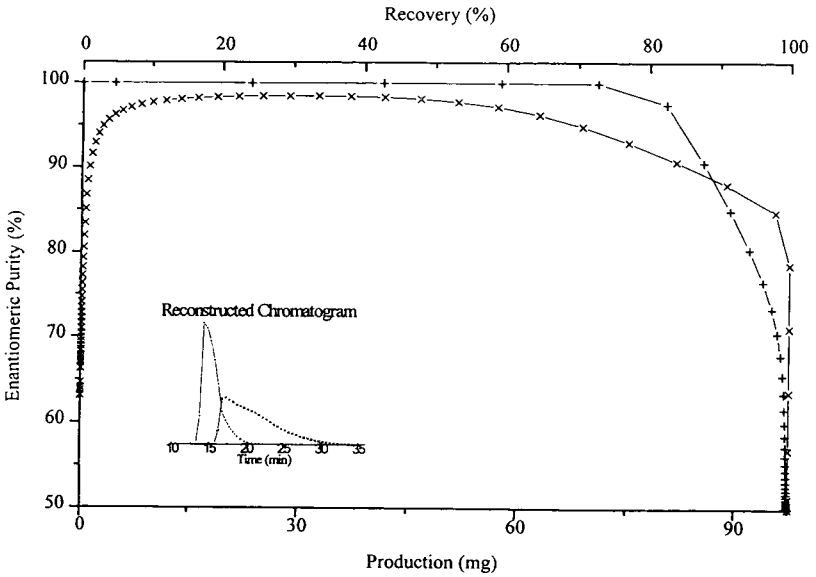

Fig. 5. Cumulative enantiomeric purity of the effluent as a function of enantiomer production (mg) on the lower horizontal axis, recovery (%) on the upper horizontal axis, with the reconstructed chromatogram shown in the inset. Sample load: 195 mg racemic mixture. Symbols as in Fig. 4.

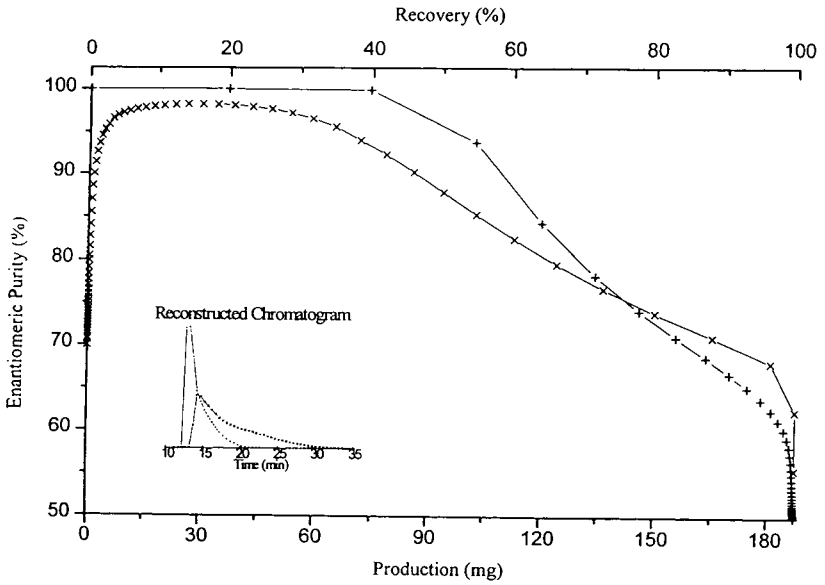

Fig. 6. Cumulative enantiomeric purity of the effluent as a function of enantiomer production (mg) on the lower horizontal axis, recovery (%) on the upper horizontal axis, with the reconstructed chromatogram shown in the inset. Sample load: 325 mg racemic mixture. Symbols as in Fig. 4.

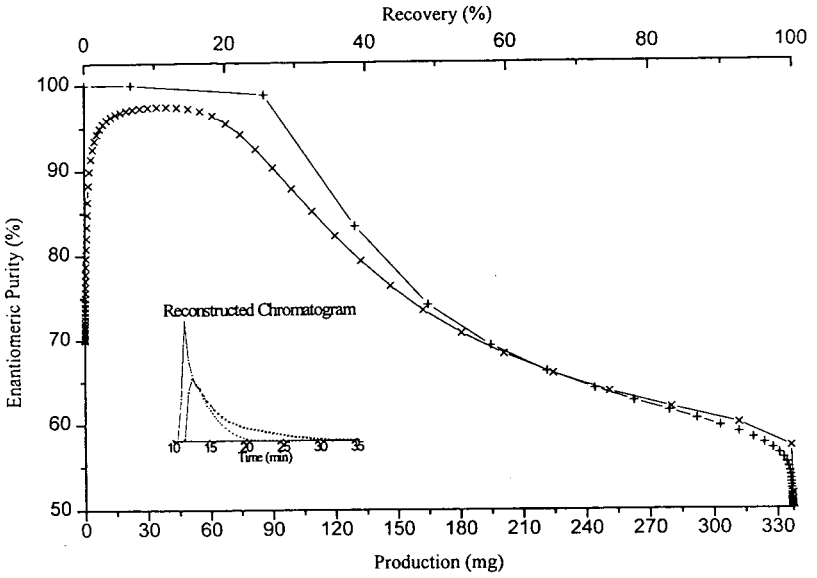

Fig. 7. Cumulative enantiomeric purity of the effluent as a function of enantiomer production (mg) on the lower horizontal axis, recovery (%) on the upper horizontal axis, with the reconstructed chromatogram shown in the inset. Sample load: 675 mg racemic mixture. Symbols as in Fig. 4.

production rate *vs.* sample load curves for both enantiomers at 99, 97 and 95% purity levels are shown in Fig. 8. It can be concluded that, with the help of the on-line fraction analysis method, the production rate can be steadily increased by increasing the size of the injected sample up to 395 mg. Above this point, increased load does not result in increased production rates.

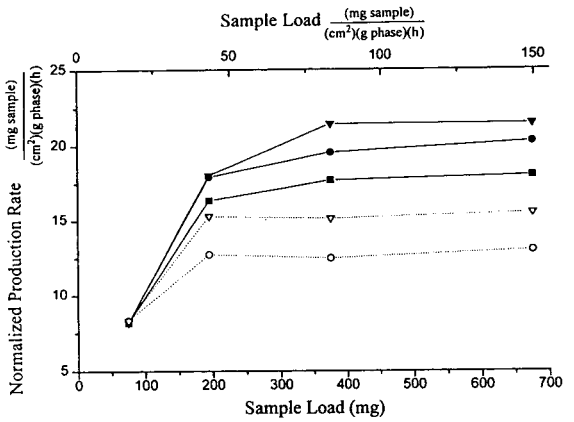

Fig. 8. Normalized production rate as a function of the sample load for various levels of product purity. Production rate has been normalized for column cross-section, stationary phase load and cycle time. Symbols: ▼ = (+)-isoflurane at 95 + % purity; ● = (+)-isoflurane at 97 + % purity; ■ = (+)-isoflurane at 99 + % purity; ▽ = (−)-isoflurane at 95 + % purity; ○ = (-)-isoflurane at 97 + % purity.

4. Conclusions

By maximizing the value of the separation selectivity factor through the selection of the appropriate cyclodextrin derivative to be used as the chiral stationary phase, and the column temperature as a compromise between high selectivity and strong retention, small-scale preparative GC separations of the enantiomers of isoflurane, a volatile anesthetic, have been successfully realized using 2 m × 10 mm I.D. columns. The sampling and switching interface allowed for the on-line analysis, in an efficient capillary column connected to the TCD exit of the preparative GC system, of the enantiomeric purity of the effluent stream and the aggressive, yet safe selection of the cut-points for fraction collections. Further work is under way in our laboratory to extend the method to the production of other valuable enantiomers.

5. Acknowledgements

Partial financial support for this project by the National Science Foundation (CH-8919151), the US Department of Education (415004), Anaquest Inc. and the Dow Chemical Company is gratefully acknowledged. ASTEC is acknowledged for providing the stationary phase used in this study.

6. References

[1] E. Bayer, K.P. Hupe and H. Mack, *Anal. Chem.*, 35 (1963) 492.
[2] M. Verzele, in J. Krugers (Editor), *Instrumentation in Gas Chromatography*, Centrex, Eindhoven, 1968, p. 159.
[3] A. Zlatkis and V. Pretorius, *Preparative Gas Chromatography*, Wiley-Interscience, New York, 1971, p. 73.
[4] R. Bonmati, G. Chapelet-Letourneux and G. Guiochon, *Sep. Sci. Technol.*, 19 (1984) 113.
[5] S.C. Stinson, *Chem. Eng. News*, 71 (1993) 38.
[6] V. Schurig, *Naturwissenschaften*, 74 (1987) 190.
[7] V. Schurig and U. Leyrer, *Tetrahedron: Asymmetry*, 1 (1990) 865.
[8] W.A. König, *Gas Chromatographic Enantiomer Separation with Modified Cyclodextrins*, Hüthig, Heidelberg, 1992.
[9] V. Schurig, M. Jung, D. Schmalzing, M. Schleimer, C. Duvekot, J.C. Buyten, J.A. Peene and P. Mussche, *J. High Resolut. Chromatogr.*, 13 (1990) 470.
[10] D.W. Armstrong, W. Li, A.M. Stalcup, H.V. Secor, R.R. Izac and J.I. Seeman, *Anal. Chim. Acta.*, 234 (1990) 365.
[11] A. Shitangkoon and Gy. Vigh, *J. High Resolut. Chromatogr.*, 16 (1993) 504.
[12] J. Meinwald, W.R. Thompson, D.L. Pearson, W.A. König, T. Runge and W. Francke, *Science*, 251 (1991) 560.
[13] A. Shitangkoon, D.U. Staerk and Gy. Vigh, *J. Chromatogr. A*, 657 (1993) 387.
[14] Gy. Vigh, G. Quintero and Gy. Farkas, in Cs. Horváth and J. Nikely (Editors), *Analytical Biotechnology*, American Chemical Society, Washington, DC, 1990, p. 181.
[15] J. Bouche and M. Verzele, *J. Gas Chromatogr.*, 6 (1968) 501.

ELSEVIER

Journal of Chromatography A, 663 (1994) 87–95

JOURNAL OF CHROMATOGRAPHY A

Optimization of supercritical carbon dioxide extraction for polychlorinated biphenyls and chlorinated benzenes from sediments

Hing-Biu Lee*, Thomas E. Peart

Research and Applications Branch, National Water Research Institute, Environment Canada, P.O. Box 5050, Burlington, Ontario L7R 4A6, Canada

(Received November 3rd, 1993)

Abstract

A method for the simultaneous extraction of polychlorinated biphenyls (PCBs) and chlorinated benzenes in sediments using supercritical fluid extraction (SFE) technique was developed. The best recovery of the above chlorinated pollutants was obtained by using non-modified carbon dioxide at 35 MPa and an extraction temperature of 100°C with a sediment moisture content in the 11 to 50% range. Cleanup of SFE extract was performed on a miniature Florisil column followed by sulfur removal with mercury. PCB levels were quantitated by a mixture of selected PCB congeners using a mass-selective detector so that the level of each PCB homologue series as well as the total PCB concentration in the sample extract could be evaluated. Under the optimized conditions, an extraction time of only 21 minutes was needed to produce PCB results comparable to a 7-h Soxhlet extraction. Meanwhile, the SFE recovery of chlorinated benzenes was up to 50% higher than for the Soxhlet results due to lower evaporative losses in the former procedure.

1. Introduction

Polychlorinated biphenyls (PCBs) contamination in the environment was first reported in 1966 [1]. Since then, there have been numerous indications of PCB pollution in various parts of the world. Because of their toxicity and suspected carcinogenicity to humans and wildlife [2], the levels of PCBs in water, sediments and biota samples are monitored in almost all water quality monitoring programs for organics. Considerable interest has also been focused on the determination of non-*ortho* substituted or coplanar PCB congeners as they exhibited toxicity at a level similar to 2,3,7,8-tetrachlorodibenzo-*p*-dioxin [3]. Although the manufacture and use of PCBs have ceased in the 1970s, environmental pollution of PCB may still arise from leaking storage tanks and improper disposal in landfill sites. In contrast, the contamination of chlorinated benzenes was not as widespread as PCBs. Their occurrence has been documented in Lake Ontario, particularly near the Niagara River, as well as the connecting channels of the Great Lakes [4–7]. Due to their persistence and tendency to accumulate in sediments and biota samples, PCBs and chlorinated benzenes pollution will remain as an environmental concern for many years to come.

* Corresponding author.

0021-9673/94/$07.00
SSDI 0021-9673(93)E0012-J

In the past, several hundred millilitres of solvent were used in all extraction methodologies developed for the determination of PCBs and chlorinated benzenes in sediments [8]. With the exception of the steam distillation procedure, there was no substitute for organic solvent until the advent of supercritical fluid extraction (SFE). Solvent extraction not only generated a large amount of waste, but also required lengthy evaporation and cleanup steps. For the determination of chlorinated benzenes, improper evaporation of sample extracts also led to losses of these volatile compounds.

SFE extraction of Aroclor 1254 from sediment was first reported by Schantz and Chesler [9]. Comparable amounts of PCBs were obtained either by Soxhlet extraction with dichloromethane or by a 4-h extraction at room temperature using supercritical carbon dioxide at 35.5 MPa. Later on, quantitative recovery of total PCBs from sediments have also been reported by other investigators in shorter extraction times using carbon dioxide modified by methanol and higher extraction temperatures [10,11]. Recently, Langenfeld *et al.* [12] have studied the effects of temperature and pressure on the SFE efficiency for selected PCB congeners. Their results indicated that, at 200°C, PCBs were effectively extracted by pure carbon dioxide at 15.5, 36.2 or 67.2 MPa. Lower PCB recovery was obtained for all congeners at an extraction temperature of 50°C, regardless of the fluid pressure used. Yet, these authors did not study the recovery of PCBs at extraction temperatures between the above extremes. Meanwhile, no results have ever been reported on the effect of SFE conditions on the recovery of PCBs at different level of chlorination, and there were few publications on the extraction of chlorinated benzenes by supercritical fluids. In this report, we describe the optimization of SFE conditions for PCBs and chlorinated benzenes in sediment samples.

2. Experimental

2.1. Reagents and chemicals

[$^2H_{12}$]Chrysene and [$^2H_4$]1,4-dichlorobenzene were products of MSD Isotopes (Pointe Claire, Canada). PCB congener standard solutions at 200 μg/ml in hexane were purchased from Ultra Scientific (North Kingstown, RI, USA). A mixture made up of the nine congeners (Table 1) at 10 μg/ml in isooctane was prepared by mixing appropriate amounts of the concentrated stock solutions. This mixture was further diluted to 1000, 250 and 100 pg/μl in the presence of [$^2H_{12}$]chrysene (500 pg/μl) as internal standard. Chlorinated benzenes and hexachloro-1,3-butadiene (HCBD) were obtained from Aldrich (Milwaukee, WI, USA). Octachlorostyrene (OCS) was also obtained from Ultra Scientific. Calibration mixtures of chlorinated benzenes, HCBD and OCS from 50 to 500 pg/μl were prepared in isooctane. Distilled-in-glass grade

Table 1
List of PCB calibration congeners and their quantitation and confirmation ions

Chlorobiphenyl	BZ No.	Chlorine substitution	Quantitation ion	Confirmation ion
Mono-	1	2	188	190
Di-	5	2,3	222	224
Tri-	29	2,4,5	256	258
Tetra-	50	2,2′,4,6	292	290
Penta-	87	2,2′,3,4,5′	326	328
Hexa-	154	2,2′,4,4′,5,6′	360	362
Hepta-	188	2,2′,3,4′,5,6,6′	394	396
Octa-	200	2,2′,3,3′4,5′,6,6′	430	432
Nona-	209	2,2′,3,3′,4,4′,5,5′,6,6′	464	466
Deca-	209	2,2′,3,3′,4,4′,5,5′,6,6′	498	500

solvents were purchased from Burdick & Jackson (Muskegon, MI, USA). SFE-Grade carbon dioxide without a helium head pressure was supplied by Air Products (Nepean, Canada).

2.2. Extraction of sediments

All SFE extractions were performed with a Hewlett-Packard 7680T module. Typically, a 7-ml thimble was prepared by placing two layers of Whatman GFC filter paper and 200 mg of Celite after the bottom thimble cap was installed. A 1-g sample was weighed into the thimble and then it was mixed with 500 μl of water by a vortex mixer. SFE was carried out at 100°C and 35 MPa (5000 p.s.i.) with unmodified carbon dioxide for 21 min (1 min static extraction and 20 min dynamic extraction). During the extraction, the octadecylsilane (ODS) trap was maintained at 15°C (see later discussion) for the sorption of extracts. Upon completion of extraction, the trap was warmed up to 45°C before the organics were eluted with two 1-ml aliquots of isooctane–hexane (1:1). The entire extraction–desorption cycle required *ca.* 35 min. For extractions using the modified carbon dioxide, a procedure previously described for polycyclic aromatic hydrocarbons (PAHs) was used [13].

For comparison, Soxhlet extraction was performed by refluxing the sediment with 300 ml of an acetone–hexane (59:41) mixture for 7 h. Evaporation of sediment extracts was performed with a three-stage Snyder column.

2.3. Cleanup procedure

The SFE extract was cleaned up on a 5-cm activated Florisil column packed in a 20 × 0.7 cm I.D. disposable Pasteur pipette. After pre-elution with 3 ml of pentane, the combined SFE extract was applied to the cleanup column. The chlorinated pollutants were eluted by another 10 ml of pentane and this fraction was then evaporated down to *ca.* 1 ml in a 40°C bath under a gentle stream of nitrogen. (Note: if the determination of chlorinated benzenes is not needed, hexane can be used instead of the less commonly available pentane.) The concentrated extract was then vigorously shaken with a drop of mercury and this step was repeated until the metal remained shiny. The extract was transferred to a calibrated test tube with several pentane rinses and the volume was brought down to just *ca.* 0.9 ml. Finally, 500 ng of the internal standard was added and the volume adjusted to 1 ml for GC–MS and GC–electron-capture detection (ECD) analyses.

2.4. Chromatographic analysis

Instrumental analysis of PCBs and chlorinated benzenes was carried out by a Hewlett-Packard (HP) 5890 Series II gas chromatograph equipped with a HP 5972A mass-selective detector, an electron-capture detector and a 30 m × 0.25 mm I.D. HP-5-MS capillary column. Splitless injections (1 μl) were made by the HP 7673A autosampler. The operation of the gas chromatograph, detectors, autosampler and the acquisition of data were all controlled by a personal computer running dedicated ChemStation and mass-selective detector softwares. The injection port and electron-capture detector were kept at 250 and 300°C, respectively while the mass-selective detector interface temperature was set at 280°C. The temperature program for PCB analysis was: initial oven temperature 70°C with a 1-min hold; programming rate 1, 30°C/min from 70 to 160°C; rate 2, 2.5°C/min from 160 to 260°C, and the final temperature was held for 10 min. The temperature program for chlorinated benzene analysis was: initial oven temperature 60°C with a 1-min hold; programming rate 1, 5°C/min from 60 to 150°C; rate 2, 10°C/min from 150 to 250°C and a 15-min hold at the final temperature. Splitless time was 1 min. Carrier gas was helium and constant column flow at 0.85 ml/min (MS work) or 1.2 ml/min (ECD work) was maintained by the electronic pressure controller. ECD make-up gas was argon–methane (95:5) at 30 ml/min. Electron energy and electron multiplier voltage of 70 eV and 2000 V, respectively, were used for all MS operations.

2.5. Acquisition of MS data

Prior to sample analysis, the mass-selective detector was tuned with perfluorotributyl-amine

(PFTBA) using the standard spectra autotune program. Mass spectral data for the PCBs were acquired in the selected ion monitoring mode using the characteristic and confirmation ions listed in Table 1 according to a previously published procedure [14]. Response factors for the calibration congeners relative to the internal standard [$^2H_{12}$]chrysene were determined. For samples, the peak areas for all PCB congeners at each level of chlorination were summed and quantitated against the calibration congener with the same number of chlorine atoms to yield the concentration of PCBs for each homologue series. Total PCB concentration in a sample was the sum of its PCB concentrations at each chlorination level. For better selectivity, dichlorobenzenes in sediment extracts were also analyzed by MS. In this case, masses m/z 146 and 148 (native dichlorobenzenes) and m/z 152 ([$^2H_4$]1,4-dichlorobenzene, internal standard) were monitored.

3. Results and discussion

Two lake sediments, one collected from the Hamilton Bay and the other from Lake Ontario at a site near the Niagara River, were used in development and optimization of the SFE method. Conventional analyses have previously been performed on these samples: the Hamilton Bay sediment was shown to be naturally contaminated with PCBs, and the Lake Ontario one with chlorinated benzenes and a few other chlorinated hydrocarbons. Both samples have been freeze-dried and homogenized before use. In order to determine the efficiency of the new extraction procedure, the SFE recoveries relative to the Soxhlet results were generated.

There are numerous factors that can affect the results in a SFE experiment. The ones that have a more significant effect on the recovery include the selection of extraction fluid, the density or pressure of the supercritical fluid, extraction temperature, flow-rates and extraction times, the nature and amount of modifier(s), and the collection technique for the extracts. Many of these factors are inter-related and optimal recovery of organics from a sample can often be obtained by different combinations of the above factors. Our aim in this work was to develop a method that is quantitative compared to Soxhlet, efficient (short extraction times), environmentally friendly and easy to adopt. Among all the supercritical fluid in use for extraction, carbon dioxide is by far the most widely used because of its availability, high purity, lower cost, ideal physical and chemical properties and environmental friendliness. Therefore other supercritical fluids were not evaluated in this study. Sorbent traps made of ODS have been shown to be highly efficient for the collection of a wide variety of semi-volatile and non-volatile organics in off-line SFE systems [15], thus they are most suitable for the collection of these chlorinated compounds. In our work, an extraction fluid pressure of 35 MPa and a flow-rate of 4 ml/min were chosen for more efficient extraction since the use of lower supercritical fluid pressures (or densities) usually and lower flow-rates usually requires a longer extraction time to achieve quantitative recovery.

3.1. SFE of PCBs from sediments

Nearly all sediment samples received for PCB analysis were wet, water was therefore added to our freeze-dried reference sample before the extraction was performed. In beginning of this work, the moisture content in our Hamilton Bay sediment was arbitrarily adjusted to 33%. Previously, we have shown that a higher extraction temperature results in a large improvement in the recovery of PAHs [13]. Using the Hamilton Bay sediment as a model sample, the recovery of PCBs in each homologous series was studied over the temperature range of 40 to 120°C in 20°C increments (Fig. 1). It should be noted that mono-, di, nona- and decachlorobiphenyls are either undetected or present in minute amounts in our reference sample and nearly all other sediments, their results were not evaluated. When SFE was carried out at 35 MPa with a flow-rate of 4 ml/min, PCBs are readily extracted by supercritical carbon dioxide. Even at low extraction temperatures of 40 and 60°C, the recovery of *total* PCBs was 73 and 82%, respec-

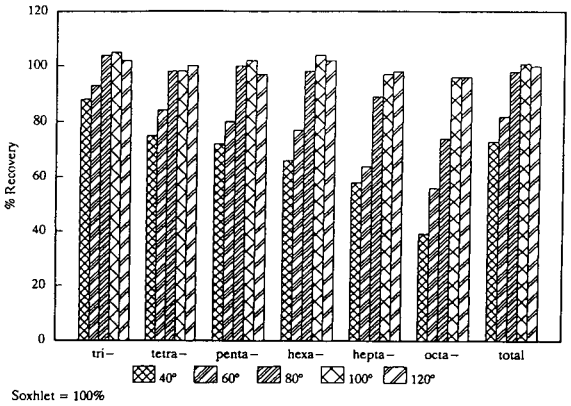

Fig. 1. Effect of extraction temperature (°C) on the SFE recovery of chlorobiphenyls and total PCBs from the Hamilton Bay sediment.

tively of the Soxhlet result. A closer look at Fig. 1 indicates that while the trichlorobiphenyls were nearly 90% recovered at 40°C, the recoveries of other chlorinated biphenyls continuously dropped when the level of chlorination increased. For example, the recovery of octachlorobiphenyls was down to 39% at this temperature. Higher temperatures produced higher recoveries of all PCBs, particularly those with higher chlorination. This observation is consistent with our work on PAHs where the higher-molecular-mass PAHs were more readily recovered at higher extraction temperatures. Over 95% recovery of all PCBs was obtained at 100°C. A further increase of extraction temperature to 120°C did not improve the recovery of PCBs, including the hepta- and octa-chlorobiphenyls.

The levels of PCBs from trichlorobiphenyls to octachlorobiphenyls in the Hamilton Bay sample determined by Soxhlet and SFE at 100°C were summarized in the second and third columns of Table 2. The precision and accuracy of the results indicated that both techniques produced data in good agreement with each other. Since the levels of hepta- and octachlorobiphenyls are relatively low in this sample, the *total* PCBs result obtained at 80°C was therefore nearly the same as the 100 or 120°C results (Fig. 1).

Sediment samples from the field had varying amounts of water, it was therefore interesting to find out if the moisture content in a sample also played a role in the recovery of PCBs under SFE conditions. Various amounts of water were added to the freeze-dried reference sample so that the resulting moisture content is 0, 11, 20, 33 or 50% before they were extracted by carbon dioxide at 100°C and 35.1 MPa (5000 p.s.i.). For all samples with 11 to 50% moisture content, the recoveries of PCBs in each homologous series were very similar to the results given in column three of Table 2. For the samples with zero moisture content, lower recoveries from 90 (for the trichlorobiphenyls) to 75% (for the hepta- and octachlorobiphenyls) were obtained. For this reason, extraction of completely dry sediment with pure carbon dioxide for PCB determination

Table 2
Mean levels of PCBs (ng/g) in the Hamilton Bay sediment by homologue series obtained under different extraction conditions

	Soxhlet ($n = 3$)	SFE 1 ($n = 6$)	SFE 2 ($n = 2$)	SFE 3 ($n = 2$)
Trichlorobiphenyls	275 ± 25	288 ± 17	287	299
Tetrachlorobiphenyls	681 ± 58	667 ± 49	654	687
Pentachlorobiphenyls	712 ± 63	726 ± 42	693	700
Hexachlorobiphenyls	310 ± 20	322 ± 21	298	341
Heptachlorobiphenyls	85 ± 12	82 ± 10	75	78
Ocatachlorobiphenyls	31 ± 3	29 ± 3	27	30
Total PCBs	2094 ± 182	2114 ± 161	2034	2135

Extraction conditions: Soxhlet: 300 ml of acetone–hexane (59:41, v/v), extraction time 7 h. SFE 1: 100°C extraction temperature and 35 MPa carbon dioxide pressure, no solvent modifier, extraction time 21 min. SFE 2: Same as SFE 1 except that 500 μl of dichloromethane–methanol (1:1, v/v) was spiked to the sediment prior to extraction. SFE 3: 120°C extraction temperature and 35 MPa carbon dioxide modified by 4% dichloromethane and 1% methanol, extraction time 42.5 min. See ref. 13 for details.

is not recommended. Attempts have also been made to extract PCBs from sediments in the presence of solvent modifier to see if higher recovery could be obtained. In these cases, the modifiers were introduced by either adding 500 μl methanol–dichloromethane (1:1) directly to the sample before extraction or mixing with the carbon dioxide with the assistance of a high-pressure modifier pump during the dynamic extraction [13]. In contrast with the SFE of PAHs from sediment, the recovery of all PCBs could not be further improved in the presence of solvent modifiers (fourth and fifth columns of Table 2). Since fewer coextractives such as PAHs and humic substances were obtained by pure carbon dioxide, it is therefore suggested that no additional modifier should be used for the SFE of PCBs from sediments.

The effect of extraction time on the recovery of PCBs was also studied. Within experimental errors, the PCB results were the same for extraction times of either 20 or 10 min. Approximately 70% of the total PCB was recovered for a 5 minutes dynamic extraction time.

3.2. SFE of chlorinated benzenes and some chlorinated hydrocarbons

For the work on chlorinated benzenes and a few other chlorinated hydrocarbons, the Lake Ontario sediment sample collected near Niagara River, NY, USA, was used. Similar to the SFE of PCBs, our work on chlorobenzenes and HCBD in sediments were carried out with a 33% moisture content. As shown in Fig. 2, low extraction temperatures were again unfavourable for the extraction of all compounds of interest. For example, less than 65% of all chlorinated benzenes and HCBD were recovered at 40°C compared to the Soxhlet results. Higher extraction temperature improved recovery of all compounds, and the highest recovery was obtained at either 100 or 120°C. Since similar results were obtained at these two temperatures, 100°C was used for the result of the experiment as a shorter cycling time (heating and cooling) was achieved at a lower extraction temperature.

The concentrations of chlorinated benzenes in

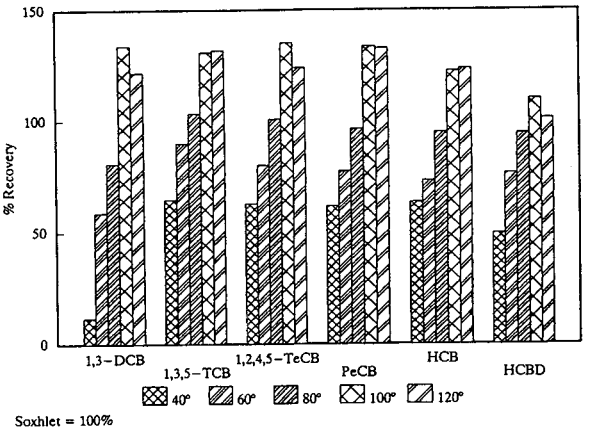

Fig. 2. Effect of extraction temperature (°C) on the SFE recovery of chlorinated benzenes and hexachloro-1,3-diene from the Lake Ontario sediment.

the Lake Ontario sediment obtained by Soxhlet as well as SFE procedures were summarized in Table 3. In contrast to the PCB results, at 100°C, the SFE recoveries of the chlorinated benzenes and HCBD were from *ca.* 10 to 35% higher than the Soxhlet values. Similar to our findings for naphthalene and methylnaphthalenes, the higher SFE results likely resulted from less evaporative losses in the SFE procedure since the latter required only one, instead of two, evaporations. This hypothesis was further supported by the results of the evaporation of Soxhlet extracts with known amounts of chlorobenzenes. Typically, only 65 to 85% of the chlorobenzenes could be recovered when 300 ml of the extract was concentrated to 1 to 2 ml, even if isooctane was used as a keeper in the evaporation.

We have also examined the effects of modifiers, extraction time and the ODS trap temperature on the recovery of chlorinated benzenes. Again, the addition of modifier (500 μl of dichloromethane–methanol, 1:1) to the sample prior to extraction did not improve the recovery of chlorobenzenes (Table 3, fourth column). Although there was no significant difference in chlorinated benzene results for extraction times of 15, 20 and 30 min, lower recoveries (from 55 to 85%) of all compounds were observed if the dynamic extraction time was reduced to 5 or 10 min. While lowering the trap temperature from

Table 3
Mean recovery of chlorobenzenes and chlorinated hydrocarbons (ng/g) in the Lake Ontario sediment by Soxhlet and SFE procedures

	Soxhlet ($n = 3$)	SFE 1 ($n = 6$)	SFE 2 ($n = 2$)	SFE 3 ($n = 2$)
1,3-Dichlorobenzene	84.8 ± 8	114 ± 10	105	156
1,4-Dichlorobenzene	66.0 ± 5	89.0 ± 8	87.2	127
1,3,5-Trichlorobenzene	72.5 ± 8.3	95.0 ± 8.3	95.7	97.3
1,2,4-Trichlorobenzene	100 ± 9	146 ± 12	151	143
1,2,4,5-Tetrachlorobenzene	114 ± 10	169 ± 11	174	169
1,2,3,4-Tetrachlorobenzene	30.8 ± 2.9	44.3 ± 3.1	42.4	43.9
Pentachlorobenzene	46.2 ± 5.8	64.5 ± 5.5	63.1	60.1
Hexachlorobenzene	195 ± 15	239 ± 13	225	227
Hexachloro-1,3-butadiene	42.8 ± 5.1	47.1 ± 3.6	43.9	46.2
Octachlorostyrene	36.4 ± 4.7	33.0 ± 2.9	37.4	31.9

Extraction conditions: Soxhlet: 300 mL of 51/49 (v/v) acetone–hexane (51:49, v/v), extraction time 7 h. SFE 1: 100°C extraction temperature and 35 MPa carbon dioxide pressure, no solvent modifier. Extraction time 21 min. SFE 2: Same as SFE 1 except that 500 μl of dichloromethane–methanol (1:1, v/v) was spiked to the sample prior to extraction. SFE 3: Same as SFE 1 except that the ODS trap temperature was kept at 0°C instead of 15°C during extraction.

15 to 0°C had no positive effects on the recoveries of trichlorobenzenes and other compounds of higher molecular masses, there was a *ca.* 40% increase in the recovery of the dichlorobenzenes (Table 3, fifth column). Trap temperatures of lower than 0°C were not used since plugging of the restrictor nozzle occasionally occurred during the extraction of wet sediments under such conditions.

3.3. Cleanup of SFE extracts

In addition to the chlorinated compounds of interest, the SFE extract also contained coextractives that could interfere with the GC analysis when ECD was used. In comparison to Soxhlet extraction, SFE was far more selective especially if no solvent modifier was used. Thus, a less stringent cleanup procedure can be used. In this work, PCBs, chlorinated benzenes and the other chlorinated hydrocarbons were eluted from a miniature (5 cm) fully activated Florisil column with pentane while the more polar coextractives in the sediment extracts stayed on the column. Pentane instead of hexane was used whenever the determination of the more volatile chlorinated benzenes was required since pentane has a lower boiling point and thus will minimize losses in the solvent evaporation step. After concentration, the sample was further treated with mercury to remove elemental sulfur and sulfur-containing compounds which were not removed by the Florisil cleanup.

3.4. Final analysis of SFE extracts

Because of the large number of PCB congeners present in environmental samples, a total congener analysis is extremely tedious. That approach is further complicated by the availability and purity of authentic standards as well as the GC resolution of the congeners. For the purpose of this work, PCB samples were analyzed by MS using a method developed by Gebhart *et al.* [14]. In this case, a selected PCB congener from each homologue series was employed to quantitate all isomers at the same level of chlorination since the congener was shown to have a response factor nearly identical to the mean of the entire group. As PCB homologues have overlapping retention time windows, special precautions was taken to eliminate interferences by PCB congeners containing more chlorine atoms. Under electron impact ionization conditions, a chlorobiphenyl molecule undergoes fragmentation by the loss of two Cl, and to a

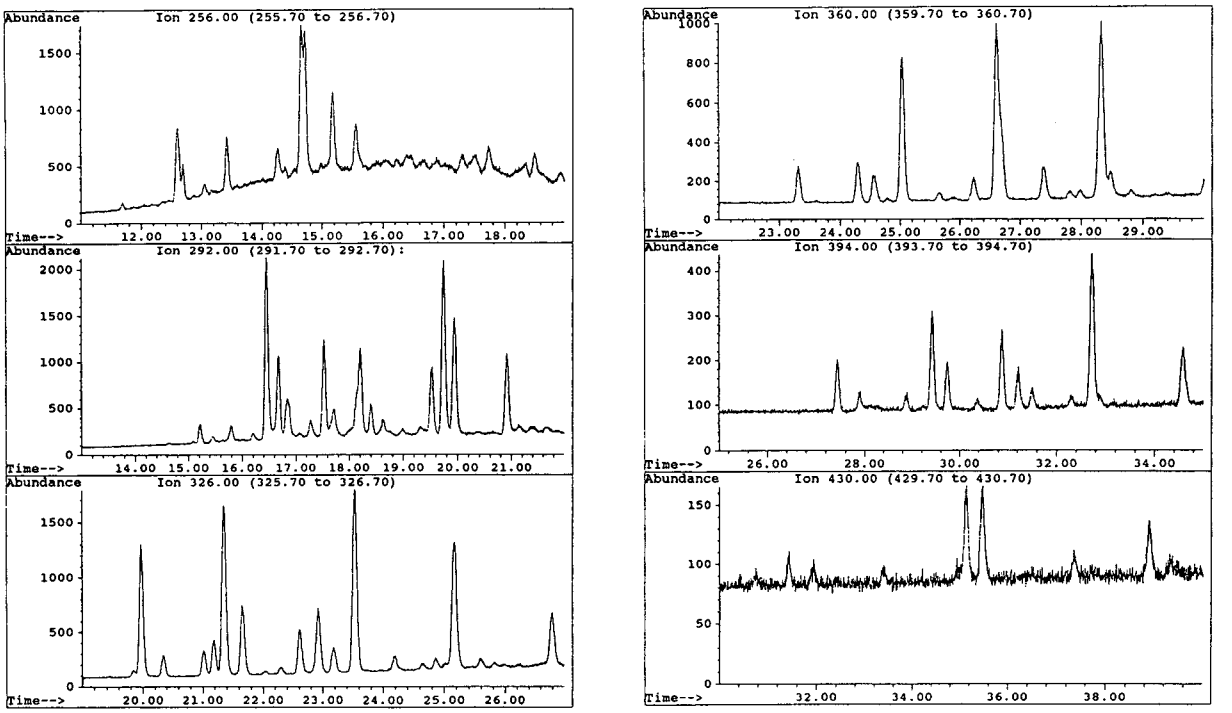

Fig. 3. Reconstructed single ion chromatograms for tri- (ion 256), tetra- (ion 292), penta- (ion 326), hexa- (ion 360), hepta- (ion 394) and octa- (ion 430) chlorobiphenyls in a SFE extract of the Hamilton Bay sediment after cleanup. Time in min.

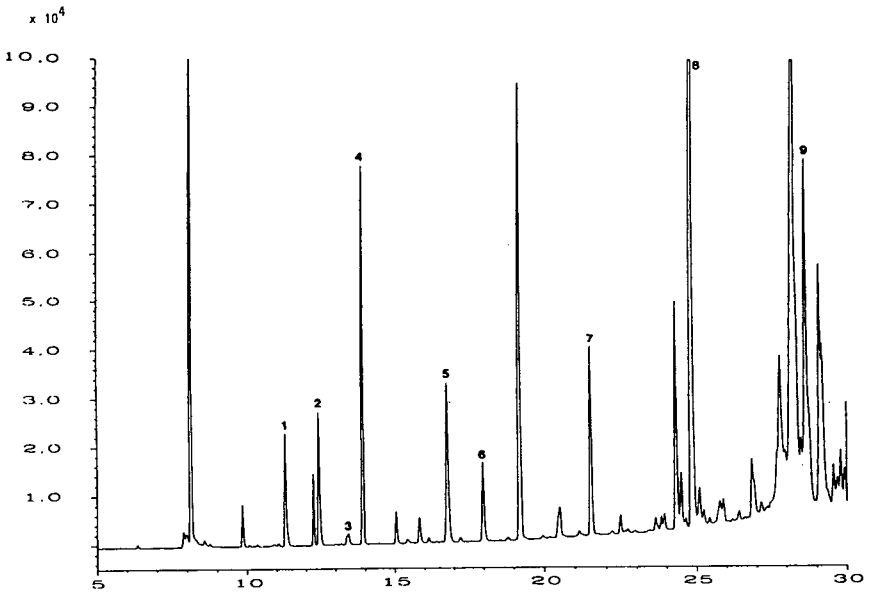

Fig. 4. Electron-capture chromatogram of a SFE extract for the Lake Ontario sediment contaminated by chlorobenzenes, hexachloro-1,3-butadiene and octachlorostyrene. Peaks: 1 = 1,3,5-trichlorobenzene; 2 = 1,2,4-trichlorobenzene; 3 = 1,2,3-trichlorobenzene; 4 = hexachloro-1,3-butadiene; 5 = 1,2,4,5-tetrachlorobenzene; 6 = 1,2,3,4-tetrachlorobenzene; 7 = pentachlorobenzene; 8 = hexachlorobenzene; 9 = octachlorostyrene. Time in min.

lesser extent, HCl and Cl, thus causing interference in the determination of PCBs with one or two less chlorine atoms [16,17]. Thus the absence of $(M + 70)^+$ and $(M + 35)^+$ ions was used to confirm the level of chlorination for each peak. With this selective quantitation technique, we were able to evaluate the recovery of chlorobiphenyls at each level of chlorination as well as the total PCB concentration of a sample in the SFE experiments. While the dichlorobenzenes were also analyzed by MS, the other chlorinated benzenes, hexachloro-1,3-butadiene and octachlorostyrene were analyzed by ECD for better sensitivity. Reconstructed single ion chromatograms depicting the PCB from tri- to octachlorobiphenyls in the SFE extract of the Hamilton Bay sample are shown in Fig. 3. An ECD chromatogram illustrating the chlorinated benzenes in the extract of a Lake Ontario sediment is shown in Fig. 4.

4. Conclusions

In summary, a SFE method using unmodified supercritical carbon dioxide was developed and optimized for the simultaneous extraction of native PCBs, chlorinated benzenes, hexachloro-1,3-butadiene and octachlorostyrene from sediments. While PCBs were similarly recovered by either SFE and Soxhlet extraction, the SFE recovery for chlorinated benzenes and HCBD exceeded the Soxhlet results due to less evaporative loss. The new technique is more efficient since it requires only 21 min and no organic solvent in the extraction steps. A simplified cleanup procedure and much less solvent evaporation are also the other advantages of the SFE approach. For the above reasons, the SFE approach is a better alternative than conventional solvent extraction techniques in routine and analyses of PCBs and chlorinated benzenes.

5. References

[1] S. Jensen, *New Sci.*, 32 (1966) 612.
[2] O. Hutzinger, S. Safe and V. Zitko, *The Chemistry of PCBs*, CRC Press, Boca Raton, FL, 1980.
[3] S. Safe, *CRC Crit. Rev. Toxicol.*, 13 (1984) 319.
[4] B.G. Oliver and K.D. Nicol, *Environ. Sci. Technol.*, 16 (1982) 532.
[5] B.G. Oliver and K.D. Nicol, *Sci. Tot. Environ.*, 39 (1984) 57.
[6] B.G. Oliver, *Water Poll. Res. J. Can.*, 19 (1984) 47.
[7] B.G. Oliver and R.A. Bourbonniere, *J. Great Lakes Res.*, 11 (1985) 366.
[8] B.G. Oliver, R.M. Baxter and H.B. Lee, in B.K. Afghan and A.S.Y. Chan (Editors), *Analysis of Trace Organics in the Aquatic Environment*, CRC Press, Boca Raton, FL, 1988, pp. 31–68.
[9] M.M. Schantz and S.N. Chesler, *J. Chromatogr.*, 363 (1986) 397.
[10] F.I. Onuska and K.A. Terry, *J. High Resolut. Chromatogr.*, 12 (1989) 527.
[11] S.B. Hawthorne, J.J. Langenfeld, D.J. Miller and M.D. Burford, *Anal. Chem.*, 64 (1992) 1614.
[12] J.J. Langenfeld, S.B. Hawthorne, D.J. Miller and J. Pawliszyn, *Anal. Chem.*, 65 (1993) 338.
[13] H.B. Lee, T.E. Peart, R.L. Hong-you and D.R. Gere, *J. Chromatogr. A*, 653 (1993) 83–91.
[14] J.E. Gebhart, T.L. Hayes, A.L. Alford-Stevens and W.L. Budde, *Anal. Chem.*, 57 (1985) 2458.
[15] L.J. Mulcahey, J.L. Hedrick and L.T. Taylor, *Anal. Chem.*, 63 (1991) 2225.
[16] S. Safe and O. Hutzinger, *J. Chem. Soc., Perkin Trans. I*, (1972) 686.
[17] G.W. Tindall and P.E. Wininger, *J. Chromatogr.*, 196 (1980) 109.

ELSEVIER

Journal of Chromatography A, 663 (1994) 97–104

JOURNAL OF CHROMATOGRAPHY A

Capillary zone electrophoresis of basic proteins with chitosan as a capillary modifier

Y.J. Yao, S.F.Y. Li *

Department of Chemistry, National University of Singapore, Kent Ridge, Singapore 0511, Singapore

(First received July 20th, 1993; revised manuscript received November 30th, 1993)

Abstract

Two new approaches based on the use of chitosan, a cationic natural polymer, have been developed for free solution capillary electrophoretic analysis of basic proteins. In the first method, chitosan was employed as a buffer additive in untreated fused-silica capillaries. The polymer interacts with the capillary surface, causes a reversal in the direction of the electroosmotic flow and reduces solute–wall interaction of basic proteins at pH values below their isoelectric points. High efficiencies ($\geq 400\,000$ theoretical plates/m) can be attained for most of the basic model proteins investigated in the pH range 3.0–5.5, except for lysozyme. Chitosan was also used as a capillary modifying reagent. Efficiencies obtained using the chitosan-modified capillary were generally lower than those with chitosan as a buffer additive. However, improvement in peak shape was obtained for lysozyme. In both cases, good migration time reproducibilities (R.S.D. $< 1\%$) were obtained.

1. Introduction

Analysis of basic proteins by free solution capillary electrophoresis using fused-silica column presents a unique challenge due to non-specific adsorption of the protein onto the capillary wall. Unless the acidic silanol (Si–OH) groups on the surface of the capillary wall [1] are masked, the proteins strongly interact with the wall resulting in poor recovery, peak broadening and distortion. Therefore resolution and quantitative determination may also be seriously impaired. Much research has been devoted to circumventing this undesirable adsorption problem and several different approaches have been reported. These include chemical modification of the silica surface [2–7], manipulation of the buffer pH [8–10], use of additive in the sample [11], application of a radial positive potential gradient [12,13] and dynamic modification of the capillary surface by buffer additives [14–23].

In the last approach, various different types of reagents have been used. These buffer additives eliminate or minimize protein adsorption either through (i) competition between proteins and high concentration of zwitterionic salts [14] and/or alkali metal salts for cation-exchange sites on the silica surfaces [15,16], (ii) suppression of ionic interaction by the use of amine additives [9,17,18] or fluorinated cationic surfactants [19,20], or (iii) shielding of the silanols by coating with amphipathic polymer column coating reagent [21,22] or non-ionic polyvinyl alcohol [23]. The use of buffer additives to suppress protein adsorption offers several advantages. The buffer pH can remain an adjustable parame-

* Corresponding author.

0021-9673/94/$07.00
SSDI 0021-9673(93)E1284-7

ter for optimizing the selectivity and avoiding denaturation of proteins. A moderate electroosmotic flow (EOF) can still be maintained which contributes to the separation power of capillary electrophoresis by magnifying the velocity differences of similar migrating analytes when the direction of their electrophoretic mobilities is countered by the direction of the EOF. In addition, the method is simple and good stability and reproducibility of the surface coating can be easily attained. However, the success of this method depends on the degree to which the additives interact with the analytes.

Chitosan, or (1→4)-2-amino-2-deoxy-β-D-glucan, is a hydrophilic polyelectrolyte obtained by deacetylation of chitin [24]. Chitosan has been shown to be an effective chelating material for the removal of toxic metals from water in pollution studies [24] and it was also widely employed as support in chromatographic separations of nucleotides, amino acids and inorganic ions [25,26]. In this work, the suitability of chitosan as a column coating reagent for analyzing basic model proteins was investigated. The properties and performance of the chitosan-modified capillary were evaluated in terms of the useful working pH range, the plate efficiency and its applications.

2. Experimental

2.1. Reagents

All proteins used were purchased as lyophilized powders from Sigma (St. Louis, MO, USA): β-lactoglobulin A and B (bovine milk, p*I* 5.1 and 5.3 respectively), carbonic anhydrase I (human erythrocytes, p*I* 6.6), myoglobin (horse heart, p*I* 7.4), α-chymotrypsinogen A (bovine pancreas, p*I* 9.1), trypsin (bovine pancreas, p*I* 9.3), trypsinogen (bovine pancreas, p*I* 9.3), ribonuclease A (bovine pancreas, p*I* 9.5), cytochrome *c* (horse heart, p*I* 10.5) and lysozyme (chicken egg white, p*I* 11.0). Reagent-grade sodium acetate and chitosan (average molecular mass *ca.* 70 000) were obtained from Fluka (Buchs, Switzerland). Water purified with a Milli-Q system (Millipore, Bedford, MA, USA) was used.

2.2. Buffer and sample preparations

Protein samples were diluted in deionised water at a concentration of 200 μg/ml. Chitosan stock solution, *ca.* 2% (w/v) in 1% aqueous acetic acid was prepared by stirring at room temperature until complete dissolution. Sodium acetate buffers were adjusted to the desired pH by the addition of glacial acetic acid or NaOH solution. Buffers with chitosan as additive were prepared by weighing out the required amount of the stock chitosan solution and made up to the volume with the buffer solution. The solutions were allowed to equilibrate for about 1 h. For solutions of higher pH, a longer period of time was required, *e.g.*, *ca.* 2 h for solution at pH 5. The equilibration step is necessary to achieve good migration time reproducibility. The pH of the buffer solution with chitosan was measured after equilibration. Buffer solutions were filtered through a 0.45-μm membrane (Whatman, Ann Arbor, MI, USA) before use.

Tryptic digest of cytochrome *c* was performed by incubating 1 volume of cytochrome *c* (10 mg/ml) with 0.2 volumes of 0.5 *M* ammonium hydrogencarbonate and 0.2 volumes of 1 mg/ml trypsin at 37°C. The ratio of the concentration of trypsin to cytochrome *c* was 1:50. Following incubation, trypsin was deactivated by heating at 100°C for 5 min. Before analysis, the digest was diluted 1:5 with water. The final tryptic digest sample concentration was *ca.* 1 mg/ml.

2.3. Capillary electrophoresis

All separations were performed using an Applied Biosystems Model 270A capillary electrophoresis system (ABI, Foster City, CA, USA). Fresh fused-silica capillary of 50 μm I.D. and 375 μm O.D. obtained from Polymicro Technologies (Phoenix, AZ, USA) was flushed under vacuum (508 mmHg; 1 mmHg = 133.322 Pa) with water (10 min), 1 *M* NaOH (10 min), water (5 min), 1% aqueous acetic acid (20 min), water again (5 min), and finally the run buffer con-

taining chitosan (5 min). This washing sequence was repeated whenever a new pH was used. In the case where chitosan was not added into the run buffer, the capillary was modified with chitosan by flushing with buffer containing 0.1% chitosan for 5 min and was allowed to contact statically with the capillary for 15 min. Prior to each sample analysis, the capillary was rinsed with the buffer containing 0.1% chitosan for 1 min, followed by a 2-min rinse with the buffer free of chitosan. Samples were injected by application of vacuum for 0.5 s at 127 mmHg. Electrophoresis was carried out at − 15 kV, with UV detection at 214 nm. The temperature of the column was maintained at 30°C. Electropherograms were recorded with a HP 3390A integrator (Hewlett-Packard, Palo Alto, CA, USA). The EOF was monitored by the water peak.

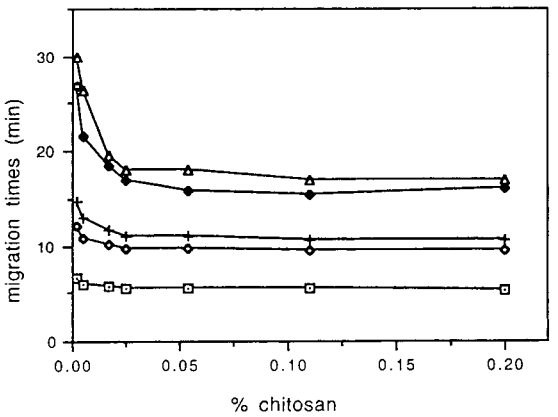

Fig. 1. Influence of chitosan concentration in the separation buffer on the EOF (□) and the migration times of four basic model proteins in free solution capillary electrophoresis: trypsinogen (◇), ribonuclease A (+), lysozyme (◆) and cytochrome *c* (△). Capillary: 53 cm (31 cm to the detector) × 50 μm; applied voltage: − 15 kV; current: 30 μA; run buffer: 50 m*M* sodium acetate, pH 4.0; detection: 214 nm; injection: 0.5 s at 127 mmHg.

3. Results and discussion

3.1. Effect of chitosan concentration

Due to its abundance of amino groups, chitosan exhibits high density of positive charge in aqueous acidic solutions. Through dominantly electrostatic interaction, the polycationic chitosan can adsorb to negatively charged surface of the inner surface of the fused-silica capillary. As a result of this interaction, the overall charge of the capillary wall is reversed [27].

To study the adsorption of chitosan onto the capillary wall, the magnitude of the EOF and the migration times of four basic proteins (*i.e.* trypsinogen, ribonuclease A, lysozyme and cytochrome *c*) were measured at various concentrations of chitosan added to the electrophoretic buffer. The results are summarized in Fig. 1. At pH 4.0 and in the absence of chitosan in the buffer, the direction of the EOF in an untreated capillary was towards the cathode, but no distinct peaks were observed for the proteins. At this pH, the proteins are highly cationic and would interact strongly with the negatively charged silanoate ($Si–O^-$) groups on the capillary surface. However, in the presence of just 0.002% of chitosan in the buffer, an inversion in the direction of the EOF towards the anode was exhibited, indicating that the interfacial double layer had been modified by the adsorption of chitosan. In addition, reasonably symmetrical peaks were obtained, presumably as a result of significant reduction of solute adsorption due to coulombic repulsion from the positively charged capillary surface. As the concentration of chitosan in the buffer increases, faster EOF was observed, due to increasing ζ potential of the electric double layer at the capillary surface as more chitosan molecules were adsorbed to the surface. With above 0.05% of chitosan in the buffer, the capillary exhibited relatively constant EOF (variation *ca.* 1%), indicating a saturation of chitosan coverage at the capillary surface.

Besides a faster EOF, better migration time reproducibility was also obtained upon increasing the concentration of chitosan up to about 0.05% in the electrophoretic buffer (see Table 1). Reproducibility of migration times was better than 0.4% for all the four proteins at chitosan concentrations greater than 0.1%. No buffer replenishment between injections was necessary to achieve such reproducibility.

Table 1
Reproducibility of migration time of the four basic model proteins with different concentrations of chitosan in the buffer

Chitosan (%)	Relative standard deviation (%, $n = 5$)				
	EOF	Trypsinogen	Ribonuclease A	Lysozyme	Cytochrome *c*
0.002	0.99	2.62	3.04	4.44	4.94
0.005	0.34	1.09	1.32	2.06	2.24
0.017	0.88	1.65	1.89	2.84	3.04
0.025	0.36	0.68	0.77	0.98	1.03
0.054	0.28	0.26	0.23	0.25	0.29
0.11	0.01	0.21	0.14	0.04	0.16
0.2	0.01	0.26	0.29	0.01	0.39

Capillary: 53 cm (31 cm to the detector) × 50 μm I.D.; buffer: 50 m*M* sodium acetate at pH 4.0; applied voltage: − 15 kV.

The reduction in protein–wall interaction is also reflected in the improved peak efficiency. As shown in Fig. 2, there is an improvement in the column efficiency, in terms of theoretical plate number N, with higher chitosan concentrations in the buffer. The higher viscosity of the buffer solution at high chitosan concentrations might have also contributed in minimizing band broadening by restricting the diffusion of the protein within the bands. This increase in efficiency is most clearly observed for ribonuclease A. In the case of trypsinogen and cytochrome *c*, their efficiencies remain relatively constant at chitosan concentrations of about 0.1%. Lysozyme, however, exhibit decreasing peak efficiency. The nature of this interaction is not fully understood.

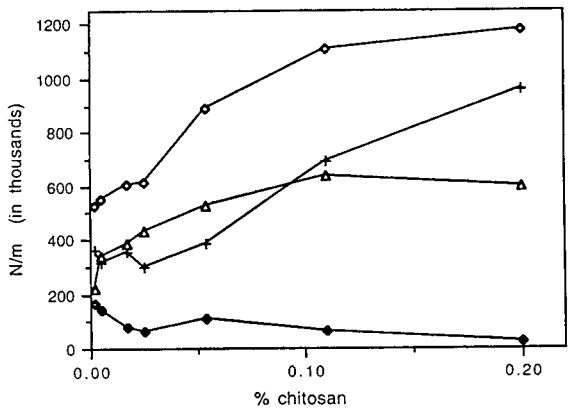

Fig. 2. Influence of chitosan concentration in the run buffer on the separation efficiency. Conditions and symbols as in Fig. 1.

3.2. Effect of pH

The pH of the operating buffer influences the charges on the proteins, the dissociation of the buffer ions and the charge density on chitosan. The charges on chitosan arises from the primary amino group of the glucosamine monomer, which has a pK_a value around 6.3 [28]. Increasing the pH of the electrolyte therefore reduces the net charge on chitosan. As a result, dissolved chitosan usually flocculates at pH values above *ca.* 6, limiting the useful pH range available. From the above experiments performed at pH 4.0, since satisfactory migration time reproducibility and separation efficiency can be obtained with 0.05% chitosan in the running buffer, this concentration was initially considered for further investigations. However, with 0.05% chitosan in the buffer, it was found that migration time reproducibility deteriorated at higher pH. It was believed that as the positive charge density on chitosan decreases with increasing pH, chitosan coverage on the capillary wall becomes less effective in masking the ionized surface silanols and preventing the adsorptive protein–wall interaction. To compensate for the decreasing coverage, 0.1% chitosan was used instead in all further experiments.

Fig. 3 shows a plot of the rate of the EOF and the electrophoretic mobilities of four proteins as a function of the pH of the run buffer containing 0.1% chitosan. From pH 3.05 to pH 3.65, there is an increase in the EOF, followed by a nearly

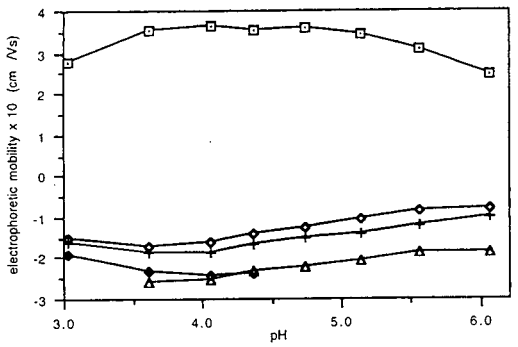

Fig. 3. Plot of EOF and electrophoretic mobilities of the four proteins as a function of buffer pH. Run buffer: 50 m*M* sodium acetate containing 0.1% chitosan. Other conditions and symbols as in Fig. 1.

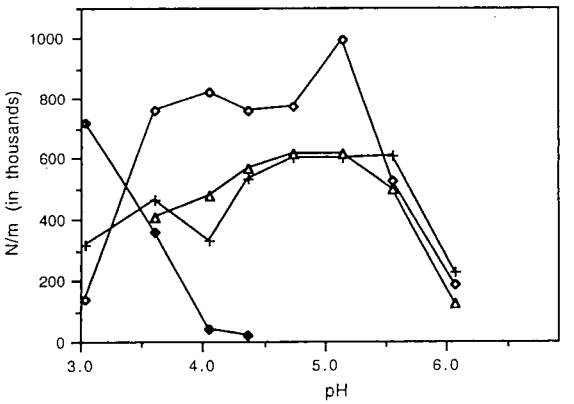

Fig. 4. Plot of peak efficiency *versus* buffer pH. Run buffer: 50 m*M* sodium acetate containing 0.1% chitosan. Other conditions and symbols as in Fig. 1.

constant EOF from pH 3.65 to pH 4.70. Further increase in pH causes a reduction in the EOF as deprotonation of the amino groups on chitosan occurred. It would be expected that with a higher degree of ionization of chitosan at lower pH, a faster anodal EOF should result. However, this was not observed at pH 3.05. It has been reported that chitosan molecules in dilute solutions (concentration between 0.01 and 0.1%, w/v) behave like worm-like molecules with some degree of stiffness, depending on the degree of ionization of chitosan and the counterion concentration [29]. As the number of charges on chitosan backbone increased with lowering of the buffer pH, the electrostatic repulsive forces between neighbouring charged groups resulted in an expansion and stiffening of the chitosan molecules; subsequently, a higher intrinsic viscosity of chitosan in solution was obtained. The result is slower EOF and electrophoretic mobilities of the proteins at lower buffer pH.

At pH 3.05, cytochrome *c* was not eluted as its electrophoretic mobility approached the magnitude of the EOF, but in the opposite direction. Generally, the mobilities of the proteins decreased with increasing pH as anticipated, with the exception of lysozyme. At higher pH, the electrophoretic mobility of lysozyme increased, and was accompanied by a drastic drop in its peak efficiency (see Fig. 4). It was postulated that repulsion between the proteins and chitosan molecules would decrease as the buffer pH approaches the pK_a value of chitosan. Possible interactions arising from hydrogen bonding between the hydroxyl groups and the deprotonated amino groups on chitosan and similar functional groups on the side chains of the proteins could have contributed to the reduction in peak efficiencies of the proteins at pH above 5.5.

3.3. Chitosan-modified capillary

The above observation suggested possible interference of chitosan in the buffer with the analytes. During the course of the work, it was noted that even after prolonged washing of the capillary with aqueous acetic acid, a solvent for chitosan, the direction of the EOF is still anodal. It appeared that the interaction of chitosan with the capillary surface is relatively strong, resulting in a stable coating of chitosan such that inclusion of chitosan in the run buffer is not necessary. The potential advantages of this approach are that possible interactions between the analytes and free chitosan in the buffer could be minimized, and sensitivity could be improved due to a reduction in the background signal originated from the UV absorbance of chitosan.

To achieve satisfactory run-to-run reproducibility of the migration time, between-run wash procedures were evaluated. It was found that when the capillary was washed with a solution containing 0.1% chitosan for 1 min, followed by

a 2-min rinse with run buffer free of chitosan, the relative standard deviation (R.S.D.) of the migration time of the proteins can be kept below 1%, in the pH range investigated.

Fig. 5 displays the change in the peak efficiency of the four basic model proteins with pH in a chitosan-modified column. Over the pH range studied, lysozyme was eluted with better efficiency than in the case when chitosan was included in the buffer. This suggested that interaction between lysozyme and chitosan in the buffer is most probably responsible for the poor peak shape. On the other hand, for the other proteins investigated, a slight decrease in efficiency was observed. This general lowering of peak efficiency in buffer solutions without chitosan might be due to the reduced solution viscosity, and hence allowing band diffusion.

An interesting point to note is the migration order for cytochrome *c* and lysozyme (Fig. 3). Despite the fact that cytochrome *c* has a lower p*I* (10.5) than lysozyme (11.0), it was eluted after lysozyme. In addition, we observed during our experiment that cytochrome *c* exhibited higher electrophoretic mobilities than lysozyme did at pH less than 4.36 and 4.74 for buffers with and without chitosan, respectively. The same migration behaviour has been observed by other workers [5,18,30,31], using either buffer additives (*e.g.* 1,3-diaminopropane) [18] or capillaries chemically coated with polymers (*e.g.* cross-linked polyacrylamide, polyhydroxyalkylmethacrylate, and polyethers with terminal hydroxyl groups) [5,30,31] for the separation of these basic proteins at pH *ca.* 4.7. The peculiar migration order for cytochrome *c* and lysozyme may be due to properties intrinsic to the proteins. For instance, lysozyme has been observed to undergo an unusual transition at around pH 4 [32].

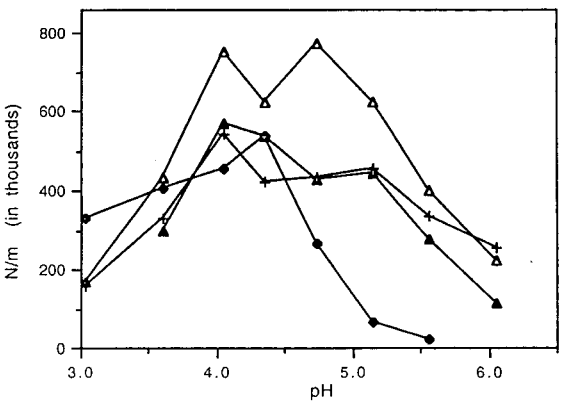

Fig. 5. Effect of buffer pH on the peak efficiency of proteins on a chitosan-modified capillary in 50 m*M* sodium acetate buffer free of chitosan. Other conditions as in Fig. 1. Symbols: △ = trypsinogen; + = ribonuclease A; ▲ = cytochrome *c*; ◆ = lysozyme.

3.4. Applications

As shown above, the use of chitosan-modified capillary is effective in reducing protein–wall interactions over the pH range 3.0–5.5. This narrow pH range, however, does not limit the applicability of the method. The high peak efficiency attained enhances the resolution and thus the separation power of the method. Fig. 6 shows an electropherogram obtained for a group of standard proteins (p*I* ranging from 5.1 to 11.0) with 0.05% chitosan in pH 3.5 buffer. The same group of proteins were also separated in

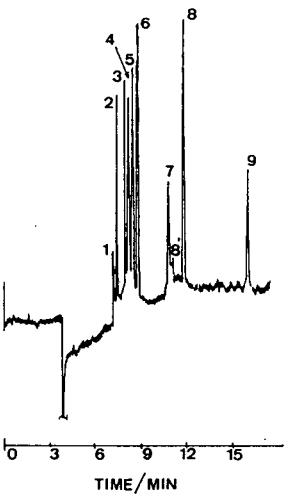

Fig. 6. Separation of standard proteins by free solution capillary electrophoresis. Buffer: pH 3.5 sodium acetate (50 m*M*) containing 0.05% chitosan. About 2 nl of protein mixture, corresponding to 0.4 μg of each protein was injected. Other conditions as in Fig. 1. Peaks: 1 = carbonic anhydrase I; 2 = α-chymotrypsinogen A; 3 = trypsinogen; 4 = β-lactoglobulin A; 5 = β-lactoglobulin B; 6 = ribonuclease A; 7 = myoglobin; 8 = lysozyme; 9 = cytochrome *c*.

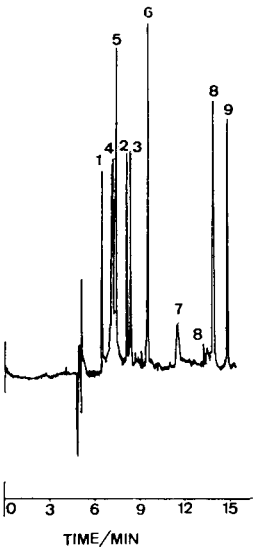

Fig. 7. Capillary electrophoretic separation of standard proteins on a chitosan-modified capillary with pH 4.36 sodium acetate (50 m*M*) buffer free of chitosan. Peaks as in Fig. 6. Other conditions as in Fig. 1.

the absence of chitosan in pH 4.36 buffer (Fig. 7). In both cases, narrow and symmetrical peaks were obtained for the proteins. The ability of the chitosan-modified columns to analyze complex mixtures is again demonstrated in Fig. 8. The electropherogram shows the analysis of a tryptic digest of horse heart cytochrome *c* performed at pH 4.0. It can be seen that the mixture contains at least 25 tryptic peptides, including some negatively charged peptides, which migrated out before the water peak (corresponding to the baseline dip at around 6 min). Capillary electrophoretic separation of tryptic digest of the same protein was also recently assessed by Wheat *et al.* [33] using an untreated fused-silica capillary. A comparison of the electropherograms revealed two rather different electropherogram profiles, suggesting the possibility of employing the present approach as an alternative method for peptide mapping.

In conclusion, the results in this work demonstrated that chitosan can be used as a capillary modifier in capillary electrophoresis. The approaches investigated in this work effectively suppresses protein–wall interaction, resulting in

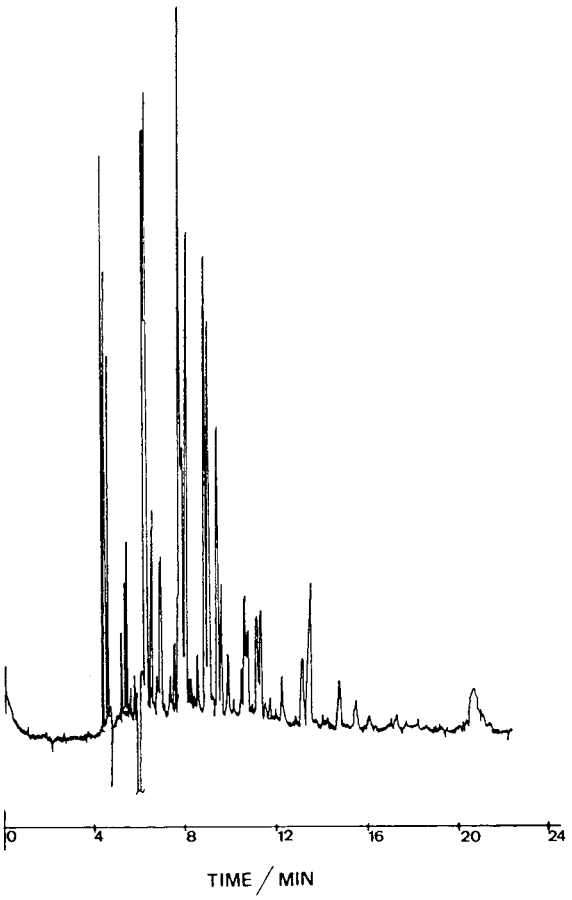

Fig. 8. Capillary electrophoretic separation of a tryptic digest of horse heart cytochrome *c* on a chitosan-modified capillary with pH 4.0 sodium acetate (50 m*M*) buffer free of chitosan. Capillary: 58.5 cm (38.5 cm to the detector) × 50 μm; applied voltage: − 17 kV; current: 28 μA; detection: 214 nm; injection: 0.5 s at 127 mmHg.

separations of basic proteins and peptides with high efficiency. Despite the narrow useful pH range, the present approach has the advantages that it does not require the use of undesirable extreme pH values and high ionic strength buffers.

4. Acknowledgements

The authors gratefully acknowledge the loan of the ABI Model 270A capillary electrophoresis system from Applied Biosystems. Thanks are

also due to the National University of Singapore for financial support.

5. References

[1] K.K. Unger, *Porous silica —Its Properties and Uses as Support in Column Liquid Chromatography*, Elsevier, Amsterdam, 1977, p. 130.
[2] S. Hjertén, *J. Chromatogr.*, 347 (1985) 191.
[3] J.T. Smith and Z. El Rassi, *J. High Resolut. Chromatogr.*, 15 (1992) 573.
[4] J.K. Towns and F.E. Regnier, *Anal. Chem.*, 63 (1991) 1126.
[5] M.X. Huang, W.P. Vorkink and M.L. Lee, *J. Microcol. Sep.*, 4 (1992) 233.
[6] K.A. Cobb, V. Dolnik and M. Novotny, *Anal. Chem.*, 62 (1990) 2478.
[7] Y.F. Maa, K.J. Hyver and S.A. Swedberg, *J. High Resolut. Chromatogr.*, 14 (1991) 65.
[8] F.T.A. Chen, *J. Chromatogr.*, 559 (1991) 445.
[9] R.M. McCormick, *Anal. Chem.*, 60 (1988) 2322.
[10] H.H. Lauer and D. McManigill, *Anal. Chem.*, 58 (1986) 166.
[11] M.J. Gordon, K.J. Lee, A.A. Arias and R.N. Zare, *Anal. Chem.*, 63 (1991) 69.
[12] K. Ghowsi and R.J. Gale, *J. Chromatogr.*, 559 (1991) 95.
[13] C.T. Wu, T. Lopes, B. Patel and C.S. Lee, *Anal. Chem.*, 64 (1992) 886.
[14] M.M. Bushey and J.W. Jorgenson, *J. Chromatogr.*, 480 (1989) 301.
[15] J.S. Green and J.W. Jorgenson, *J. Chromatogr.*, 478 (1989) 63.
[16] S.A. Swedberg, *Anal. Biochem.*, 185 (1990) 51.
[17] V. Rohlicek and Z. Deyl, *J. Chromatogr.*, 494 (1989) 87.
[18] J.A. Bullock and L.C. Yuan, *J. Microcol. Sep.*, 3 (1991) 241.
[19] W.G.H.M. Muijselaar, C.H.M.M. de Bruijn and F.M. Everaerts, *J. Chromatogr.*, 605 (1992) 115.
[20] A. Emmer, M. Jansson and J. Roeraade, *J. High Resolut. Chromatogr.*, 14 (1991) 738.
[21] K. Tsuji and R.J. Little, *J. Chromatogr.*, 594 (1992) 317.
[22] J.E. Wiktorowicz and J.C. Colburn, *Electrophoresis*, 11 (1990) 769.
[23] M. Gilges, H. Husmann, M.H. Kleemiß, S.R. Motsch and G. Schomburg, *J. High Resolut. Chromatogr.*, 15 (1992) 452.
[24] R.A.A. Muzzarelli, *Natural Chelating Polymers*, Pergamon Press, New York, 1973.
[25] V. Carunchio, A.M. Girelli and A. Messina, *Chromatographia*, 23 (1987) 731.
[26] L. Lepri, P.G. Desideri and G. Tanturli, *J. Chromatogr.*, 147 (1978) 375.
[27] R.J. Hunter, *Zeta Potential in Colloid Science: Principles and Applications*, Academic Press, New York, 1981.
[28] M. Rinaudo and A. Domard, in G.S. Braek, T. Anthonsen and P. Sandford (Editors), *Chitin and Chitosan*, Elsevier Applied Science, London, 1989, p. 71.
[29] C.K. Sterzer, D.R. Sanchez and C. Rha, in J.P. Zikakis (Editor), *Chitin, Chitosan and Related Enzymes*, Academic Press, London, 1984, p. 383.
[30] M.X. Huang and M.L. Lee, *J. Microcol. Sep.*, 4 (1992) 491.
[31] A. Malik, Z.X. Zhao and M.L. Lee, *J. Microcol. Sep.*, 5 (1993) 119.
[32] S. Beychok and R.C. Warner, *J. Am. Chem. Soc.*, 81 (1959) 1892.
[33] T.E. Wheat, P.M. Young and N.E. Astephen, *J. Liq. Chromatogr.*, 14 (1991) 987.

Journal of Chromatography A, 663 (1994) 105–113
Elsevier Science B.V., Amsterdam

CHROM. 25 753

Monitoring and analysis of antisense DNA by high-performance capillary gel electrophoresis

Maria Vilenchik, Alexei Belenky and Aharon S. Cohen*

Hybridon Inc., Worcester, MA 01605 (USA)

(First received August 26th, 1993; revised manuscript received November 19th, 1993)

ABSTRACT

The use of antisense DNA to modulate human immunodeficiency virus gene expression *in vitro* has increased the need for analytical methods to support clinical studies. High-performance capillary electrophoresis and slab gel electrophoresis are useful methods for the analysis. Especially important is low level and rapid monitoring of phosphorothioate DNA (SODNs) in biological fluids. The method presented here is based on Watson–Crick hydribization between phosphodiester and the target DNA. Various techniques of staining or labeling are investigated to improve detection limits. The sensitivity of this method is 0.1 ng/ml.

INTRODUCTION

Recent advances in antisense DNA analogues, especially phosphorothioates, have generated a tremendous demand for the characterization of phosphorothioate oligodeoxynucleotides (SODNs). As a result, new challenges for analytical research have surfaced including the need for rapid determination of molecular mass, purity, sequence and base composition.

SODNs have a non-bridging oxygen-to-sulfur substitution per phosphate in the oligomer chain (*i.e.*, P–O to P–S) and therefore are expected to behave very similarly to phosphodiesters. Unfortunately, this is not the case. Charge localization in the species is not the same. In aqueous solutions a negative charge localized on sulfur is far more stable than the same charge localized on an oxygen atom. The larger size and polarity of sulfur relative to oxygen allow the charge density of a thioate anion to be less than that of oxyanions. This difference contributes to the greater acid strength of thioates (P–O and P–S bond lengths are 1.48 and 1.95 nm, respectively) and changes their characters substantially [1]. As a result, analytical methods that were developed for phosphodiesters should be adapted, but in many cases new methods need to be developed for SODNs.

As we mentioned earlier, analysis of phosphorothioates needs to address the general issues of oligomer length, base composition, base sequence, chemical purity and stereochemical purity. The absolute length and the degree of length heterogeneity are currently assessed by ion exchange and reversed phase HPLC [2,3] though there can be separation problems due to hydrophobic interactions. Gel electrophoresis, either in the slab or capillary format, is an alternative method [3,4]. Both allow the achievement of single base resolution of phosphorothioates. Unfortunately none of these techniques has demonstrated quantitation capability. Slab gel electrophoresis coupled with laser densitometry is not a quantitative technique because there is no quantitative dye binding to SODNs; besides, slab gel procedures are long, tedious and labor ineffec-

* Corresponding author.

0021-9673/94/$07.00
SSDI 0021-9673(93)E1232-0

tive. High-performance capillary gel electrophoresis (gel HPCE) is very promising since UV detection can be done on-line, and neither staining or destaining procedures are needed; however, quantitation has not been demonstrated thus far.

Clinical studies of SODNs antisense effects are close to being realized in humans. In providing successful therapy and proper patient care, the development of quantitative analysis becomes one of the most important issues. Pharmacokinetic measurements are often concerned with relatively low concentrations of a drug and its metabolites in a sample of blood, tissue, urine, etc. However, to the best of our knowledge, only one non-radioactive work on the quantitative analysis of SODNs has been reported thus far [5].

This paper addresses "on-line quantitative Southern blotting" using gel HPCE as a quantitative analytical tool for antisense DNA monitoring. Laser-induced fluorescence (LIF) detection coupled with gel HPCE demonstrates detection at the (ng/ml) level for the targeted phosphorothioate DNA (GEM).

EXPERIMENTAL

Chemicals and reagents

Sequagel Sequencing System (acrylamide–bisacrylamide, 19:1) purchased from National Diagnostics (Manville, NJ, USA) was used for slab gel preparations. Ultra-pure Tris base, urea, acrylamide and EDTA were purchased from Schwartz/Mann Biotech (Cleveland, OH, USA). N,N,N′,N′-tetramethylethylenediamine (TEMED) and ammonium persulfate were purchased from Bio-Rad (Richmond, CA, USA). Boric acid was obtained from Sigma (St. Louis, MO, USA). All SODNs were synthesized in the laboratory, desalted, lyophilized and reconstituted in sterile water for injection (Lyphomed, a division of Fujisawa USA, Deerfield, IL, USA). Stains-All (4,5,4′5′-dibenzo-3,3′-diethyl-9-methylcarbocyanine bromide) was purchased from Eastman Kodak (Rochester, NY, USA) and ISS Oligo Staining System was received from Integrated Separation Systems (Natick, MA, USA).

Slab gel apparatus

Electrophoresis was carried out in a vertical slab gel apparatus (Model V16; GIBCO BRL, Gaithersburg, MD, USA). The electric field was supplied by a regulated power supply (Model FB 400; Fisher, Pittsburg, PA, USA). The applied voltage was 250 V, which corresponds to an electric field strength of 19.2 V/cm. Gels were stained with Stains-All or ISS Oligo Staining System and dried on a gel dryer (Buchler Instruments, Lenexa, KA, USA).

HPCE Apparatus

The CE apparatus with UV and LIF detection and the preparation of gel-filled capillaries for the separation of DNA molecules have been described previously [6]. A 30 kV, 500 μA direct current high-voltage power supply (Model ER/DM; Glassman, Whitehouse Station, NJ, USA) was used to generate the potential across the capillary. UV detection of phosphorothioates at 270 nm was accomplished with a Spectra 100 (Spectra-Physics, San Jose, CA, USA). For LIF detection an argon ion laser (Model 543 100BS; Omnichrom, Chino, CA, USA) was employed. The data were acquired and stored on an Acer-Power 486/33 computer (Acer American Corp, San Jose CA, USA) through an analog-to-digital converter (Model 970; Nelson Analytical, Cupertino, CA, USA).

Gel-filled capillaries

Fused-silica capillary tubing (Polymicro Technologies, Phoenix, AZ, USA) with an inner diameter of 75 μm, an outer diameter of 375 μm, an effective length of 15–20 cm and a total length of 30–60 cm was treated with (methylacryloxypropyl)trimethoxysilane (Petrarch Systems, Bristol, PA, USA) and then filled with a degassed solution of polymerizing acrylamide in aqueous or formamide media [0.1–0.3 *M* Tris–borate, 2–6 m*M* EDTA (TBE buffer), pH 8.3 containing 7–8.3 *M* urea]. Polymerization was achieved by adding ammonium persulfate solution and TEMED.

RESULTS AND DISCUSSION

Conventionally, Southern blotting is performed to identify the nucleotide sequence of a

DNA molecule [7]. The process involves the separation of DNA species by gel electrophoresis, transfer and immobilization onto a membrane support, and hydridization with a radioactively labeled probe. An autoradiogram is developed, and the molecules carrying the complementary sequence to the probe are identified (by Watson–Crick hybridization). Although this method is a powerful tool, it is a time-consuming and laborious process.

This study describes the analysis of GEM in human serum by gel HPCE coupled with LIF that significantly extends detection limits.

Antisense phosphorothioate oligomer was "fished" out from a sample solution by Watson–Crick hybridization and analyzed by gel HPCE. Alternatively, polyacrylamide gel electrophoresis (PAGE) was employed for the same analysis and used as an experimental backup to verify capillary results. The former was found to be more efficient and effective than the traditional PAGE.

The major advantage of using Watson–Crick hybridization for "fishing" is that the probe, a complementary DNA molecule, hybridizes very specifically with the DNA target molecule. The probe molecule tagged with the appropriate fluorescent dye allows very low detection limits. For example, gel HPCE coupled with LIF allows detection limits in the range of 10^{-21} mol (concentration of 10^{-12} M at the sample vial). Only the hybridized duplex and the probe molecule can be detected with LIF, *i.e.*, other DNA molecules present in the sample vial will not disturb the LIF electropherogram. "Fishing" GEM from physiological fluids adds another level of complexity, since for example, serum proteins clog gel pores in the capillary and consequently, prevent DNA injection. Therefore, a physiological sample preparation step is necessary to digest or eliminate proteins from the sample vial. A detailed description of the enzymatic digestion has been published earlier [5] and a schematic diagram of the present procedure is provided in Fig. 1.

Although at the concentrations needed for HPCE with UV detection DNA hybridization can be done in water, increased ionic strength is often used to enhance the yield of hybridization of DNA molecules. It is known that the presence of significant concentrations of salt in the sample preparation greatly reduces the amount of DNA sample introduced by electrokinetic injection. Since the molecule in question is a 25-mer phosphorothioate, we first turned to optimize hybridization at very low to almost zero ionic strength, using the traditional method of slab gel electrophoresis to screen the results.

Fig. 2A and B demonstrate that the complementary probe molecule COM does hybridize the target molecule GEM. Lanes 1 and 2 in Fig. 2A and B represent the probe COM, positioned at 1III and the GEM positioned at 2II respectively. Lanes 3 and 4 in Fig. 2B represent the

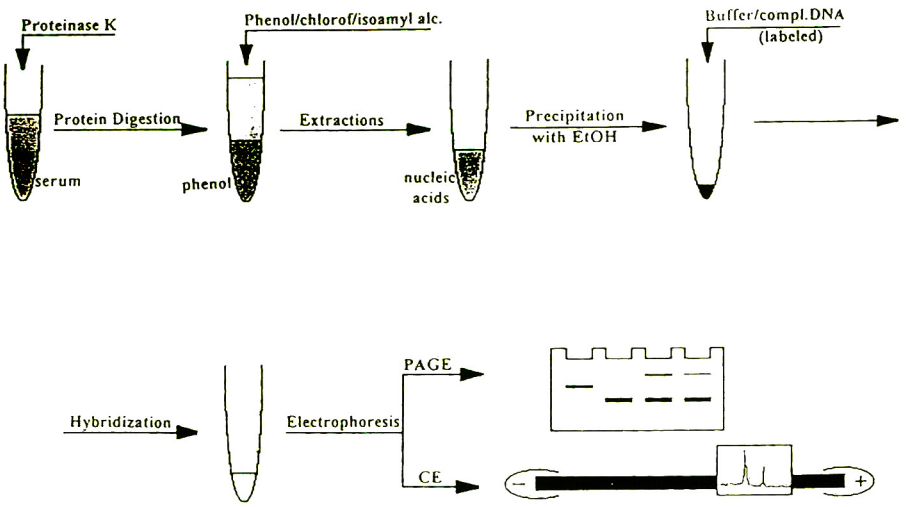

Fig. 1. Schematic diagram of analysis.

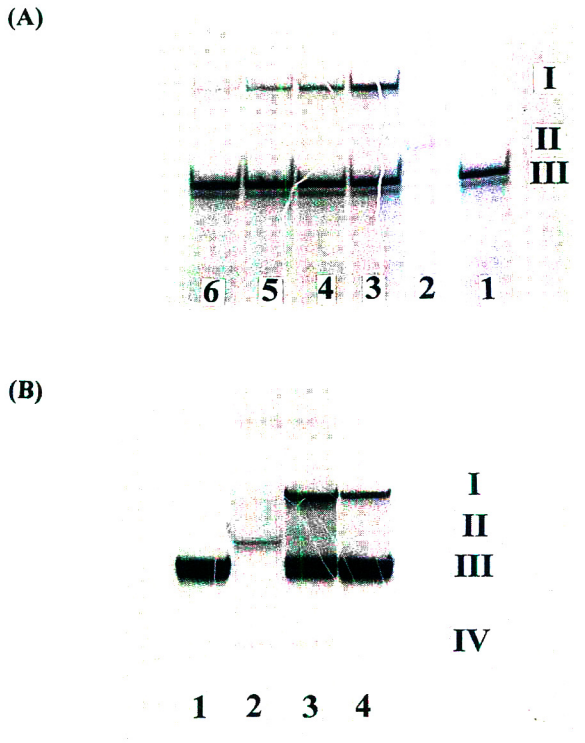

Fig. 2. Separation of analyzed GEM and COM mixture after hybridization using PAGE slab gel. (A) lanes: 1 = COM; 2 = GEM (dissolved in water); 3–6 = duplex of GEM and COM where concentrations of GEM were 100, 50, 25 and 2 μg/ml, respectively. (B) lanes: 1 = COM; 2 = GEM (extracted from human serum by enzymatic digestion); 3, and 4 = duplex of GEM and COM where concentrations of GEM were 100 and 50 μg/ml, respectively. See text for more details. Conditions: polyacrylamide gel (acrylamide–bisacrylamide, 19:1), 0.1 *M* TBE buffer, pH 8.3. Electrophoresis was performed at constant current 50 mA; stained with silver-based system. See text.

mixture of GEM and COM. The band positioned at 3III and 4III represents the excess of COM that was not hybridized while the bands positioned at 3I and 4I represent the GEM–COM duplex. Interestingly, the duplex migrates slower than the single-stranded GEM and COM under the experimental conditions. Also observed is a band positioned at 2IV and 3IV (Fig. 2B). This band represents an impurity in the serum, digested with protein kinase [5], that was not hybridized with GEM demonstrating high selective binding.

Fig. 2A demonstrates "titration" of COM with GEM in water. Differences in band intensities high to low, positioned at 3I to 6I respectively represent differences in the duplex product amount on the slab gel.

Next we turn to optimize the experimental conditions for the gel capillary. To prevent any discrepancies in sample preparation, we used the same samples as in the slab gel experiment described in Fig. 2. The samples were injected electrokinetically into two capillaries, one of which, for comparison, contained denaturing conditions. The results in a form of UV electropherogram are shown in Fig. 3. The same mixtures (1,2,3) were injected under non-denaturing (A) and denaturing (B) conditions. Three peaks are observed under non-denaturing conditions (mixtures 2 and 3). The first migrating peak was identified as COM, the last migrating peak was identified as GEM. The third peak between the first and the last was identified as the duplex. Identification was done by spiking. Since hybridization is an equilibrium process, increase in duplex peak area is well correlated with the increase in GEM concentration at a constant COM content in the injected sample mixture. GEM was completely hybridized in excess of COM (mixture 1) and therefore not observed in Fig. 3 (A1). As expected, only two peaks were observed under denaturing conditions that is illustrated on Fig. 3B. The absence of the duplex peak is not surprising, probably due to denaturation upon injection. Interestingly, the migration order of GEM and COM under non-denaturing conditions is reversed compared to denaturing conditions, most likely due to SODNs secondary structure that is well pronounced under nondenaturing conditions. With GEM hybridization under control, relative quantitation by capillary gel electrophoresis was possible. Fig. 4A illustrates a set of seven consecutive electropherograms, six of which were spiked with $pd(A)_{19-24}$ as an internal standard and titrated with known amounts of GEM (80–1330 ng/ml). Reproducibility of migration time can easily be observed. Also observed is the proportional change in duplex peak height with increased GEM amount. Fig. 4B shows a plot of the experimental results obtained from Fig. 4A.

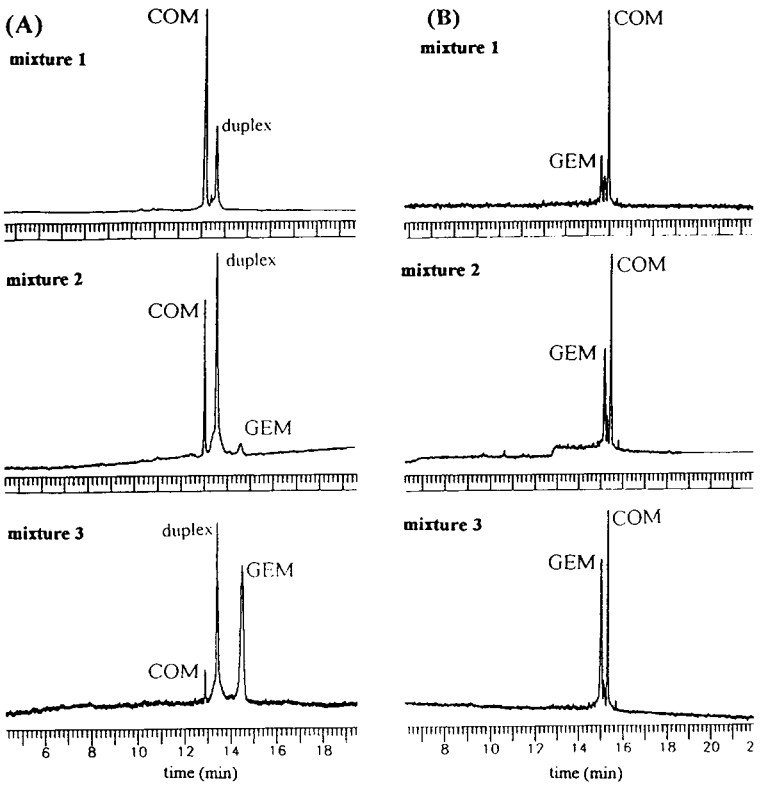

Fig. 3. The separation of GEM, COM and duplex by capillary electrophoresis using UV detection. Electropherograms 1, 2 and 3 show different amounts of GEM with constant COM concentration. (A) Non-denaturing conditions, (B) denaturing conditions. Conditions: (A) 9%T linear polyacrylamide column, effective length $l = 20$ cm, applied electric field $E = 200$ V/cm; (B) 13%T linear polyacrylamide, denaturing conditions, effective length $l = 15$ cm, applied electric field $E = 400$ V/cm.

A linear relationship between GEM concentration and normalized duplex peak height was observed over three orders of magnitude of GEM concentration. In our hands, under the experimental conditions, using UV detection and capillary gel electrophoresis the lowest detected amount of GEM (SODNs) was 80 ng/ml. The ultimate goal was to achieve low detection limits for GEM. Traditionally, slab gel and radioactive labeling by ^{32}P are used to achieve low detection limits. An alternative evolving method is LIF coupled with CE. The LIF optical setup was described previously [6]. The method requires a fluorescent dye to be chemically bound to a small complementary segment of DNA that is hybridized with the target DNA. This method is very selective because unlike UV detection, only labeled DNA or DNA that is hybridized to the labeled DNA will be detected by the LIF method. All other oligonucleotides which may be present in the sample vial will not be detected. In this experiment fluorescein was used as the dye chemically linked to COM (complementary segment of DNA). Unfortunately, the dyed COM co-migrated with the duplex DNA as shown in Fig. 5A. Using ethidium bromide (EtBr) as an additive, we were able to open a time window between the duplex and COM DNA's so that baseline separation was obtained. EtBr is known as a double-stranded DNA intercalator which induces conformational changes as well as charge changes, which result in mobility changes. Fig. 5A demonstrates the EtBr concentration effect on the separation. Since EtBr in the gel matrix can cause fluorescence interference, a concentration of 0.1 μM EtBr was found to be a good compromise as indicated by the sigmoidal curve in Fig. 5B where selectivity was

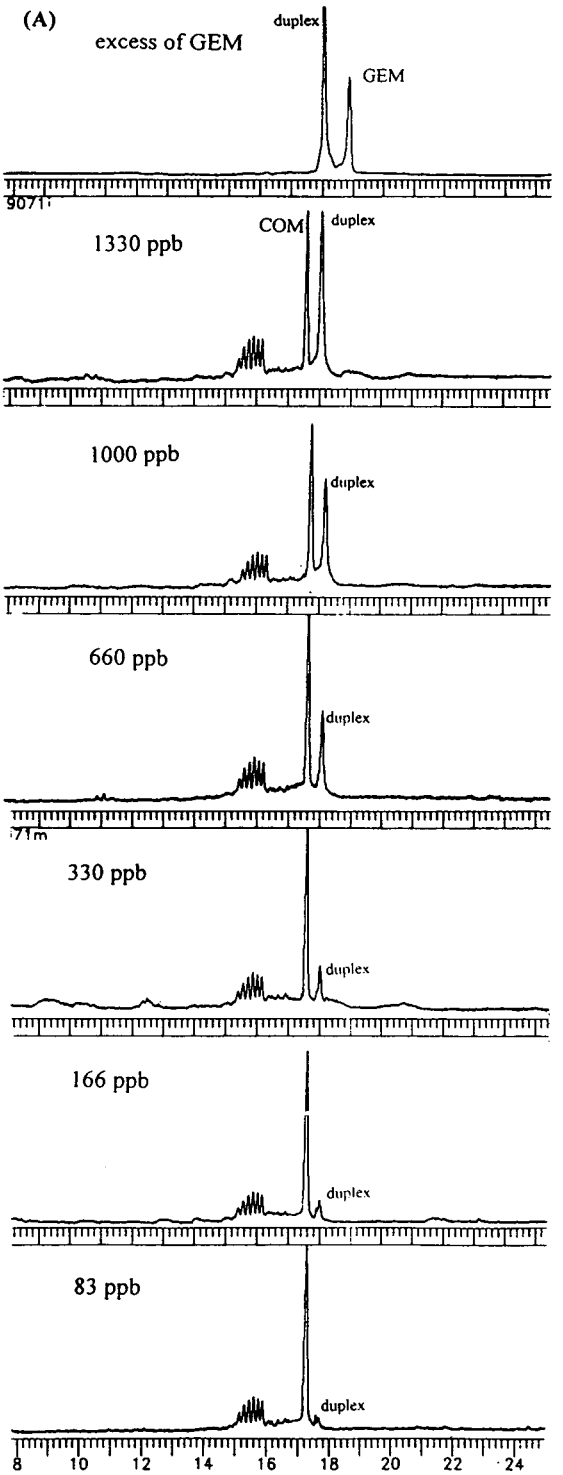

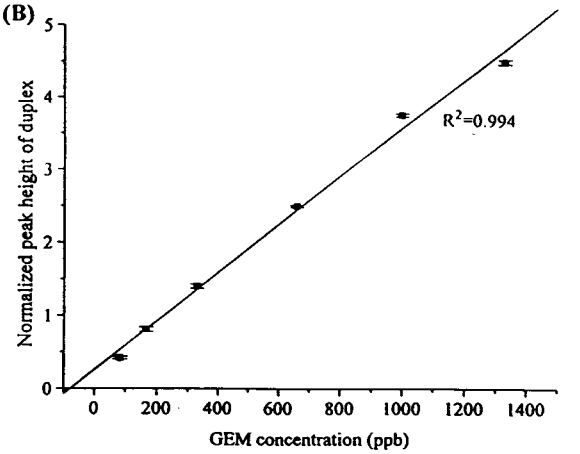

Fig. 4. Determination of GEM by capillary electrophoresis. (A) UV detection using $[pd(A)_{19-24}]$ as an internal standard, numbers indicate GEM concentration; (B) calibration curve for determination of GEM concentration relative to internal standard. Electrophoresis conditions as in Fig. 3A. Annealing was performed at 65°C for 5 min followed by cooling down at room temperature at the rate of 1°C/min. ppb = ng/ml.

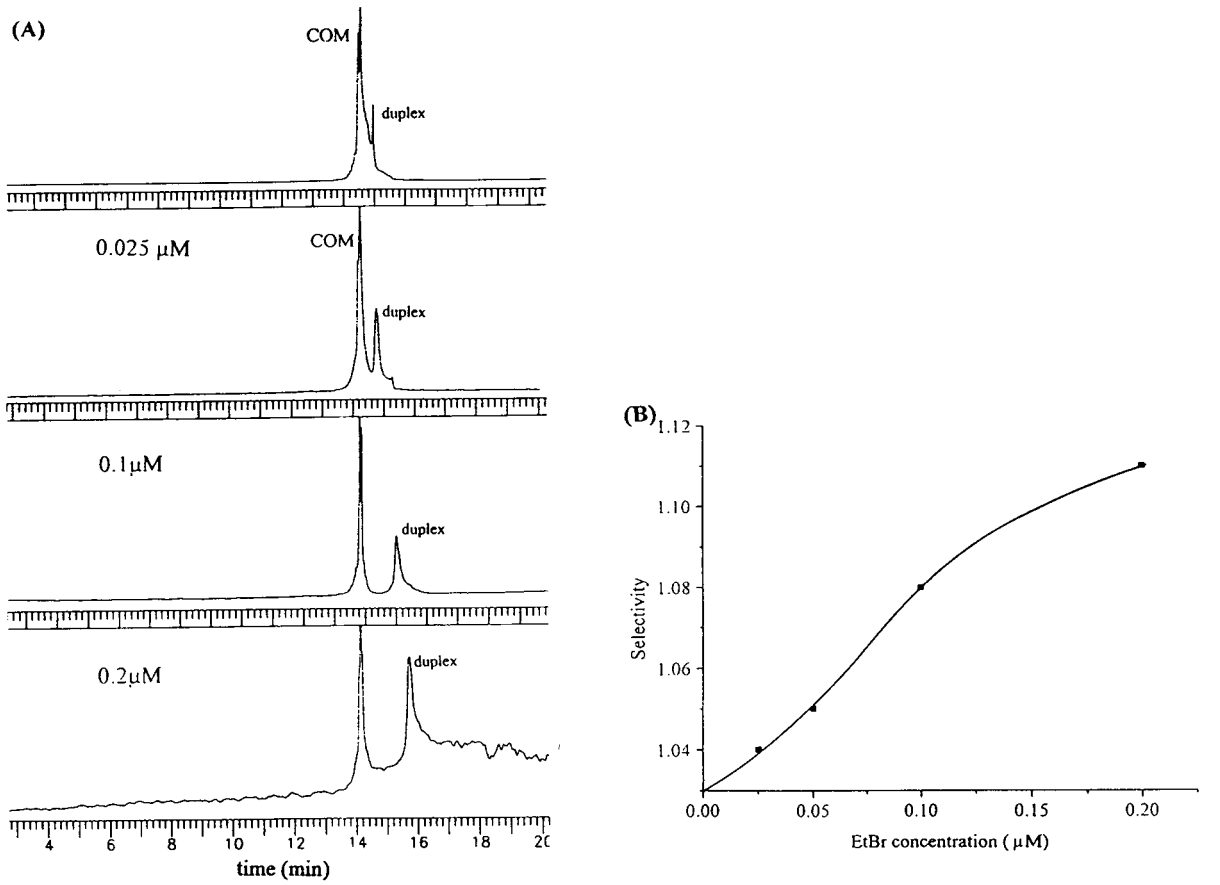

Fig. 5. Effect of intercalator concentration (EtBr) on the separation of single and double stranded oligonucleotides. (A) Electropherograms obtained using LIF detection, numbers indicate EtBr concentrations; (B) plot of selectivity *vs.* intercalator concentration; selectivity factor α is defined as $\alpha = t_B/t_A$, where t_B and t_A are the migration times of duplex and COM, respectively. Conditions as in Fig. 3A.

plotted against EtBr concentration. Experimentally, EtBr was added into the buffer reservoirs and the gel capillary was equilibrated for a few hours to distribute evenly along the capillary. GEM detection limits under these experimental conditions were found to be 2 ng/ml, and the calibration curve with a correlation coefficient of $R^2 = 0.994$ is shown in Fig. 6. Although we expect one or two orders of magnitude better detection limits, we have to remember that a good quantitative annealing reaction between COM and GEM at very low concentration is unlikely to happened unless high salt (at least 10 m*M*) is present in the sample matrix. This, of course, dramatically decreases the amount injected electrophoretically into the gel capillary as predicted by Kohlrauch's law.

Based on our experience, double-stranded DNA molecules usually migrate faster than single-stranded molecules of the same length in a capillary column [8]. However, the hybridized species observed in this study apparently migrated more slowly than the single-stranded oligonucleotide. This may be because the COM molecules are phosphodiesters and the duplex molecules is a hybrid of the COM strand and the GEM strand which is a phosphorothioate that normally migrates slower than the equivalent phosphodiester on non-denaturing polyacrylamide gels.

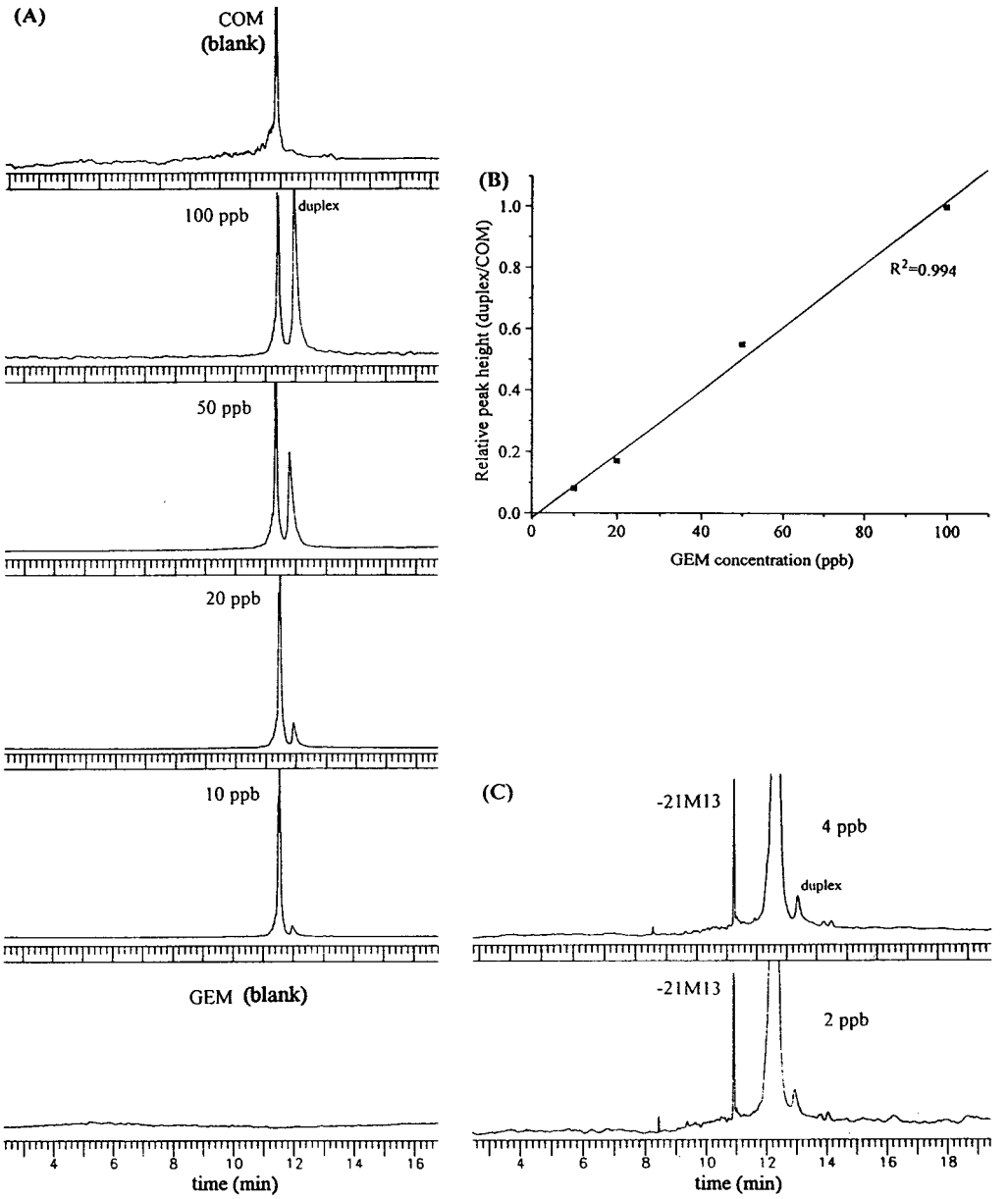

Fig. 6. (A) Low detection limits achieved by capillary electrophoresis using LIF detection, numbers indicate GEM concentrations, numbers indicate GEM concentrations; (B) plot of relative peak height duplex/COM *vs.* GEM concentration; (C) analysis under optimal conditions with the use of primer *−21M13* labeled with fluorescent dye as an internal standard, numbers indicate GEM concentrations. Conditions: 10 μM of $MgCl_2$ were added to the injected solution; electrophoresis was performed on 9%T linear polyacrylamide with 0.04 μM of EtBr, other conditions as in Fig. 3A. ppb = ng/ml.

It may be noteworthy that DNA molecules separated by capillary gel electrophoresis can also be collected and immobilized on a membrane. Additional confirmation with specific probes, similar to conventional Southern blotting could then be performed [9].

CONCLUSIONS

Conventional Southern blotting although a powerful tool, is time consuming and laborious. Previously [9] we have demonstrated how Southern blotting can be transferred from a slab gel to a capillary column with all the advantages provided by HPCE technique. If a capillary is coupled with a LIF detector, extremely low detection limits can be obtained. In this work we have demonstrated that HPCE can be used not only as new approach to Southern blotting with very high sensitivity, but also as a quantitative tool. The three elements (ease of handling, sensitivity and quantitation) which are so important for bioanalysis are combined. The extremely high efficiency and resolution obtained in capillary gel electrophoresis operation are advantageous and make this method unique. The presence of background DNA in the detection cell or sample vial, can be problematic in UV detection, but do not affect the analysis when LIF detection is used. This enables us to detect low concentrations of specific DNA fragments in large DNA bulk by "fishing" out the target oligonucleotide. The technique of capillary gel electrophoresis that is now widely accepted as a standard analytical tool for studying and separating biopolymers has much potential for as yet undiscovered applications. The invention of novel gel matrices and various detection systems opens new horizons for capillary electrophoresis in its role in biochemistry.

REFERENCES

1 M. Matsukura, A. Shinozuka, G. Zong, H. Mitsuya, M. Reitz, J.S. Cohen and S. Broder, *Proc. Natl. Acad. Sci. U.S.A.*, 84 (1987) 7706–7710.
2 S. Agrawal, J.Y. Tang and D.M. Brown, *J. Chromatogr.*, 509 (1990) 396–399.
3 A.S. Cohen, M. Vilenchik, J.L. Dudley, M.W. Gemborys and A.J. Bourque, *J. Chromatogr.*, 638 (1993) 293–301.
4 L.A. DeDionisio, *J. Chromatogr. A*, 652 (1993) 101.
5 A.J. Bourque and A.S. Cohen, *J. Chromatogr.*, 617 (1993) 43–49.
6 A.S. Cohen, D.R. Najarian and B.L. Karger, *J. Chromatogr.*, 516 (1990) 49–60.
7 E.M. Southern, *J. Mol. Biol.*, 98 (1975) 503–517.
8 K. Krapko, J.S. Hanekamp, W.G. Thilly, A. Belenkii, F. Foret and B.L. Karger, *Proc. Natl. Acad. Sci. U.S.A.*, (1993) in press.
9 J.W. Chen, A.S. Cohen and B.L. Karger, *J. Chromatogr.*, 559 (1991) 295–305.

ELSEVIER

Journal of Chromatography A, 663 (1994) 114–118

JOURNAL OF CHROMATOGRAPHY A

Short Communication

Determination of caulerpenyne, a toxin from the green alga *Caulerpa taxifolia* (Caulerpaceae)

Robert Valls*[,a], Jacques Artaud[a], Philippe Amade[b], Nardo Vincente[c], Louis Piovetti[d]

[a]*Laboratoire d'Analyse et de Valorisation des Biomolécules, Université d'Aix–Marseille III, IUT de Satint Jérôme, 142 Traverse Charles Susini, B.P. 147, F-13388 Marseille Cedex 13, France*

[b]*INSERM Unité 303, La Darse, B.P. 3, F-06230 Villefranche-sur-Mer, France*

[c]*Centre d'Études des Ressources Animales Marines, Université d'Aix-Marseille III, B.P. 552, F-13397 Marseille Cedex 13, France*

[d]*Laboratoire de Recherches de Chimie Marine des Organométalliques, Université de Toulon et du Var, B.P. 132, F-83957 La Garde Cedex, France*

(First received September 29th, 1993; revised manuscript received November 30th, 1994)

Abstract

A high-performance liquid chromatographic method is described for the determination of caulerpenyne, a neurotoxic sesquiterpenoid isolated from the green alga *Caulerpa taxifolia*. UV and refractometric detection were compared in order to determine the amounts of this toxin in the alga and the alimentary chain. UV detection at 252 nm was more sensitive and could be applied to the determination of very low concentrations of caulerpenyne (the detection limit per gram of dried seaweed was 27 μg/g). The chromatographic conditions adopted were a 5-μm silica column with isocratic binary elution with ethyl acetate–hexane (23:77, v/v) at a flow-rate of 1 ml/min.

1. Introduction

The genus *Caulerpa* has been widely studied and the structures of many new compounds have been described [1–12]. Secondary metabolites isolated from the lipid extract are deterrent or toxic towards fish, sea urchin larvae, bacteria and fungi, and are probably implicated in the defence of algae against predators in tropical regions [1,13]. Amico *et al.* [9] first reported the structure of caulerpenyne (**1**) (Fig. 1) isolated from *Caulerpa prolifera*. This neurotoxic sesquiterpenoid is also present, with some new derivatives, in the tropical alga *C. taxifolia* (Vahl) C. Agardh [1], recently introduced in the Mediterranean Sea [14]. In this work, high-performance liquid chromatography (HPLC) was used in order to prepare and purify **1** and its derivatives (it must be noted that **1** was the major compound of the lipid extract from *C. taxifolia* [1]). However, to our knowledge there has been no attempt to determine precisely the amount of **1** in the alga. Such an investigation could be useful in evaluating the toxicity of this

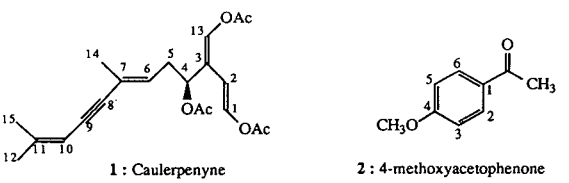

1 : Caulerpenyne **2** : 4-methoxyacetophenone

Fig. 1. Structures of compounds **1** and **2**.

* Corresponding author.

0021-9673/94/$07.00
SSDI 0021-9673(93)E1281-4

species and its variability according to the season of collection and the geographical location. Moreover, the yield and the accumulation of the toxin **1** in the alimentary chain could be quantified.

In this paper, we report a method for the determination of caulerpenyne (**1**) from green seaweed belonging to the Caulerpaceae family using normal-phase HPLC. This work, which can be applied to related compounds characterized by similar UV absorption, completes our previous study on the determination of sterols and diterpenoids from brown algae [15] in the field of sesquiterpenoids from green seaweed.

2. Experimental

2.1. Instrumentation

Separation and purification were carried out on a Model L6000 liquid chromatograph equipped with a mono-pump system (Merck, Darmstadt, Germany). A Merck L4250 variable-wavelength UV–Vis detector set at 252 nm, with a 15-μl flow cell, was used for the analysis of samples with low concentrations of caulerpenyne, whereas a Merck L8810 differential refractometer was used for the detection of samples with high concentrations. Retention times and peak areas were obtained with a Shimadzu (Kyoto, Japan) Chromatopac C-R5A integrator. The column (Interchrom, 250 × 4 mm I.D.) was packed with 5-μm silica (Intersphere ID; Interchim, Montluçon, France) and used at a temperature of 22°C. The flow-rate was 1 ml/min and the injection volume was 20 μl.

2.2. Mobile phase

The solvents were freshly distilled and then filtered and degassed *in vacuo* through a sintered-glass filter. The composition of mobile phase was ethyl acetate–hexane (23:77, v/v).

2.3. Standards

Reference samples for the standardization were commercial 4-methoxyacetophenone (**2**) (Carlo Erba, Milan, Italy), used as an internal standard for both UV and refractive index (RI) detection, and caulerpenyne (**1**), which was isolated directly from a diethyl ether extract of *C. taxifolia*.

2.4. Sample preparation for HPLC analysis

Caulerpenyne (**1**) was extracted and purified form a diethyl ether extract of *C. taxifolia* by normal-phase semi-preparative HPLC using a 5-μm silica column (Interchrom, 250 × 10 mm I.D.) with ethyl acetate–hexane (25:75, v/v) as the mobile phase at a flow-rate of 3 ml/min. The testing of purity was performed using NMR and analytical HPLC. Reference mixtures of caulerpenyne were obtained form stock standard solutions of each standard: 6.35–25.38 mg/l in ethyl acetate for UV detection and about 1000 times more concentrated (2.86–11.44 mg/ml) for RI detection. Calibration was achieved using 4-methoxyacetophenone (**2**) as the internal standard with a stock standard solution of 16.83 mg/l for UV detection and 10.10 mg/ml for RI detection. For the preparation of the reference mixtures, 100 μl of internal standard solution were added to give volumes of each standard solution and diluted to 200 μl with ethyl acetate–hexane (23:77, v/v). Under identical conditions, a diethyl ether extract of the alga [stock standard solution of 106.00 mg of extract per litre and 22.38 mg/l (UV detection) or 11.34 mg/ml (RI detection)] was mixed with 100 μl of internal standard solution and diluted with ethyl acetate–hexane (23:77, v/v). This solution was injected directly into the HPLC apparatus.

2.5. Standardization

Calibration graphs $m_i/m_{is} = f(A_i/A_{is})$, where m_i/m_{is} = sample mass per unit mass of internal standard weight and A_i/A_{is} = sample peak area per unit internal standard peak area, were straight lines (regression lines were obtained from four points). Equations and correlation coefficients (r) are given in Table 1 for UV (252 nm) and RI detection; the internal standard was 4-methoxyacetophenone for both detection methods.

3. Results and discussion

Caulerpenyne (**1**) was determined by normal-phase HPLC with isocratic binary elution with ethyl acetate–hexane (23:77, v/v). Its retention time is given in Table 1.

Under these conditions, the capacity factor (k') for **1** is 1.53 and the resolution (R_s) between **1** and **2** is 2.53, showing that 4-methoxyacetophenone (**2**) could be used as an internal standard if no secondary compounds with similar retention times (t_R) are present in the studied extracts. Moreover, **2** with UV spectroscopic data ($\lambda_{max} = 262$ nm; molar absorptivity $\varepsilon = 19\,500$) near to those of **1** ($\lambda_{max} = 252$, 265 and 280 nm; $\varepsilon = 33\,100$, 27 900 and 17 000), is suitable as internal standard not only with RI but also with UV detection.

After several preliminary experiments, including gradient elution in combination with UV detection, we selected the binary eluant system ethyl acetate-hexane (23:77, v/v), allowing an optimum separation of the analyte compounds from *Caulerpa taxifolia*. After many experiments at different wavelengths, the wavelength chosen for UV detection was 252 nm. UV detection, which is generally more sensitive than RI detection, was found to be about 500 times more sensitive for **1**. It could be used for the determination of very small amounts of **1** (the detection limit per gram of dried seaweed was 27 μg/g), whereas under the same conditions RI detection could only be used for samples containing high concentrations of **1** (the detection limit value per gram of dried seaweed was 16.6 mg/g).

The standardization of **1** was achieved under these conditions, with **2** as an internal standard for both UV (252 nm) and RI detection. Equations and correlation coefficients for the calibration graphs obtained with standard caulerpenyne are given in Table 1. The standard deviation of residues (R.S.D.) from the regression line of this standard is also given (based on four points).

In the determination of **1**, the accuracy of the method is calculated from difference ($d = m_i - m_i$) between a known mass of the sample studied and the mean of the calculated values from the calibration graph (Table 2). The value of the experimental coefficient ($t_{exp.}$) is lower than the corresponding Fischer coefficient (t) evaluated with a confidence level of 99%. On this basis, the method is not burdened with a systematic error.

Fig. 2 and Table 3 show that the diethyl ether extracts from *C. taxifolia* with a low concentration of **1** can only be analysed using UV detection. The precision given in Table 3 as a percentage with a confidence level of 99% was obtained from four measurements on the same sample.

4. Conclusions

This work was undertaken with two purposes: to determine the seasonal variation of the pro-

Table 1
Retention times and equations of calibration graphs for standard caulerpenyne

Detection method	Retention time (min)		Equation[a]	Correlation coefficient (r)	R.S.D.[b] (%)
	1	2			
UV	9.36	10.23	$y = 1.677\,x - 0.006$	0.999	0.0019
RI	9.36	10.23	$y = 1.863\,x + 0.001$	0.999	0.0016

HPLC with a normal-phase silica (5 μm) column (250 × 4 mm I.D.), eluted with ethyl acetate–hexane (23:77, v/v) at a flow-rate of 1 ml/min and with UV (252 nm) and RI detection. Internal standard, 4-methoxyacetophenone.

[a] $y = m_i/m_{is}$ (sample mass per unit mass of internal standard); $x = A_i/A_{is}$ (sample peak area per unit internal standard peak area). Number of points on the calibration graphs: four ($y = 0.38$, 0.75, 1.13, 1.51 and $x = 0.23$, 0.45, 0.68, 0.90 for UV detection; $y = 0.,28$, 0.57, 0.85, 1.13 and $x = 0.15$, 0.30, 0.46, 0.61 for RI detection). Number of points at each level: four.

[b] Relative standard deviation of the residues.

Table 2
Comparison of a known mass of standard with the calculated value

Detection method	$\bar{m}_i$ (mg)	s (mg)	$d = m_i - \bar{m}_i$	$t_{exp.}$ [a]
UV (252 nm)	1.27	0.003	0.004	2.60
	1.90	0.005	0.003	1.20
	2.54	0.005	0.006	2.40
RI	5.74	0.165	0.024	0.29
	8.58	0.159	0.007	0.09
	11.43	0.131	0.011	0.17

$\bar{m}_i$ = Mean mass of sample calculated fro calibration graph; s = standard deviation from four measurements (n); m_i = known mass of sample; $t_{exp.} = d\sqrt{n}/s$; t = corresponding Fischer coefficient for a confidence level of 99%.
[a] Fischer coefficient for a confidence level of 99% *is* $t = 5.84$.

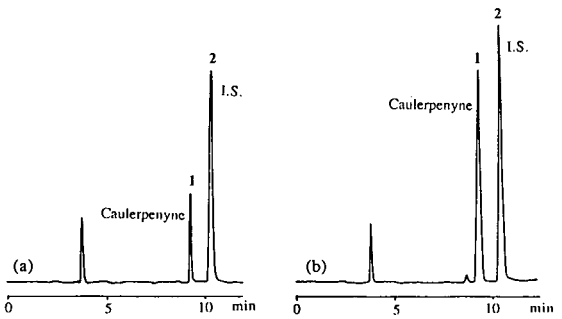

Fig. 2. Examples of HPLC analyses with UV detection of diethyl ether extracts from *C. taxifolia*: (a) extract with a low concentration of **1**; (b) extract with a high concentration of **1**. For experimental conditions, see Table 1.

duction of toxin **1** from *C. taxifolia* recently introduced in the Mediterranean Sea and to follow it in the alimentary chain. A rapid, simple and reproducible method was developed that could be applied to the determination of other sesquiterpenoids from green algae, structurally related to **1**. Moreover, this method is able to analyse precisely either very low-concentration extracts using UV detection (*e.g.*, to determine **1** in the alimentary chain), or high-concentration samples using UV or RI detection (*e.g.*, for seaweed extract analysis).

5. Acknowledgements

The work was supported financially by European contract CEE DGXI LIFE. We thank Dr. R. Le Mée, Laboratory "Environnement Marin Littoral", University of Nice–Sophia Antipolis, Nice, France, for the plant material.

Table 3
Composition of extracts originating from the green alga *C. taxifolia*

Detection method	Low concentration of **1** (mg/g)	Precision (%)[a]	High concentration of **1** (mg/g)	Precision (%)[a]
UV (252 nm)	1.06	1.9	20.7	1.5
RI	–[b]	–[b]	18.9	10.0

Concentration of caulerpenyne (**1**) in diethyl ether extracts from *Caulerpa taxifolia*. For both extracts, alga was collected at a 5-m depth at Cap Martin (French Mediterranean coast) in February and May 1993. Results are given in mg/g of dried seaweed. Analyses were carried out in quadruplicate on the same sample.
[a] Precision for a confidence level of 99%.
[b] Not detected.

6. References

[1] A. Guerreiro, A. Meinez, M. D'Ambrosio and F. Pietra, *Helv. Chim. Acta*, 73 (1992) 689.
[2] R.J. Capon, E.L. Ghisalberti and P.R. Jefferies, *Phytochemistry*, 22 (1983) 1465.
[3] M.S. Doty and G. Aguilar-Santos, *Pacific Sci.*, 24 (1970) 351.
[4] G. Aguilar-Santos, *J. Chem. Soc. C* (1970) 842.
[5] J.P. Vidal, D. Laurent, S.A. Kabore, E. Rechencq, M. Boucard, J.P. Girard, R. Escale and J.C. Rossi, *Bot. Mar.*, 27 (1984) 533.
[6] A.R.S. Anjaneyulu, C.V.S. Prakash and U.V. Mallavadhani, *Phytochemistry*, 30 (1991) 3041.
[7] J.G. Schwede, J.H. Cardellina, S.H. Grode, T.R. James and A.J. Blackman, *Phytochemistry*, 26 (1987) 155.
[8] M.F. Raub, J.H. Cardellina and J.G. Schwede, *Phytochemistry*, 26 (1987) 619.
[9] V. Amico, G. Oriente, M. Piattelli and C. Tringali, *Tetrahedron Lett.*, 38 (1978) 3593.
[10] V.J. Paul and W. Fenical, *Bioorg. Mar. Chem.*, 1 (1987) 1.
[11] P.G. Nielsen, J.S. Carle and Christophersen, *Phytochemistry*, 21 (1982) 1643.
[12] V.J. Paul and W. Fenical, *Tetrahedron Lett.*, 23 (1982) 5017.
[13] V.J. Paul and W. Fenical, *Mar. Ecol. Prog. Ser.*, 34 (1986) 157.
[14] A. Meinesz and B. Hesse, *Ocean. Acta*, 14 (1991) 415.
[15] L. Piovetti, P. Deffo, R. Valls and G. Peiffer, *J. Chromatogr.*, 558 (1991) 99.

ELSEVIER

Journal of Chromatography A, 663 (1994) 119–122

JOURNAL OF CHROMATOGRAPHY A

Short Communication

High-performance liquid chromatographic determination of atractyloside and carboxyatractyloside from *Atractylis gummifera* L.

M. Calmes, F. Crespin, C. Maillard, E. Ollivier, G. Balansard*

Laboratoire de Pharmacognosie, Faculté de Pharmacie, 27 Boulevard Jean Moulin, 13385 Marseille cédex 5, France

(First received July 27th, 1993; revised manuscript received November 23rd, 1993)

Abstract

A reversed-phase high-performance liquid chromatographic method is described for the identification and determination of two toxic compounds, atractyloside and carboxyatractyloside, in a 60% methanolic extract of *Atractylis gummifera* L. roots. Separation was achieved in 55 min with a water–acetonitile gradient in the presence of trifluoroacetic acid. Detection was effected with a light-scattering detector. The detection limit was determined and was *ca.* 9 μg of atractyloside standard injected. The method of quantification was validated.

1. Introduction

Atractylis gummifera L. (Asteraceae) is a toxic plant widely distributed in mediterranean countries. In the north of Africa many intoxications from *Atractylis gummifera* have been reported, mainly accidental but also criminal or suicidal. Intoxications are fatal in most cases because there is no effective treatment. Symptoms are respiratory, vascular and nervous difficulties and disturbance of glycaemia and anuria. Intoxications are induced by oral, respiratory and cutaneous routes [1–3]. This toxicity is related mainly to two heterosides: atractyloside (or atractyline) and carboxyatractyloside (or gummiferine) (Fig. 1) [4]. Atractyloside and carboxyatractyloside are both specific inhibitors of mitochondrial oxidative phosphorylation; this inhibition is more important from carboxyatractyloside [5,6].

Several quantitative assays but no specific methods for these compounds have been described. All used spectrophotometric measurement after a chromogenic reaction [7–10]. The

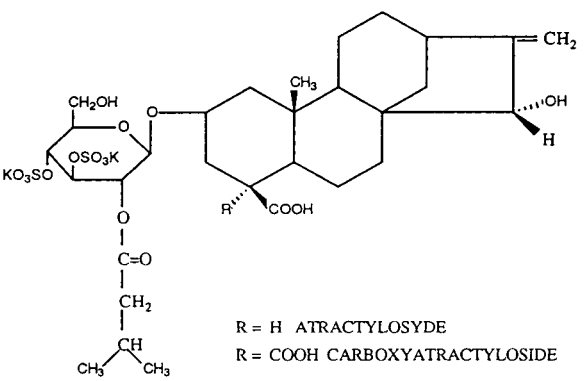

Fig. 1. Structure of atractyloside and carboxyatractyloside.

* Corresponding author.

0021-9673/94/$07.00
SSDI 0021-9673(93)E1255-X

limit of detection is *ca.* 1 μg. No HPLC method has been reported because these compounds are not detectable by UV spectrophotometry.

In this paper we describe a procedure for the determination of these two toxic compounds by HPLC with light-scattering detection.

2. Experimental

2.1. Sample preparation

Fresh roots of *Atractylis gummifera* (5 g), collected in Tunisia (Zaghouan), were lyophilized and extracted with 40 ml of water–methanol (40:60, v/v) under reflux for 30 min and filtered without cooling. The volume was completed to 50 ml with the same solvent. A 20-ml volume of this solution was evaporated to dryness under vacuum. The residue was dissolved in 10 ml of water–methanol (40:60, v/v).

Standard (atractyloside) was dissolved in water–methanol (60:40, v/v) to give a concentration of 1 mg/ml. All samples were filtered on a 0.2-μm Dynagard filter (Merck, Montluçon, France).

2.2. Apparatus and conditions

The liquid chromatograph consisted of a U6K universal injector, two M 501 solvent-delivery systems (Waters, St. Quentin en Yveline, France) and a Cunow DDL 21 light-scattering detector (Waters) connected to an NEC computer to monitor chromatographic parameters and process data.

The column was LiChrosorb RP-8 (7 μm) (250 × 4 mm I.D.) from Merck and a μBondapak C_8 (15–20 μm) guard column (25 × 4 mm I.D.) from Waters.

The eluent was water containing 0.05% trifluoroacetic acid (TFA). (Merck) (solvent A) and acetonitrile (pesticide residue analysis grade; Prolabo, Paris, France) (solvent B), with a linear gradient from 10 to 30% of solvent B over 40 min. The solvents were filtered through a 0.45-μm Millipore filter. A re-equilibration period of 10 min was necessary. The flow-rate was 1 ml/min and the injection volume was 20 μl.

For evaporative light-scattering detection, nebulization of the eluent was provided by a stream of pressurized air at 2.2 bar. The nebulized solvent was evapored at 64 ± 2°C. The pressurized air was filtered through a Millex FG_{50} filter (0.2 μm) (Millipore).

3. Results and discussion

3.1. Optimization of detection conditions

The optimum operatory conditions were established by studying the temperature of evaporation and the pressure of nebulization. At low temperature the detector response was maximum, but the noise level was too high. The signal-to-noise ratio was better at 64 ± 2°C. On the other hand, at low pressures the noise level was high. To obtain an acceptable noise level it was necessary to work at an evaporation temperature of about 64 ± 2°C and a nebulization pressure of 2.2 bar.

3.2. Chromatography

A chromatogram of *Atractylis gummifera* L. root extract was obtained with a water–acetonitrile gradient in the presence of TFA in 55 min, as shown in Fig. 2.

Two compounds were identified by means of authentic standards: carboxyatractyloside (Fluka, St. Quentin Fallavier, France) and atractyloside (Extrasynthèse, Lyon, France), the retention times of which were 22.77 and 27.21 min, respectively. Determination of carboxyatracthyloside and atractyloside in this extract was achieved by the external standard method with the atractyloside standard. The contents of carboxyatractyloside and atractyloside were expressed as atractyloside.

Extract of *Atractylis gummifera* L. roots was analysed using the above procedure. Roots were extracted with water–methanol (40:60, v/v) as described previously. The contents of atrac-

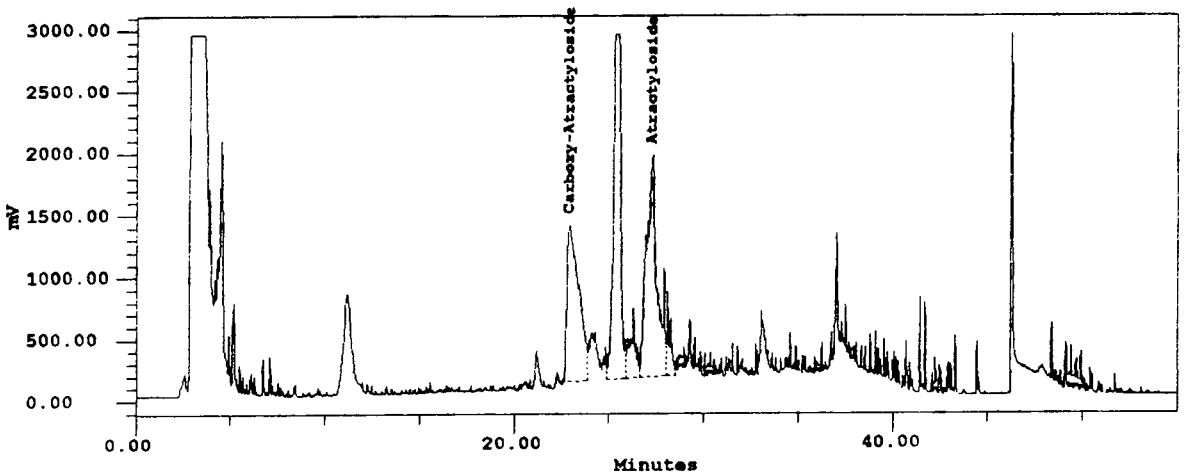

Fig. 2. Chromatogram of *Atractylis gummifera* extract.

tyloside and carboxyatractyloside in the roots were 0.981% and 0.63%, respectively, or 1.45% expressed as atractyloside.

3.3. Validation

The method was tested on atractyloside as the external standard. The regression curve calculated by assaying standard solutions three times consecutively showed a sigmoidal response of the detector in the concentration range 0.6–2.4 mg/ml; a plot of peak area *versus* sample concentration in double logarithmic coordinates was linear. The calibration graph is shown in Fig. 3. The results of the regression analysis and the correlation coefficient (r) were $\log C = 0.610 \log A - 4.386$ ($r = 0.9990$), where C is the concentration in mg/ml and A is the peak area.

Repeatability at 0.95 mg/ml ($n = 10$) gave a relative standard deviation (R.S.D.) of 1.064%. The reproducibility for a standard preparation tested by assaying four solutions at a concentration of 1.25 mg/ml showed an R.S.D. of 1.51%. The reproducibility of the extraction method displayed an R.S.D. of 2.89% ($n = 8$).

The detection limit was determined and was *ca.* 9 μg of atractyloside standard injected, corresponding to a methanolic solution of 0.450 mg/ml.

4. Conclusions

This method is not as sensitive as spectrophotometric methods [7–10], but it is more specific. The complete separation and the simultaneous determination of the two toxic compounds in *Atractylis gummifera* L., atractyloside and carboxyatractyloside, can be achieved in 55 min. This is the first HPLC method to be described for these compounds using light-scattering detection.

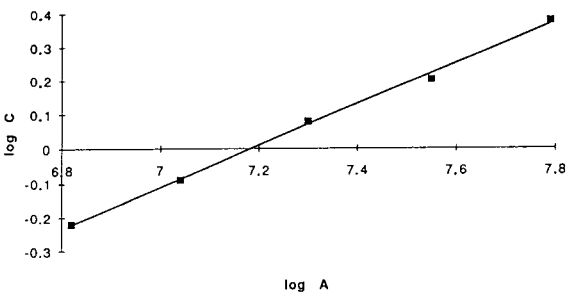

Fig. 3. Calibration graph for atractyloside.

5. References

[1] G. Chardon, A. Viala, P. Vignais and E. Stanislas, *Therapie*, 19 (1964) 1313.
[2] M. Georgiou, D. Biol, L. Sianidou, T. Hatzis, J. Papadatos and A. Koutselinis, *Clin. Toxicol.*, 26 (1988) 487.
[3] M.L. Martin, A. Moran and L. San-Roman, *An. R. Acad. Farm.*, 51 (1985) 751.
[4] F. Piozzi and A. Quilico, *Tetrahedron Lett.*, 23 (1965) 1829.
[5] A.C. Passam and J.O.D. Coleman, *J. Exp. Bot.*, 26 (1975) 536.
[6] A. Hedili, J.M. Warnet, M. Thevenin, C. Martin, M. Yacoub and J.R. Claude, *Arch. Toxicol., Suppl.*, 13 (1989) 312.
[7] E. Stanislas, A. Viala and P. Tourte, *Toulouse Pharm.*, 7 (1960) 1.
[8] A. Viala and J.P. Cano, *Bull. Soc. Pharm. Marseille*, 59 (1966) 161.
[9] A. Viala and J.P. Cano, *Bull. Soc. Pharm. Marseille*, 59 (1966) 167.
[10] A. Viala and J.P. Cano, *Bull. Soc. Pharm. Marseille*, 59 (1966) 175.

ELSEVIER

Journal of Chromatography A, 663 (1994) 123–126

JOURNAL OF CHROMATOGRAPHY A

Short Communication

Simple method for preventing unsuitable solvents from entering gas chromatographic detectors

Hai Bin Wan, Ming Keong Wong*, Chup Yew Mok

Department of Chemistry, National University of Singapore, Lower Kent Ridge Road, Singapore 0511, Singapore

(First received October 18th, 1993; revised manuscript received November 30th, 1993)

Abstract

A simple method for preventing unsuitable solvents and other substances from entering gas chromatographic detectors is described. A split vent was constructed by connecting the outlet of the column to the unused injector and the detector with a press-tight Y-splitter and two short capillary columns. Unsuitable solvents and other substances can be discharged through the unused injector by keeping the injector open for a few minutes. When the nut on the injector is tightened, all the effluent from the analytical column enters the detector. Use of this split vent can avoid or reduce the adverse effects of unsuitable solvents on the detector performance.

1. Introduction

Many gas chromatographic (GC) detectors are used with unsuitable solvents. Electron-capture detectors are not suitable for samples that involve solvents containing halogen or nitro groups [1], and solvents containing nitrogen or phosphorus, such as acetonitrile and dimethylformamide, are not suitable for nitrogen–phosphorus detectors. Water is a very difficult solvent for GC owing to its high surface tension, the very large volume of vapour produced per unit volume of the liquid and the poor properties concerning solvent effects. In addition to the problems with the influence on injection techniques [2] and the column lifetime, water is also an unsuitable solvent for many detectors [1,3]. Water may upset electron-capture detectors. Samples containing large amount of water may also damage the rubidium salts of nitrogen–phosphorus detectors.

The most common approach to avoid the effects of unsuitable solvents on detectors is to replace them with more suitable solvents during sample preparation. For instance, in some methods that use dichloromethane to extract pesticides from water, dichloromethane is removed by evaporation and the extract residue is then dissolved in hexane before being analysed by GC with electron-capture detection (ECD). Some valve systems have also been used for this purpose [2,4,5]. Switching valves are installed either between the outlet of the column and the detector inlet or between two columns, using the first column to produce a retention gap. Unsuitable solvents can also be discharged by using a temperature-programmed injection port [6]. The retention gap between the solvent and the analytes is created by keeping the temperature relatively low at the beginning and then rapidly increasing it. Simmonds and Kerns [7] used a permselective membrane to remove water selectively prior to the sample entering the chromatographic column. The problem with this method is

* Corresponding author.

0021-9673/94/$07.00
SSDI 0021-9673(93)E1282-5

that different membranes are required for different solvents and analytes.

Most gas chromatographs are not installed with the above-mentioned valve systems when they are purchased, and it is not easy to select suitable valves and to install them in the instruments. This paper describes a simple method that can be easily adopted to avoid or minimize the adverse effects of unsuitable solvents and other substances on GC detectors. The method uses a Y-splitter and the unused injector in the instrument to construct a split vent. Unsuitable solvents and other substances can be discharged through this split vent before the sample enters the detector.

2. Experimental

2.1. Instrumentation

The construction of the split vent is shown in Fig. 1. The outlet of the analytical column is connected to the detector and injector B by a Y-splitter and two very short capillary columns. The dimensions are 10 cm × 0.53 mm I.D. for the column between the Y-splitter and injector B and 25 cm × 0.32 mm I.D. for the column between the Y-splitter and the detector. The press-tight Y-splitter was purchased from Hewlett-Packard (Avondale, PA, USA). Capillary columns with different diameters can be fitted into the splitter by gently pressing the column against the splitter. When the nut on injector B is fully loosened, all the effluent from the analytical column is discharged through injector B. When injector B is closed, all the effluent enters the detector. Unsuitable solvents can be discharged through injector B by keeping the nut on injector B fully open for several minutes. The time elapsed can be monitored using the clock installed on the instrument. When a HP-5890A gas chromatograph was used, the septum in injector B was cut smaller so that it would not stick to the mouth of the injector when the nut was loosened.

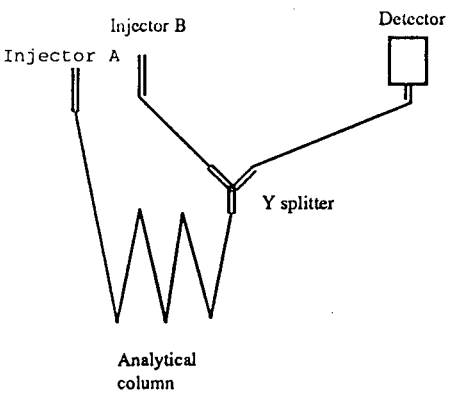

Fig. 1. Schematic diagram of the instrumental set-up.

An HP-5890 Series II gas chromatograph equipped with an electron-capture detector was used for estimating the split vent.

2.2. Gas chromatography

The pesticides lindane and methyl parathion dissolved in methanol and methanol–water (7:3) at a concentration of 1 μg ml^{-1} were determined by GC–ECD. An HP-1 capillary column (12 m × 0.2 mm I.D.) was used for isolation. The oven temperature was programmed from 130°C (held for 1.0 min) to 250°C at 15°C min^{-1}. The injection volume was 1 μl.

3. Results and discussion

When the nut on injector B was fully loosened, the effluent from the analytical column was distributed between injector B and the detector. According to the flow-rate measurement, the ratio was about 12:1 at room temperature, that is, about 92% of the effluent was discharged through injector B. When the oven temperature was increased to >60°C, no effluent entered the detector. The flat baseline at the solvent peak positions on the chromatogram (Fig. 2B) also indicates that no effluent entered the detector.

The relationship between the gas flow-rate (F) and the column dimensions can be described as

$$F = 3.14\Delta PD^4/32\eta L \quad (1)$$

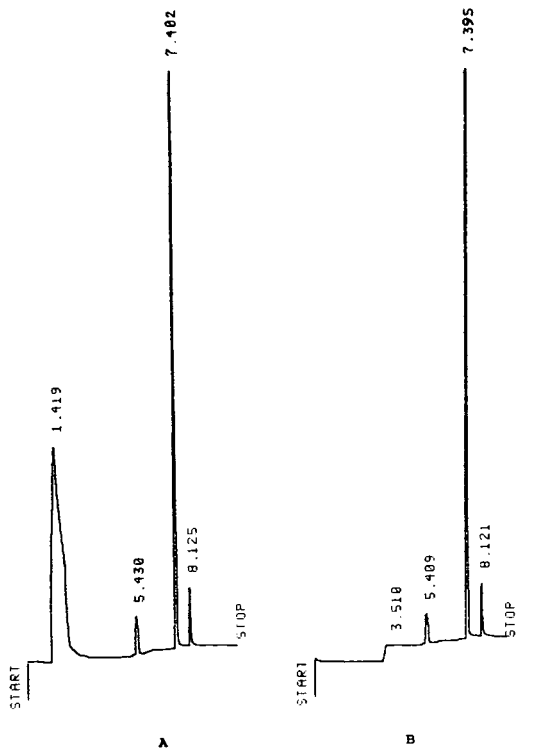

Fig. 2. Chromatograms of lindane (retention time = 7.4 min) and methyl parathion (retention time = 8.1 min) dissolved in methanol–water (7:3) obtained on an HP-5890 II gas chromatograph equipped with an electron-capture detector, (A) without using the split vent and (B) with the split vent. The oven temperature was programmed from 130°C (held for 1.0 min) to 250°C at 15°C min^{-1}.

where ΔP is the difference in pressure between the inlet and outlet of the column, D and L are the inner diameter and length of the column, respectively, and η is the viscosity of the gas [8]. Therefore, the distribution ratio of the effluent between injector B and the detector can be calculated using the equation

$$F_1/F_2 = D_1^4 L_2 / L_1 D_2^4 \quad (2)$$

The result obtained is 15:1 under the conditions used. The change in the ratio when the temperature was increased was unlikely to be due to thermal expansion of the columns, as quartz has a very low thermal expansion coefficient (*ca.* $5 \cdot 10^{-7}$ $°C^{-1}$). The effect of temperature on the distribution ratio might be due to other factors.

The influence of the split vent on the accuracy and the instrument performance were studied with pesticide solutions. The results, given in Table 1, indicate that the use of the split vent did not affect the accuracy and reproducibility of the analysis when a sample using pure methanol as solvent was analysed. This is reasonable, because the carrier gas from the analytical column accounts for only 3% of the total gas flow of the detector (the rest is the make-up gas), so the interruption of the carrier gas flow should not have a noticeable effect on the detector performance. When the solvent of the sample contained 30% of water, discharging the solvent before the sample entered the detector was able to prevent the adverse effects of water on the detector response and the reproducibility. Without using the split vent, the average peak area was smaller and the relative standard deviation was larger. The chromatograms in Fig. 2 were obtained by injecting lindane and methyl parathion dissolved in methanol–water (7:3) with and without using the split vent. They suggest that the use of the split vent will not affect the retention time of the analytes.

Table 1
Effect of the split vent on the response of an electron-capture detector to lindane and reproducibility of the analysis

Sample solvent	Split	Mean response[a] (μV s)	R.S.D. (%)
Methanol	Yes	2 287 202	6.26
Methanol	No	2 340 731	5.42
Methanol–water (7:3)	Yes	2 289 558	7.23
Methanol–water (7:3)	No	1 863 029	13.5

[a] Mean of four replicates.

In addition to direct analysis of samples containing unsuitable solvents, the split vent may be used to prevent other unsuitable substances from entering detectors, provided that there is an appropriate retention gap between the substance and the analyte. The split vent is also useful in column conditioning. Column bleeding can be discharged from injector B without disconnecting the column from the detector.

4. Acknowledgements

H.B.W. thanks the National University of Singapore for award of a research scholarship. Very helpful suggestions by Dr. Sam F.Y. Li are greatly appreciated.

5. References

[1] F.I. Onuska and F.W. Karasek, *Open Tubular Column Gas Chromatography in Environmental Sciences*, Plenum Press, New York, 1984, p. 99.
[2] K. Grob, Jr., and E. Muller, *J. Chromatogr.*, 473 (1989) 411.
[3] R. Villalobos, *Instrum. Technol.*, 14 (1967) 59.
[4] F.I. Onuska and F.W. Karasek, *Open Tubular Column Gas Chromatography in Environmental Sciences*, Plenum Press, New York, 1984, p. 83.
[5] B.B. Gerhart and H.J. Cortes, *J. Chromatogr.*, 503 (1990) 377.
[6] C.F. Poole and S.K. Poole, *Chromatography, Part A: Fundamentals and Techniques*, Elsevier, Amsterdam, 1992, p. 425.
[7] P.G. Simmonds and E. Kerns, *J. Chromatogr.*, 186 (1979) 785.
[8] C.J. Geankoplis, *Transport Processes and Unit Operation*, Allyn & Bacon, Boston, 1983, p. 91.

ELSEVIER

Journal of Chromatography A, 663 (1994) 127–131

JOURNAL OF CHROMATOGRAPHY A

Short Communication

Application of trifluoroacetic anhydride–sodium iodide reagent for selective detection in thin-layer chromatography IV. Thin-layer chromatographic differentiation of nitrones, nitroxide radicals and nitrosoamines in mixtures

Andrzej Kotyński[a], Zbigniew H. Kudzin*[,b]

[a]*Institute of Chemistry, Faculty of Pharmacy, Medical University of Łódź, Narutowicza 120A, Łódź, Poland*
[b]*Department of Organic Chemistry, University of Łódź, Narutowicza 68, Łódź 90-136, Poland*

(First received September 27th, 1993; revised manuscript received November 24th, 1993)

Abstract

Trifluoroacetic anhydride–sodium iodide mixture (TFAA-I) reacts with nitroxide radicals, nitrones and nitrosoamines with release of iodine. Methods for the differentiation of these groups of nitrogen derivatives containing the N–O moiety using TLC systems with TFAA-I detection reagent are described.

1. Introduction

In previous papers we have described the analytical application of trifluoroacetic anhydride–sodium iodide (TFAA-I) reagent for the TLC determination of nitrones (**1**) [1–3], nitroxide radicals (**2**) [1,2] and nitrosamines (**3**) [1,4]. TFAA-I reagent has been found to react very fast with these compounds with quantitative formation of iodine, according to Eqs. 1–3, and this feature constituted the basis of their detection, determination and micro-determination.

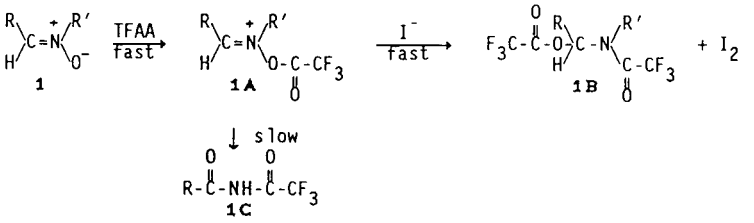

(1)

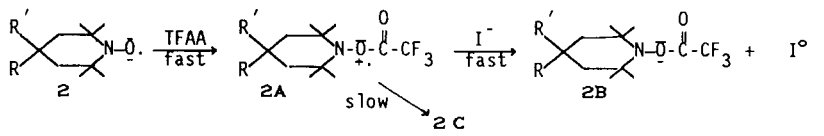

(2)

* Corresponding author.

0021-9673/94/$07.00
SSDI 0021-9673(93)E1262-X

(3)

In this paper we present our findings on the selective group determination of these compounds when they are present in mixtures.

2. Experimental

2.1. Materials

All reagents and solvents were purchased from Aldrich (Milwaukee, WI, USA) if is not stated otherwise. N-Phenyl-α-phenyl nitrone (**1a**) and N-nitrosomethylphenylamine (**3a**) were prepared according to Refs. 5 and 6, respectively.

2.2. Solutions

N-Phenyl-α-phenyl nitrone (**1a**), 4-oxo-2,2,6,6-tetramethyl-1-piperidinyloxy free radical (4-oxo-TEMPO; **2a**), N-nitroso-methylphenylamine (**3a**) solutions containing 2 mg of the compound in 1 ml of methanol (or acetic acid) were prepared. Other solutions used were a 0.5 *M* solution of sodium iodide in anhydrous acetone, a 1 *M* solution of trifluoroacetic anhydride in anhydrous acetone and a 1.5 *M* solution of ethanethiol in methanol.

2.3. Thin-layer chromatography

Procedure I. TFAA-I detection

Precoated silica gel 60 F_{254} aluminium sheets and (10 cm × 5 cm) with a 0.2-mm thick layer (Merck, Darmstadt, Germany) were used for all TLC experiments. The plates were spotted with an appropriate amounts of compound (*ca.* 5 μg), developed for a distance of 8 cm with appropriate solvent [methanol or chloroform–acetone (4:1)], air dried and sprayed with sodium iodide solution, again air dried and subsequently sprayed with TFAA solution. Nitrones (**1**), nitroxide radicals (**2**) and nitrosoamines (**3**) appeared almost immediately as brown spots on a white background, and were stable for more than 20 min.

Procedure II. EtSH–TFAA-I detection

To 0.5 ml of a solution of **1**, **2** or **3** in methanol, 0.5 ml of a 1.5 *M* solution of ethanethiol in methanol was added. The mixture was allowed to stand for 3 h, then analysed according to procedure I.

Procedure III. Ascorbic acid–TFAA-I detection

To 1 ml of a solution of **1**, **2** or **3** in methanol, ascorbic acid (5 mg) was added and the mixture was stirred for 10 min and then analysed as according to procedure I.

Procedure IV. Hydrogenation–TFAA-I detection

To 1 ml of a solution of **1**, **2** or **3** in acetic acid–formic acid (9:1), palladium (10% Pd–C) (5 mg) was added. This mixture was stirred for 30 min and analysed according to procedure I.

Procedure V. Silane–TFAA-I detection

To 1 ml of a solution of **1**, **2** or **3** in acetic acid, triethylsilane (Et_3SiH) (3 drops) and trifluoroacetic acid (TFA) (3 drops) were added. The mixture was stirred for 20 min and analysed according to procedure I.

Procedure VI. TFAA–TFAA-I detection

Procedure I was followed but the final detection with TFAA-I was preceded by spraying the plate with TFAA solution (three times in 3-min periods). The plates were then sprayed with NaI and TFAA solutions.

Procedure VII. Acidic treatment

The plates were spotted with an appropriate amount (*ca.* 5 μg of each component) of compound **1**, **2** or **3**, developed (see procedure I), air dried and exposed to HCl vapour for 5 min (tank) or sprayed with TFA.

Procedure VIII. TFAA–(TFAA-I)–NaI detection

Two plates were spotted with a mixture of nitrone (**1a**), nitroxide radical (**2a**) and nitrosoamine (**3a**) (5 μg of each component), developed according to procedure I and sprayed

with TFAA solution (three times in 3-min periods). One of these plates was treated with TFAA-I reagent (see procedure I) and the other was sprayed with NaI solution.

Procedure IX. Ascorbic acid–(TFAA-I)–HCl–NaI detection

A solution of a mixture of nitrone (**1a**), nitroxide radical (**2a**) and nitrosoamine (**3a**) was treated with ascorbic acid according to procedure III. Two plates were spotted with an appropriate amount of this solution (to deposit *ca.* 5 μg of each component) and developed according to procedure I. One of these plates was treated with TFAA-I reagent (see procedure I). The other plate was exposed to HCl vapours (tank) for 5 min (or sprayed with TFA), air dried and sprayed with NaI solution.

3. Results and discussion

In order to determine selectively each of the N-oxy derivatives **1**, **2** and **3** in the mixture, some additional treatments are required that would allow their gradual selection, prior to the final detection with TFAA-I. Thus, nitrones (**1**) and nitroxide radicals (**2**) exhibit different redox properties; whereas nitrones are reduction-resistant compounds, nitroxide radicals are reduced easily various reagents, *e.g.*, hydroiodic acid [7], ascorbic acid [8], ethanethiol [9] and rhodizonic acid and its analogue [10]. The corresponding amines or hydroxylamines formed in this reaction are totally inactive towards TFAA-I.

We established analytical conditions for the selective reduction of nitrones in the presence of nitroxide radicals. Thus, the combination of the selective pre-reduction of nitroxide radicals into hydroxylamines or amines (by means of ascorbic acid, thiols or formate–palladium hydrogenation), with detection by means of the TFAA-I reagent of the reduction-resistant nitrones, allows the selective TLC differentiation of these two classes of N-oxy compounds:

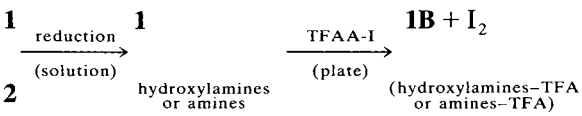

Another possibility for the TLC differentiation of nitrones and nitroxide radicals is to use of the reverse mode of the TFAA-I procedure (TFAA is used in first stage, followed by addition of NaI). Thus, the corresponding N-O-trifluoroacetyl derivatives **1A** and **2A**, formed during the treatment of **1** and **2** with TFAA, rearrange to **1C** or **2C**, respectively, which are not able to oxidize iodide anion [1,3].

As these reactions proceed at different rates (reaction **1** → **1C** is much faster than reaction **2** → **2C**), the application of the reverse mode of TFAA-I detection permits the differentiation of these two types of N-oxy compounds according to:

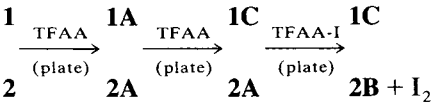

The instability of nitrosoamines (**3**) in the presence of acid provides an opportunity for the elimination of these derivatives from their mixtures with nitrones and/or nitroxide radicals (all these N-O-derivatives are positive in TFAA-I detection). The subsequent decomposition of nitrosoamines in HCl vapour, followed by TFAA-I detection of the residual component, allows the selective detection of nitrones and/or nitroxide radicals in the two-component mixtures with nitrosoamines (**1** + **2** and **1** + **3**). Such TLC plates (after TFAA-I detection) revealed only the spots of the nitrones and/or nitroxide radicals, respectively.

We also attempted the selective detection of three-component mixtures of **1**, **2** and **3**:

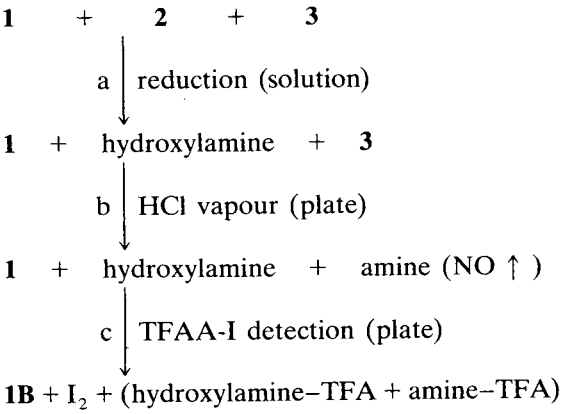

Table 1
Comparison of procedures for the selective detection of nitrones (**1a**), nitroxide free radicals (**2a**) and nitrosoamines (**3a**) by TLC

Compound applied[a]	Procedure[b]						
	I TFAA-I[c]	II EtSH[d] TFAA-I[c]	III Ascor.[d] TFAA-I[c]	IV H-Pd[d] TFAA-I[c]	V SiH-TFA[d] TFAA-I[c]	VI TFAA[c] TFAA-I[c]	VII HCl[c,e]
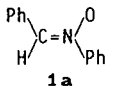 **1a**	++	++	++	++	++	–	–
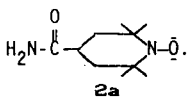 **2a**	++	++	–	–	–	++	–
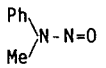 **3a**	++	–/+	++	–	–/+	++	++[f]

Abbreviations: Me = methyl; Ph = phenyl; Ascor. = ascorbic acid; SiH = triethylsilane; TFA = trifluoroacetic acid; TFAA = trifluoroacetic anhydride. ++ = Strong detection; + = distinct detection; –/+ = spot is detectable; – = not detected.
[a] The amounts of **1**, **2** or **3** spotted were *ca.* 5 μg per spot (2–3 mm in diameter).
[b] Brown spots.
[c] The reaction was carried out on the TLC plate.
[d] The reaction was carried out in solution.
[e] HCl vapour.
[f] Brown spot turning green and subsequently blue on air exposure.

Table 2
Comparison of procedures for the TLC analysis of mixtures of nitrones (**1a**), nitroxide radicals (**2a**) and nitrosoamines (**3a**)

Applied mixture of **1**, **2** and **3**[a]	TLC		VIII		IX		
	TFAA-I[b]	R_F[c]	TFAA[d] (TFAA-I[b,e])	NaI[d]	Ascor.[f] (TFAA-I[b,e])	HCl[d]	NaI[d]
1a	++	0.57	– (–)[e]	–	– (++)[e]	–	–/+[b]
2a	++	0.13	– (++)[e]	++	– (–)[e]	– –	– –
3a	++	0.65	++[g]		– (++)[e]	++[g]	–

Abbreviations and symbols as in Table 1.
[a] The mixture contained *ca.* 5 μg of each components.
[b] Brown spots on a white background.
[c] Silica plates. Solvent, chloroform–acetone (4:1).
[d] The reaction was carried out on the TLC plate.
[e] Detection with TFAA-I on the second plate.
[f] The reaction was carried out in solution.
[g] Brown spot turning green, and subsequently blue on air exposure.

The subsequent treatment of the three-component mixture with (a) ascorbic acid (in the starting solution) and (b) HCl vapour (on the TLC plate) allows the gradual elimination of nitroxide radicals (reduced to inactive hydroxylamines in stage a) and nitrosoamines (decomposed into amines in stage b), prior to the final detection of nitrones with TFAA-I reagent (stage c).

Comparison of this plate with the corresponding plates obtained (1) by instant TFAA-I detection of the starting mixture of **1**, **2** and **3** and (2) by HCl treatment followed by TFAA-I detection, permits the full TLC differentiation of all the N-oxy components in these mixtures.

The results of the differential detection of various compounds containing a semi-polar X–O bond with the TFAA-I as the final detection reagent are given in Tables 1 and 2.

4. References

[1] W. Ciesielski, W. Jędrzejewski, J. Drabowicz, Z.H. Kudzin and R. Skowroński, presented at the *Polish Chemical Society Congress, Łódź, Poland, 1988.*
[2] J. Drabowicz, A. Kotyński, Z.H. Kudzin and R. Skowroński, *J. Chromatogr.*, 473 (1989) 287.
[3] W. Ciesielski, Z.H. Kudzin, M. Tasz and J. Drabowicz, *Can. J. Chem.*, 68 (1990) 679.
[4] Z.H. Kudzin, A. Kotyński and R. Skowroński, *J. Chromatogr.*, 516 (1990) 467.
[5] O.H. Wheeler and P.H. Gore, *J. Am. Chem. Soc.*, 78 (1956) 3363.
[6] H. Soll, in E. Muller (Editor), *Methoden der Organischen Chemie (Houben–Weyl)*, Vol. XI-2, Georg Thieme, Stuttgart, 1958, p. 178.
[7] V.A. Golubev, M. Neiman and E.G. Rozantsev, *Izv. Akad. Nauk SSSR*, (1965) 345.
[8] C.M. Paleos and P. Dais, *J. Chem. Soc., Chem. Commun.*, (1977) 345.
[9] J. Zakrzewski, *Monatsh. Chem.*, 121 (1990) 803.
[10] M.E. Brik, *Synth. Commun.*, 20 (1990) 3283.

ELSEVIER

Journal of Chromatography A, 663 (1994) 132–133

JOURNAL OF CHROMATOGRAPHY A

Book Review

Practical HPLC Methodology and Applications, by B.A. Bidlingmeyer, Wiley-Interscience, New York, Chichester, 1992, X + 452 pp., price £45.50, ISBN 0-471-57246-2.

The author has written a practical monograph on high-performance liquid chromatography (HPLC) for readers with a limited knowledge of the basic principles of this technique, who just want to use it as a separation tool. The most important features and parameters are explained in a simple way using a minimum of mathematical equations. A very useful part is the glossary of the most important definitions used in HPLC.

An overview is given of how HPLC can be used in the biotechnological industry, in environmental research, for therapeutic drug monitoring or as a qualitative analytical tool. The most important features and parts (*e.g.*, connections, guard columns) of an HPLC system are briefly explained, followed by the basic principles of the different forms of HPLC. A general strategy and the basic tactics of how to choose the most suitable approach for a certain analyte are also treated. These basic tactics are developed in more detail for reversed-phase, ion-pair, ion-exchange and normal-phase HPLC and gel permeation and preparative chromatography. In this respect it is disappointing that the influence of the matrix is hardly discussed.

Useful strategies for optimizing resolution in HPLC and quantitative aspects of this separation technique are considered. In the section on solid-phase extraction (SPE), which will be of interest to many potential readers, surprisingly, mainly manually packed minicolumns are discussed and the nowadays frequently applied commercially available SPE cartridges are hardly mentioned. The chapter on gradient elution provides useful information on how to develop the optimum gradient conditions and discusses the problems that may occur during the development of a gradient separation (*e.g.*, viscosity and refractive index effects, degassing problems).

In the last ten chapters, practical experiments are given to demonstrate the use of normal-phase HPLC, the effect of column length and recycling of the eluent, the use of gel permeation chromatography in combination with dual detectors, the use of reversed-phase HPLC, quantitation effects, preparative HPLC and gradient elution, etc. All these chapters have the same sub-divisions: objective, background, additional materials, safety and disposal, experiments, evaluation, discussion, self-help questions and additional experiments.

Positive aspects of this publication are the extensive discussion on choosing the best solvents for the mobile phase, the effects of eluent recirculation, the quality of the water used to prepare mobile phases and the large number of applications, illustrated by chromatograms, tables and schemes.

Limitations are that the theoretical background and the practical considerations needed to develop an HPLC method are found in different chapters and that the majority of the theoretical discussions are rather concise. For example, even the most critical parameters in ion-pair HPLC, *i.e.*, the effect (type and concentration) of the organic solvent, counter ions,

SSDI 0021-9673(93)E1289-C

buffer ions and pH, or the fact that the potential of ion-suppression HPLC for bases is limited, are not discussed in detail. Further, the number of references is small and those cited are not always the most up-to-date. Also, there are a number of small inaccuracies in the figures and schemes; for example, the information indicated in the text cannot always be found in the mentioned figure or scheme. Especially in the last chapters the information is given in a way that is difficult to understand without reading the first chapters of the book.

The overall conclusion is that this book is an interesting tool for non-chromatographers during the development of a new HPLC method, but that for experienced analytical chemists the information is rather superficial and, as a result, the monograph will not be a real help in developing HPLC procedures.

Amsterdam (Netherlands) Henk Lingeman

Journal of Chromatography

Request for Manuscripts

Ralph Riggin and Gregory Davis will edit a special, thematic issue of the *Journal of Chromatography* entitled "**Analytical Biotechnology**". Both reviews and research articles will be included.

Topics such as the following will be covered:

- Sequencing
- Host Cell Protein Determination
- Peptide Mapping
- Electrophoretic Methods
- Capillary Electrophoresis/Electrokinetic Chromatography
- Protein Mass Spectrometry
- Glycoprotein Characterization
- High-Speed Separations
- Chromatographic Methods
- Residual DNA Determination
- Immunochemical Assays
- Moisture Determination

Potential authors of reviews should contact Roger Giese, Editor, prior to any submission. Address: Mugar Building Rm 122, Northeastern University, Boston, MA 02115, USA; tel.: (617) 373-3227; fax: (617) 373-8720.

The deadline for receipt of submissions is **April 30, 1994**. Manuscripts submitted after this date can still be published in the Journal, but then there is no guarantee that an accepted article will appear in this special, thematic issue. Four copies of the manuscript, citing this issue, should be submitted to the Editorial Office, Journal of Chromatography, P.O. Box 681, NL-1000 AR Amsterdam, The Netherlands. All manuscripts will be reviewed and acceptance will be based on the usual criteria for publishing in the *Journal of Chromatography*.

PUBLICATION SCHEDULE FOR THE 1994 SUBSCRIPTION

Journal of Chromatography A and *Journal of Chromatography B: Biomedical Applications*

MONTH	O 1993	N 1993	D 1993	J	F	M	A	
Journal of Chromatography A	652/1 652/2 653/1	653/2 654/1 654/2 655/1	655/2 656/1 + 2 657/1 657/2	658/1 658/2 659/1 659/2	660/1 + 2 661/1 + 2 662/1 662/2	663/1 663/2 664/1	664/2 665/1 665/2 666/1 + 2 667/1	The publication schedule for further issues will be published later.
Bibliography Section						681/1		
Journal of Chromatography B: Biomedical Applications				652/1	652/2 653/1	653/2 654/1	654/2 655/1	

INFORMATION FOR AUTHORS

(Detailed *Instructions to Authors* were published in *J. Chromatogr. A*, Vol. 657, pp. 463–469. A free reprint can be obtained by application to the publisher, Elsevier Science B.V., P.O. Box 330, 1000 AH Amsterdam, Netherlands.)

Types of Contributions. The following types of papers are published: Regular research papers (full-length papers), Review articles, Short Communications and Discussions. Short Communications are usually descriptions of short investigations, or they can report minor technical improvements of previously published procedures; they reflect the same quality of research as full-length papers, but should preferably not exceed five printed pages. Discussions (one or two pages) should explain, amplify, correct or otherwise comment substantively upon an article recently published in the journal. For Review articles, see inside front cover under Submission of Papers.

Submission. Every paper must be accompanied by a letter from the senior author, stating that he/she is submitting the paper for publication in the *Journal of Chromatography A* or *B*.

Manuscripts. Manuscripts should be typed in **double spacing** on consecutively numbered pages of uniform size. The manuscript should be preceded by a sheet of manuscript paper carrying the title of the paper and the name and full postal address of the person to whom the proofs are to be sent. As a rule, papers should be divided into sections, headed by a caption (*e.g.*, Abstract, Introduction, Experimental, Results, Discussion, etc.). All illustrations, photographs, tables, etc., should be on separate sheets.

Abstract. All articles should have an abstract of 50–100 words which clearly and briefly indicates what is new, different and significant. No references should be given.

Introduction. Every paper must have a concise introduction mentioning what has been done before on the topic described, and stating clearly what is new in the paper now submitted.

Experimental conditions should preferably be given on a *separate* sheet, headed "Conditions". These conditions will, if appropriate, be printed in a block, directly following the heading "Experimental".

Illustrations. The figures should be submitted in a form suitable for reproduction, drawn in Indian ink on drawing or tracing paper. Each illustration should have a caption, all the *captions* being typed (with double spacing) together on a *separate sheet*. If structures are given in the text, the original drawings should be provided. Coloured illustrations are reproduced at the author's expense, the cost being determined by the number of pages and by the number of colours needed. The written permission of the author and publisher must be obtained for the use of any figure already published. Its source must be indicated in the legend.

References. References should be numbered in the order in which they are cited in the text, and listed in numerical sequence on a separate sheet at the end of the article. Please check a recent issue for the layout of the reference list. Abbreviations for the titles of journals should follow the system used by *Chemical Abstracts*. Articles not yet published should be given as "in press" (journal should be specified), "submitted for publication" (journal should be specified), "in preparation" or "personal communication".

Vols. 1–651 of the *Journal of Chromatography*; *Journal of Chromatography, Biomedical Applications* and *Journal of Chromatography, Symposium Volumes* should be cited as *J. Chromatogr.* From Vol. 652 on, *Journal of Chromatography A* (incl. Symposium Volumes) should be cited as *J. Chromatogr. A* and *Journal of Chromatography B: Biomedical Applications* as *J. Chromatogr. B*.

Dispatch. Before sending the manuscript to the Editor please check that the envelope contains four copies of the paper complete with references, captions and figures. One of the sets of figures must be the originals suitable for direct reproduction. Please also ensure that permission to publish has been obtained from your institute.

Proofs. One set of proofs will be sent to the author to be carefully checked for printer's errors. Corrections must be restricted to instances in which the proof is at variance with the manuscript.

Reprints. Fifty reprints will be supplied free of charge. Additional reprints can be ordered by the authors. An order form containing price quotations will be sent to the authors together with the proofs of their article.

Analytical Applications of Circular Dichroism

Edited by **N. Purdie** and **H.G. Brittain**

Techniques and Instrumentation in Analytical Chemistry Volume 14

Circular dichroism is a special technique which provides unique information on dissymmetric molecules. Such compounds are becoming increasingly important in a wide variety of fields, such as natural products chemistry, pharmaceutics, molecular biology, etc. The content of this book has been selected in order to feature the unique aspects of circular dichroism, and how these strengths can be of assistance to workers in the field.

Substantial discussions have been provided regarding the particular phenomena associated with dissymmetric compounds which give rise to the circular dichroism effect. Reviews are also given of the type of instrumentation available for the measurement of these effects. A number of chapters cover the wide range of applications illustrating the power of the method.

Owing to its broad appeal, the book will be of interest to workers in all areas of chemistry and pharmaceutical science.

Contents:

© 1994 360 pages Hardbound
Price: Dfl. 355.00 (US $ 202.75)
ISBN 0-444-89508-6

ORDER INFORMATION

For USA and Canada
ELSEVIER SCIENCE INC.
P.O. Box 945
Madison Square Station
New York, NY 10160-0757
Fax: (212) 633 3880

In all other countries
ELSEVIER SCIENCE B.V.
P.O. Box 330
1000 AH Amsterdam
The Netherlands
Fax: (+31-20) 5862 845

US$ prices are valid only for the USA & Canada and are subject to exchange rate fluctuations; in all other countries the Dutch guilder price (Dfl.) is definitive. Customers in the European Community should add the appropriate VAT rate applicable in their country to the price(s). Books are sent postfree if prepaid.

ELSEVIER SCIENCE B.V.

0021-9673(19940304)663:1;1-Z